Developing an *in vitro* repeat-dose approach to detect non-genotoxic carcinogens (NGCs)

Demi Jade Pritchard, B.Sc.

Submitted to Swansea University in fulfilment of the requirements for the Degree of Doctor of Philosophy

Swansea University

2023

Abstract

This work aimed to develop an *in vitro* testing battery, to detect non-genotoxic carcinogens (NGCs). Currently, *in vitro* test systems aim at detecting genotoxic carcinogens (GCs) whereas, the gold standard test for NGCs is the two-year rodent bioassay. There are numerous problems with this method such as long experimental periods, high costs and many ethical concerns. NGCs make up ~15% of all carcinogens, highlighting the importance of their correct detection and labelling.

The *in vitro* test battery includes a selection of endpoints comprised primarily from the hallmarks of cancer. The endpoints explored were acute and chronic genotoxicity assessment via the mononucleated micronucleus (Mn) assay; cytotoxicity assessment utilising RPD; cell cycle and apoptosis assessment using flow cytometry; gene expression analysis using a PCR array and determining mitochondrial health using the Seahorse analyser.

Six carcinogens were assessed using the multi-endpoint, *in vitro* testing system. These chemicals included nickel chloride ($NiCl_2$), sodium meta arsenite (NaMAr), cacodylic acid (GC- included to compare with NaMAr), rosuvastatin, chloroprene and 2,3,7,8-tetrachlorodibenzodioxin (TCDD). This work showed that some NGCs can behave as GCs so there may be some mislabelling of carcinogens. NaMAr indicated genotoxicity due to a chronic dosing approachand $NiCl_2$ also showed genotoxicity but in an acute setting. The correct categorisation of these carcinogens is of increasing importance due to the use in consumer product for example.

The *in vitro* battery appears to be a promising first step in detecting and understanding the mechanism(s) of action (MoA) used by different NGCs. This work highlighted some potentially mislabelled NGCs, such as $NiCl_2$ and NaMAr, which is an important novel finding. The PCR array proved to be very useful to identify genes of interest, that could help unpick the MoA of each diverse NGC. Next steps could include utilising a targeted three-dimensional (3D) spheroid approach based on the exposure route (E.g. Rosuvastatin is ingested so a gut model). Chronic dosing is an important real-life component of the test battery and is required to improve the whole picture. These additional approaches, together with an *in vitro* test battery, could improve detection and provide a complete narrative of the MoAs utilized by these complex carcinogens.

Declarations and Statements

This work has not previously been accepted in substance for any degree and is not being concurrently submitted in candidature for any degree.

Signed: [redacted]

Date: 14th March 2023

This thesis is the result of my own investigations, except where otherwise stated. Other sources are acknowledged by footnotes giving explicit references. A bibliography is appended. Signed:

Signed: [redacted]

Date: 14th March 2023

I hereby give consent for my thesis, if accepted, to be available for photocopying and for inter-library loan, and for the title and summary to be made available to outside organisations. Signed:

Signed: [redacted]

Date: 14th March 2023

The University's ethical procedures have been followed and, where appropriate, that ethical approval has been granted. Signed:

Signed: [redacted]

Date: 14th March 2023

Covid-19 Statement

The Covid-19 pandemic drastically impacted my PhD and affected the amount of work I was able to produce. I was not able to enter the laboratory from Monday 23rd March 2020 until 20th July 2020. This 4-month period of lockdown occurred at a very inconvenient time for myself, as I should have been collecting a large portion of my data during this time. It was not possible to make up this time due to the stage of PhD I was in. Due to extra delays when ordering resources, chemicals, getting cells up and running, securing time in tissue culture laminar flow hoods and on machines such as the metafer system, more time was lost upon the return to the lab.

I tried to use my time as wisely as possible during lockdown by collating my data, doing any outstanding statistics, joining webinars, summer schools, registering for virtual conferences, writing a review research paper with a colleague (manuscript in preparation), writing backgrounds for my non-genotoxic carcinogens and making a detailed experimental plan for my return.

Lockdown was an unfamiliar and difficult time with increased stress and anxiety, which made working from home very challenging. I also had extra stress during this time as my father has a heart condition and was in hospitals twice over the period due to heart problems and once due to an ablation operation. During the waiting time for the heart operation, he was classified as 'at high risk', so I did any food shopping and errands required whilst he remained completely isolated and shielded by my mum. I was his lift to and from the hospital on the day of the operation and all distancing measures were in place such as him sitting in the back of the car, both of us wearing facemasks and with windows opened.

If the Covid-19 lockdown had not taken place, I believe I could have completed some of the work I have suggested as future work. I wanted to carry out some follow up qPCR to further confirm what the qRT-PCR microarray (Bio-Rad general cancer panel) showed. Further delays were also seen upon my return to the lab due to Brexit. Any orders placed took longer than expected to arrive, meaning the actual time lost from the lab was even longer than the 4 months originally stated.

Table of Contents

Acknowledgements

First, I would like to thank my supervisor, Professor Gareth Jenkins for the opportunity to complete this PhD. I am also very grateful for his continued support and guidance throughout my PhD. I am thankful for the input from my second and third supervisors Professor Shareen Doak and Dr Kate Chapman respectively. I would also like to thank my funder, The NC3Rs for making this work possible. I appreciate the opportunities and experience I have gained through attending conferences both nationally and internationally throughout my studies. I would like to thank UKEMs for providing the funding to make this possible.

Thanks to each member of the In Vitro Toxicology Group for your friendship, help and support. Thank you to my friends outside of the lab for your constant support and welcome laughs and distractions. I would like to thank my parents for their constant encouragement, care and understanding. Thank you to my grandparents for always believing in me and being proud of whatever I achieve. Without the reassurance from my family, this PhD would not have been possible. I am also very thankful to all the stress relief I received in the way of cwtches from my dog, Misty.

Finally, I would like to thank my extremely helpful and supportive partner Matthew for always cheering me up and cheering me on. I could not have done it without all of the fantastic support I have received, and I am grateful to each and every one who helped me.

Tables and Illustrations

Definitions / Abbreviations

µl	Microlitre
µM	Micromolar
3D	3-Dimensional
3RS	Replacement, Reduction and Refinement
7-AAD	7-Aminoactinomycin D
8-OHdG	8-Hydroxy-2'-Deoxyguanosine
ADI	Acceptable Daily Intake
Ah	Aryl Hydrocarbon
AhR	Aryl Hydrocarbon Receptor
ANOVA	Analysis of Variance
AOX	Antioxidant
APL	Acute Promyeloid Leukaemia
As	Arsenic
ATCC	American Type Culture Collection
ATP	Adenosine Triphosphate
Av	Average
BAX	BCL-2 Associated X Protein
BBC	British Broadcasting Corporation
BCL-2	B-Cell Lymphoma 2
BN	Binucleate
BSA	Bovine Serum Albumin
CA	Chromosome Aberration
Ca^{2+}	Calcium
Caco	Cacodylic Acid
CBMN	Cytokinesis Block Micronucleus Assay
CBPI	Cytokinesis Block Proliferation Index
CCND1	Cyclin D1
CD4	Cluster of Differentiation 4
CDKN2A	Cyclin Dependent Kinase Inhibitor 2A
cDNA	Complementary DNA
CO_2	Carbon Dioxide
CTA	Cell Transformation Assay
CYP	Cytochrome P450
cytoB	Cytochalasin B
DAPI	4,6-Diamidino-2-Phenylindole
DCF	Dichlorodihydrofluorescein
DCFDA	Dichlorodihydrofluorescein Diacetate
DEA	Diethanolamine
DMA	Dimethylarsinic Acid
DMEM	Dulbecco's Modified Eagle Medium
DMSO	Dimethyl sulphoxide
DNA	Deoxyribunucleic Acid
ECAR	Extracellular Acidification Rate
EPA	Environmental Protection Agency

ESR	Electron Spin Resonance
EthBr	Ethidium Bromide
FACS	Fluorescence Activated Single Cell Sorting
FCCP	(Carbonyl cyanide-p-trifluoromethoxy) Phenylhydrazone
FCS	Flow Cytometry Standard
FITC	Fluorescein Isothiocyanate
Fix	Fixative
G	Gravitational Force
G1	Gap 1 (cell cycle)
G2	Gap 2 (cell cycle)
GC	Genotoxic Carcinogen
gDNA	Genomic DNA
GJIC	Gap Junction Intercellular Communication
GSH	Glutathione
GSSG	Glutathione Disulphide
h/s	hours/seconds
H_20	Water
H_2O_2	Hydrogen Peroxide
HIF	Hypoxia Inducible Factor
HMG-CoA	3-Hydroxy-3-Methylglutaryl-CoenzymeA Reductase
HRAS	Harvey Rat Sarcoma Virus
HRP	Horseradish Peroxidase
Hygro B	Hygromycin B
IARC	International Agency for Research on Cancer
IGF1	Insulin Like Growth Factor 1
IGF-BP	Insulin Like Growth Factor Binding Protein
IPA	Ingenuity Pathway Analysis
KCC	Key Characteristics of Carcinogens
kg	Kilogram
KRAS	Kirsten Rat Sarcoma Virus
LDL	Low Density Lipoprotein
M	Molar
MAPK	Map Kinases
MDA	Malondialdehyde
MDM2	Mouse Double Minute 2
MEGA	Multi-End Point Genotoxicity Assessment
min	Minutes
ml	Millilitre
MLA	Mouse Lymphoma Assay
mM	Millimolar
MMA	Monomethylarsonic Acid
MMS	Methylmethane sulphonate
Mn	Micronucleus
MoA	Mechanism of Action
mRNA	Messenger RNA

NAC	N-Acetyl Cysteine
NAM	New Approach Methodologies
NaMAr	Sodium Meta Arsenite
NC3Rs	National Centre for the Replacement, Refinement and Reduction of Animals in Research
Neg	Negative
NFKB	Nuclear Factor Kappa B
ng	Nanogram
NGC	Non-genotoxic Carcinogen
$NiCl_2$	Nickel Chloride
Ni_3S_2 / NiS	Nickel Sulphide
nm	Nanometer
NOAEL	No Observed Adverse Effect Level
NRAS	Neuroblastoma Rat Sarcoma Virus
NTP	National Toxicology Program
O_2	Oxygen
OCR	Oxygen Consumption Rate
OECD	The Organisation for Economic Cooperation and Development
OH/OH^-	Hydroxide
PAH	Polycyclic Aromatic Hydrocarbon
PBS	Phosphate Buffered Saline
PCR	Polymerase Chain Reaction
PD	Population Doubling
PI	Propidium Iodide
PI3K	Phosphatidylinositol 3-Kinase
POS	Positive
PS	Phosphatidylserine
PTEN	Phosphatase and Tensin Homolog
Q1	Quartile 1
Q2	Quartile 2
Q3	Quartile 3
Q4	Quartile 4
qPCR	Quantitative PCR
QSAR	Quantitative Structure Activity Relationship
REACH	Registration, Evaluation, Authorisation and Restriction of Chemicals
Rep	Repetition
RET	Receptor Tyrosine
RNA	Ribonucleic Acid
RoC	Report on Carcinogens
ROS	Reactive Oxygen Species
RPD	Relative Population Doubling
RPMI	Roswell Park Memorial Institute
RT	Reverse Transcription
SHE	Syrian Hamster Embryo
Tbl1x	Transducin Beta Like 1 X Linked

TCDD	2,3,7,8-Tetrachlorodibenzodioxin
TF	Transferrin
TG487	Test Guideline 487
TGFß / TGFß1	Transforming Growth Factor Beta (1)
TNF	Tumour Necrosis Factor
TOP1	DNA Topoisomerase 1
TP53	Tumour Protein 53
TTC	Threshold of Toxicological Concern
UV	Ultraviolet
VEGF / VEGFA	Vascular Endothelial Growth Factor (A)
VHL	von Hippel Lindau
WHO	World Health Organisation
XF	Extracellular Flux

Chapter 1: Introduction

1.1 Environmental agent exposure

Humans are exposed to a plethora of environmental agents throughout their lifetime. Between 70% and 90% of human cancers are developed due to exposure to environmental agents (Wu *et al*., 2016). Lifestyle choices are the risk factors associated with the onset of carcinogenesis and are often well-documented because of epidemiological studies. However, environmental agents are so diverse, numerous and often able to integrate into the environment, making them difficult to pinpoint and understand (Irigaray *et al*., 2007). A study carried out in identical twins demonstrated that environmental factors appeared more important in cancer aetiology than genetic factors (Lichtenstein *et al*., 2000). This highlights the significance of understanding these environmental agents as they have such an impact on human health.

Over 87,000 chemicals have been accepted for use commercially since 1970, however only 1 thousand of those chemicals have been tested for their carcinogenic potential (Cohen and Jefferies, 2019). Humans are estimated to be exposed to around 80,000 environmental toxicants each year (Ward *et al*., 2003). There are different categories used to describe these chemicals, such as 'known' carcinogen, 'possibly' carcinogenic and a newly emerging category of endocrine disrupting chemicals (EDCs). These carcinogens can be found in the environment, in our food products and/or within the substances we put on our bodies. Human beings are exposed to a low level of a mixture of environmental toxins daily (Cohen and Jefferies, 2019). The regulations covering carcinogens are currently complex but are incomplete and require intervention and improvement in order to improve public health (Suarez-Torres *et al.*, 2019).

1.2 Toxicology

Toxicology is an area of science that investigates the harmful effects of different chemicals to the environment and to animals. Numerous factors must be taken into consideration to understand if an individual exposed to a toxic chemical will develop a disease, such as the duration of exposure, a person's age, and their susceptibility to chemicals (NIH, 2023). Paracelsus (1493-1541) was an alchemist and physician and is known as a significant figure of medical history and is one of the pioneers of toxicology (Michaleas *et al*., 2021). He coined the important phrase "What is there that is not poison? All things are poison, and nothing is without poison. Solely the

dose determines that a thing is not a poison" (Grandjean, 2016). This highlights the importance of the dose in toxic responses.

Another extremely important figure in this field is Mathieu Joseph Bonaventura Orfila, who is known as the founder of modern toxicology. His contributions were great, and they advanced several different fields including medical, chemical and legal sciences (Michaleas *et al*., 2022). Perhaps his most profound contributions were his treatises such as 'Traité des Poisons Tirés des Règnes Minéral, Végétal et Animal ou Toxicologie Générale' which is translated as 'A treatise on poisons found in the mineral, vegetable and animal kingdoms, or a general system of toxicology' and this was published in 1814. He also designed a method for detecting poisonous substances such as arsenic (As) in the human body (Michaleas *et al*., 2022). Toxicological risk assessment aims to provide rationale to regulatory bodies with a decision of classification regarding certain chemicals in order to avoid adverse outcomes. The results and decisions from toxicology studies are discussed not only among scientists and the regulatory bodies but also within the public when it involves public health advice (Schrenk, 2018).

1.2.1 Genetic toxicology

Genotoxicity refers to damage to the genetic material from harmful substances. Chemical, physical, and biological agent exposure can lead to genomic instability which is responsible for the onset of numerous diseases including cancer (Ren *et al*., 2017). Genotoxicity is often confused with mutagenicity; this describes the process of inducing permanent transformations by altering the structure and quality of the genetic material which can in turn lead to further mutations. Mutagenicity is therefore a long-term process as there is a permanent mutation which can be passed on (Hsu *et al.,* 2016). Whereas, genotoxicity can be short term, transient and can be repaired, therefore not resulting in permanent inherited mutations (Ren *et al*., 2017). The action of numerous DNA repair pathways such as nucleotide excision repair, base excision repair, mismatch repair and direct reversal, can prevent the DNA damage causing a permanent gene mutation (Nagarathna *et al.,* 2013).

The work of Hermann J Muller is an important first step in mutagenesis and genetic toxicology (Muller, 1927). In 1927, he described introducing gene mutations in *Drosophila* and explained the theory of point mutations for which he received a Nobel prize in 1946 (Calabrese, 2018). Auerbach, Robson and Carr, (1947) continued Mullers work and further found that chemicals such as mustard gas are also capable of causing mutations in *Drosophila*.

Hazard identification and cancer risk estimation is an important factor of genetic toxicology. For assessing genotoxic hazard, regulatory agencies request a battery of tests to be performed to cover the different types of DNA damage. The current safety testing battery is made up of the Ames bacterial mutagenesis test, *in vitro* cytogenetics and *in vivo* genotoxicity assays. There are some suggestions regarding modernising the current testing battery. Newer approaches are becoming more popular and carry more weight, including *in silico* approaches and genomics for instance which may provide more of an understanding for indirect carcinogens (Mahadevan *et al*., 2011).

There have been several advances in the field of toxicology, more specifically genetic toxicology, in the last two decades. There are developments in the knowledge of gene function and improved databases of genetic sequence information. This had led to the formation of toxicogenomics which also encompasses other stages of assessment such as toxicokinetics and toxicodynamics (Martins *et al.*, 2019). Toxicogenomics studies the relationship between adverse effects from environmental agents and the activity of the genome (Aardema and MacGregor, 2003). These advances are beneficial in terms of the aims of this work as these progressive techniques provide promise in allowing the detection of carcinogens *in vitro*.

1.3 Cancer

Cancer arises when a cell is able to escape the usual control and regulation of cell proliferation (Weinberg, 1996). Cancer can originate as a result of both genotoxic and non-genotoxic carcinogens (NGCs) (Hanahan and Weinberg, 2000). The term NGC is defined as a chemical that can cause cancer as a result of a secondary mechanism, not by direct deoxyribonucleic acid (DNA) damage, which is true for genotoxic carcinogens (GCs) (Hayashi, 1992). This work focusses on the *in vitro* detection of NGCs and understanding their unique mechanism of actions (MoAs). Understanding the mechanisms behind how certain NGCs initiate oncogenesis would ensure they are correctly classified. These classifications are important to inform the regulations in place for different chemicals and therefore making accurate decisions regarding their use in everyday products (Suarez-Torres *et al.*, 2019). It is thought that NGCs make up 10-20% of all carcinogens (Bartsch and Malaveille, 1989). Considering that they lack an appropriate means of detection, this is an alarming statistic.

The initiation of cancer is a multi-step process, which arises as a result of multiple mutations in a number of genes (Hernández *et al*., 2009). It is known for the uncontrolled cellular growth and division as well as acquiring a metastatic potential. The inhibition of tumour suppressor genes and initiation of oncogenes work together to evade apoptosis and lead to uncontrollable progress through the cell cycle (Sarkar *et al*., 2013). These examples of characteristics and hallmarks are important as they form the basis of this work. Some common causes of cancer are occupational exposure and some lifestyle factors such as smoking tobacco and drinking alcoholic beverages (Wilde *et al*., 2017). In order to understand unknown carcinogenic mechanisms, multiple endpoint analysis is important, understanding whether the chemical is a GC or NGC (Wilde *et al*., 2017).

There is a growing incidence of cancer, largely as a result of the aging population and better control of communicative diseases, but also as a result of improved diagnosis and screening procedures (Irigaray *et al*., 2007). Only 1.7% of cancer related deaths occur before the age of 40 years in America and 90% of cancers are diagnosed in individuals over the age of 50 (Siegel *et al*., 2018). The UK has seen 375,000 new cancer cases between 2016 and 2018 and as a result there has been 167,142 cancer deaths between 2017 and 2019 (CRUK, 2022). Childhood cancer is rare, although it can occur, and is often misunderstood. There are approximately 1,800 new cases diagnosed in the UK each year (Children with cancer UK, 2023). This highlights that in childhood cancer, age is not the problem, this occurs due to the random mutations that can take place in the growing cells (Children with cancer UK, 2023). The most common cancer types in the UK are breast, prostate, lung and bowel cancers which amounts to 53% of new cancer cases in 2016-2018 (CRUK, 2022). It is also thought that around 38% of cancer cases in the UK in 2015 were preventable (CRUK, 2022) which is important as this PhD focuses on aspects of cancer prevention.

Humans are made up of over 40 trillion cells, so to be able to avoid cancer for around 50 years is remarkable (Bianconi *et al*., 2013). Due to numerous factors such as pathogens, limited food supply and predation, humans often did not live >50 years, so did not encounter diseases of old age such as cancer (Caspari and Lee, 2004). Evolution plays a role in oncogenesis, as cancer is a microevolutionary process (Alberts *et al*., 2002), and the mechanisms of cancer prevention are most prevalent during reproductive ages. Then after 50 years, there is more chance of a mutation leading to the development of cancer (Laconi *et al*., 2020).

Cancer is the leading cause of mortality world-wide (WHO, 2023). In 2020, there was an estimated 10 million cancer related deaths worldwide (CRUK, 2022). Cancer has numerous different causes; however, many cancers can be cured if they are detected and treated early enough (WHO, 2023). The cancer burden can be reduced due to preventing key risk factors and early detection coupled with successful treatment. Some prevention strategies include a healthy diet with fruit and vegetables, regular physical activity and avoiding ultraviolet (UV) exposure. Both screening and early diagnosis are the components of early detection and therefore a better prognosis (WHO, 2023). "Prevention is better than cure" was a phrase coined by Desiderius Erasmus in 1500 (RCN, 2023) however it is still used in campaigns to improve public health today. If the carcinogens that lead to the initiation of cancer were better understood and controlled, then perhaps the cancer incidence would be reduced.

1.3.1 Hallmarks of cancer

The hallmarks of cancer concept were originally outlined in 2000 by Hanahan and Weinberg, (2000). They demonstrated several of the capabilities acquired during the multi-step process of tumourigenesis as seen in **Figure 1.1a & b**. It was stated that as normal cells become neoplastic, they obtain a series of the hallmarks and therefore can progress into a tumour (Hanahan and Weinberg, 2000). The hallmarks consist of a series of commonalities uniting all cancer cell types at a phenotypic level. They are comprised of the core hallmarks and enabling characteristics which together allow for further understanding into the mechanisms of cancer development and malignancy (Hanahan, 2022).

Although cancer describes a heterogeneous collection of diseases, the hallmarks are a series of characteristics common throughout different cancer types (Gutschner and Diederichs, 2012). The battery of *in vitro* tests used in carcinogen hazard identification aims to target some of the hallmarks of cancer such as resisting cell death, genome instability, mutation and sustaining proliferative signalling.

The hallmarks attempt to provide an organised understanding of the complex disease and it is demonstrated how normal cells progress to be neoplastic. Tumours are complex tissues comprised of multiple different cell types which are all capable of interacting with each other in the tumour microenvironment (Hanahan and Weinberg, 2011).

The hallmarks of cancer are particularly important to this work, and they have formed the basis of how the endpoints were chosen for the test battery. The endpoints chosen, aim to measure

selected hallmarks of cancer and are being assessed as an approach to detect NGCs. The selected endpoints will form part of a multi-endpoint *in vitro* testing approach.

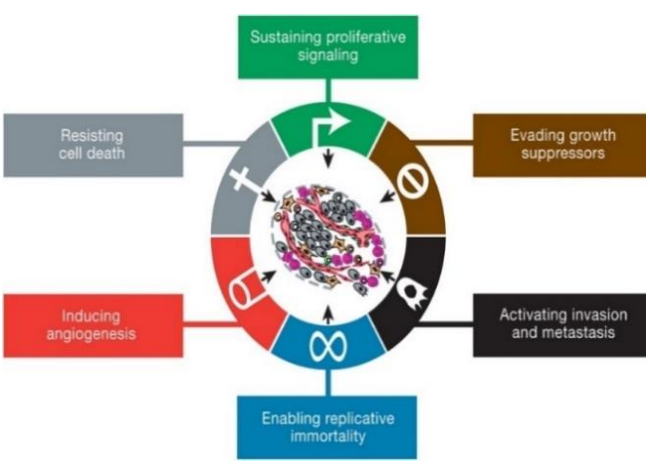

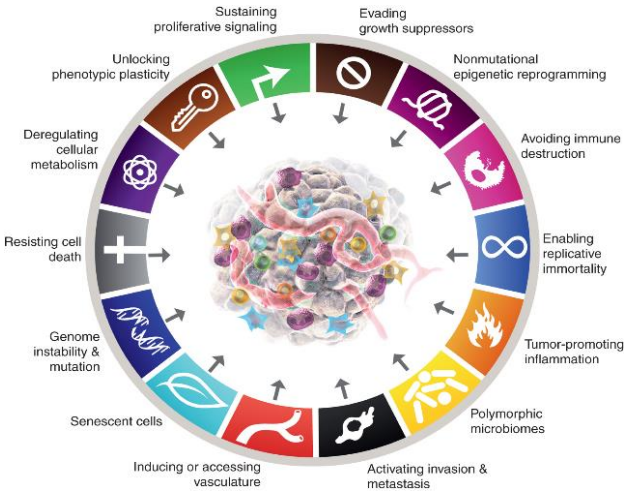

1.1a **1.1b**

Figure 1.1 (a and b): The original 6 hallmarks of cancer (**Figure 1.1a**) taken from (Hanahan and Weinberg, 2011) with permission and the most up-to-date version including the full 14 hallmarks of cancer (**Figure 1.1b**) taken from (Hanahan, 2022) with permission.

1.4 Carcinogens

A carcinogen is a compound capable of causing cancer in experimental animals and humans (Schrenk, 2018). Carcinogens are divided into 2 main groups; GCs and NGCs. GCs are known as the chemicals that interact directly with the DNA thereby damaging it. GCs are thought to have no safe exposure threshold, due to their DNA reactive properties, meaning that they pose a risk of cancer to humans even at low doses. GCs use is not usually permitted in products, such as pharmaceuticals, food stuffs, lifestyle products, and there are strict regulations surrounding them (Nohmi, 2018). Whereas NGCs are capable of inducing cancer via alternative mechanisms, not acting directly on the DNA. NGCs are thought to have a safe exposure threshold; therefore, they are used in society providing the threshold is not exceeded (Nohmi, 2018). Carcinogens can also be divided into 3 types; biological carcinogens such as viruses human papillomavirus (HPV), parasites and bacteria; chemical carcinogens such as aflatoxin, asbestos and the components of tobacco smoke and physical carcinogens such as ionising radiation and UV light (WHO, 2023).

It has proven difficult to detect NGCs *in vitro*, which means there is a requirement to find an *in vitro* testing system capable of this. The importance of mechanistic understanding is apparent when trying to distinguish between NGCs and GCs as there are some overlaps and misleading results specifically referring to NGCs in the wider literature. Mixed results are common in the field and some carcinogens give negative results in the *in vitro* bacterial mutation assays however provide positive results in the *in vivo* gene mutation assay and vice versa. For example, two NGCs; dicyclanil and ochratoxin A, both give negative results for *in vitro* mutagenicity but are positive for *in vivo* mutagenicity assays (Nohmi, 2018). Allemang *et al*., (2020) also provides a comparison of different *in vitro* positives and negatives for both GCs and NGCs. NGCs are also occasionally capable of producing positive results in the *in vitro* genotoxicity tests such as the micronucleus (Mn) assay and the chromosome aberration (CA) assay as a result of indirect effects such as spindle poisons or topoisomerase II inhibition for example (Nohmi, 2018).

As previously stated, Paracelsus devised the principle "The dose makes the poison". This principle suggests that any chemical can be toxic above a certain threshold and a toxic chemical can also be non-toxic below a certain threshold. However, this phrase is not always deemed true for GCs (Nohmi, 2018). Chemicals within pesticides, veterinary drugs and food additives for example are subject to regulatory toxicological testing before they reach the market (Nohmi, 2018). The adoption of threshold dose responses for GCs is now becoming more common when backed up by reliable data and a biologically plausible mechanism (COM, 2010). It has been highlighted that different classes of rodent carcinogens can behave differently in different species, as NGCs routinely give positive results for either rats or mice (single-species carcinogens) whereas GCs are normally capable of induce tumours in both mice and rats (Hayashi, 1992). Human beings are subject to a number of genotoxic and non-genotoxic agents within the current polluted environments and unpicking the role of individual compounds from a mixture can be complicated (Sommer *et al*., 2020).

Genotoxic and NGCs have differences in their sub-mechanisms which similarly affects the cells gene expression profiles. This is a promising approach for distinguishing between GC and NGCs in toxicological studies (Zhao *et al*., 2012). Some of the similarities and differences between genotoxic and NGCs are highlighted in **Table 1.1** below.

Table 1.1: Detailing some of the main differences between genotoxic and non-genotoxic carcinogens.

Genotoxic carcinogens	**Non-genotoxic carcinogens**
Directly acts on the DNA (covalently binding to the DNA or inserting into the DNA-helix) (van Delft *et al*., 2004)	Indirect carcinogen, acts via a variety of mechanisms (stimulating oxidative stress, inducing proliferation and altering cellular communication etc.) (van Delft *et al*., 2004)
Positive results in *in vitro* genotoxicity tests (with exceptions) (Kirkland *et al*., 2016).	Negative results in *in vitro* genotoxicity tests (with exceptions) (Kirkland *et al*., 2016).
Positive results in *in vivo* genotoxicity tests (with exceptions) (Kirkland *et al*., 2016).	Positive results in *in vivo* genotoxicity tests (with exceptions) (Kirkland *et al*., 2016).
Carcinogenic in multiple organs and multiple rodent species (Nohmi, 2018)	Carcinogenic in single organ/single species of rodents (Nohmi, 2018)

As it is currently understood, there are three main stages of carcinogenesis: initiation, promotion and finally progression, with multiple mechanisms of carcinogenesis across the 3 elements often targeted alongside each other (Jacobs *et al*., 2016). Synergism between genotoxic and non-genotoxic factors can be responsible for the initiation of carcinogenesis (Zoumpourlis *et al*., 2003).

In order to understand the risk that carcinogens pose, numerous methods are used to protect the public, for example, setting as low as reasonably achievable (ALARA) levels, the threshold of toxicological concern (TTC) approach and the margin of exposure (MoE) approach. Conversely, these methods all have pros and cons and although they are easy to communicate, they often lack toxicological data and rationale (Schrenk, 2018).

1.4.1 Key characteristics of carcinogens (KCCs)

The KCC concept was proposed to identify common characteristics of carcinogenic chemicals (Smith *et al*., 2016). As already stated, the formation of cancer involves multiple steps including the initiation, promotion and progression of the process. Therefore, any of these processes can be altered by the two main types of carcinogens; genotoxic and NGCs. The DNA of cells can be damaged and can contain multiple mutations in one or more of the critical genes. NGCs can induce cancer through numerous different indirect mechanisms as stated in the KCCs such as immunosuppression, receptor mediation, endocrine modification (Hernández *et al*., 2009), oxidative stress, disruption of apoptosis, peroxisome proliferation and many more (Silva Lima and Van der Laan, 2000). NGCs are also able to utilize several MoA pathways at once, to elicit oncogenesis (van Delft *et al*., 2004). Predicting the carcinogenicity of NGCs is difficult due to the complexity and diversity of the MoAs used (Hernández *et al*., 2009). This highlights the need to employ an *in vitro* test battery to try to determine the MoAs of NGCs in order to detect and correctly classify these chemicals. The KCCs described in **Table 1.2** below, show how each

of the characteristics behave and give some examples of this. The majority of the characteristics are utilized by NGCs as well as GCs apart from characteristic 1 and 2. The KCCs, along with the hallmarks of cancer were considered when developing the *in vitro* test battery. Again, the KCCs also highlight the requirement for mechanistic understanding when evaluating carcinogens. Due to the variety of MoAs used by NGCs, multiple endpoint analysis is necessary.

Table 1.2: Detailing the 10 key characteristics of carcinogens (KCCs) including multiple examples of the characteristic. Abbreviations are listed at the bottom of the table. Taken directly from (Smith *et al*., 2016) with permission.

Characteristic	Examples of relevant evidence
1. Is electrophilic or can be metabolically activated	Parent compound or metabolite with an electrophilic structure (e.g., epoxide, quinone), formation of DNA and protein adducts
2. Is genotoxic	DNA damage (DNA strand breaks, DNA–protein cross-links, unscheduled DNA synthesis), intercalation, gene mutations, cytogenetic changes (e.g., chromosome aberrations, micronuclei)
3. Alters DNA repair or causes genomic instability	Alterations of DNA replication or repair (e.g., topoisomerase II, base-excision or double-strand break repair)
4. Induces epigenetic alterations	DNA methylation, histone modification, microRNA expression
5. Induces oxidative stress	Oxygen radicals, oxidative stress, oxidative damage to macromolecules (e.g., DNA, lipids)
6. Induces chronic inflammation	Elevated white blood cells, myeloperoxidase activity, altered cytokine and/or chemokine production
7. Is immunosuppressive	Decreased immunosurveillance, immune system dysfunction
8. Modulates receptor-mediated effects	Receptor in/activation (e.g., ER, PPAR, AhR) or modulation of endogenous ligands (including hormones)
9. Causes immortalization	Inhibition of senescence, cell transformation
10. Alters cell proliferation, cell death or nutrient supply	Increased proliferation, decreased apoptosis, changes in growth factors, energetics and signaling pathways related to cellular replication or cell cycle control, angiogenesis

Abbreviations: AhR, aryl hydrocarbon receptor; ER, estrogen receptor; PPAR, peroxisome proliferator–activated receptor. Any of the 10 characteristics in this table could interact with any other (e.g., oxidative stress, DNA damage, and chronic inflammation), which when combined provides stronger evidence for a cancer mechanism than would oxidative stress alone.

1.4.2 Genotoxic carcinogens

GCs were named following a large chemical screening initiative by the National Toxicology Programme (NTP) (Ashby and Tennant, 1988). Genotoxicity has an important toxicological link to cancer (Di Bucchiano *et al*., 2018) due to the mutation-cancer axis. Druckery, (1973) was an important figure and revised relationships between carcinogenicity, genotoxicity, mutagenicity, and teratogenicity. He also made progress into identifying NGCs due to the wording used in his definition of GCs (Ashby, 1995). He defined genotoxicity as "Any agent which, by virtue of its physical or chemical properties, can induce or produce heritable changes in those parts of the genetic apparatus that exercise homeostatic control over somatic cells, thereby determining their malignant transformation" (Ashby, 1995).

Most GCs are electrophilic and nucleophilic, so are capable of interacting with the DNA directly via covalent bonds causing DNA adduct formation which is a DNA-carcinogen complex (Lee *et al.,* 2013). These DNA adducts can cause several forms of DNA damage such as the removal of DNA bases (abasic sites), forming cross links between the helices, creating bonds between adjacent bases and cleaving DNA strands. These DNA adducts confuse DNA polymerase and mutations ensue after replication of adducted DNA bases. These mutations all modify the information held in the DNA (Lee *et al.,* 2013). The original DNA damage could be repaired by DNA repair mechanisms unless replication occurs before repair has taken place or unless there are problems with DNA repair machinery. If the mutations are not repaired they can go on to contribute to the formation of tumours (Lee *et al.,* 2013).

As GCs are capable of covalently binding to the DNA directly, this means that there is interference with the DNA helix structure or post activation via metabolizing enzymes. Due to the cellular DNA damage, p53 (tumour suppressor) is activated and in turn activates a number of cellular processes for example DNA repair, cell cycle arrest and apoptosis (Levine, 1997). The DNA damage caused by GCs, can lead to the initiation of sub-mechanisms such as apoptosis and cell cycle arrest (Ellinger-Ziegelbauer *et al*., 2004).

In genotoxicity assessment, there can be false positives generated *in vitro*, as chemicals that are not genotoxic can occasionally give positive results for genotoxicity tests. NGC chemicals can also induce some positive genotoxic responses even if the manner in which they cause cancer is not through genotoxicity (Walmsley and Billinton, 2011). This was another important factor to consider when designing the multi-component *in vitro* test battery. It highlights that genotoxicity assessment should still be carried out for NGCs. Even with GCs, a battery of *in vitro* and *in vivo* tests is required such as the COM tiered approach, when trying to detect all possible candidates to improve the prediction of genotoxicity (Cimino, 2006). If this is the case for GCs, then the multiple endpoint approach is definitely necessary when testing for NGCs as they are considered very complex and diverse in their MoAs.

1.4.3 Non-genotoxic carcinogens

As mentioned above, NGCs use secondary/indirect mechanisms, which do not involve direct DNA interactions, to cause cancer (Jacobs *et al*., 2016). NGCs are thought to cause tumours by increasing the risk of inducing genetic error and they can do this by altering the cellular proliferation rate and disturbing cellular organisation (Lee *et al*., 2013). The term ‘non-genotoxic carcinogen’ can be misunderstood as it can give the pretence that the chemical is

harmless to humans, though this is not the case (Hayashi, 1992). The MoA of NGCs may include complex regulations and interactions of chemicals and proteins. Some NGCs can indeed lead to indirect genotoxicity e.g. through downstream reactive oxygen species (ROS) induction, which can complicate characterisation (Hayashi, 1992).

There is a wide selection of mechanism(s) employed by NGCs in order to initiate oncogenesis such as gap junction intercellular communication (GJIC), tumour promotion and tissue-specific toxicity to name a few (Hernández *et al*., 2009). Some more of the mechanisms of action used by NGCs are displayed in **Figure 1.2**. Jacobs *et al*., (2016) has comprised a list of some of the main mechanisms utilized by NGCs with examples of some of the chemicals that employ these mechanisms. This was useful alongwith numerous other lists, when selecting the carcinogens to study in this work. **Figure 1.2** highlights some of the MoAs chosen to investigate within the multi-endpoint *in vitro* test battery. These endpoints include ROS, cell cycle, apoptosis, genotoxicity for example.

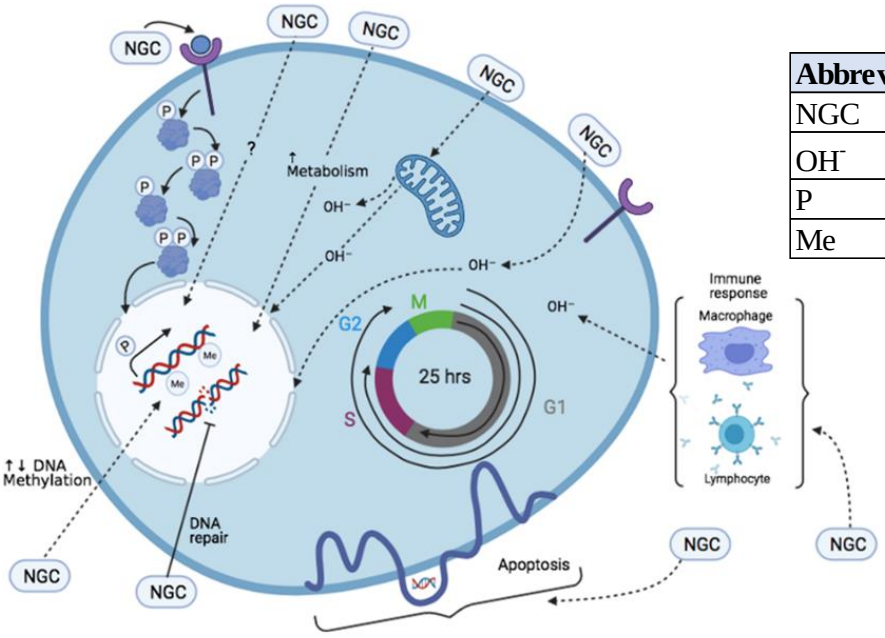

Key

Abbreviation	Description
NGC	Non genotoxic carcinogen
OH^-	Hydroxide
P	Phosphate
Me	Methyl

Figure 1.2: Demonstrates some of the mechanisms utilized by non-genotoxic carcinogens such as apoptosis, affecting cell cycle and inducing reactive oxygen species for instance. Figure was designed using biorender.com. The key denotes the abbreviations used within the diagram. The dotted arrows show potential routes of NGC action. The solid DNA repair line represents a route of inhibition. Solid arrows show processes that take place, such as cell cycle and phosphorylation. The apoptosis MoA is represented by a disrupted cellular membrane.

Chemical compounds undergo a screening process for numerous hazardous and carcinogenic properties using a series of *in vitro* and *in vivo* tests to classify them as shown in **Figure 1.3** (van Delft *et al*., 2004). The current testing system for NGCs is the 2-year rodent bioassay, which is expensive, labour intensive and time-consuming together with associated ethical concerns. More of an updated *in vitro* approach to predicting NGC's carcinogenic potential and MoA is required with these complex chemicals, in order to reduce the testing on animals and to save time and money. Methods such as gene expression profiling through toxicogenomics and computational models using quantitative structure-activity relationship (QSAR) (Tung and Jheng, 2014) show promise.

NGCs are of increasing concern as they are still largely misunderstood, and their hazards are also largely undetermined. Health-based guidance values are important in order to protect against the carcinogenic effects of NGCs and consequently protecting against cancer (Braakhuis *et al*., 2018). It is thought that if use of the 2-year rodent bioassay is restricted, then NGCs may be completely undetected unless a more modern alternative approach is taken (Hernández *et al*., 2009). Some examples of commonly studied NGCs include 2,3,7,8-tetrachlorodibenzodioxin (TCDD); dichlorodiphenyltrichloroethane (DDT) and cyclosporine (Hernández *et al*., 2009). Due to the potency of a number of these chemicals, there is increasing requirements to develop an accurate *in vitro* testing system to detect them.

Hormesis is defined as a dose response in which there is evidence of a biological activation at a specified dose. This could be activation at high doses but not low or more characteristically activation at low doses but not high. Hormesis can result in a J-shape, U-shape or an inverted U-shape curve (Calabrese, 2002). There is substantial evidence for hormesis and biphasic dose responses with NGC treatment especially with *in vivo* studies (Fukushima *et al*., 2005). Hormesis or also known as a biphasic dose response tends to exert the opposite effect than what is expected. Hormesis also means that threshold dose levels exist (Kinoshita *et al*., 2006). It also means that NGCs that cause hormesis are trying to maintain homeostasis as a result of adaptive responses such as DNA damage and repair, cellular proliferation and apoptosis to name a few (Kinoshita *et al*., 2006).

Understanding NGCs, despite their complex mechanisms and unpredictable nature is the main aim of this work. NGCs are known for behaving unusually and occasionally going against expected test results, meaning they could slip through the net in terms of safety testing. If an *in vitro* detection system was proposed for these carcinogens then this would be a novel step

forward towards understanding these carcinogens and also reducing the numbers of animals used in their testing.

1.5 Regulatory testing

Current regulatory testing requirements include a genotoxicity testing battery which means that positive results in the *in vitro* genotoxicity tests lead to *in vivo* genotoxicity tests. This can then lead to more mammalian *in vivo* genotoxicity testing and occasionally the gold standard 2-year rodent bioassay is carried out. Bridges (1974;1976;1984) had a significant impact on the regulatory testing approaches by pioneering the three-tier screening system. A lot of the regulatory testing carried out still use these three-tiered approaches for GCs (Ashby, 1986), highlighting the need of a tiered testing approach for NGCs. The existing *in vitro* genotoxicity testing battery consists of the Ames test, mouse lymphoma assay (MLA) and either the *in vitro* Mn or CA (Kirkland *et al*., 2005). The up-to-date battery requires further thought as NGCs seem to be left behind as they are not detected in this way. The flow charts in **Figure 1.3** are useful to understand how the decisions are made based on the classification of chemicals by the Committee on Mutagenicity (COM). It is evident that NGCs require a separate detection approach, and it would be beneficial if there was a similar strategy in place for NGCs.

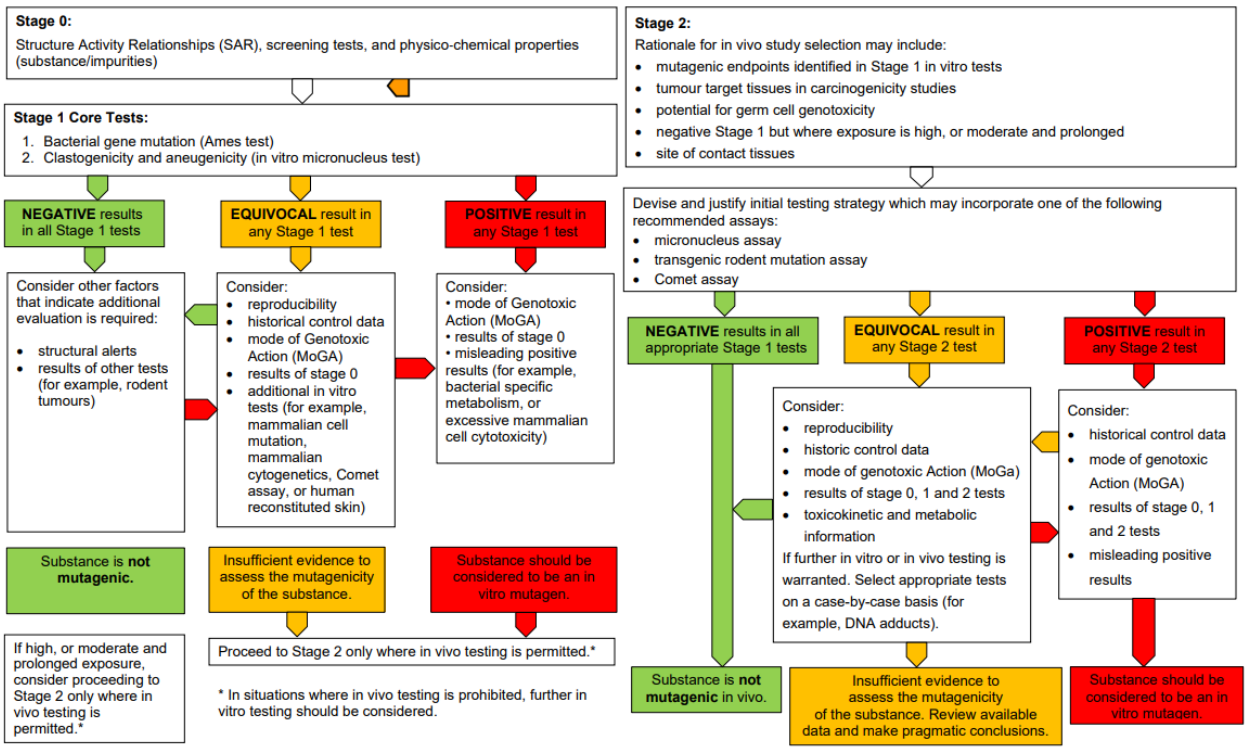

Figure 1.3: A flow chart representing the strategy for testing of chemicals for genotoxicity (both *in vitro and in vivo*) taken from the Committee on Mutagenicity (COM) of Chemicals in Food, Consumer Products and the Environment 2021 with permission.

As mentioned, GCs have a specific strategy for detection, but no similar approach exists for NGCs. Therefore, this work focuses on trying to create a comparable strategy for NGCs. The 2-year rodent bioassay is capable of detecting NGCs, although not all chemicals are subject to this test and there are a number of limitations with this assay (Jacobs *et al*., 2016). There are numerous problems with the current long-term rodent studies, where the chemicals tested often have to use high doses for extended periods before observing carcinogenic effects. The results of these rodent bioassays are often not useful as the effects can be species and organ specific. The current testing strategies for NGCs are not adequate due to the lack of relevance of rodent studies when translating to humans (Holmes and Rainsford, 2001).

The NTP estimates that each 2-year rodent bioassay requires 860 animals to be killed, costs about $2-4 million dollars and takes 5 years to plan and conduct the experiment and analysis, meaning that limiting this assay is of great interest (Manuppello and Willett, 2008). There are various ethical issues with the rodent bioassay and animals suffer during the process. They live in stressful conditions within the laboratory and are subject to force feeding, inhalation or injections of certain chemicals (Manuppello and Willett, 2008). If an *in vitro* testing battery can at least compliment the 2-year bioassay, hopefully this would mean that the numbers of animals used can be reduced, as we are not yet at the stage of completely replacing the assay

unfortunately. High throughput *in vitro* methods, toxicogenomics and computational methods are also required as a complete replacement.

Pharmaceuticals have to undergo the 2-year bioassay as part of their regulatory requirements, however human clinical trial data is of the greatest importance. More recently, other chemicals such as agricultural or food additives have been subject to the bioassay on a case-by-case basis (Marone *et al*., 2014). A sub-chronic toxicity study is usually carried out for 90 days (3 months) (Rhiaouani *et al*., 2008) which is considerably shorter than the gold-standard 2-year rodent bioassay. There does not seem to be much additional benefit by conducting the 2-year assay over the 90-sub chronic study (Braahuis *et al*., 2018). There are numerous questions around the use of the 2-year bioassay. Although it is a useful tool to test for carcinogenicity, it can identify rodent only carcinogens, predicting that the chemical is possibly carcinogenic to humans but could also represent a false positive (Suarez-Torres *et al*., 2021).

There is a great requirement of a reliable NGC *in vitro* testing system comprised of distinct end points. This would significantly reduce the need for animal testing, reduce financial costs and improve the accuracy of data using human cells submitted to regulatory authorities (Holmes and Rainsford, 2001). In agreement with the 3R's principles, there has been a reduction of animal testing as standard requirements under Registration, Evaluation, Authorization and Restriction of Chemicals (REACH) regulations (EC, 2008). In 2022, it was reported that there has been a 10% decrease in the number of procedures involving living animals (Home office, 2023). This makes 2.76 million, the total of scientific procedures carried out in the UK, which is the lowest in around 2 decades (Home office, 2023). The updated regulation states that a rodent carcinogenicity study should only be conducted if there are concerns with a chemical. New carcinogenicity studies are rarely performed since this testing restriction was put in place (Jacobs *et al*., 2016). Although protecting the animals, this still leaves questions around numerous chemicals.

About 12% of carcinogens classified by International Agency for Research on Cancer (IARC) into Group 1, 2A and 2B carcinogens are thought to be non-genotoxic (Hernández *et al*., 2009). As previously stated, NGCs are currently tested for and detected using the *in vivo* two-year rodent bioassay. However, the *in vitro* cell transformation assays (CTAs) also attempt to mimic the *in vivo* processes better so have been recommended to detect NGCs (Meyer, 1983). However, these CTAs are not strictly *in vitro* assays so do not comply with the 3R's principles as hamster embryo cells are often harvested and grown. CTAs utilising Bhas 42 cells have been

validated due to their ability to detect promoter activity without the need for treatment with initiators (Hayashi *et al*., 2012) and are therefore included in The Organisation for Economic Cooperation and Development (OECD) guidelines (OECD, 2016b). The Bhas 42 cell line was established as a result of the BALB/c 3T3 cells being transfected with a Harvey rat sarcoma viral mutated oncogene called v-Ha-ras. The Bhas 42 CTA aims to detect the carcinogenic potential of carcinogens (European commission, 2012). The Syrian hamster embryo (SHE) assay is another example of a CTA. It has a high specificity and sensitivity for carcinogenic testing. The SHE cells are genetically stable, have metabolic competency and are capable of detecting both GCs and NGCs. However, it is time consuming, strenuous and the scoring can be subjective (Ahmadzai *et al*., 2011).

1.6 The *in vitro* test battery used in this work

The test battery was defined as a result of a large literature search in order to gain information based on the complex mechanism(s) of action utilized by NGCs. It has been previously suggested that a multiple endpoint approach is most beneficial when trying to understand NGCs (Wilde *et al.,* 2017; Chapman *et al.,* 2021). It is comprised of a series of *in vitro* tests targeting different mechanisms of carcinogenesis such as genotoxicity, cytotoxicity, ROS, cell cycle, apoptosis, gene expression and mitochondrial health. Although this test battery is only comprised of 7 endpoints, other methods could also be included if this battery proves successful, such as toxicogenomic analysis. It has been shown that mechanistic information is of increasing importance when trying to understand carcinogens. Below are outlines of the 7 endpoints included in the test battery.

The hallmarks of cancer are the key influence behind the rationale for the endpoints chosen within this *in vitro* test battery. As shown in **Figure 1.4**, the circled hallmarks all link to the endpoints in the test battery. Four out of the six original hallmarks are important and six out of the updated hallmarks were used to build the test battery. Certain hallmarks are very difficult to model *in vitro* such as angiogenesis, so there was not a specific endpoint dedicated to this. However some angiogenesis genes had altered expression in the polymerase chain reaction (PCR) array. Evading growth suppressors was modelled using cell cycle analysis, resisting cell death was investigated using the apoptosis assay and enabling replicative immortality was probed using relative population doubling (RPD) to understand any cytotoxic effects and understand cellular proliferation. Sustaining proliferative signalling refers to gene expression changes which were explored with the PCR array, deregulating cellular metabolism was studied

with Seahorse analysis and genome instability and mutation was considered using both genotoxicity analysis through Mn and ROS analysis using the dichlorodihydrofluorescein diacetate (DCFDA) assay. Although this was a proposed battery for NGCs, genotoxicity assessment was still an important component of the *in vitro* test battery.

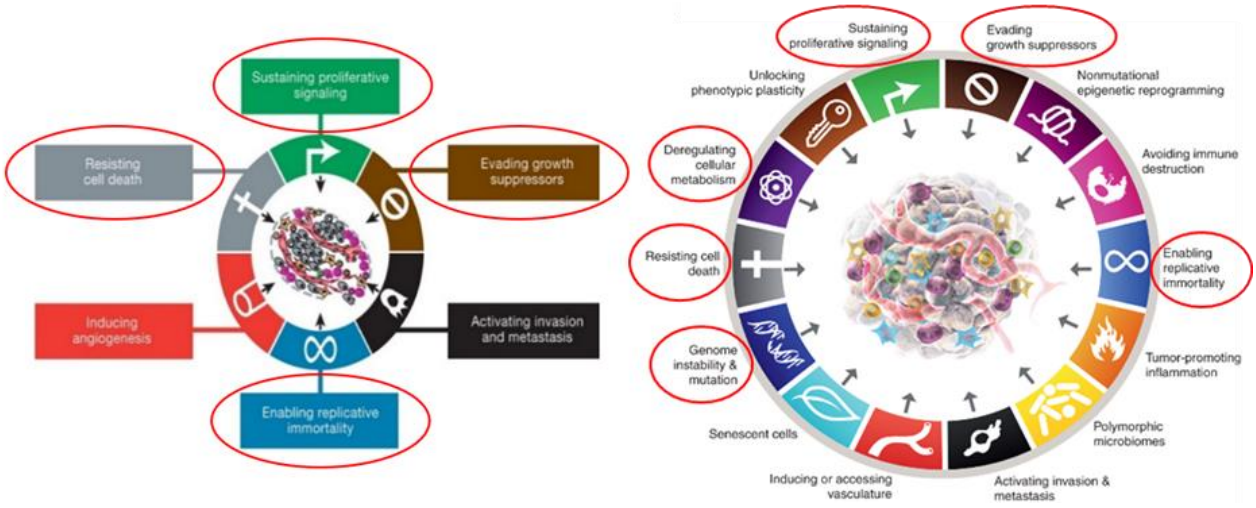

Figure 1.4: An adaptation of Figure 1.1 (a and b) to highlight the rationale for the endpoints chosen in this work. The red circles in the diagram represent the hallmarks of cancer targeted by the *in vitro* test battery.

1.6.1 Micronucleus assay (genotoxicity assessment)

Micronuclei are defined as a small extra nuclear body, present in interphase cells as a result of a broken chromosome (clastogenic) or a whole chromosome lag (aneugenic), left behind during cellular division and not combined into the main nucleus (Seager *et al*., 2014). The Mn assay has been utilized for over 40 years (Sommer *et al*., 2020). W Schmid first introduced the Mn assay in 1976, explaining what a Mn is and how they form, mentioning both clastogenic and aneugenic mechanisms (Schmid, 1976). The development of the cytokinesis-block Mn assay involves the addition of cytochalasin B (cytoB), an actin polymerisation inhibitor that targets mitosis. This method allows the identification of nuclei that have undergone one cellular division and therefore forming binucleated (BN) cells. Therefore, the micronuclei present in these BN cells develop as a result of the test chemical (Fenech and Morley, 1986). The most commonly used methodology in genotoxicity testing is the cytokinesis block micronucleus assay (CBMN) (Fenech and Morley, 1985). The most reliable way to determine Mn frequency is to score the Mn in BN cells (Fenech, 2000). This method allows the discrimination of cells that completed

division once, more than once or not at all producing BN cells, multinucleated cells and mononucleated cells respectively (Kirsch-Volders and Fenech, 2001).

NGCs could benefit from Mn assessment to determine any genotoxicity that is present as they can utilize a number of mechanisms and do not have a unifying characteristic (Hernández *et al*., 2009). Also, NGCs can be detected using the 2-year rodent bioassay (Hernández *et al*., 2009), so it was thought that chronic dosing would more closely mimic this and may pick up any indirect genotoxicity.

A lot of evidence suggests that traditional Mn scoring is very tedious, time consuming and subjective, meaning the results are not consistent (Lukamowicz *et al*., 2011). The semi-automated metafer system proposes numerous advantages over the conventional scoring method such as reduced subjectivity and labour and an increased scoring output and statistical power (Seager *et al*., 2014). Micronuclei are a well-accepted biomarker of chromosomal damage (Fenech, 1993).

1.6.2 Mononucleated micronucleus assay

In this work, the mononucleated version of the Mn assay is used, although it is less common and has less power, it is advantageous when comparing acute and chronic data. If cytoB was utilized in the chronic exposure work, only the micronuclei produced after the addition of this chemical would be scored (counted), which does not account for any build-up of genotoxicity. There would also be an underestimation of micronuclei counted so there would be a misinterpretation of the results. Despite this, numerous studies have reported a significant induction of Mn when using the mononucleate version of the Mn assay highlighting it as an advantageous approach (Hasimoto *et al*., 2011; Lorge, 2010; Elhajouji, 2010).Micronuclei present in mononuclear cells give an approximation of the genome instability accumulated over an extended period, whereas micronuclei in binuclear cells give an understanding of the immediate effect of an exposure (Kirsch-Volders and Fenech, 2001). When it comes to evaluating mononucleated Mn, the exposure time is most important (Kirsch-Volders and Fenech, 2001). The micronuclei scoring criteria has been documented in Fenech, (2007), highlighting when to count a micronucleus based on its appearance. This criterion includes size and staining intensity of the Mn (Fenech, 2007).

It has often been shown that evaluating mononucleated Mn as well as BN Mn is useful in the detection of aneugens (Clare *et al*., 2006). There is an underestimation of micronuclei frequencies in mononucleated cells which is due to the cells being scored whether they have

divided or not (Channarayappa *et al*., 1990). However, in order to allow for the comparison of acute and chronic Mn exposures the mononucleate version of the assay was utilized (Dural *et al*., 2021). As stated above, it has been shown that the mononucleated version of Mn assay is less sensitive than the CBMN (Chapman *et al*., 2014). This is largely due to the fact that cells in cell cycle arrest, senescent cells and pre-apoptotic cells would not have undergone nuclear division and will not contain micronuclei (Fenech, 2000).

Another study also compared both acute and chronic treatments with genotoxic and NGCs and utilized the *in vitro* Mn assay without the addition of cytoB (Jossé *et al*., 2012). This study used HepaRG cells and investigated mononucleated micronuclei which is in agreement with the work in this PhD.

It has been mentioned in the OECD 487 test guideline that TK6 cells can be used for the genotoxicity assessment using the *in vitro* Mn assay of test chemicals (Lorge *et al*., 2006). As MCL5 cells are a derivative cell line of TK6 cells it also confirms their use in genotoxicity tests where metabolic activation is required (Yamakage *et al*., 1998).

The mononucleated Mn can be visualised in **Figure 1.5** below, which are checked against the scoring criteria using the semi-automated Metafer4 system. The Metafer system was used to score mononucleated micronuclei using a specific classifier to detect cells bearing a Mn. The slide is scanned using the x10 objective lens and picks up the cells both with and without micronuclei (Chapman *et al*., 2014). A greater cell number can be scored using this system as 2000 cells are required per dose for BN cells, 4000 cells can be scored for mononucleate cells. Gallery images display the mononucleated cells seen in **Figure 1.5**, which can be detected and can be checked using the microscope for final confirmation, making this method semi-automated (Chapman *et al*., 2014).

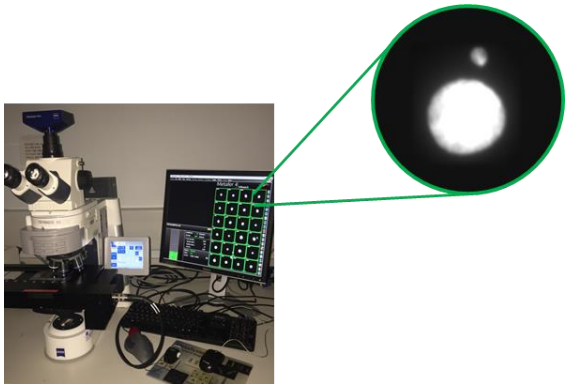

Figure 1.5: The semi-automated Metafer4 system showing an enlarged image of a mononucleated cell with a Mn.

4′,6-diamidino-2-phenylindole, more commonly known as DAPI, is a DNA stain often used in microscopy, chromosome staining and in flow cytometry. It has a great affinity for the AT regions of double stranded DNA. DAPI is usually used in staining cells that are fixed as the dye is impermeable to the cell membranes unless used at high concentrations (Thermofisher, 2023). During the preparation of slides for analysis on the metafer, the cells are fixed in a number of steps (detailed in the main methods **section 2.4.3**) which permeabilises the cell membrane. This allows the nucleus and any micronuclei to be stained (**Figure 1.5**). However, this can cause some subjectivity as the cell membrane is not visible so the micronuclei needs to be close enough to the main nucleus in order to be counted. This is kept as constant as possible in order to ensure data integrity.

Acute and chronic dosing

Acute dosing of chemicals is a single exposure of between 6 and 72 hours. Although traditional acute toxicity is an important aspect of regulatory toxicity, it does not take into account accumulative toxicity (Macko *et al*., 2021). Acute and chronic dosing can produce completely different results, hence the investigation of a chronic dosing system and comparing this with an acute dosing system in this work. Chronic dosing could lead to a bioaccumulation and therefore cause metabolic saturation and potentially overwhelming the system with toxicity (Wills *et al*., 2017).

Chronic dosing

Chronic dosing more closely mimics a real-life exposure, so is more relevant than a one-off spiked dose. It has been shown that chronic dosing can reduce cytotoxicity and genotoxicity with a chronic system (Dural *et al*., 2020). This could be due to a better tolerance of the chemical in a chronic system as cell resilience factors including DNA repair can take place (Dural *et al*., 2020). It is thought that cells can overcome the doses delivered in low-dose chronic dosing which can make the cells more resilient as cell death was not activated. This cell resilience can be modelled by gene expression changes or epigenetic modulations for example (Smirnova *et al*., 2015).

Mechanistic studies conducted on NGCs show that chronic exposure means there is extensive interference with homeostasis (Silva and Van der Laan, 2000). Some NGCs are capable of inducing increased hormone levels which causes increased cell proliferation, therefore contributing to tumour promotion (Benigni *et al*., 2013). It has also been stated that if the dose is

low enough, then hormonal imbalances will not occur therefore not causing carcinogenesis. This is the same principle for other NGC mechanisms (Braakhuis *et al*., 2018).

Acute dosing

Acute toxicity is very important to identify the toxicity of cells or target organs, to offer information regarding the dose selection for long-term studies and to design a testing program. Toxicity testing is also vital order to allow the classification, labelling and transportation of different chemicals (Arome and Chinedu, 2013). However, it is also thought that there can be an over-estimate of genotoxicity as a result of an acute test system as the cellular defences can be overwhelmed (Dural *et al*., 2020). The 24-hour spiked dose is the gold standard in most toxicity testing as a first step which is outlined in the OECD guidelines.

Acute testing has been questioned as common human exposures are mostly chronic in nature (Swenberg *et al*., 1987). *In vitro* toxicity testing is still dominated by high dose acute treatments (Blakey *et al*., 2008). Therefore, chronic dosing requires more of a focus and further investigation as it is not widely studied in the literature (Chapman *et al*., 2015).

1.6.3 Relative population doubling

RPD is fully documented in the OECD guidelines as test no. 487 (OECD, 2016a). RPD is a measure of cell viability and therefore cytotoxicity and is capable of detecting both cell death and cytostasis. Using RPD we can study both effects on cell proliferation and effects on cell viability. It is important for the Mn assay to understand whether the cells in culture have undergone cellular division post chemical treatment. It has been shown that RPD can be used when cytoB has not been used in the assay (Fowler *et al*., 2010). RPD was conducted here alongside the Mn assay in order to calculate cytotoxicity. However, cell counts were also carried out alongside numerous other endpoints as it was an easy way to monitor cellular proliferation and if there were any problems with the cell counts the experiment could not go ahead. The accepted guideline for cytotoxicity parameters for RPD is that the maximum is 55% ± 5% cytotoxicity induction (OECD, 2016a). Cytotoxicity higher than this level could lead to false positives as a result of chromosome damage (Lukamowicz *et al*., 2011).

1.6.4 Reactive oxygen species (ROS)

Maintaining cellular homeostasis is extremely important to the normal functioning of cells and all cellular functions require energy to take place. Mitochondria produce most of the energy to support the life of the cell, however as a consequence of this energy production, ROS are also produced (Murphy, 2009). ROS are initiated as a result of two main processes: they can originate

as a reaction to xenobiotics or cytokines due to cellular defence procedures or released during mitochondrial respiration as a waste product of oxidative metabolism (Finkel, 2011). The DCFDA assay is the most popular method of ROS detection (Szychowski *et al*., 2016). The ROS assay was conducted here in conjunction with an omega plate reader as seen in **Figure 1.6** below.

Figure 1.6: Demonstrates the omega plate reader (right) and output on the connected computer screen (left). The computer screen is displaying the real-time output of the DCFDA assay at a singular time point. The data can be exported from the omega software to Microsoft Excel for analysis.

Microplate assays are beneficial for a number of reasons including their affordability, high throughput results and the optimisation and analysis time (Ng and Ooi, 2021). The DCFDA assay is comprised of a non-fluorescent origin probe capable of detecting oxidative stress. DCFHDA is a cell permeable molecule, which then cleaves to produce H_2DCF which accumulates and oxidation then yields the fluorescent dichlorodihydrofluorescein (DCF) product (Eruslanov and Kusmartsev, 2010). The DCF fluorescence can be measured at numerous time points using a plate reader. ROS are known for being short- lived, extremely reactive and fast acting molecules which can be generated almost immediately after exposure (Figueroa *et al*., 2018).

1.6.5 Cell cycle dysregulation

The cell cycle is comprised of four phases, two gap phases (G1 and G2), a synthesis phase (S) and a mitosis/meiosis (M). If a full cell cycle has been completed then two daughter cells are the result. G1 phase is where the cell grows in size and the genes that control cell cycle, cyclins are transcribed and translated. A series of checkpoints are carried out before the cell progresses into S phase and once in S phase, a copy is made of the entire genome through DNA polymerase. In G2 phase, the cell is first checked for any errors and to make sure the size is correct before organising the cell ready for division. Then in M phase, the actual division takes place; the nuclear envelope disperses, the chromatin condenses in order for the cell to split into two

daughter cells with their own nuclei. After the full cell cycle, cells can either remain dormant in G0 or re-enter the cell cycle in order to divide again (Nurse *et al*., 1998).

There are many ways in which the cell cycle distribution of a cell population can be assessed. The method utilized in this work included fixing the cells with ethanol and then propidium iodide (PI) was used to stain the cellular DNA content, revealing the distribution of cells in G1, S and G2 cell cycle phases after flow cytometry which assessed cell and nuclear size. This method is described as a single time point measurement (Pozarowski and Darzynkiewicz, 2004). As PI is also capable of staining double stranded ribonucleic acid (RNA), it is removed using RNase alongside PI in the protocol (Pozarowski and Darzynkiewicz, 2004). The cells were then sorted into the different cell cycle stages depending on the proportion of DNA using the Novocyte flow cytometer as seen in **Figure 1.7a**. **Figure 1.7b** represents the gating of cells for cell cycle analysis. This is done as initial gating for live cells, then gating for single cells (both done during the experiment). Finally the single cells are used to produce a histogram against PE-Texas Red which is performed using FlowJ and carried out during the analysis. Gating for G1, S and G2 are performed manually by keeping the criteria consistent with each experiment. In **Figure 1.7b** the screen is divided into 4 sections, the first section represents the live cell gating, the second section represents the single cell gating and the fourth section represents the gated single cell population. Section 3 could contain a histogram template, however within this work it was found that manual gating was more accurate, so the template was not used.

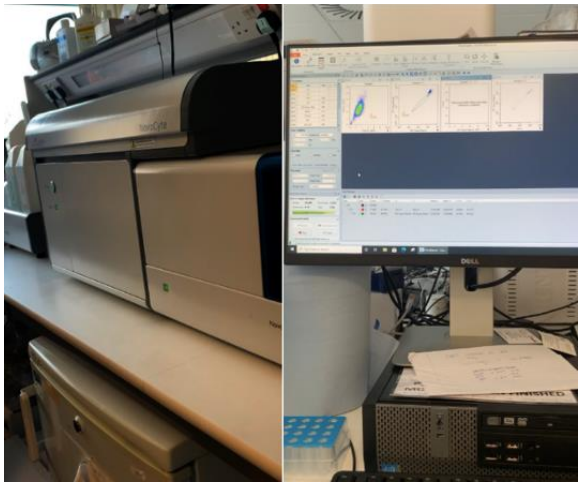

A

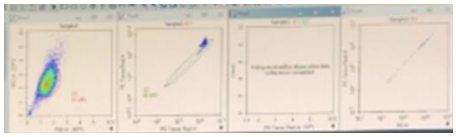

B

Figure 1.7 (a and b): Figure 1.7a shows the Novocyte flow cytometer (left) is imaged alongside the connected computer (right), collecting the cell cycle data. The data can be exported as Flow Cytometry Standard (FCS) files for analysis. **Figure 1.7b** is a close-up of how the cells are gated for cell cycle analysis.

The lowest level of PI intensity represents the cells in the G1 phase, the cells in S phase have more PI intensity than those in G1 and the highest PI intensity, approx. double that in G1, represents the cells in the G2 phase (Blasi *et al*., 2016).

1.6.6 Apoptosis

Apoptosis is a form of regulated cell death and is an important feature in maintaining homeostasis and cellular development. It is characterised by morphological changes such as nuclear fragmentation, cell shrinkage and chromatin condensation (Dong *et al*., 2009). Apoptosis is a tightly controlled cellular process and any failure in the course of this event can result in numerous pathological conditions including cancer, neurodegeneration and autoimmune diseases (Fadeel and Orrenius, 2005).

Phosphatidylserine (PS) is usually located on the internal surface of the plasma membrane within the cytoplasm (Dong *et al*., 2009). However, during apoptosis the PS is externalised and this process is seen with numerous cell types (Rimon *et al*., 1997). Annexin V has a high binding affinity for PS (Tait *et al*., 1989) and is used alongside a membrane impermeable DNA stain. 7-amino-actinomycin D (7-AAD) when used in conjunction with annexin V, can discriminate between live, early and late apoptotic and necrotic cells (Rimon *et al*., 1997). The grid with the 4 different quartiles represents the 4 stages of live and dead cells, seen in **Figure 1.8 (a and b)**. Q1 represents necrotic cells, Q2 which has a small cluster represents late apoptosis, Q3 represents live cells and has the largest proportion of cells in that quartile and finally Q4 represents early apoptosis and there are some cells transitioning in this quartile.

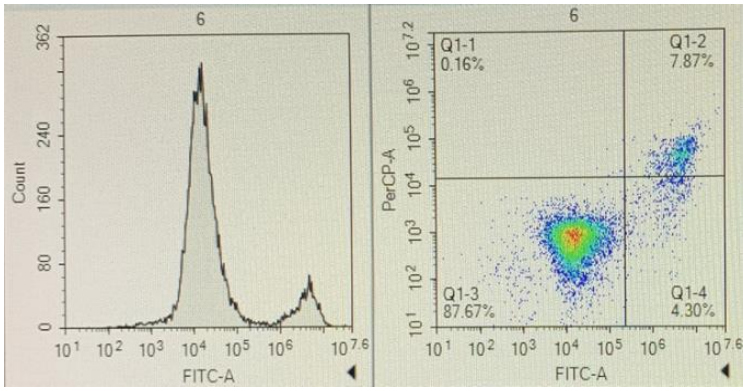

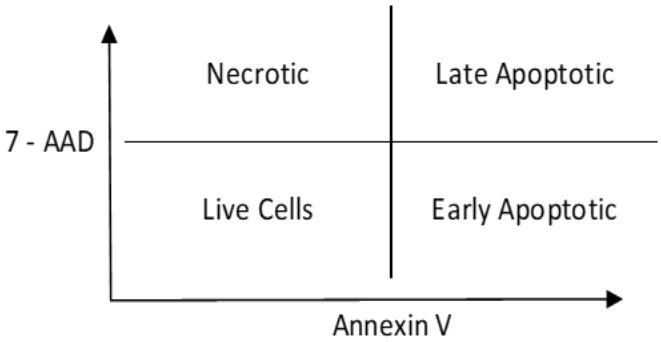

1.8a **1.8b**

Figure 1.8 (a and b): An example output read from the Novocyte flow cytometer collecting apoptosis data (**Figure 1.8a**). The cells appear within each of the 4 quartiles representing live cells (Q3), early apoptotic (Q4), late apoptotic (Q2) and necrotic cells (Q1). The 4 quartiles seen in **Figure 1.8a** are explained in **Figure 1.8b.** This diagram represents the sections where the cells should appear after apoptosis analysis.

1.6.7 Gene expression changes

Toxicogenomics has been shown to be useful in identifying carcinogenic modes of action. PCR arrays are a quantitative, accurate and a reliable tool to investigate a panel of target genes commonly linked to cancer pathways or the disease state (Alvarez and Doné, 2014). PCR arrays have been used in high-throughput gene profiling and are cost effective when compared to RNA-seq methodologies (Veselenak *et al*., 2015). GCs and NGCs use largely different sub-mechanisms to induce carcinogenesis and so gene expression methods are favoured (Lee *et al*., 2013).

Gene expression was investigated using predefined cancer gene panel arrays, comprised of genes commonly altered in cancer. Some of the equipment used to perform the PCR array such as the thermocycler and the quantitative PCR (qPCR) machine can be seen in **Figure 1.9.** In order to identify some of the pathways significantly altered as a result of NGC treatment, PCR arrays are very useful. It allows for functional pathway analysis and further follow up investigation using qPCR. Some studies have used gene profiling to map specific mechanistic pathways of carcinogens (Lee *et al*., 2013). This would be a useful tool to see whether the mechanistic studies conducted in the test battery confirm what is seen in the gene profiles.

Similar to other PCR arrays, it comprises of a number of different cancer genes, a positive PCR control, a DNA contamination control, RNA quality controls and a reverse transcription (RT) control (Nacif-Pimenta *et al*., 2019). The up and down regulation of different genes can provide some insight into the mechanism(s) utilized by the individual NGC. The up/downregulated ± 2-fold difference represents the biologically significant genes. PCR arrays are very useful tools, to provide an indication of the mechanism(s) of action utilized by the chemical, which has proven very important for the *in vitro* test battery to detect NGCs.

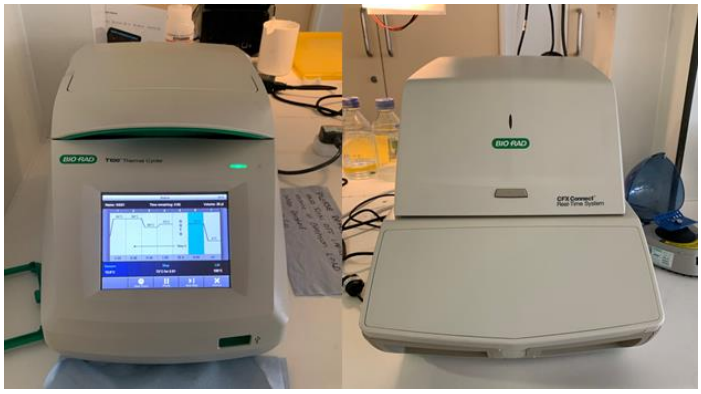

Figure 1.9: The thermocycler (left) and the qPCR machine (right), both used to perform the PCR array of a general panel of cancer genes.

1.6.8 Mitochondrial function

The Seahorse mito stress test is considered the gold standard assay for mitochondrial function. This assay is useful to understand mitochondrial dysfunction and provides an insight into the metabolic pathway used as a result of the bioenergetic trace. Mitochondrial health and function assessment has allowed further understanding of metabolism's role in different diseases, including cancer (Agilent, 2023a).

Mitochondria control several cellular processes such as controlling redox homeostasis, apoptosis and oncogenic signalling. This means that mitochondria play a pivotal role in tumourigenesis and are often targeted in therapy (Zong *et al*., 2016). The importance of mitochondrial function has been documented in numerous diseases, for example the energy generated by mitochondria can impact the effectiveness of immune responses (Nicholas *et al*., 2017). An advantage of extracellular flux (XF) analysis is that numerous outputs can result from one experiment. Only a small number of cells are required to measure the oxygen consumption rate (OCR) per well (Nicholas *et al*., 2017). A test compound is administered prior to 3 serial injections of the modulators: oligomycin, (carbonyl cyanide-p-trifluoromethoxy) phenylhydrazone (FCCP) and rotenone/antimycin A, which together indicate the OCR and therefore the mitochondrial function (Agilent, 2023a). **Figure 1.10** demonstrates an example output from the Seahorse XF analyser, showing an overall picture of the water-soluble compounds investigated and how they compare to each other.

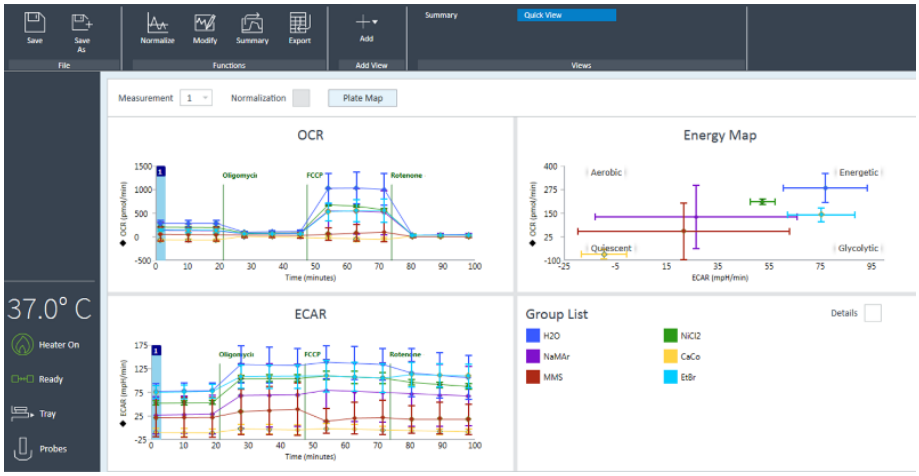

Figure 1.10: An output from the Seahorse extracellular flux (XF) analyser displaying the oxygen consumption rate (OCR), extracellular acidification rate (ECAR) and an energy map comparison of the water-soluble chemicals.

1.7 Chemical selection

A comprehensive literature search was conducted early in this study, reviewing numerous lists of NGCs in order to select the chemicals to assess (Kirkland *et al*., 2016; Hernández *et al*., 2009; Vinken *et al*., 2008; Hwang *et al*., 2020). The chemicals chosen for investigation here were selected on the basis of having varied and interesting mechanisms of action, useful when trying to design an *in vitro* test battery.

The NGCs picked for assessment were: nickel chloride ($NiCl_2$); sodium meta arsenite (NaMAr); rosuvastatin; chloroprene and 2,3,7,8-tetrachlorodibenzo-p-dioxin (TCDD). Cacodylic acid (Caco) was also assessed, although not an NGC but actually a GC, it was selected on the basis that it formed a contrast to the other NGC As compound, NaMAr. Two more chemicals were chosen; cholic acid and diethanolamine (DEA). However, these NGCs had to be discounted due to problems with dissolution and precipitation but preliminary data for these can be found in the Appendix (**Appendices Figures A1, A2 and A3)**. The selected carcinogens were also included as they each have a different purpose and impact, some being occupational hazards, some being drugs and environmental contaminants etc. More information on each of the chemicals and the negative and positive controls can be found in the main methods and the respective chapters.

Six chemicals in total were taken forward to study in this work, five NGCs and one GC, these can be seen in **Table 1.3.** There was varied rationale behind choosing each of the NGCs studied. This included varied MoAs, interesting chemicals and some historical NGCs as explained above. Cacodylic acid is a GC, which was chosen in order to form a comparison with NaMAr as the two types of arsenic.

Table 1.3: Literature classifications of the chemicals chosen to study detailing the rationale for the classification of each chemical as an NGC.

Chemical	**NGC classification**
Nickel chloride	(Hernández *et al*., 2009)
Sodium meta arsenite	(Vinken *et al*., 2008)
Rosuvastatin	(Kirkland *et al*., 2016; Hwang *et al*., 2020)
Chloroprene	(Vinken *et al*., 2008)
2,3,7,8-tetrachlorodibenzo-*p*-dioxin (TCDD)	(Hernández *et al*., 2009; Vinken *et al*., 2008; Hwang *et al*., 2020)
Cholic acid	(Hwang *et al*., 2020)
Diethanolamine	(Hwang *et al*., 2020)
Cacodylic acid (GC)	N/A

1.8 3Rs goals

The funder for this work was the NC3Rs, the national centre for the Replacement, Refinement and Reduction of animals in research. These principles were developed by Russel and Burch, (1959) in order to encourage more ethical practices when working with animals. The NC3Rs are a national organisation that focus on the scientific benefits of re-defining and updating the framework of the original 3Rs (NC3Rs, 2022).

Replacement describes practices that completely avoid the use of animals or directly replace the use of animals where they would have been used. Full replacement concerns non-animal technologies such as the use of cell lines or computational models for example. It can also include any updated scientific methods such as new approach methodologies (NAMs). Partial replacement includes using animals that are not thought to suffer such as *Drosophila* and nematodes. Reduction means minimising the number of animals used in each study to ensure there is not an over estimation of animals used unnecessarily. This includes any acceptable repeat sampling from an individual animal and the sharing of data and resources between research groups to minimise waste. Refinement indicates any method that could minimise the suffering, distress or pain of the research animals in order to improve their welfare. It can include improvements in their housing and any procedures performed. Some examples are minimising pain by utilising pain relief such as anaesthesia and training animals to cooperate with certain procedures in order to minimise their distress. It has also been demonstrated that suffering and stress can affect the results of the experiment (NC3Rs, 2022).

Recently there has been a lot of focus on whether it is possible to no longer use the 2-year rodent bioassay as it is not providing robust data for human carcinogenicity assessment (Goodman, 2018). The current gold standard test for NGCs is the 2-year rodent bioassay (Cohen *et al*., 2001). There are a number of motivations to use human relevant *in vitro* and *in silico* testing strategies such as for ethical reasons, financial reasons and to improve scientific quality. There are vast improvements in the animal alternative approaches and they are continuously being developed, validated and improved (Groff *et al*., 2021). A poll showed that a high proportion of the population, 44% of adults did not agree with testing on animals (Jones, 2017). In 2013, animal testing for cosmetics purposes was banned. Instead, there has been a lot of focus on animal alternatives and New Approach Methodologies (NAMa) (Silva and Tamburic, 2022). Rodent studies are very time consuming as well as costly, there are extra costs associated with

the care and breeding of the animals. These studies also lack physiological relevance when translating the data to humans and are not very reproducible (Luechtefeld *et al*., 2016).

Within this PhD, the work was conducted entirely *in vitro* and with the aim to introduce an *in vitro* testing battery for NGCs in order to reduce the number of animals used in the current 2-year rodent bioassay.

1.9 Cells lines

1.9.1 TK6 cells

TK6 cells are a human lymphoblastoid cell line, established from the WI-L2 parent cell line, originally derived from a 5-year-old male with hereditary spherocytosis (Lorge *et al*., 2016). TK6 cells are a suspension cell line, extensively used in *in vitro* genotoxicity testing due to the expression of the p53 protein, which is encoded by the *TP53* gene in humans (Kirkland *et al*., 2007). Some of the *in vitro* genotoxicity testing carried out in the TK6 cell line are the chromosomal aberration assay and the Mn (Li *et al*., 2020). Fowler *et al*., (2014) has shown that genotoxicity test results in TK6 cells gave analogous results to primary human lymphocytes, unlike rodent and liver cell lines. These cells were used for all chemicals bar one as most chemicals did not require metabolic activation and TK6 cells were suitable. TK6 cells doubling time is 16 hours to 18 hours (Brüsehafer *et al*., 2015).

1.9.2 MCL5 cells

AHH-1 cells, like TK6 cells, are a human lymphoblastoid cell line which has been transfected with CYP1A1 (Crofton-Sleigh *et al*., 1993). MCL5 cells are derived from AHH-1 cells but they have been transfected with a plasmid encoding cytochrome P450s (CYP1A2, CYP2A6, CYP2E1, and CYP3A4) and microsomal epoxide hydrolase in order to facilitate metabolic activation (Yamakage *et al*., 1998). Both AHH-1 cells and MCL5 cells have a heterozygous mutation in the *TP53* locus (Guest and Parry, 1999). Along with the cytochromes transfected into MCL5 cells via a plasmid, a hygromycin B (Hygro B) resistance gene is also carried as complimentary DNA (cDNA) (Brüsehafer *et al*., 2015) to selectively maintain the plasmid. The doubling time for both AHH-1 and MCL5 cells was approximately 22 hours to 24-hours (Brüsehafer *et al*., 2015).

TK6 cells are p53 competent, however both AHH-1 and MCL5 have a *TP53* mutation, meaning there may be a restriction of p53 function in these cell lines (Li *et al*., 2020). It has been shown

that there is a higher level of Mn formation and decreased cytotoxicity as a result of the genotoxicity in MCL5 and AHH-1 cells when compared to the TK6 cell line (Brüsehafer *et al*., 2015). AHH-1 cells were not used in this work and MCL5 cells were only used with TCDD due to the requirement of metabolic activation (Wilde *et al*., 2017). Some chemicals were initially tested using both cell lines, however only taken forward using one cell line. The literature was consulted before conducting experiments with each chemical and recommendations regarding the requirement of metabolic activation was taken from there.

1.10 Aims and hypotheses

Hypotheses

- NGCs can be detected using an *in vitro* testing battery.
- NGCs can be detected using chronic dosing following by the *in vitro* Mn assay.
- Identify the mechanism(s) of action (MoA) of NGCs using multiple endpoint analysis.

Aims

The main aims of this PhD were to design an *in vitro* detection system for NGCs. In order to try to plan a successful test system, it was thought that a multi-endpoint battery would be the most beneficial. Numerous endpoints were picked as a result of information in the literature and each chemical assessed was subject to each endpoint. Mechanistic understanding is increasingly important, especially with NGCs as they are so complex and can use a combination of mechanisms in order to initiate oncogenesis (Hernández *et al*., 2009). Chronic dosing was utilized to encompass a more 'real-life' exposure (Kermanizadeh *et al*., 2019) and this was compared to the traditional acute testing. Chronic dosing also aims to allow the potential build-up of DNA damage (Wills *et al*., 2017) which may be seen in *in vitro* genotoxicity or mechanistic assays. In contrast, it could also represent an adaptive response where the stress could be better tolerated (Dural *et al*., 2020). It was thought possible that some NGCs with their indirect activity might produce genotoxicity through chronic but not acute exposures. The aims all link to the 3Rs as this work was funded by the NC3Rs and this project focused on replacement of animals in research as it was a solely *in vitro* PhD.

Chapter 2: General Materials and Methods

2.1 Materials

2.1.1 Equipment and reagents used

The reagents used throughout this work are included in **Table 2.1** below and most of these reagents were used during cell culture (**Section 2.2.3**).

Table 2.1. The reagents used with the providing supplier.

Reagents	**Supplier**
RPMI 1640 media	GIBCO®, Life Technologies
L-Glutamine	GIBCO®, Life Technologies
Horse serum	GIBCO®, Life Technologies
DMSO (CAS:67-68-5)	Fisher Scientific
Hygromycin B	Merck
PBS	GIBCO®, Life Technologies
D_2H_2O	MilliQ
Methanol (CAS:67-56-1)	VWR
Cell tak (CAS: 243984-11-4)	Corning
DAPI (28718-90-3)	Sigma Aldrich (Merck), Dorset
RNAse	Thermofisher
PI	BioLegend
Annexin V	BioLegend
7-AAD	BioLegend
Annexin buffer	BioLegend
Ethanol (CAS:64-17-5)	VWR

The equipment used throughout this PhD are listed in **Table 2.2** below.

Table 2.2. The equipment used with the providing supplier.

Equipment	**Supplier**
Axiovert 40C microscope	Zeiss
Biological safety cabinet class 2- Mars	Labogene (Scanlaf)
Centrifuge 5810R	Eppendorf Ltd
Coulter Z1 particle counter	Beckman Coulter
CO_2 Air jacketed incubator	Nuaire
ErgoOne Fast pipette controller	Starlab
Grant sub aqua 18water bath	Eppendorf, Stevenage, UK
Gilson pipette set	Fischer scientific
Heraeus ™ Pico ™ 17 microcentrifuge	Thermo Fisher Scientific
Metafer	Metasytems
Nanodrop spectrophotometer ND1000	Labtech
Novocyte flow cytometer	Agilent technologies
Seahorse XFe24 Analyzer	Agilent technologies
T100 thermal cycler	Bio-Rad Laboratories
Whirlmixer Vortexer	Thermo Fisher Scientific
Cell Freezing chambers	Mr Frosty, Thermo Fisher Scientific, UK
2 ml Cryovials	ALKAY
-80°C freezer	New Brunswick Freezer
15 ml centrifuge tubes	Corning

50 ml unskirted falcon tubes	Corning
1000 µl tips (Sterile, filter tips)	Starlab
200 µl tips (Sterile, filter tips)	Starlab
20 µl tips (Sterile, filter tips)	Starlab
10 µl tips (Sterile, filter tips)	Starlab
FLUOstar Omega multimode microplate reader	BMG LABTECH Ltd, UK
T75 flasks	Cell Star®, Greiner
T25 flasks	Cell Star®, Greiner
6 well plates	Cell Star®, Greiner

2.1.2 Test Chemicals

The test chemicals; including NGCs, comparative GCs and positive controls utilized in this PhD are detailed in **Table 2.3** below.

Table 2.3. The chemicals used with the providing supplier.

Chemical	**CAS**	**Supplier**
Nickel chloride	7718-54-9	Sigma Aldrich (Merck), Dorset
Sodium meta arsenite	7784-46-5	
Cacodylic acid	75-60-5	
Rosuvastatin	147098-20-2	
Chloroprene	126-99-8	
2,3,7,8-tetrachlorodibenzo-*p*-dioxin (TCDD)	1746-01-6	LGC Standards, Teddington
Methyl methanesulphonate (MMS)	66-27-3	Sigma Aldrich (Merck), Dorset
Ethidium bromide	1239-45-8	
Staurosporine	62996-74-1	
Hydrogen peroxide H_2O_2	7722-84-1	

2.2 Cell Culture and Cell Lines

2.2.1 TK6 cell line

TK6 (American Type Culture Collection (ATCC)) suspension cells were mainly utilized throughout this work and were maintained in a T75 flasks (Cell Star®, Greiner) in 30 ml of RPMI medium supplemented as described in **section 2.2.3**. The cells were subcultured between $2x10^5$ and $1x10^6$ cells/ml and seeded into either T25 flasks (Cell Star®, Greiner) (10 ml total volume) or 6-well plates (Cell Star®, Greiner) at a seeding density of $1x10^5$ (5 ml total volume).

2.2.2 MCL5 cell line

MCL5 suspension cells were also utilized where metabolic activation was required,for example it was used with TCDD assessment. They were cultured the same as TK6 cells, they were maintained in a T75 flask with 30 ml total volume growth medium with added supplements. They were also sub cultured between $2x10^5$ and $1x10^6$ and seeded into mainly 6-well plates at a seeding density of $1x10^5$ (5 ml total volume). MCL5 cells were sourced from the ATCC, (Middlesex, UK). MCL5 cells contain a plasmid with a vector containing Hygro B resistance as

a selector for CYP1A2 and CYP2A6. There is another vector conferring resistance to 1-histidinol that contains cDNA encoding for CYP2E1 and CYP3A4, however this was not selected for in this work. In order to ensure that the cells within the culture contain the CYPs, the addition of the Hygro B selector is necessary (Crespi *et al*., 1991). Hygro B was added to MCL5 cell cultures at 4 µl per 1 ml.

2.2.3 Cell culture

All cell culture procedures are performed in a class II laminar flow cabinet with a hepa filter as imaged in **Figure 2.1** (VWR International, Lutterworth, UK). The hood utilized had to contain a hepa filter as the chemicals used were toxic and 4 out of the 6 arrived as a powder. Cell culture was carried out entirely in sterile working conditions, with the use of 70% ethanol (diluted with tap water) spray on any equipment required in the laminar flow cabinet. The cells were maintained at 37°C and 5% Carbon Dioxide (CO_2) in a humidified incubator (NU-5510); NuAire, Plymouth, USA). All cell types used were sub-cultured as described in **section 2.2.4** and maintained in their exponential growth phase. Both cell lines (TK6 and MCL5) were maintained in the same media composition; Roswell Park Memorial Institute, RPMI-1640 (Gibco Invitrogen, Paisley, UK) media with the addition of 2 mM L-glutamine (Gibco Invitrogen, Paisley, UK) and 10% horse serum (Gibco Invitrogen, Paisley, UK). The RPMI-1640 with the additional supplements (stated previously) which can be collectively termed Growth medium, was stored at 4°C in the dark and was warmed to 37°C in a water bath (Eppendorf, Stevenage, UK) prior to use. RPMI 1640 is often used to culture suspension cells whereas Dulbecco's Modified Eagle Medium (DMEM) is commonly used to culture adherent cells. RPMI 1640 medium contains vitamins such as B12, choline, biotin and glutathione (GSH), unlike DMEM (Sigma Aldrich, 2023).

Figure 2.1: Shows a class II laminar flow cabinet with a hepa filter. The hood pictured was used for all toxic work and was being used at the time for cell counts in order to calculate the relative population doubling (RPD) alongside micronucleus (Mn) analysis.

2.2.4 Cell counts and seeding

Cells were counted twice per culture in order to take an average and could be recounted if there were large differences between the counts. Counts were taken at multiple stages in order to calculate cytotoxicity and monitor growth throughout different experimental procedures using the Beckman coulter counter (Beckman-Coulter, Wycombe, UK). Cell counts were carried out in the laminar flow hood pictured in **Figure 2.1**. Cells were gently shaken within the culture flask and 100 µl of cell suspension was added to 10 ml diluent (Beckman-Coulter, Wycombe, UK) and were counted by the Beckman coulter counter. A cell count reading was given as cells/ml which allows the calculation of the required volume of cells and volume of media to seed at a given cell concentration (using $C_1V_1=C_2V_2$). All experiments were seeded at a seeding density of $1x10^5$. After seeding, cells were left to grow at 37°C and 5% CO_2 in a humidified incubator for 24-hours prior to treatment with the test chemicals.

2.2.5 Cryopreservation, thawing and culture

In order to store cells for extended periods cryopreservation is necessary. Cells were spun using a centrifuge at 107xg (gravitational Force) for 5 minutes and the supernatant was discarded. The cells were then suspended in 1 ml of freezing medium consisting of horse serum and dimethyl sulphoxide (DMSO) (Fischer scientific, Loughborough, UK) at the ratio 9:1 respectively. 1 ml of cells suspended in the freezing medium solution is added to cryovials (Elkay Laboratories, Basingstoke, UK) and they were kept in -80°C freezers (Fisher Scientific, Loughborough, UK) overnight before being stored in the liquid nitrogen containers (ThermoFisher Scientific, Rugby, UK) for long-term storage. Personal protective equipment such as goggles, gloves and lab coats were worn when transferring cells to and from the liquid nitrogen containers.

In order to thaw cells taken from liquid nitrogen storage, a T75 flask (Greiner BioOne, Stonehouse, UK) is filled with 29 ml of supplemented medium. The cells removed from liquid nitrogen in the cryovial were placed in the water bath to allow rapid thawing and were then added to the T75 culture flask using a Pasteur pipette (VWR International, Lutterworth, UK).

2.3 Test Chemicals and exposure regime

There are numerous test chemicals that are prepared by weighing out the required mass of chemical before dissolving in the appropriate volume of solvent.

2.3.1 Negative controls

. Negative controls are all solvent controls and were added as 1% volume of the whole system. For example, with $NiCl_2$, the treatments are carried out in T25 flasks with a total volume of 10 ml, meaning that 100 µl of d_2H_2O is added to the negative control flask.

The chemicals prepared in d_2H_2O are; $NiCl_2$; NaMAr; Caco as they are all soluble in water (H_2O). Both TCDD and rosuvastatin arrive in sealed glass vials, already dissolved in DMSO. The pre-dissolved chemicals are further diluted to produce the dose ranges using the DMSO solvent and/or media as required. Chloroprene was more difficult to dissolve and was soluble in methanol, so this was taken further as the solvent and therefore negative control. The solvents can be seen in **Table 2.4** below.

Table 2.4: The negative controls used throughout all endpoints for each of the chemicals used.

Chemical	**Negative controls (solvent control)**
Nickel chloride	H_2O
Sodium meta arsenite	
Cacodylic acid	
Rosuvastatin	DMSO
2,3,7,8-tetrachlorodibenzo-*p*-dioxin (TCDD)	
Chloroprene	Methanol

2.3.2 Exposure Regimes

Acute

The acute exposures carried out in this work were 24-hour exposures as standard (unless stated otherwise). Acute treatments were carried out with each endpoint. Acute treatments were seeded on day 1 as stated in **section 2.2.4**. Acute treatments for Mn assessment include a 24-hour recovery time.

Chronic

The chronic treatment of chemicals for Mn analysis is displayed in **Figure 2.2**, where it clearly demonstrates the series of events from cell seeding to the semi-automated scoring final stage. Chronic treatment was only utilized with the Mn endpoint. Chronic treatments for Mn assessment include a 24-hour recovery time.

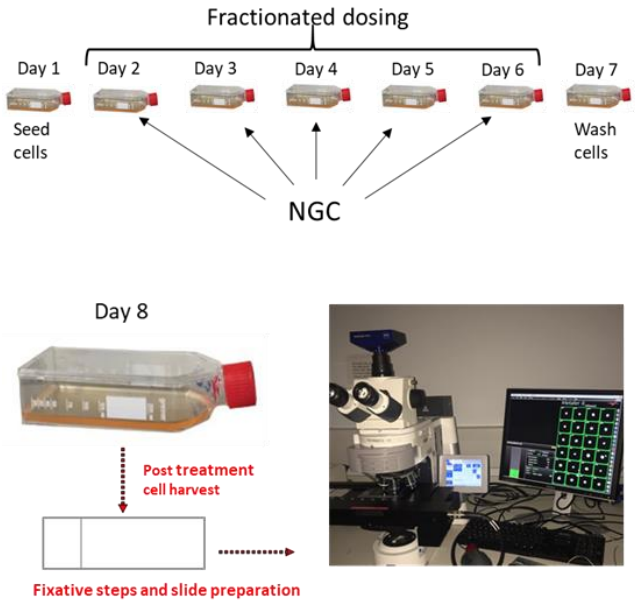

Figure 2.2: The chronic dosing regime is shown by the diagram. It shows the cells grown in culture treated chronically for 5 days at fractionated doses, washed, harvested and then they undergo a series of fixative steps before the cells are attached to the slides. The semi-automated metafer system is used to score 4000 cells per replicate.

2.3.3 Test chemicals

T25 flasks or 6 well plates were used depending on the chemical assessed, in order to have enough chemical and to reach the dose requirements of some NGCs, a smaller volume was required due to restrictions in the chemical stock. Doses of test chemicals were based on previous work conducted in the Swansea laboratory, thorough literature searches and as a result of dose finding experiments such as RPD, excluding doses beyond the threshold from the OECD 487 guidelines (OECD, 2016a). The negative controls are always 1% of the solvent used. For the endpoints that required a one-off dose and time-point, these were decided based on the first dose that showed significance or

T25 flasks with 10 ml total volume used for the analysis of the chemicals below:-

Nickel chloride; doses include d_2H_2O as the solvent negative control, 50 µM, 100 µM, 125 µM, 150 µM and a positive control from the list below, depending on the endpoint.

Sodium meta arsenite; doses include d_2H_2O as the solvent negative control, 2 µM, 4 µM, 6 µM, 8 µM, 10 µM and a positive control from the list below, depending on the endpoint.

Cacodylic acid; doses include d_2H_2O as the solvent negative control, 500 µM, 1000 µM, 2000 µM, 3000 µM, 5000 µM and a positive control from the list below, depending on the endpoint.

6 well plates with 5 ml total volume used for the analysis of the chemicals below:-

Chloroprene; doses include methanol as the solvent negative control, 2 µM, 20 µM, 100 µM, 200 µM, 400 µM and a positive control from the list below, depending on the endpoint.

Rosuvastatin; doses include DMSO as the solvent negative control, 2 µM, 20 µM, 100 µM, 200 µM, 400 µM and a positive control from the list below, depending on the endpoint.

2,3,7,8-tetrachlorodibenzo-p-dioxin; doses include DMSO as the solvent negative control, 0.1 µM, 0.5 µM, 1 µM, 2 µM, 3 µM (doses 2 µM and 3 µM were only added for chronic exposure) and a positive control from the list below, depending on the endpoint.

Table 2.5 below documents the one chosen dose which will be used for the endpoints that require a single exposure such as the PCR array and the Seahorse XF analyser. These doses are based primarily on the acute Mn and RPD data. This could be the first dose where there is a significant increase of Mn, if the RPD is above the 50% threshold. If the RPD drops below the 50% threshold, then the selected dose is the one before the drop in RPD. This is all based on recommendations detailed in the OECD guidelines.

Table 2.5: The selected dose used for the endpoints that require a single exposure.

Chemical	Chosen dose (µM)
Nickel chloride	125
Sodium meta arsenite	6
Cacodylic acid	5000
Rosuvastatin	200
2,3,7,8-tetrachlorodibenzo-*p*-dioxin (TCDD)	2
Chloroprene	400

2.3.4 Positive controls

All the chemicals below use d_2H_2O as the solvent. The positive control doses were chosen based on previous data produced in Swansea University, the literature and dose finding experiments.

Methyl methanesulphonate; was utilized at 10 µM for RPD, Mn, cell cycle and PCR.

Ethidium bromide; was utilized at 100 mM for the Seahorse assay.

Staurosporine; was utilized at 0.1 µM for the apoptosis assay.

Hydrogen peroxide; was utilized at 100 µM for DCFDA assay.

2.3.5 Treatment times

The regulatory toxicity assessment treatment time of 24-hours was utilized for each chemical when exploring genotoxicity. The 24-hour treatment is the gold standard because it allows a complete cell cycle to take place post treatment. The cell cycle duration varies in different cell types however a typical human cell cycle takes approximately 24-hours. G1 lasts around 11 hours, S phase around 8, G2 around 4 and finally M phase takes about 1 hour (Cooper, 2000). This 24-hour treatment was employed in order to form comparisons between the acute spiked doses of a chemical to the more human relevant chronic dosing exposures (EMA, 2013). It is suggested that a 24-hour time point should be assessed with both *in vivo* and *in vitro* treatments (EMA, 2013).

The chronic exposure was the same total dose as the acute treatment but was fractionated over 5 days as this was used previously in this laboratory (Chapman *et al*., 2015). For example, if the total dose was 100 µM the chronic treatment would receive 5 x 20 µM doses. The exposure regime is indicated in **Figure 2.2** above where it demonstrated the series of events in a chronic Mn treatment.

For cell cycle exposure, apoptosis, the PCR array and Seahorse analysis, a 24-hour time point was used in order to maintain consistency across the test battery.

For DCFDA analysis a series of time points were assessed due to the fast action of ROS. After dosing, the time points investigated were 30 minutes, 1hr, 2hr, 3hr, 4hr, 5hr, 6hr and 24hr. The 24-hour time point remains consistent with the other assays within the test battery.

2.4 Endpoints

2.4.1 Exposure regime

Acute Vs chronic endpoints were carried out just for the mononucleate Mn assay and RPD. It was thought that chronic dosing may allow for the accumulation of DNA damage therefore may be detectable (Stannard *et al*., 2017). However, the other endpoints such as cell cycle, apoptosis, Seahorse etc. are thought to give a more immediate response so this is why the 24-hour acute time point was utilized.

2.4.2 Cytotoxicity assessment (RPD assay)

RPD assessment was carried out alongside the mononucleate Mn assay as it considers the dividing portion of the population when cytoB (Merck) is not used (OECD, 2010b). In order to maintain consistency, RPD was conducted alongside other endpoints such as; cell cycle, apoptosis and the PCR array. It is useful to assess cytotoxicity alongside other endpoints to understand the cells' ability to tolerate the chemicals at a range of doses.

The initial cell value comes from the day 2 count pre-treatment and then the cells are counted on the final day (cell harvest) and this value is also included in the PD calculation. In order to calculate RPD, the full dose range of the treated samples take the solvent control into account. The population doubling (PD) and RPD were calculated using the formulas included below.

PD = (Log(Final/Initial))/Log2

RPD = (Treated/Control)x100

2.4.3 Genotoxicity assessment (Mononucleate Micronucleus assay)

Acute dosing/ exposure

The CBMN (OECD, 2010b) is the most frequently used and well-known version of the assay. The CBMN utilizes cytoB, which is capable of blocking cytokinesis by inhibiting microfilament assembly (Fenech, 2000).

The mononucleate Mn assay was utilized to allow comparison with the chronic Mn assay (Dural *et al*., 2021), cytoB (Merck) was not added as Mn could have been induced prior to the addition to cytoB. It is important to know that the cells have undergone division post chemical treatment. CytoB is a microfilament assembly inhibitor, therefore blocking cytokinesis (Fenech, 2000).

Cells were seeded as described above (**Section 2.2.4**). On day 2, cells are then counted again prior to chemical treatment and this value becomes the initial value in the RPD calculation. The flasks were then dosed with the total dose, vehicle (solvent) control or positive control. The flasks were incubated for 24h following each treatment with the test chemical (37^{o}C, 5% CO_2). On day 3, after the 24-hours of chemical treatment, cells are counted as described in **Section 2.2.4**, transferred to 15 ml centrifuge tubes (corning) pelleted by centrifugation at 279xg for 5 minutes, suspended in 5 ml and washed using phosphate buffered saline (PBS) before replacing with fresh media, transferred to fresh cell culture flasks/ plates as necessary and allowed a 24-hour recovery period (37^{o}C, 5% CO_2). On day 4, the cells were harvested, after the final

incubation, the number of cells/ml in all experimental flasks were counted (as cell number is used to calculate RPD values) and the samples were harvested for microscopic slide preparation, for scanning with the automated Metafer system (Metasystems Metafer 4, Zeiss). The Zeiss Metafer system is a semi-automated microscopy platform that uses algorithms based on machine learning and deep learning (GmbH, 2023).

On day 4, after 2 x PBS wash stages, cells were then treated with 0.56% potassium chloride) and centrifuged at 123xg 4°C for 10 minutes. The function of the hypotonic solution is to increase the cell size in order to analyse the cytogenetics easier (Dhawan and Bajpayee, 2019). The same centrifugation settings were utilized for the remaining stages of fixation. Following this, the addition of 10 ml ice-cold fixative (Fix) 1 was carried out (composed of methanol, 0.09% sodium chloride and acetic acid, at ratios of 5:1:6), then leaving at 4ºC for 10 minutes incubation before centrifugation. The supernatant was then discarded and 10 ml ice-cold Fix 2 added (methanol and acetic acid, at ratios of 5:1) which was incubated for 10 minutes before the first centrifugation step. The supernatant was again discarded and the process of re-suspending in 10 ml Fix 2, followed by centrifugation was repeated 3 times. Cells were then stored overnight at 4°C suspended in Fix 2.

Cells were then mounted onto microscope slides on day 5, applied with a Gilson pipette at a volume between 50 and 100 µL. These slides had been stored overnight submerged in Fix 2, before rinsing in distilled water and wiping with soft tissue. A total of 5 slides were prepared for each concentration to enable repetition of analysis if required. The distribution of cells was assessed using a light microscope (Olympus, BX51) to ensure adequate spacing. Cells were then air dried for approximately 3 hours.

Immediately before analysis of Mn content, slides were stained with ~20 µL Vectashield® mounting medium with DAPI for 15 minutes whilst protected from light, then a 25 x 60 mm coverslip was added. A total of 4000 cells were analysed per replicate (2000 cells per slide) for the presence of Mn using the Metafer 4 program using the automated Mn slide-scanning system (MetaSystems, Oxon, United Kingdom). This involved use of the 10x objective lens to achieve automated mononucleated cell identification, with verification of selected cells and Mn content carried out utilising the 60x objective lens. Three replicates were performed for each compound.

Chronic dosing/ exposure

Follows the same protocol as the acute dosing however the dosing regimen takes place over 5 days, using a fractionated proportion of the total dose.

On day 1, TK6/MCL5 cells were seeded at $1x10^5$ cells/ml in a T25 flask with a 10 ml total volume or 6 well plates with a 5 ml total volume and maintained in 37ºC and 5% CO_2 conditions.

On day 2, the number of cells/ml in all of the flasks were counted (cell number should have doubled). The flasks were then dosed with the fractioned dose (one fifth of the final dose), vehicle (solvent) control and positive control consecutively. The flasks were incubated for 24h following each treatment (37ºC, 5% CO_2). On day 3, the cells were counted, dosed and incubated as explained previously. On day 4, the cells may be confluent (~$1x10^6$ cells/ml) therefore, they required subculturing to $2x10^5$ cells/ml and resuspension with fresh medium before the test chemical treatment (this dilution factor was accounted for in future calculations). Cells were then dosed and incubated as explained previously. On days 5 and 6, the cells were counted, dosed and incubated as explained previously. On day 7, the cells were washed with PBS after the final treatment had been incubated for 24h. The contents of the flasks were transferred into labelled 15 ml centrifuge tubes and centrifuged to collect the cell pellet (193xg for 5 minutes). The supernatant was discarded and 10 ml fresh media was added to each sample. The cell samples were then transferred to new flasks, and incubated for 24h (37ºC, 5% CO_2). On day 8, after the final incubation, the number of cells/ml in all flasks were counted and the samples were harvested for the metafer slide preparation as explained in the acute section and 4000 cells/treatment/replicate were scored. On day 9, the slides were prepared as outlined in the acute section and each chemical was completed as n=3.

The scoring criteria of the Mn was mainly documented in (Fenech *et al*., 2003) and includes characteristics such as: Mn needs to be between 1/3 and 1/16 size of the main nucleus, they are round or slightly oval, not connected or overlapping with the main nuclei and have the same staining intensity as the main nucleus (Fenech *et al*., 2003). As this work utilized the mononucleated version of the assay, the Mn needs to be within the immediate surroundings of an individual nucleus, with no other nuclei present within the metafer grid and can only be counted if there is enough distance between other nuclei. This parameter is kept as constant as possible.

2.4.4 Cell cycle analysis

This protocol was carried out on fixed cells. On day 1, TK6/MCL5 cells (as required for metabolic activation) were seeded at $1x10^5$ cells/ml in either a T25 flask with a 10 ml total volume or 6 well plates with a 5 ml total volume (see **section 2.3**) and maintained in 37ºC and 5% CO_2 conditions. On day 2, the flasks were counted and dosed with their respective doses

including positive and negative controls (see **section 2.3** and **Table 2.3**). The negative controls are solvent controls and the positive control in this instance was methylmethane sulphonate (MMS) as it was aiming to keep the positive control constant with the Mn data. On day 3, the cells were centrifuged and then washed with PBS, before vortexing and mixing with 1 ml of -20^{o}C ethanol and storing at -20^{o}C for fixation overnight. On day 4, the cells were ready for flow cytometry analysis, so the cells are washed twice with PBS in order to remove the ethanol ready for flow cytometry preparation. The cells were then resuspended in 50 µl RNase solution (Thermofisher scientific) in order to remove any RNA present as PI is used to proportionately stain the cellular DNA content (Pozarowski and Darzynkiewicz, 2004). However, PI is also able to bind with the double stranded RNA, so this needs to be removed using RNase (Pozarowski and Darzynkiewicz, 2004). Then the RNase suspended cells are added to 200 µl PI solution (BioLegend) and transferred to fluorescence activated single cell sorting (facs) tubes (Fisher scientific) and kept on ice and in the dark for 30 minutes before running the cells through the flow cytometer (Novocyte).

PI is a fluorescent dye, excited by a blue 488 nm laser and uses the PE-Texas Red channel for detection. PI should be stored between 2 and 8^{o}C undiluted (BioLegend, 2023). The cell number and therefore running time varies based on the cytotoxicity of the assessed chemical. The settings on the flow cytometer indicate that 20,000 events should be recorded with each sample assessed. The gating is firstly based on the live cell population, then gated for single cells and further sorting and analysis was done in FlowJ. The data was exported from the Novocyte via Flow Cytometry Standard (FCS) files which are compatible with FlowJ. First, the data was changed into a histogram and then each cell cycle stage assessed (G1, S, G2) was individually gated using FlowJ. The data was conducted with 3 technical replicates and 3 biological replicates. Data analysis was conducted using Graphpad prysm software.

2.4.5 Apoptosis analysis

Apoptosis analysis was carried out in unfixed cells as it is measuring live cells, early apoptotic, late apoptotic and necrotic cells. Staurosporin was used as a positive control, the vehicle was used as a negative control (see **section 2.3** and **Table 2.3**) and the chemical doses were also investigated (see **section 2.3.3**). On day 1, TK6/MCL5 cells were seeded at 1x10^{5} cells/ml in a T25 flask with a 10 ml total volume or 6 well plates with a 5 ml total volume and maintained in 37^{o}C and 5% CO_2 conditions. On day 2, the cells were counted to check the cells were dividing as normal and they were then treated with their respective doses including controls. On day 3, the cells were counted again as 1x10^{6} cells/ml were required for the assay. The cells were

centrifuged and then washed twice with 0.2 % facs buffer (125 ml PBS and 0.25 g BSA mixed), before suspending in an appropriate volume of Annexin buffer solution. Annexin V and 7-AAD (BioLegend) used in parallel allow for the discrimination of the different stages of apoptosis including live cells, early and late apoptotic cells as well as necrotic cells (Rimon *et al*., 1997). Then 100 µl of the cells suspended in annexin buffer solution were added into a facs tube. Next, 5 µl of annexin V and 5 µl of 7-AAD were added to each 100 µl cell suspension. The cells were incubated for 15 minutes in the dark and then topped up with 400 µl of annexin buffer before being run on the flow cytometer (Novocyte).

The results from the flow cytometry apoptosis assessment can be visualised in **Figure 1.8b**. The grid represents where each cellular parameter should fall as a result of the different dyes.

Compensation

Compensation refers to the correction of any spectral overlap of fluorescence (Bio-rad, 2023). Compensation is the mathematical correction due to spill over from the emission spectra (Roederer, 2001). Annexin V uses the Fluorescein Isothiocyanate (FITC) channel of detection, whereas 7-AAD is excited at 488 nm and uses the PE-Texas Red channel. Compensation was required as the wavelengths of the dyes overlapped slightly which can be seen in **Figure 2.3**. This compensation was carried out and then applied to all samples. The data is exported from the Novocyte via FCS files which are compatible with FlowJ. The gating was based on the entire cell population, including live and dead cells, then gated for single cells and further sorting and analysis is done in FlowJ. The data was conducted with 3 technical replicates and 3 biological replicates. Data analysis was conducted using Graphpad prysm software.

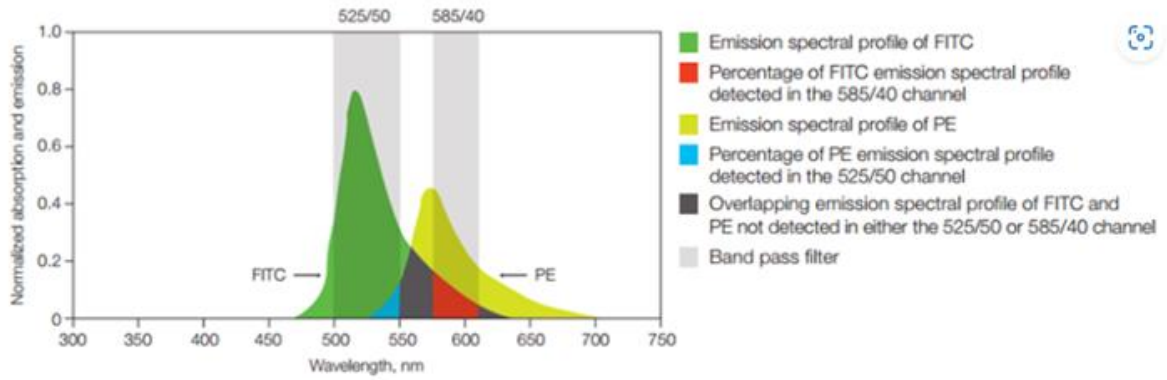

Figure 2.3: Shows the emission spectra of FITC and PE-Texas Red and indicates the portions in which they can overlap. The potential for FITC and PE-Texas Red to overlap explains the requirement for compensation. Image is taken from (Bio-Rad, 2023).

Compensation was carried out using a live cell and dead cell mix with different stains as seen in **Figure 2.4.** The necrotic cells were killed with a heat shock at 90°C for 5 minutes. The apoptotic cells, had been Staurosporine treated. The cells were put into 4 facs tubes of cell populations- 1 tube contains live cells only with no fluorescent dyes; the second tube contained live unstained cells and the heat shocked dead cells with just the 7-AAD dye; the third tube contained the unstained live cells and the staurosporine treated cells with the annexin V dye and the fourth tube contains a mixed cell population of untreated cells and both dyes. This was then all run through the Novocyte flow cytometer and saved as a compensation template that could be applied into each apoptosis experiment to avoid having to run a new compensation experiment alongside each experiment.

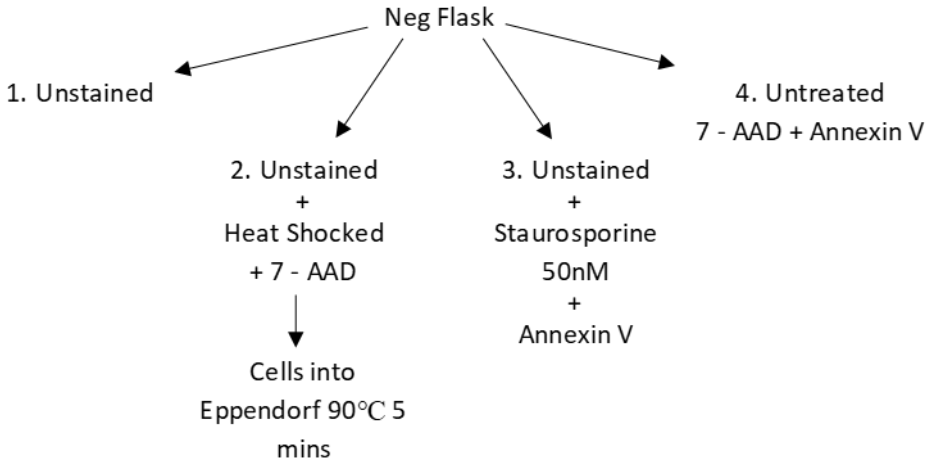

Figure 2.4: This diagram shows how the cells and treatments were divided into the four tubes for compensation. It represents the basis of how the compensation was carried out. Neg stands for the negative control flask of untreated cells at the beginning.

2.4.6 Reactive oxygen species (ROS) assay

The cells were seeded at 1 x10^5 cells/ml in T25 flasks (10 ml total volume) or 6-well plate (5 ml total volume) depending on the chemical assessed. The cells were incubated overnight at 37°C and 5% CO_2 and after 24-hours the test chemical, negative and positive control were added to the cells. After 15 minutes, 100 µl cells (with each of the treatments) were added to a black 96-well plate (clear bottom) (greiner) with 100 µl DCFDA (Sigma-Aldrich) working solution at 20 µM. The DCFDA powder was weighed out and dissolved in DMSO to give the main stock of 100 mM and then further diluted to a working solution of 20 µM.

The outer wells around the edge of the 96-well plate were left for PBS only and then also one row for DCFDA only and one row for cells only. There is an edge effect when using 96-well

plates, the corner and outer edge wells are more susceptible to evaporation. As the whole plate was not required for analysis, it is more favourable to use the inner wells for the assay (Mansoury *et al.*, 2021). Cells only and DCFDA only serve as controls and can also be monitored over time.

After 15 minutes of treating the cells, they are mixed with DCFDA, the first reading was taken (30 minutes from dosing). The time points assessed were 30 minutes, 1h, 2h, 3h, 4h, 5h, 6h and 24h in order to see how the ROS levels change over time. ROS have different half-lives and this can therefore the affect they exert over time. For example, OH radicals have a fairly short half-life, meaning the effects they exert are usually close to the generation site (Lautraite *et al.*, 2003). Other ROS molecules such as hydrogen peroxide (H_2O_2) and Oxygen (O_2^-) have a longer half-life which means their effects can be seen a long time after generation and there is a greater diffusion distance (Forkink *et al.*, 2010). The readings were taken using a FLUOstar Omega multimode microplate reader (BMG LABTECH Ltd, UK) with an excitation/emission set to 485/535nm respectively in order to reduce background noise and to obtain the best possible results (Abcam, 2023).

2.4.7 PCR arrays

RNA extraction

Cells were seeded at 1 x10^5 in T25 flasks (10 ml total volume) or 6-well plate (5 ml total volume) and incubated overnight at 37ºC and 5% CO_2. After 24-hours, the test chemical, negative and positive controls were added to the cells and left to incubate overnight at 37ºC and 5% CO_2. Cells were centrifuged, washed with PBS and resuspended in fresh media and left to recover for a further 24-hours. RNA extraction was carried out using the RNeasy micro kit (74004, Qiagen). Then cells were centrifuged, washed with PBS and resuspended in 600 µl RLT buffer with vigorous pipetting. The lysate was pipetted into a QIAshredder column inside a 2 ml collection tube and was centrifuged for 2 minutes at 8000xg. Next, 600 µl of 70% ethanol was added to the lysate and was mixed by pipetting. Using ~700 µl of sample at a time, transfer to an Rneasy spin column in a 2 ml collection tube. Microfuge (Biorad) for 15 seconds at 8000xg and the flow through was discarded and then the remaining volume was added to the same column and centrifuged at the same settings before discarding the flow through. Following this, 700 µl RW1 buffer was added to the spin column and was centrifuged for 15 seconds at 8000xg and the flow through was discarded. Then, 500 µl RPE buffer was added to the Rneasy spin column before centrifugation for 2 minutes at 8000xg and the flow through was again discarded. The Rneasy column was placed into a new 1.5 ml collection tube and ~50 µl Rnase free water was

added to the column and was centrifuged for 1 minute at 8000xg in order to elute the RNA. The RNA was then tested for yield and quality on the nanodrop. RNA samples can be stored at -80°C in aliquots until the cDNA synthesis step.

cDNA synthesis

The cDNA synthesis was carried out according to the manufacturer's instructions for the iScript genomic DNA (gDNA) Clear cDNA synthesis kit (172-5034, Bio-rad). The cDNA synthesis was carried out in the laminar flow PCR hood, which was wiped down with 70% ethanol and Rnase Zap (Biorad) before use. All equipment was also wiped using 70% ethanol and Rnase Zap. The components of the cDNA synthesis kit were thawed on ice. First, a Dnase master mix was formed as in **Table 2.6**, (scaled up for each sample), it was mixed thoroughly by pipetting.

Table 2.6: DNA master mix per reaction

Component of master mix	**Volume per reaction (µl)**
iScript Dnase	0.5
iScript Dnase buffer	1.5
Total	2.0

Using the same amount of RNA in each cDNA synthesis reaction (each PCR array was carried out separately). For each RNA sample, an RNA/DNA reaction mix was prepared on ice, volumes can be seen in **Table 2.7**. A RT control was prepared using 1 µl of the control RNA template (provided with the PCR arrays, Biorad).

Table 2.7 RNA/Dnase reaction mix

Component of RNA/Dnase reaction mix	**Volume per reaction (µl)**
Dnase master mix	2
RNA template (1 µg)	Variable
Nuclease free water	Variable
Total	16

After thorough mixing by pipetting, the tubes were centrifuged to remove bubbles and collect the volume at the bottom of the Eppendorf. It was then placed into the T100 Thermal cycler (Bio-Rad) and was set to the Dnase reaction protocol with the conditions seen in **Table 2.8**.

Table 2.8: Dnase Reaction protocol

Step of Dnase reaction	**Temperature (ºC)**	**Time (minutes)**
Dnase digestion	25	5
Dnase inactivation	75	5
Storage	4 (or in ice)	Until RT PCR step

The RT master mix was made by adding the iScript RT supermix (or the no RT control) to Dnase treated RNA template. For each RNA sample prepared, a no-RT control must also be carried out (it was set up as described in **Table 2.9**, the RT Supermix was replaced with the no-RT Supermix.

Table 2.9: RT master mix set up

Component of master mix	**Volume per reaction (µl)**
iScript RT supermix (or no RT control)	4
Dnase treated RNA	16
Total	20

Again, it was mixed thoroughly by pipetting and centrifuged. The reaction tubes were incubated in the T100 thermal cycler using the conditions in **Table 2.10**.

Table 2.10: cDNA synthesis thermal cycler conditions

Thermal cycler stage	**Thermal cycler conditions**
Priming	5 minutes at 25ºC
Reverse transcription	20 minutes at 46ºC
RT inactivation	1 minute at 95ºC
Hold	4ºC

The cDNA can be stored at this point at -80ºC for an extended period.

Quantitative PCR (qPCR) using the Bio-Rad general cancer panel PCR array

qPCR is conducted as per manufacturer's instructions using SYBR green super mix (1725121, Biorad) and the cancer panel tier 1 PCR array (10025137, Biorad) as seen in **Figure 2.5.**

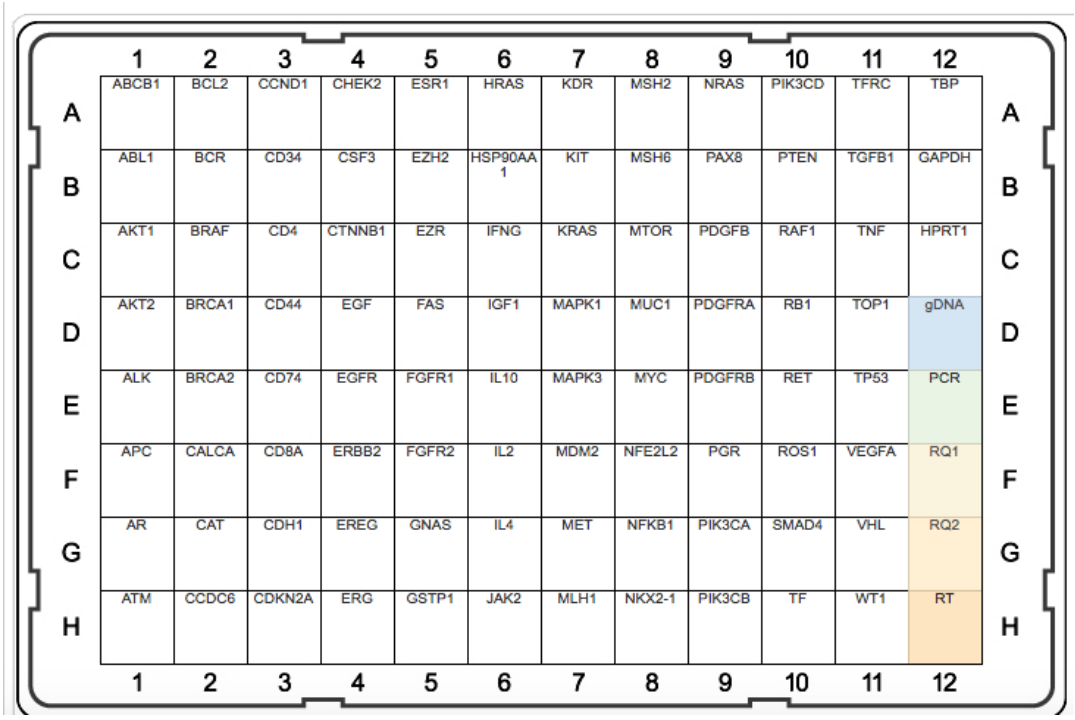

Figure 2.5: Plate layout of cancer panel tier 1 PCR array genes in the order they were assessed. 12 D-H represent controls and 12 A-C represent housekeeping genes (taken from Bio-Rad.com).

Again, conducted in the PCR hood with everything sprayed with 70% ethanol and Rnase Zap. The PCR arrays are allowed to come to room temperature from the fridge (4^{o}C). The SYBR green Supermix, cDNA samples (including no-RT and RT control), positive PCR control were allowed to thaw on ice in the PCR hood (kept away from direct light where possible). All tubes of SYBR green and cDNA samples were mixed by inversion and centrifugation using the microcentrifuge. Each cDNA sample was diluted to give a total of 100 µl using nuclease free water. In order to account for any pipetting error, more master mix was made than the volume needed. The master mix was scaled up to 100 wells to make it easier to pipette. The individual well volumes are stated in **Table 2.11** below.

Table 2.11: qPCR reaction master mix

Component of master mix	**Volume per reaction (µl)**	**Final Concentration**
SYBR green supermix	10	1x
PCR primer	Lyophilised on plate	-
cDNA sample	1	10 ng
Nuclease free water	Variable	-
Total volume	20	-

A total of 20 µl qPCR reaction mix was pipetted into each well of the PCR array plate (except for gDNA and RT control wells). The gDNA and RT controls were made as per **Table 2.11**,

except the no-RT control and RT control cDNA was used (20 µl of controls were added to the specific wells). Add 1 µl of the PCR control tube into the PCR control well with the 20 µl of master mix (this well has a total volume of 21 µl). The plate was then sealed with a plate sealer and centrifuged for 2 minutes at 2600xg at room temperature. The plate was run using the Bio-Rad CFX qPCR machine as per the conditions in **Table 2.12**.

Table 2.12: PCR cycling protocol

qPCR protocol	**Temperature (ºC)**	**Time (s)**	**Number of cycles**
Activation	95	120	1
Denaturation	95	5	40
Annealing/extension	60	30	
Melt curve	65-95 (0.5ºC increments)	5 (s/step)	1

The values produced for the PCR array quality controls are then checked to ensure the data can be used.

2.4.8 Mitochondrial stress test (Seahorse assay)

One day prior to Seahorse run the cell culture microplate (Agilent, California, U.S) was coated with Cell Tak as suspension cells were used throughout this work. Cell Tak is a cell and tissue adhesive which is capable of adhering a monolayer of suspension cells such as lymphocytes to a plate in order to conduct the Seahorse mitochondrial stress test as often adherent cell lines are used (Agilent, 2023b). The cells need to be attached to the plate in the Seahorse assay so that the probes capable of measuring OCR/extracellular acidification rate (ECAR) are directly above the cells and are able to monitor any changes to the measurements (Plitzko and Loesgen, 2018; Robertson Lab, 2023). In order to dilute the Cell Tak, 29 µl was taken from the main stock and was added to 221 µl sterile double distilled water (d_2H_2O) and was added to the plate within 10 minutes of preparation. Then, 10 µl of diluted Cell Tak was pipetted into each well and 40 µl sodium bicarbonate (0.1 M, filter sterilised: 1.26 g + 150 ml H_2O) was added to each well and was left to dry in the hood for 20 minutes. The 50 µl of solution was removed from the plate and 500 µl H_2O was added to the plate to wash which was then removed without scratching the base of the well (taking care not to remove the Cell Tak). The plate was left to air dry in the hood again and was then stored at 4°C (for up to 1 week).

The Mitochondrial stress test medium was prepared a day prior to the assay run. The XF based DMEM medium (Agilent, California, U.S) was warmed in the water bath as well as the supplements: sodium pyruvate (Agilent, California, U.S), glucose (Agilent, California, U.S) and defrost L-glutamine (GIBCO®, Life Technologies). Two x 50 ml tubes of medium were

prepared, 1 for sterile use and 1 for non-sterile use, these were stored at 4°C until use. A volume of 48.5 ml medium was added to a sterile 50 ml storage container and 500 µl of each of the supplements (sodium pyruvate, glucose and L-glutamine) were added. The sterile media was used to suspend the correct cell number in order to allow for correct quantification and comparison between different chemicals. The non-sterile medium was utilized to make the correct volume of the injections before adding into the bioanalyser.

The Seahorse cartridge also required hydration a day prior to the assay run. The lid, hydrobooster and cartridge were removed and 1 ml of calibrant was dispensed into each well of the 24-well plate. The cartridge, hydro booster and lid were replaced allowing the probes to be submerged in the calibrant. The cartridge was stored overnight in a non-CO_2 incubator at 37°C and was kept in a sealed bag in the incubator so the calibrant does not evaporate.

On the day of the Seahorse run, which was 24-hours after treatment, the cells were counted and centrifuged at 10,000xg for 5 minutes in order to work out the cell concentration required for 4 million cells per well.

$$\frac{\text{Cell number x number of millilitres of cells}}{4000000} = \text{Volume of resuspension Seahorse media}$$

A volume of 100 µl of cell suspension was added to the wells containing Cell Tak, they were spun for 1 minute at 21°C (acceleration at 4 and brake at 0) to ensure attachment of cells to the plate. Then 400 µl Seahorse medium (non-sterile) was added to the cells (giving a total of 500 µl per well) in order to keep everything constant throughout the plate and so the wells have sufficient media in them to monitor OCR/ECAR. The cartridge and cell plate were inserted into the Seahorse 24 machine (Agilent, California, U.S).

The pre-prepared injections (Agilent, California, U.S) were diluted using set volumes of assay medium to give 100 µM concentration for Oligomycin (+ 630 µl assay medium) and FCCP (+ 720 µl assay medium). The rotenone/antimycin A has a 50 µM injection (+ 540 µl assay medium). The injections were further diluted with media to give final well concentrations of 1.5 µM oligomycin (port A), 1.0 µM FCCP (port B) and 0.5 µM rotenone/antimycin A (port C). Oligomycin is used to inhibit the adenosine triphosphate (ATP) synthesis that should take place directly after the basal measurements are taken. It works by decreasing the flow of electrons through the electron transport chain meaning there should be a reduction of mitochondrial respiration (Agilent, 2023a). FCCP causes a rapid and maximum rate of respiration and means in

order to meet the metabolic demand, oxidation of any substrates such as sugars and fats takes place (Agilent, 2023a). Rotenone is a complex I inhibitor and antimycin A is a complex III inhibitor of the electron transport chain. This means that mitochondrial respiration is inhibited and only respirational processes outside of the mitochondria can take place (Agilent, 2023a). These inhibitors mean that different measurements can be taken as a result of the addition of these complexes. These final well concentrations are added into the correct ports of the cartridge, taking care not to add bubbles during this process. The wave programme was used, the XF mito stress test was selected and the chemicals were filled into the groups section of the template. The hydro booster and lid were both removed before the plate was run. The data was removed from the Seahorse XF Analyzer via excel files. One of the outputs produced as a result of the mitochondrial stress test can be seen in **Figure 2.6** below.

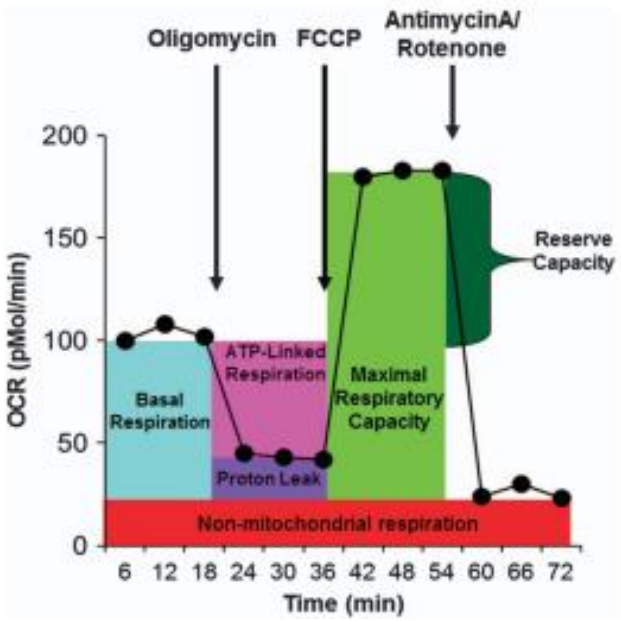

Figure 2.6: The bioenergetic profile for lymphoblastoid cell lines representing the mitochondrial function. The shape of the graph is as a result of the addition of several pharmacological agents, intended to challenge mitochondrial function. Figure taken from (Rose *et al.*, 2014) with permission.

2.5 Statistical analysis

The statistical programmes used to analyse the data produced were Mutait, (http://www.mutait.org/) and Graphpad (Dotmatics). Statistical tests carried out were Bartletts, Shapiro Wilk, Dunnets and both one and two-way Analysis of Variance (ANOVAs). Where the data is nonparametric, the Dunns test was carried out.

Mn (acute and chronic assessment); the DCFDA assay; the cell cycle data and the apoptosis data were analysed using a two-way ANOVA. The PCR array was n=1 so could not be analysed, it was used as an indicator. Seahorse analysis was a series of T-tests, both paired and unpaired were used.

As the assays used are the same throughout each chapter of this thesis, the same statistical analysis for each endpoint was carried out. Statistical significance was represented by a series of asterisks:-

If the p value is *<0.05, **<0.005, ***<0.0005, ****<0.00005 etc.

Chapter 3: Investigations of TCDD, Chloroprene and Rosuvastatin

3.1 Introduction

3.1.1 General background

The exposure to man-made chemical agents within the environment, workplaces and through food and water is inevitable. Some of the chemicals we are exposed to are hazardous to human health (Nohmi, 2018). NGCs initiate cancer using indirect mechanisms of action, not related to direct DNA damage. There are inconsistencies in the classification of NGCs due to the vast range of MoAs used by these chemicals (Hayashi, 1992), some NGCs appear to show some genotoxicity (see **chapters 4 and 5**). GCs are thought to be genotoxic even at very low levels, so their use in food additives, pesticides and drugs for instance, is restricted. In contrast to GCs, NGCs are thought to be more likely to have a safe exposure threshold, so they can be used in products unless the level exceeds the threshold (Nohmi, 2018). Therefore, the correct classification of these compounds is highly important as it corresponds to their regulatory pathway for use in everyday products and consumables. Although, NGCs are deemed less potent, less harmful and can be licensed for use in society, these chemicals are still able to cause cancer so perhaps their use should be reconsidered. NGCs are such complex chemicals, it makes their detection very difficult and they can even produce conflicting results between different species, cell types and doses (Rieswijk *et al*., 2015).

3.1.2 Selecting chemicals

Here, data is shown for 3 known NGCs. These were selected from the literature to study alongside the ones also seen in **Chapters 4 and 5**. There are several published lists of NGCs suggesting and categorizing chemicals based on their *in vitro* and *in vivo* results to a series of recommended genotoxicity tests. These lists are useful when choosing the NGCs to further investigate as there are often suggestions of possible mechanisms (Kirkland *et al*., 2016; Hwang *et al*., 2020) (see **Table 1.3**). Whilst assessing if an *in vitro* multi-endpoint approach can detect NGCs, an idea of the mechanism utilized is useful in selecting chemicals. A thorough literature review was carried out and NGCs were chosen based on numerous factors such as; a diverse suggested MoA, understudied chemicals, a range of different types of chemicals (i.e. herbicide, clinical drug and synthetic rubber), solubility and availability to purchase. Some NGCs such as DEA and cholic acid were selected and then discounted due to problems determining doses as a result of chemical viscosity, precipitation out of solution and pH changes etc. (see **Appendices Figures A1, A2 and A3**).

The battery of tests chosen to screen the NGCs in this research, as also used in **chapters 4 and 5**, focused on a range of different mechanisms which are linked to the KCC (Smith *et al*., 2016) in order to try to decipher the exact mechanisms used by different NGCs.

3.1.3 Negative data

In general, negative results are important to the wider field, allowing other scientists to access the information and adjust their research appropriately. However, there is a known publication bias against negative data with editors preferring to publish positive results. Hence, much negative data remains unpublished and unavailable to researchers. If negative data was more widely published in the literature, it would allow for a comparative point and change of direction with the future research. By publishing negative results it allows the whole picture to be understood and informed decisions to be made (Weintraub, 2016). Begley and Ellis, (2012) suggested that in order to improve the reliability of preclinical cancer research, there should be more chances to present negative data through means of papers and conferences for example. There should be a requirement to report all findings and there should be a general view that negative data is as informative as positive data.

This chapter contains data for 3 NGCs (rosuvastatin, chloroprene and TCDD) which show largely negative data when applying the multi-endpoint testing battery used in other chapters. The complexity of NGCs may explain some of the negative results using the novel testing battery, seen with these chemicals. So, even with a wide range of endpoints tested it still does not capture all the mechanisms used by NGCs. It highlights the fact that alternative approaches are required for understanding the carcinogenicity of NGCs and that a larger battery of *in vitro* tests is required to understand the MoA.

3.1.4 Chemical 1: TCDD (2,3,7,8-Tetrachlorodibenzo-p-dioxin)

Background

TCDD is primarily used as a herbicide, **Figure 3.1** demonstrates the use of this highly toxic NGC sprayed in great quantities onto crops.

Figure 3.1: TCDD was historically used as a herbicide. The image shows it being sprayed onto crops. Image taken from (Collaborative on Health and the Environment, 2016) with permission.

TCDD (2,3,7,8-tetrachlorodibenzo-*p*-dioxin) is a Seveso dioxin and it is an environmental contaminant which does not have a distinguishable odour at room temperature. It is a product of the incomplete combustion of certain organic materials as well as a product in herbicides such as agent orange (Schecter *et al*., 2006). TCDD is well known as a contaminant and component of agent orange, a potent herbicide used during the Vietnam war (Stellman and Stellman, 2018). The effects of TCDD were not fully understood until years later when 2,4,5-trichlorophenoxyacetic acid (2,4,5-T) (another component of agent orange) was banned from domestic use due to a teratogenic effect (Stellman *et al*., 2003). It was estimated that Vietnam was subject to 366 kg TCDD spray (Stellman and Stellman, 2018). TCDD containing herbicides were primarily banned from food crops and eventually banned entirely in the U.S (ATSDR, 1998). Some examples of TCDD production, as a biproduct of numerous anthropogenic processes are the combustion of hazardous, hospital and municipal waste, chlorine gas bleaching, manufacture of wood products, tobacco, iron and steel (Tanida *et al*., 2009).

TCDD belongs to the group of polycyclic aromatic hydrocarbons (PAHs), these include polychlorinated biphenyls (PCBs), polychoorinated dibenzo-p-dioxins (PCDDs) and polychlorinated dibenzofurans (PCDFs) (Koibuchi, 2006). TCDD is a persistent organic pollutant (POP) and the chemical structure can be seen in **Figure 3.2**, which means that it can exist in the environment for a long period of time. Due to its lipophilic properties, these chemicals can accumulate in fatty tissues such as the liver and brain and also in the bloodstream and in the dermal layer of the organisms. This means that by losing fat, some harmful compounds can be released. This can lead to a number of diseases affecting the reproductive system and the immune system (Lesage, 2015). These chemicals are also capable of causing cancer, endocrine disruption and developmental issues (Maqbool *et al*., 2016).

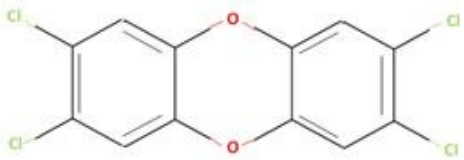

Figure 3.2: Chemical structure of TCDD. Colours represent different bonds. Red indicates an oxygen bond and green indicates a chlorine bond. Structure adapted from 2,3,7,8-tetrachlorodibenzo-p-dioxin, (2023).

TCDD is the most studied of the dioxins due to its high potency (Van den Berg *et al*., 2006). Humans are exposed to dioxins through a variety of sources such as in food products, drinking water, air, soil and dust (Tanida *et al*., 2009). Dioxins can accumulate in both plant and animal tissues, entering the food chain and therefore are a threat to human health as a result of biomagnification (Patrizi and Siciliani de Cumis, 2018). TCDD has an extended half-life ranging between 7.1 (Pirkle *et al*., 1989) and 11.3 years (Wolfe *et al*., 1994).

TCDD's cytotoxicity and genotoxicity

It is known that TCDD is carcinogenic in animal experiments however, it has not yet proven to be conclusively carcinogenic in humans. There is a lot of opposing views in the literature about the carcinogenicity potential for humans due to the widespread, low dose exposure to the contaminant. TCDD is often part of complex mixtures with other carcinogenic chemicals making it difficult to understand the effects of TCDD alone (Boffetta *et al*., 2011).

TCDD is classified as a NGC and is negative in the Ames test, the *in vitro* MLA, chromosomal aberration, sister chromatid exchange and the *in vivo* chromosomal aberration assay (Hwang *et al*., 2020). TCDD underwent ingenuity pathway analysis (IPA) of gene expression to investigate some of the potential diseases it can cause and which mechanism it uses to achieve this. It was found that cell transformation can cause oncogenesis, cell death and survival is affected due to apoptotic changes. Also, developmental and functional abnormalities of the cardiovascular system are due to systolic pressure alterations. TCDD can also affect behaviour due to disruption of the long-term recognition memory and cellular movement can be disrupted due to macrophage cellular infiltration (Hwang *et al*., 2020). Ozden *et al*., (2015) investigated whether DNA methylation could be a potential indicator for NGCs, alongside different primary MoAs. TCDD induced some gene methylation alterations, however it did not expose a mechanistic pathway utilized by TCDD to initiate oncogenesis.

TCDD exposure

Epidemiology studies for TCDD are limited and there is not enough evidence to form a solid conclusion. Although, animal studies suggest TCDD is carcinogenic, the epidemiology studies are often inconclusive or negative in association (Boffetta *et al*., 2011). There may also be some biases in regard to political and emotional issues as this research area has been active for over 40 years. Other biases that may include selective reporting due to the concerns surrounding TCDD as an environmental carcinogen (Boffetta *et al*., 2011).

TCDDs MoA

It was shown that as a result of high dose TCDD exposure there was a slight increase in the risk of cancer to humans (IARC, 1997). Mechanistic evaluation confirmed that the activation of the aryl hydrocarbon (Ah) receptor led to both animal and human carcinogenesis. This then led to the classification of TCDD as an IARC Group 1, established human carcinogen (Boffetta *et al*., 2011). It is thought that TCDD utilizes receptor binding as its MoA (Mandal, 2005) specifically the aryl hydrocarbon receptor (AhR). The AhR is recognised as a molecular switch and regulator of cell proliferation, differentiation and regulating xenobiotic metabolism. The AhR is considered to be commonly involved in many toxic responses observed even though the mechanisms of TCDD carcinogenicity are otherwise largely unknown (Bock and Köhle, 2006). TCDD exposure affects humans in a number of ways such as birth defects, chloracne and cancer (Boffetta *et al*., 2011). TCDD is able to induce a range of toxic effects including immunosuppression, teratogenesis and tumour promotion all as a result of the AhR (Mimura and Fujii-Kuriyama, 2003).

3.1.5 Chemical 2: Chloroprene

Background

The industrial area of Mississippi where chloroprene is used to produce neoprene is known as ‘Cancer alley’ and is linked to a high cancer incidence locally thought to be due to the output of smoke and fumes produced and links to epidemiological studies. The production of dense smoke from the neoprene factories can be seen in **Figure 3.3**. This issue has been highlighted by the British Broadcasting Corporation (BBC) in order to spread awareness of this issue (Wareham and Rosney, 2020).

Figure 3.3: Cancer alley image, demonstrating the level of smoke produced as a result of chloroprene production. Image taken from (EcoEnclose, 2020).

Chloroprene is largely understudied in the literature which may be as a result of the complexity of these NGC chemicals. Although chloroprene is classified as an IARC group 2b carcinogen ('possibly carcinogenic to humans'), it is also a NGC (Vinken *et al*., 2008).

Chloroprene is otherwise known as 2-chlorobuta-1,3-diene (C_4H_5Cl) it is a monomer and is a volatile and flammable liquid **(Figure 3.4)**. There are no known occurrences of chloroprene in nature and the only sources of chloroprene in the environment are from waste and emissions from the chloroprene production plants and the transportation of this chemical (EPA, 2010). As chloroprene is both volatile and lipid soluble it cannot exist in the environment and therefore does not bioaccumulate (Guo and Xing, 2016).

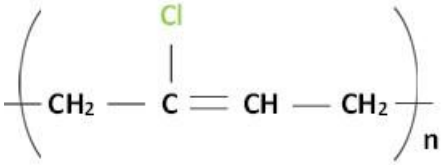

Figure 3.4: The chemical structure of chloroprene is a monomer, the polymer forms neoprene. This structure was adapted from polychloroprene: 9010-98-4, (2023). The colour green represents the chlorine bond.

The NGC, chloroprene is a colourless liquid with a strong aroma (Guo and Xing, 2016). It is used in the commercial production of synthetic rubber alongside other chemicals such as 1, 3-butadiene (Himmelstein *et al.*, 1997). Chloroprene (or ß-chloroprene) is used to produce polychloroprene (or Neoprene) which is a rubber product used in automotive purposes, wire and cable insulation and adhesives (Valentine and Himmelstein, 2001). It has an approximate atmospheric half-life of between 4 and 20 hours (Grosjean, 1990). Chloroprene is manufactured from the starting material butadiene and undergoes a 2-step process which includes both chlorination and dehydrochlorination reactions (EPA, 2010). Chloroprene is an analogue of

isoprene and is also analogous to vinyl chloride (EPA, 2010). Both butadiene and vinyl chloride are very volatile and well-known potent human carcinogens (Albertini *et al*., 2003).

Following a series of chronic inhalation studies with chloroprene, it was demonstrated that the early presentation of tumours, the further development of malignancies and occurrence of multiple tumours across animal species (NTP, 1998) all contributed to the classification of 'likely to be carcinogenic to humans. There is some, although limited, evidence of an association between lung cancer and liver cancer risk with occupational exposure to chloroprene (EPA, 2010).

Chloroprene exposure

Absorption routes for chloroprene are through the skin, inhalation, ingestion and both skin and eye contact. Leading to the main cancer types of the lung and skin. Some of the internal organs that chloroprene targets are the eyes, the respiratory system and the reproductive system. Some of the symptoms that humans have experienced from chloroprene exposure are irritated eyes, dermatitis, reproductive effects as well as change in mood and anxiety (CDC, 2022).

There is opposing information in the literature about the results of occupational exposure to chloroprene and the risk of cancer. Bulbulyan *et al*., (1999) demonstrated through epidemiological studies that both the incidence and mortality of liver, lung and digestive tract cancers were significantly higher among the workers in a chloroprene production plant. However, Acquavella and Leonard, (2001) highlighted several limitations within these epidemiological studies. Due to the low numbers of deaths, lack of information on the exposures and the lack of follow-up information on the workers, it cannot be assumed that cancer incidence and chloroprene exposure is linked in these studies.

Epidemiological studies of Chloroprene

St John the Baptist Parish on the Mississippi corridor in Louisiana, was thought to have the highest risk of cancer as a result of exposure to carcinogens such as chloroprene and ethylene. This area has gained the name 'cancer alley' as a result of the high cancer incidence. In May 2021, the Environmental protection agency (EPA) inspector announced that there needed to be updated risk reviews of the sites that release both chloroprene and ethylene oxide to protect the residents from the exposure (Randolph, 2021). Geographic information system (GIS) mapping has found pollution inconsistencies in affected people, based on race, income and education. In St James Parish in cancer alley, the highest percentage of residents are of African American

origin, the lowest average household incomes and most of the residents have not graduated from high school. The individuals who work at the plants tend to live further away, are wealthier, better educated and predominantly white (Blodgett, 2006).

Chloroprene's cytotoxicity and genotoxicity

The genotoxicity of chloroprene is often questioned due to a series of conflicting results in the literature. Chloroprene is negative for the *in vitro* Mn assay, the chromosomal aberration assay and sister chromatid exchange (Tice *et al*., 1988). Genotoxicity results for chloroprene vary greatly, further highlighting the complexity of NGCs. For example, certain strains of *Salmonella typhimurium* bacteria produce positive results in the Ames test whereas others produce negative results. The results for the *in vitro* Mn assay are negative in the multiple studies assessed (EPA, 2010).

Chloroprene is a known carcinogen in both rats and mice, predominantly causing neoplasms in the lungs of female mice (Huff *et al*., 1985). Chloroprene can give misleading results and its genotoxic potential is often discussed throughout the literature however, it is classified as a NGC (Kakiuchi-Kiyota *et al*., 2012). Even though butadiene and chloroprene are similar, they differ in their classification. Butadiene is listed in the NTP's report on carcinogens (RoC) as 'known to be a human carcinogen' due to the mechanistic and epidemiological information. However, chloroprene is listed in the RoC as 'reasonably anticipated to be a human carcinogen' (NTP, 2000). Epidemiology studies for butadiene showed an increased incidence of lymphoma and leukaemia in exposed worker (Macaluso *et al*., 1996).

Chloroprene *in vivo* studies

In vivo studies show inconsistencies when different species are tested with chloroprene, when mice are tested, they demonstrate the onset of tumours at lower concentrations when compared to other species. Due to the different response to chloroprene exposure in mice, compared to other *in vivo* studies, it indicated that mice are not the best species to assess. Thus further proving that mouse models are not comparable to humans (Sax *et al*., 2020). Animal studies demonstrate a positive response for carcinogenicity, however there are huge species-species differences between the effects exerted by chloroprene. Humans are less susceptible to the carcinogenic effects of chloroprene when compared to mice as a result of the differences in metabolism (Sax *et al*., 2019).

Chloroprene MoA

Chloroprene has been assessed via a 2-year rodent bioassay, specifically the B6C3F$_1$ mouse, which is characteristic for NGCs. The 2-year bioassay identified oncogene activating mechanisms (NTP, 1998). Both *KRAS* and *HRAS* mutations have been mutated, causing lung neoplasms (Sills *et al*., 1999). There is also a suggested mutagenic mode of action of chloroprene and structural similarities between chloroprene and 1,3-butadiene (EPA, 2010). It has been suggested that chloroprene has an alternative MoA, potentially involving chronic cytotoxicity leading to compensatory hyperplasia. It was shown that chloroprene is toxic to animals at higher doses leading to an increased mortality rate. However, *in vivo* genotoxicity was not positive, implying that the MoA of chloroprene may be target-site cytotoxicity (Shelby, 1990). This suggested cytotoxicity MoA is also supported by chloroprene treatment in F344 rats and B6C3F1 mice as a result of cell death or injury, as well as tissue regeneration (Melnick *et al*., 1996).

As previously stated, the mechanism(s) of chloroprene carcinogenicity are largely unknown however, it is known that the mechanism utilized by chloroprene is probably not genotoxic (Vinken *et al*., 2008). Histopathological target tissue evaluation in mice supported a non-genotoxic MoA (Sax *et al*., 2020). However, in contrast, it has also been suggested that chloroprene exposure gives rise to tumours in rodents using a genotoxic mode of action (Himmelstein *et al*., 2004). This is contradictory to other reports in the literature, although it is clear that chloroprene is largely misunderstood.

The exact mechanism of chloroprene carcinogenesis is largely disputed and is not understood. Most of the molecular and therapeutic targets are lacking for chloroprene induced lung cancer (Guo and Xing, 2016).

3.1.6 Chemical 3: Rosuvastatin

Background

The complicated chemical structure of rosuvastatin can be seen in **Figure 3.5** below.

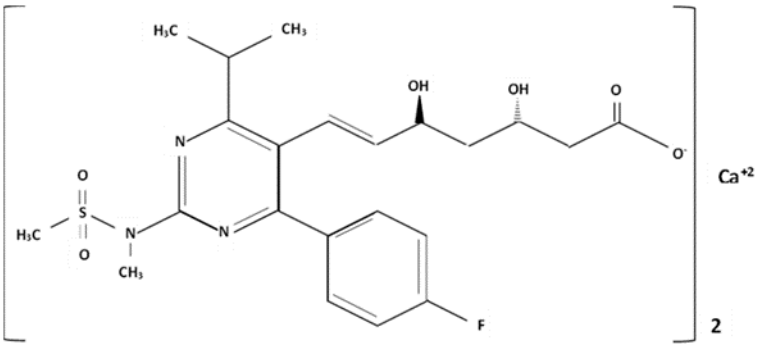

Figure 3.5: Chemical structure of rosuvastatin. This structure was adapted from Ashfaq *et al.,* (2013).

Rosuvastatin is part of the collective group of drugs called statins, which are designed to lower levels of bad cholesterols such as low-density lipoproteins (LDL) and to raise levels of good cholesterol such as high-density lipoproteins (HDL). By regulating cholesterol levels, this can help prevent heart attacks and strokes. They work by limiting the levels of cholesterol produced by the liver (Webmd.com, 2022). Rosuvastatin is in the hydrophilic class, which primarily acts in the liver (Lustman *et al*., 2013). The hydrophilic nature of rosuvastatin is important as it means that this molecule can have access to numerous cell types in the body via the passive diffusion across cellular membranes (McTaggart, 2003). It has been demonstrated that rosuvastatin only undergoes very minimal metabolism via the CYP system. Rosuvastatin seems to show the same limited metabolism both *in vitro* and *in vivo* (McTaggart, 2003). There are promising QSAR for rosuvastatin and suggests they can perform better than current statin drugs (Samizo and Kaneko, 2023).

There is opposing information in the literature regarding statins and cancer in humans. There have been studies that show that statin use can be correlated with a reduced risk of oncogenesis. Cholesterol plays a role in prostate, breast and colorectal cancer, which is reflected in the studies carried out. The results of *in vivo* studies and clinical trials on cancer incidence are being investigated for statin therapy (Barbalata *et al*., 2020). Some studies show that certain statins such as rosuvastatin, simvastatin and atorvastatin are associated with a decreased incidence of prostate cancer (Lustman *et al*., 2013).

Cardiovascular disease is constantly rising in incidence and is the leading cause of mortality in China, contributing to 40% of deaths (Sun *et al*., 2017). Statins have proven to reduce morbidity and mortality in patients with cardiovascular disease (Anderson *et al*., 2018). Statins are shown to be very effective lipid lowering drugs, capable of also reducing the total cholesterol as well as LDL (Zhao, 2016). Statins are currently the most frequently prescribed medication in numerous

countries (Salami *et al*., 2017). There is also an increase in statin use among diabetes and hyperlipidaemia patients (Liu *et al*., 2020).

The importance of statin use has been shown to play a role in both primary and secondary prevention of coronary heart disease, myocardial infarction and ischemic stroke, evident through clinical trials (Liu *et al*., 2020). Rosuvastatin had an increase in use from 2012 to 2016 and was classified as the highest ranked statin, followed by atorvastatin and then simvastatin. The three most frequently prescribed statins during 2012-2018 was rosuvastatin, atorvastatin and simvastatin. The increased statin use was mirrored world-wide, not only in China (Liu *et al*., 2020).

Rosuvastatins Mechanism of Action

Rosuvastatin is thought to act via a mechanism of inhibiting 3-hydroxy-3-methylglutaryl-coenzymeA reductase (HMG-CoA) (AstraZeneca, 2022) as demonstrated in **Figure 3.6.** Statins are capable of obstructing the key enzymes active site in the mevalonate metabolic pathway. This means that HMG-CoA is not converted to mevalonic acid and therefore hepatic cholesterol synthesis is reduced. Due to increased microsomal HMG-CoA reductase and cell surface LDL receptor expression, this allows the removal of LDL from the bloodstream (Ward *et al*., 2019).

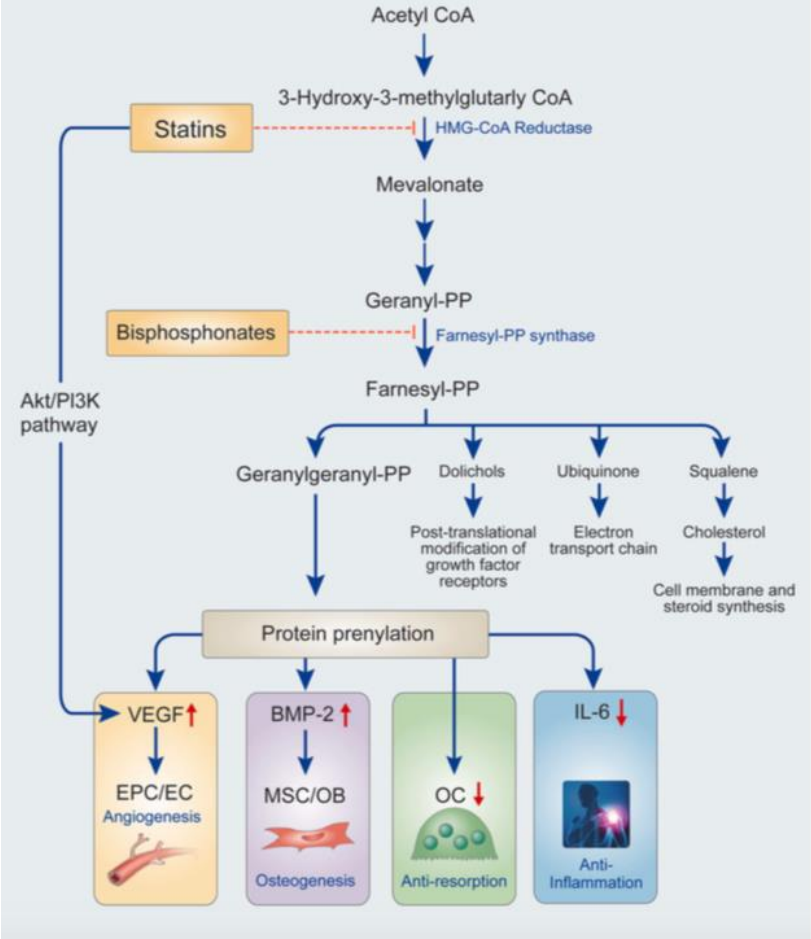

Key	
VEGF	Vascular endothelial growth factor
BMP-2	Bone morphogenetic protein 2
IL-6	Interleukin 6
OC	Osteoclast
MSC	Mesenchymal stem cells
EPC	Endothelial progenitor cells
EC	Enterochromaffin
OB	Osteoblast

Figure 3.6: A flowchart explaining how statins work, by inhibiting HMG-CoA reductase. Some of the downstream effects of statins are shown with the arrows. This image is taken from (Shah *et al*., 2014). The key explains the abbreviations used in the flowchart.

As rosuvastatin is largely understudied in the literature, the carcinogenic MoA is unknown, but it is labelled as a NGC (Hwang *et al*., 2020).

Rosuvastatins cytotoxicity and genotoxicity

Rosuvastatin is negative in the Ames test with standard strains and in *E. coli.* It was negative for cytogenetic aberrations carried out using the *in vivo* in mouse bone marrow micronuclei and also negative for *in vitro* genotoxicity tests such as the MLA and the CA. However, rosuvastatin has been classified as a NGC as it has negative results in all genotoxicity tests, but it is positive for carcinogenicity, such as the 2-year bioassay, in rats and mice (Kirkland *et al*., 2016).

There are contradicting results in the literature regarding the effects of different statins on Mn frequency. Atorvastatin has been shown to significantly decrease the Mn frequency in human lymphocytes (Hosseinimehr *et al*., 2015) however, rosuvastatin significantly increased Mn frequency in human lymphocytes (Berber *et al*., 2014). It has been suggested that rosuvastatin

gives positive results to the *in vitro* Mn assay and comet assay. This suggests that rosuvastatin is genotoxic by MoA (Berber *et al*., 2014) and therefore may have been misclassified, which is alarming, as rosuvastatin is still used clinically.

***In vivo* studies**

In a rat study it was demonstrated that rosuvastatin selectively targets the liver before uptake in any other organ. Pravastatin, a hydrophilic molecule like rosuvastatin, exhibited selectivity for the liver unlike simvastatin which showed uptake into the spleen and adrenals as well as the liver (McTaggart *et al*., 2001). It has been demonstrated in an *in vivo* study on *Drosophila melanogaster* that the anti-cancer drug doxorubicin induces cardiotoxicity and genotoxicity, however with rosuvastatin co-treatment there is a reduction in mutant spots on *D. melanogaster* which represent genotoxicity. This is also evidence of an anti-cancer effect of certain statins (Orsolin *et al*., 2015).

Rosuvastatin's clinical information

In clinical use, rosuvastatin is mainly removed by the faecal route and the plasma half-life of rosuvastatin circulation is thought to be 20 hours (McTaggart *et al*., 2001). Rosuvastatin was more effective at reducing LDL and had more beneficial effects than a lot of the comparative commercially available statins such as lovastatin, simvastatin and atorvastatin (White, 2002). Rosuvastatin was first used clinically in 2003, a long time after simvastatin which was first used in Sweden in 1988 (Hajar, 2011). There is also a noted risk of diabetes while taking statins such as rosuvastatin, commercially known as Crestor (Hajar, 2011) or formally known as ZD4522 (Olsson *et al*., 2001). Rosuvastatin has shown to have caused cases of kidney failure/damage or rhabdomyolysis before the drugs approval. The 80 mg dose of rosuvastatin has been removed by AstraZeneca however as there are still concerns of proteinuria and haematuria at the lower doses (Public Citizen, 2022). Rosuvastatin has 201 drug interactions, including 165 moderate, 25 major and 11 minor interactions (Drugs, 2022). Olsson *et al*., (2001) demonstrated that as the result of a small patient-based dose finding study, rosuvastatin seemed to be well tolerated and resulted in lowering LDL cholesterol. Some of the main side effects experienced as a result of rosuvastatin treatment were nausea, diarrhoea and abdominal pain (Olsson *et al*., 2001).

It is somewhat concerning that rosuvastatin is still available on the market despite its classification as a NGC. It is still available due to the positive benefit-risk profile if it is used at the recommended doses and the clinical advantages in successfully lowering LDL-cholesterol better than other available statins (Florentinus *et al*., 2004).

3.1.7 HepG2 spheroid model

HepG2 are derived from a hepatocellular carcinoma and the cell line was isolated in 1975 (Aden *et al.,* 1979). This cell line was among the first liver cell line to perform key hepatocytes characteristics (Arzumanian *et al*., 2021). HepG2 is the most commonly published liver cell line according to PubMed searches (Arzumanian *et al*., 2021). HepG2 is a frequently studied spheroid model in the form of the 'hanging-drop' method and with the use of a matrigel or hydrogel scaffold (Higuchi *et al.,* 2016; Shah *et al.,* 2018). One of the main negatives with the HepG2 cell line is the poor expression of the CYP enzymes (Guengerich, 2019). However most metabolic functions are well conserved in HepG2 cells, which is why they are so widely studied (Pareek *et al.,* 2013).

Liver cells such as the HepG2 cell line contain the necessary metabolism machinery required in drug testing (Shah *et al.,* 2018), so may prove to be useful in the detection of complicated NGCs. HepG2 cells have proven to have a poor metabolic capacity as a two-dimensional (2D) culture. However, when these cells are used in a three-dimensional (3D) 'hanging-drop spheroid' model, they have an increased metabolic capability (Shah *et al.,* 2018). It was thought that as these three NGCs are largely negative in most of the *in vitro* test battery, perhaps they would benefit from a more physiologically relevant model.

3.2 Methods

Methods utilised in this chapter were performed as detailed in the main methods.

3.2.1 Cell lines

The cell line used to study rosuvastatin and chloroprene was the human lymphoblastoid cell line TK6 (received from ATCC). However, TCDD requires metabolic activation so MCL5 cells were used. The MCL-5 cell line was established from human lymphoblastoid TK6 cells but was transfected with the cDNAs of certain human cytochrome P450s. Full details of both cell lines are detailed in the main introduction in **Chapter 2 in section 2.2.1 and 2.2.2**.

3.2.2 Cell culture

Both cell lines were maintained in a total volume of 30 ml cell growth medium in a 75 cm^2 flask. They are kept at a concentration of 1 x 10^5 cells/ml but not reaching 1 x 10^6 cells/ml. Cells were maintained at 37°C and 5% CO2 in a humidified incubator. However, MCL-5 cells required the addition of Hygro B (Merck) in the ratio 4 µg/ml. Further explanation of Hygro B is in sections 1.9.2 and 2.2.2. Full details are described in the main methods in **Chapter 2 section 2.2.3.**

3.2.3 TCDD test chemical

2,3,7,8-Tetrachlorodibenzo-*p*-dioxin**,** TCDD (LGC Standards, Teddington) utilized DMSO as its solvent and diluted fresh before each use. It was available as a liquid already dissolved in its solvent. Full details of all the test chemicals are detailed in the main methods in **Chapter 2 in section 2.3.3**.

3.2.4 Chloroprene test chemical

This chemical utilized methanol as its solvent as was diluted fresh before each use. It was available as a liquid already dissolved in its solvent. This chemical was available from Sigma Aldrich (Merck), Dorset. This chemical was stored at 4°C to prevent polymerization in **Chapter 2 in section 2.3.3**.

3.2.5 Rosuvastatin test chemical

This chemical utilized DMSO as its solvent as was weighed and diluted fresh before each use. This chemical was available from Sigma Aldrich (Merck), Dorset in **Chapter 2 in section 2.3.3**. Further details on negative and positive controls can be found in sections 2.3.1 and 2.3.4 respectively. Further details of the exposure regimes and the doses of each test chemicals can be found in sections 2.3.2 and 2.3.3 respectively.

3.2.6 Additional data- HepG2 3D spheroid Micronucleus and CBPI assessment

HepG2 cells

HepG2 cells (ATCC) are an adherent liver cell line with metabolic capabilities, used in this work to form a 3D spheroid microenvironment, in order to understand whether this will improve the detection of these NGCs *in vitro*. HepG2 cells were cultured using DMEM medium (Gibco, fisher scientific) with 4.5 g/L D-glucose and L-glutamine with the addition of 10% foetal bovine serum (FBS) (Gibco, fisher scientific) and 1% penicillin/streptomycin antibiotic (100 units/ml penicillin and 0.1 mg/ml streptomycin) (Gibco, fisher scientific).

Spheroid formation

HepG2 monolayers were used to make the spheroids using the hanging drop method previously used in the Swansea laboratory. The viability of the cells used for spheroids was determined using Trypan blue (CAS:72-57-1, Sigma, Dorset) and the cells were counted using a haemocytometer or the Luna II automated cell counter. Trypan blue was the first method of measuring cell viability used (Chan *et al*., 2015) and is still a commonly used technique (Pamphilion *et al*., 2013). The trypan blue is often used with a haemocytometer grid and this combination is the standardised approach for calculating the cell population (Belini *et al*., 2013).

The Initial cell density was 4,000 cells per 20 µl drop of growth media. The drops were carefully pipetted on the inner side a 9.4 cm Square Petri dish (Greiner bio-one, UK) lid. The lids contained ~100 or more drops per dose of the analysis. The cell suspension was gently aspirated by the pipette to ensure the cells were thoroughly suspended within the media. To prevent the drops from drying, the 9 cm Petri dish (inner compartment) was filled with 20 ml PBS (Gibco, fisher sci). The lid was carefully returned onto the Petri dish containing PBS and the whole set up was placed gently into the incubator at 37°C and 5% CO_2 atmosphere. The cell viability in the hanging drop was maintained by adding 6 µl of growth media to each drop on day 3.

The mononucleate micronucleus assay (Mn)

On day 1 the spheroids were prepared as mentioned above, the spheroids were left to form and grow in the incubator with 37°C and 5% CO_2. On day 3, the 6 µl of growth medium was added to the hanging drop in order to maintain cell viability. On day 4, the 100 spheroids per dose were treated with 6 µl of the test chemical for 24-hours and maintained in a non-hanging position after the dose has been delivered. The bottom part of the Petri dish, previously containing PBS was emptied and dried before being used as a lid over the spheroids. There was no recovery day with this treatment. On day 5, the spheroids are separated using 0.05% trypsin (Gibco) before the

harvest and slide preparation for Mn analysis. The Spheroids were collected in 15 ml labelled centrifuge tubes already containing 1 ml of the DMEM growth media and centrifuged at 279xg for 5 minutes. The supernatant was discarded and then the spheroids were washed once with 2 ml PBS and again centrifuged at 279xg for 5 minutes and the supernatant was discarded. The spheroids were re-suspended into 500 µl trypsin and were incubated for 8 minutes at 37°C and 5% CO_2. After the incubation, the suspension was aspirated gently up and down to ensure that spheroids were completely dissociated. This was then followed by the addition of 2 ml of PBS before centrifugation (279 xg for 5 minutes) and the supernatant was discarded. The pellet was re-suspended into 1 ml PBS. The cells were counted using trypan blue in the Luna II automated cell counter to measure the viability, which should be more than 60%. The slide preparation was carried out as described in the general methods, **section 2.4.3**. When the cells from the spheroid are being fixed, the volume of Fix solution used is much less than with the 2D cell culture documented in **section 2.4.3** as the pellet formed by the 100 spheroids is much smaller. Instead of adding > 5 ml Fix (depending on the size of the pellet) it is more likely that < 500 µl will be used in total. Scoring of mononucleate cells were performed on the Metafer 4 software of the semi-automated metafer system.

Cytotoxicity assessment

The cytokinesis block proliferation index (CBPI) was calculated using the Metafer system, however the CBPI calculation was used in the absence of cytoB, just as a snapshot measurement of the cellular proliferation rate. A total of 1000 cells were scored and separated into mononucleate cells and BN cells using the criteria highlighted by Fenech, 2000. This work was all completed with 3 replicates. This was done alongside the mononucleate Mn in order to understand the cytotoxicity present. Cytotoxicity assessment is more difficult to calculate with spheroids as the cells cannot be counted as freely as 2D cultures due to the limited volume and due to the nature of the spheroids needing to be separated using trypsin.

The calculation below was utilized to calculate the CBPI:-

$$\text{CBPI} = \frac{((\text{No. mononucleate cells}) + (2 \times \text{No. BN cells})}{(\text{Total number of cells})} \times 100$$

The BN frequency was also calculated in order to observe the natural division rate of the spheroids after treatment.

3.3 Results

The three remaining chemicals TCDD, rosuvastatin and chloroprene have here undergone the same testing battery as chemicals in **chapter 4** ($NiCl_2$) and **chapter 5** (2 forms of As). This multiple endpoint analysis includes both acute and chronic assessment with the mononucleate Mn assay, ROS analysis, cell cycle assessment, apoptotic investigation, further investigation to mitochondrial function and exploration of a general cancer gene panel. The testing battery demonstrates the importance of assessing multiple endpoints with these chemicals, highlighting the complexity of NGCs.

3.3.1 TCDD

This chemical has demonstrated very little in the way of positive effects and therefore insight into its MoA from the endpoints assessed in this testing battery. The mononucleate Mn assay was carried out in both an acute **(Figure 3.7)** and chronic **(Figure 3.8)** fashion. **Figure 3.7** shows no significant genotoxicity or cytotoxicity induced in an acute spiked dosing regimen. The doses were chosen as a result of informed literature searches. Most of the literature suggest that a nano range should be utilized for TCDD and that 0.1 µM should be the top dose (Karman *et al*., 2012). However, previous studies from our laboratory have also used doses of up to 3 µM for TCDD and it was at this top dose where a significant effect was seen for mRNA expression (Wilde *et al*., 2017). The acute treatment (**Figure 3.7**) was carried out first with 1 µM as the top dose, as DMSO levels were kept below 1% with this dose. There was enough chemical to make up extra doses for chronic treatment to see if the slightly higher doses would have an effect (**Figure 3.8**). Due to the TCDD being already dissolved in DMSO, the 3 µM dose meant that there would be 2% DMSO added to the cells, so the negative control used was also 2% DMSO.

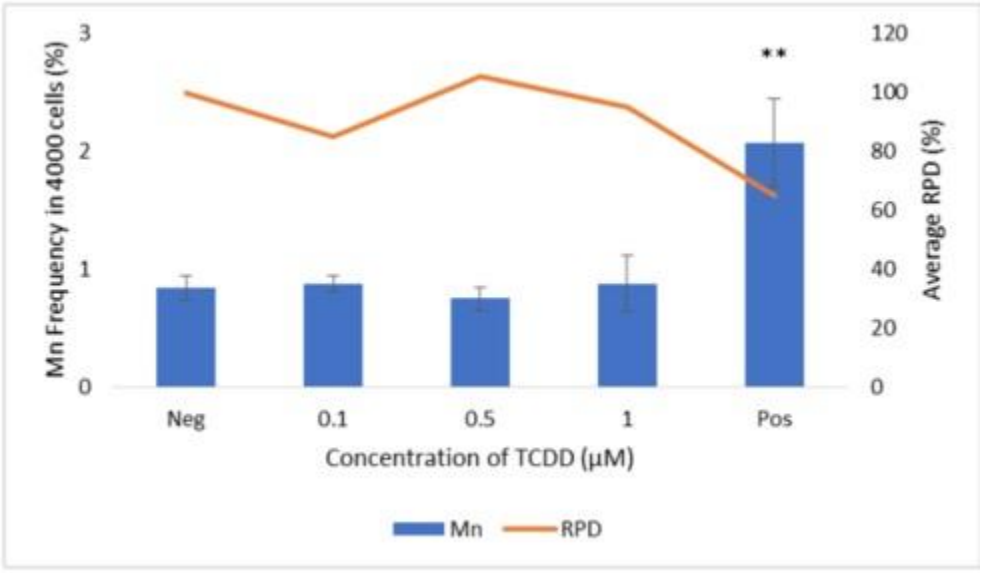

Figure 3.7: The acute (24-hour +24-hour recovery) mononucleate micronucleus (Mn) assay was carried out alongside relative population doubling. This graph shows the treatment of MCL5 cells with TCDD. This work is n=3 and the average was plotted with error bars. The negative control used here was DMSO and 10 µM MMS was used as the positive control. There is no statistical significance with the addition of TCDD, however there was significance with the addition of MMS giving a *P* value of 0.0055.

In order to assess more real-life exposures, chronic dosing was utilized, which includes a 5-day fractionated experiment with the same total doses as the acute assay. The chronic (fractionated) dosing experiment data is shown in **Figure 3.8** which comprises the same total doses as **Figure 3.7.** This again shows no induction of Mn indicating no genotoxicity induced and also no change in the cytotoxicity as measured by RPD.

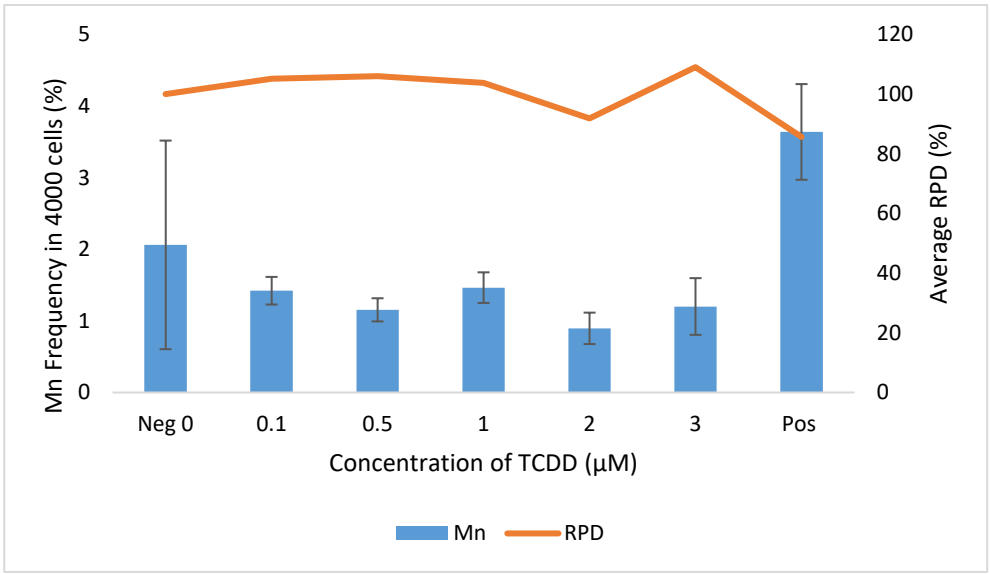

Figure 3.8: The chronic (5-day fractionated treatment) mononucleate micronucleus assay was carried out alongside relative population doubling. This graph shows the treatment of MCL5 cells with TCDD. This work is n=3 and the average was plotted with error bars. The negative control used here was DMSO and 10 µM MMS was used as the positive control. There is no statistical significance here with the addition of TCDD or MMS (due to large error bars).

As already mentioned, ROS induction are an important MoA for several NGCs. The DCFDA assay allows for the generation of quantitative fluorescence values indicating the level of ROS present at each time point. **Figure 3.9 (a and b)** shows the ROS induction data for TCDD at each of the time points and doses measured. There is no evidence of ROS induction, in fact at 2 and 3 hours there is actually a significant reduction in ROS, suggesting a possible AOX action.

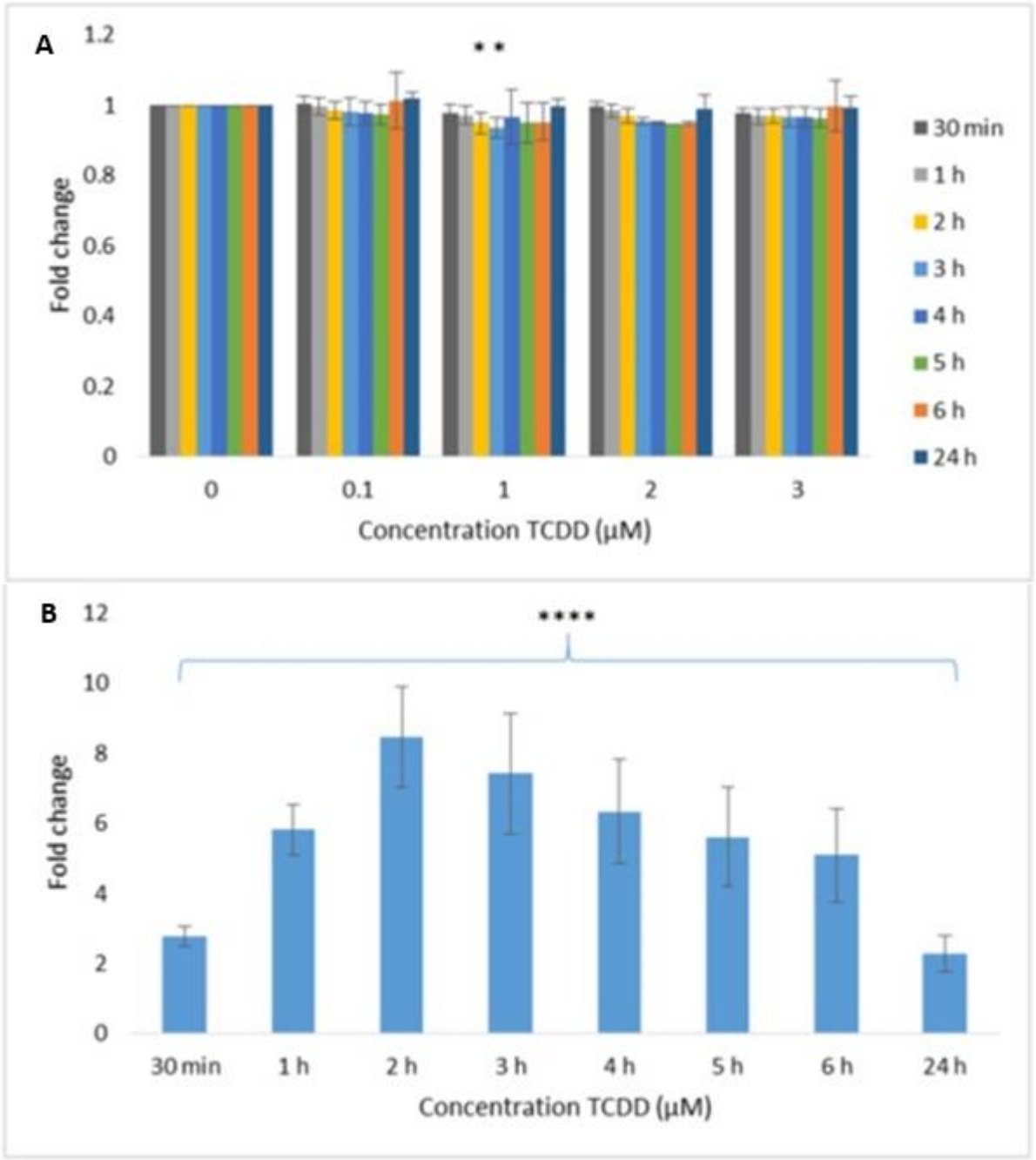

Figure 3.9 (a and b): The total reactive oxygen species (ROS) produced from 30 minutes, 1-6 hours and at 24-hour readings with no recovery. This work is n=3 and the average was plotted with error bars included. The negative/solvent control used was DMSO and hydrogen peroxide at 100 µM is the positive control (indicated as graph B). There is a statistically significant drop in ROS production at a concentration of 1 µM at 2h (P = 0.0469) and 3h (P = 0.0322) exposures. The positive control was also significantly increased when compared to the negative control with a P value of 0.00004.

Cell cycle checkpoints are closely linked with DNA damage and consequently can have an effect on tumourigenesis. TCDD has little effect on the cell cycle checkpoints **(Figure 3.10)** overall, suggesting this MoA is not utilized by TCDD.

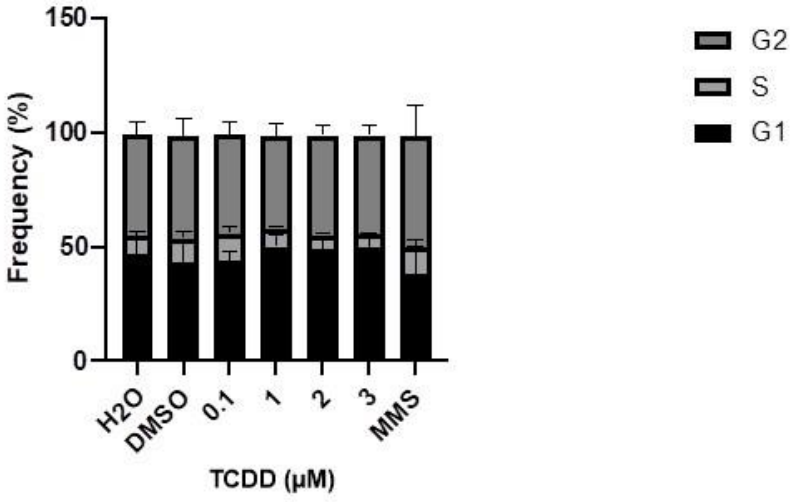

Figure 3.10: Cell cycle analysis of TCDD at 24-hours without recovery. The cell cycle stages G1, S and G2 are represented using the flow cytometric method. n=3 was performed including 3 technical replicates and the average was plotted with error bars. The negative control used here was DMSO and 10 µM MMS was used as the positive control here. The key is shown to the top right with different colours representing each cell cycle stage. No statistical significance shown here.

DNA damage induction and cell cycle stress are capable of initiating apoptosis, so they are often closely linked. In this case there are correlations among most of the endpoints for TCDD as there is largely a minimal response. Annexin V and 7-AAD dyes were therefore used in order to assess levels of apoptosis in cells exposed to the different doses of TCDD. The Q4 quadrant represents live cells, Q3 represents early apoptosis, Q2 late apoptosis and Q1 necrotic cells. **Figure 3.11** shows that TCDD has a minimal but consistent increase in apoptosis when compared to a water control but not compared to the DMSO control (in which TCDD is dissolved). However, there does not seem to be a significant increase in the induction of apoptosis, so TCDD is not utilising this MoA.

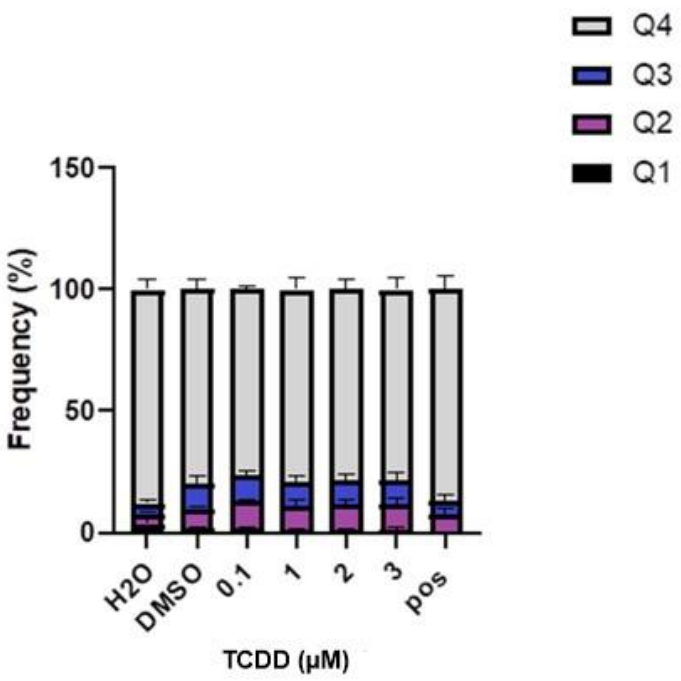

Figure 3.11: Apoptosis analysis of TCDD at 24-hours without recovery using the annexin V and 7-AAD dyes and the flow cytometry method. Q1 is the percentage of necrotic cells. Q2 is the percentage of late apoptotic cells. Q4 is the percentage of viable cells and Q3 is the percentage of early apoptotic cells. The negative control used here was DMSO and the positive control was 0.1 µM staurosporine. n=3 was performed including 3 technical replicates and the average was plotted with error bars. The key indicates the stages Q1-Q4. There was no statistical significance observed here.

A PCR array was used to further investigate the transcriptional changes that could explain the carcinogenic mechanisms utilized by TCDD. A general cancer panel was specifically used here. **Figure 3.12** shows a great number of up and down-regulated genes of interest to the MoA of TCDD. This could be vital to understanding the otherwise unknown MoA of TCDD. **Figure 3.12** shows that TCDD had the greatest number of gene expression changes when compared to all other chemicals assessed. This is an important observation as it is the only positive endpoint for TCDD, other than gene expression changes there is no other indication of the MoA utilised by this NGC. The *TF* receptor is highly upregulated for TCDD and is important to consider as TF has a role in allowing iron into the cell. This is important when considering iron dependant processes such as ferroptosis for example which is a type of iron dependant cell death (Daniels *et al*., 2012). *FGFR2* is also highly upregulated in TCDD and has been identified in several cancers. If it is deregulated it can lead to mutations in *FGFR2* and can lead to tumour promotion. *FGFR2* has a role in stimulating proliferation and migration (Szybowska *et al.,* 2019).

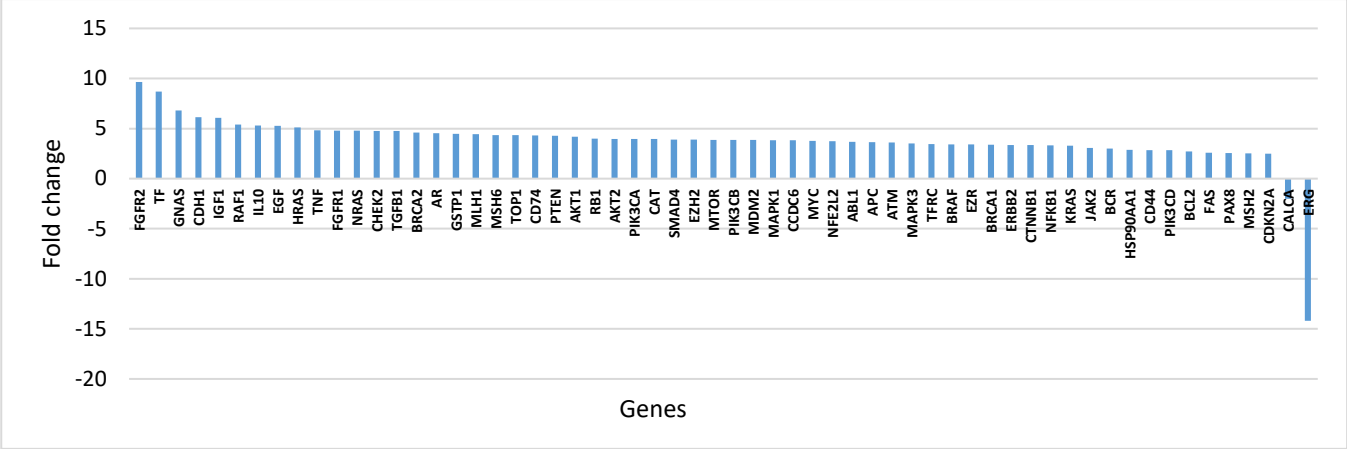

Figure 3.12: The PCR array for a general panel of cancer genes was carried out. The biologically relevant gene expression changes (±2 fold change) are represented in the graph. The MCL5 cells were dosed with 2 µM TCDD for 24-hours before the RNA was extracted for the PCR array. The PCR array was compared to the negative/solvent control which was DMSO. Most biologically relevant genes are upregulated but there are two that are also downregulated (*ERG* and *CALCA*). This work is n=1, therefore no statistical analysis was carried out.

Mitochondrial stress is often induced by toxic agents and is capable of inducing DNA damage. Mitochondrial function can be assessed using the Seahorse bioanalysis platform. The OCR for TCDD is largely unchanged **(Figure 3.13)**, it is slightly increased when compared to the DMSO control at the maximal respiratory capacity, although very similar throughout. This is rare as most NGCs cause a drop in the maximal respiratory capacity rather than an increase although it is not significant. The full Seahorse data breakdown can be found in **Figure 3.14 (A-H)** for TCDD.

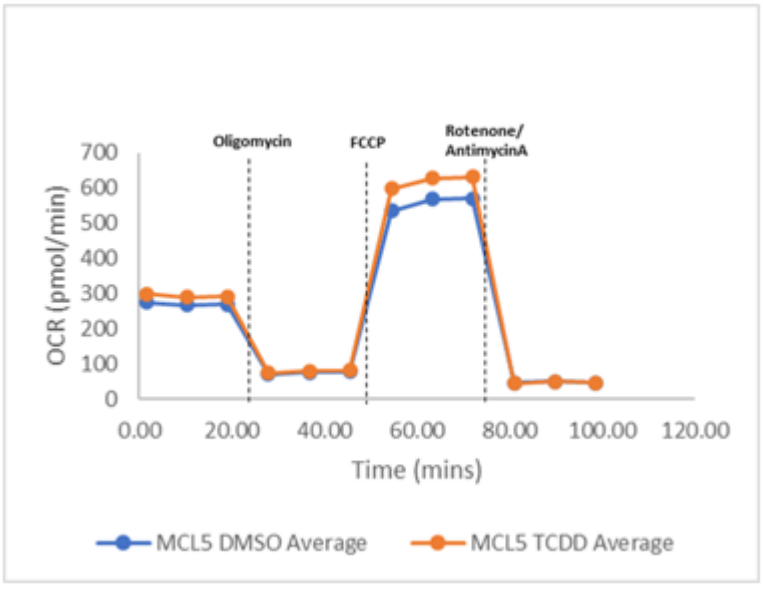

Figure 3.13: A Seahorse trace graph showing the bioenergetic flux profiles of 2 µM TCDD compared to the DMSO negative/solvent control. Oligomycin, FCCP and rotenone/antimycinA are chemical stressors

added at different time points to investigate the mitochondrial stress reaction. The full name of FCCP is (carbonyl cyanide-p-trifluoromethoxy) phenylhydrazone and it acts as a mobile ion carrier. n=3 was performed here and the average was plotted.

The 8 Seahorse XF outputs for TCDD show very little change in each of the graphs. For TCDD, the maximal respiratory capacity (B) and the ATP linked respiration (C) showed TCDD as higher than the DMSO solvent control. In all other graphs the solvent control is higher, which is to be expected. Again, TCDD is behaving unlike other chemicals and is acting in an unusual manner, making this a very complex carcinogen.

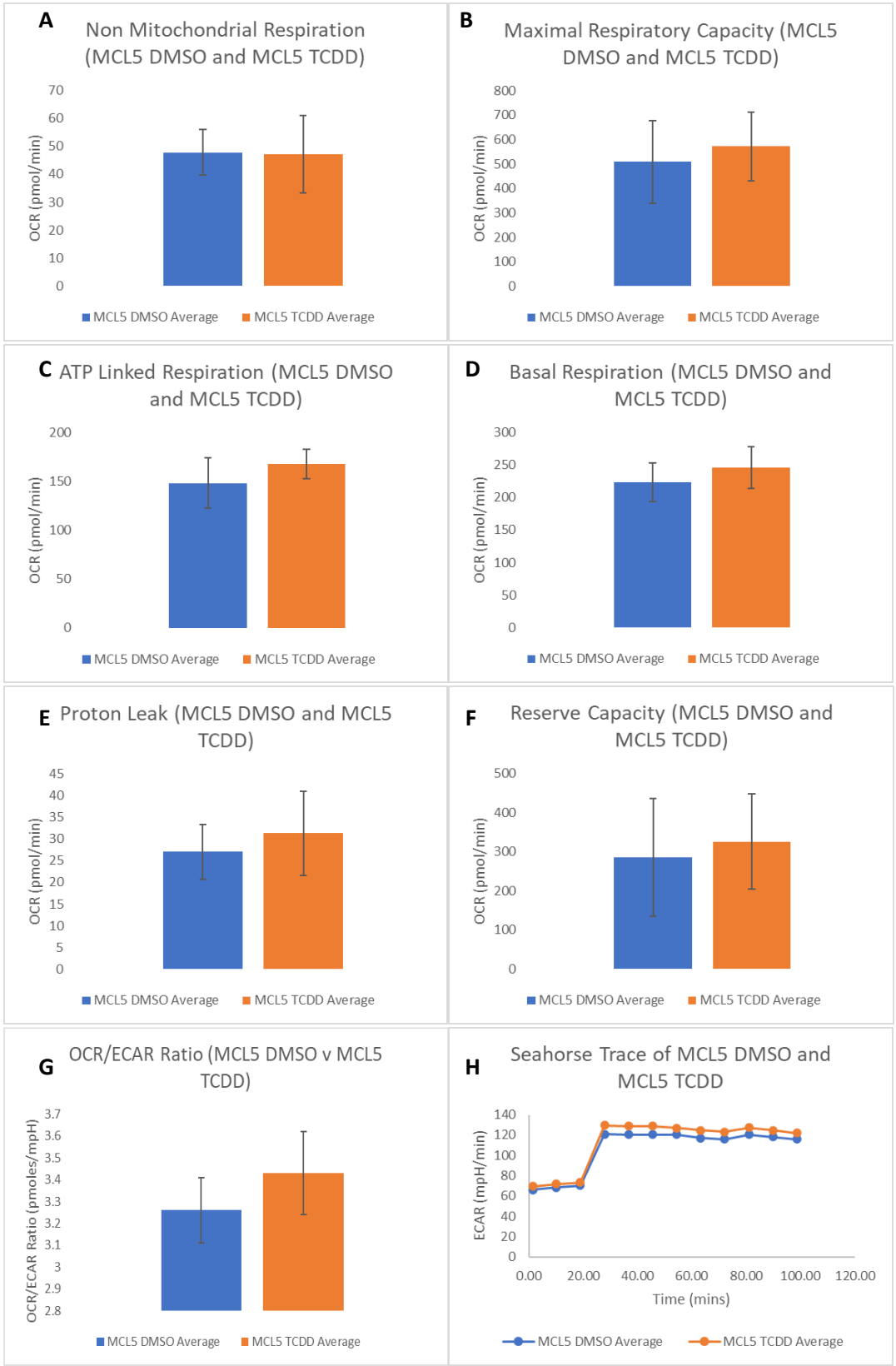

Figure 3.14 (A-H): Seahorse graphs for TCDD with MCL5 cells indicating the different respiration parameters when compared to the DMSO solvent control. **A** represents non mitochondrial respiration, **B** is the maximal respiratory capacity, **C** is the ATP linked respiration, **D** is basal respiration, **E** is proton leak, **F** is the reserve capacity, **G** demonstrates the OCR/ECAR ratio and **H** represents the ECAR graph. There was no statistical significance.

3.3.2 Chloroprene

An acute (24-hour) treatment of chloroprene using TK6 cells was employed to assess the RPD and mononucleate Mn frequency (**Figure 3.15)**. No dose dependent increase in Mn was seen, but there was a suggestion of a decrease in Mn induction from 2 µM - 100 µM. This could represent a slight biphasic response at doses from 2 to 100 µM. The RPD is largely unaffected from 2 µM – 200 µM, however at 400 µM the RPD drops to around 60%.

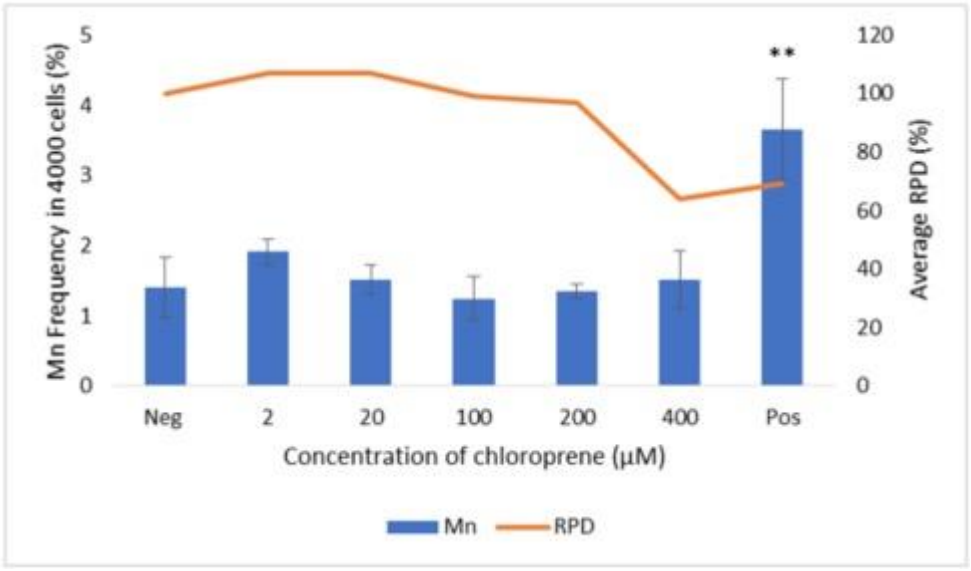

Figure 3.15: The acute mononucleate micronucleus (Mn) assay and relative population doubling (RPD) at 24-hour chloroprene exposure with 24-hours recovery in TK6 cells. n=3 was carried out for this work and the average was plotted with error bars. The negative control used here was methanol and 10 µM MMS was used as the positive control. There is no statistical significance when chloroprene was compared with the methanol control. The positive control (MMS) has a *P* value of 0.0098.

In order to assess more real-life exposures, chronic dosing was utilized, which includes a 5-day fractionated experiment with the same total doses as the acute assay **(Figure 3.16)**. Chronic dosing with chloroprene showed less toxicity (reduced RPD) suggesting that dose fractionation was largely better tolerated. From 2 µM - 100 µM the Mn induction remains largely constant and unchanged when compared to the negative control. However, the 200 µM and 400 µM doses seem to have a slightly decreased Mn induction (non-significant), which is different to what is expected. Although there are slight perturbations in RPD values, overall it remains mostly unaffected and therefore indicating cytotoxicity is not induced.

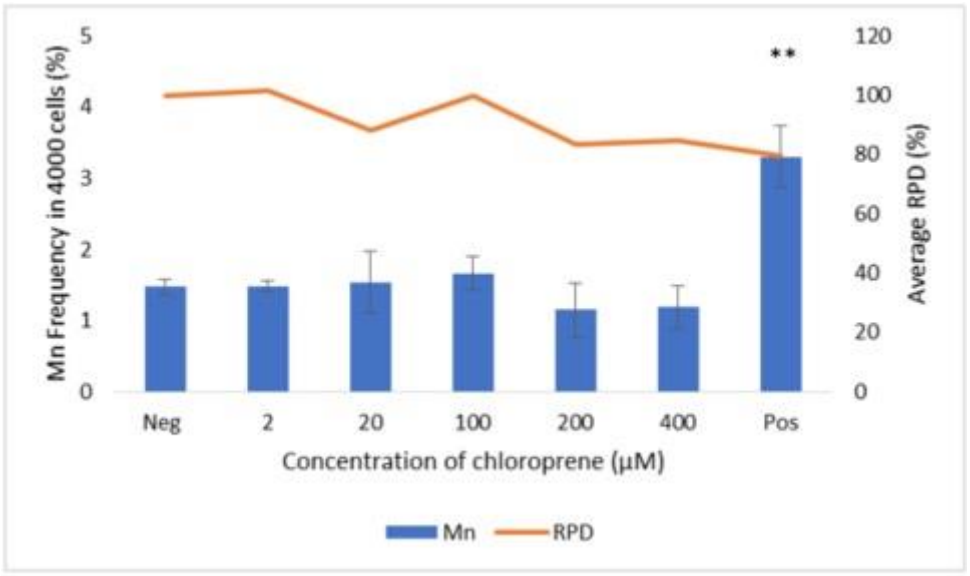

Figure 3.16: The chronic mononucleate micronucleus assay and relative population doubling at 5-day repeated exposure to fractionated chloroprene with 24-hours recovery in TK6 cells. The negative control used here was methanol and 10 µM MMS was used as the positive control. n=3 was carried out for this work and the average was plotted with error bars. There was no statistical significance when chloroprene was compared to the methanol control. The positive control (MMS) has a *P* value of 0.0021.

ROS can be an important route of carcinogenesis for NGCs. ROS measurements using the DCFDA approach at the 8 time points were compared across the chloroprene dose range. It seems as though chloroprene induces a possible AOX effect in **Figure 3.17**, as at increasing doses, the level of ROS produced is less than the negative control.

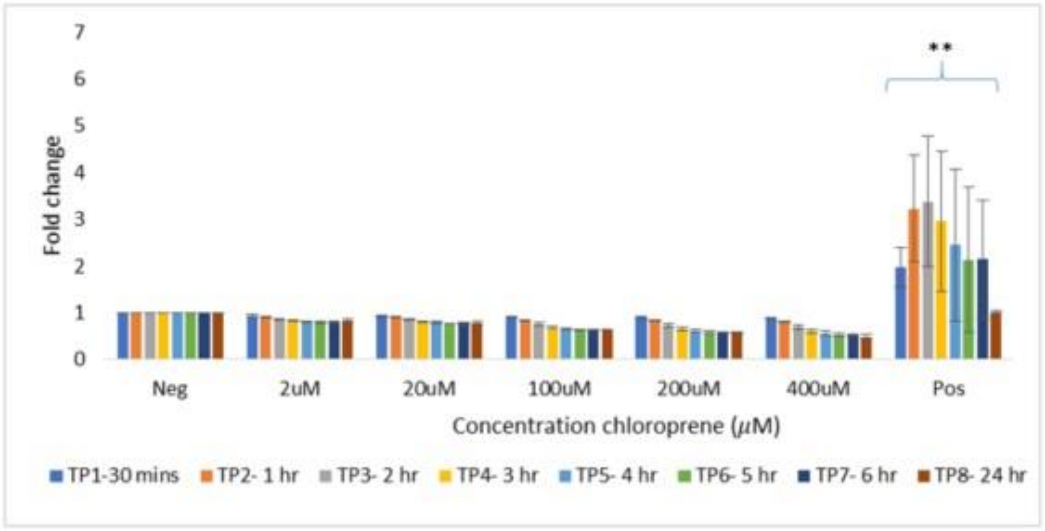

Figure 3.17: The reactive oxygen species (ROS) analysis with chloroprene as the test chemical at 8 different time points. 30 minutes, 1 hour, 2 hours, 3 hours, 4 hours, 5 hours, 6 hours and 24-hours were all measured and plotted against fold change of total ROS produced. An n=3 was carried out here and the average was plotted with error bars included. The negative/solvent control used was methanol and hydrogen peroxide at 100 µM is the positive control (indicated as pos on the graph). There was no statistical significance observed with the addition of chloroprene. However, there was a significant response in relation to H_2O_2 with a *P* value of 0.0017.

Cell cycle checkpoints are essential for progression through the cell cycle, in cancer cells there are often defects and mutations of the checkpoint proteins to encourage proliferation, meaning the cell cycle is closely linked to DNA damage. **Figure 3.18** shows the cell cycle analysis at 24-hours post-treatment with chloroprene. There is an unusual, slightly biphasic response seen with this NGC. For example at doses 2 µM and 200 µM there was an increase of cells in G1. However at 20 µM, 100 µM and 400 µM the cell cycle profile matches that of the negative control meaning that there were perturbations as the doses increased.

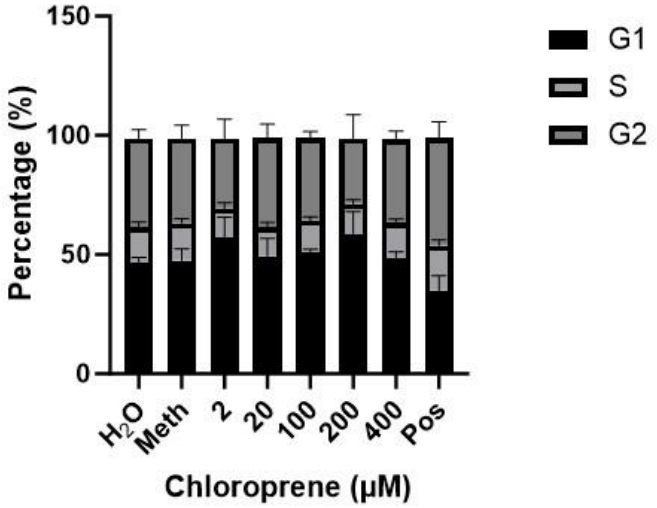

Figure 3.18: Cell cycle analysis of chloroprene at 24-hours without recovery. The cell cycle stages G1, S and G2 are represented using the flow cytometric method. n=3 was performed including 3 technical replicates and the average was plotted with error bars. The negative control used here was methanol and 10 µM MMS was used as the positive control here. The key is shown to the top right with different colours representing each cell cycle stage. No statistical significance shown here**.**

Cell cycle analysis was also carried out at both 12-hour **(Figure 3.19)** and 48-hour **(Figure 3.20)** time points as a result of significant *CCND1* upregulation in **Figure 3.22**. Both time points show a very slight dose dependent increase in G1 cells however this do not match the biphasic pattern seen in **Figure 3.18**. Overall, both graphs, **Figure 3.19** and **Figure 3.20** do not show any major changes in the cell cycle analysis. This shows that time point selection is important to assess cell cycle changes.

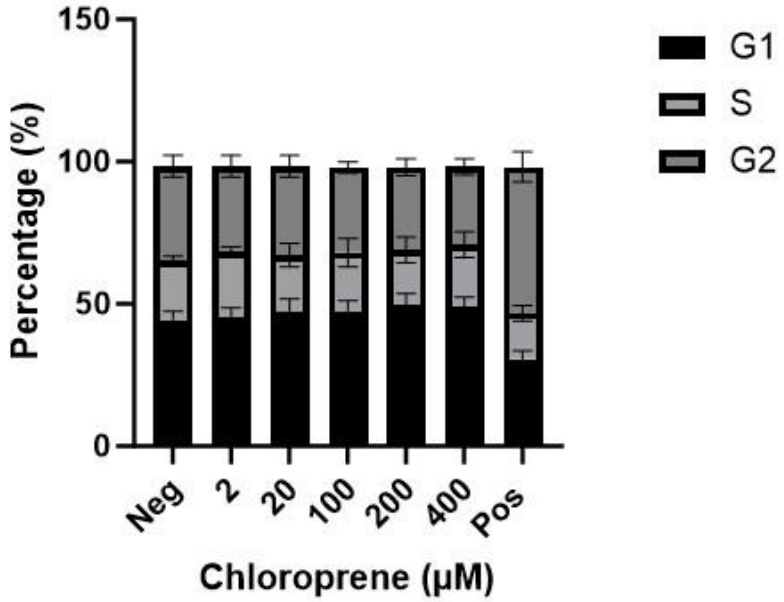

Figure 3.19: Cell cycle analysis of chloroprene at 12-hours without recovery. The cell cycle stages G1, S and G2 are represented using the flow cytometric method. n=3 was performed including 3 technical replicates and the average was plotted with error bars. The negative control used here was methanol and 10 µM MMS was used as the positive control here. The key is shown to the top right with different colours representing each cell cycle stage. No statistical significance shown here.

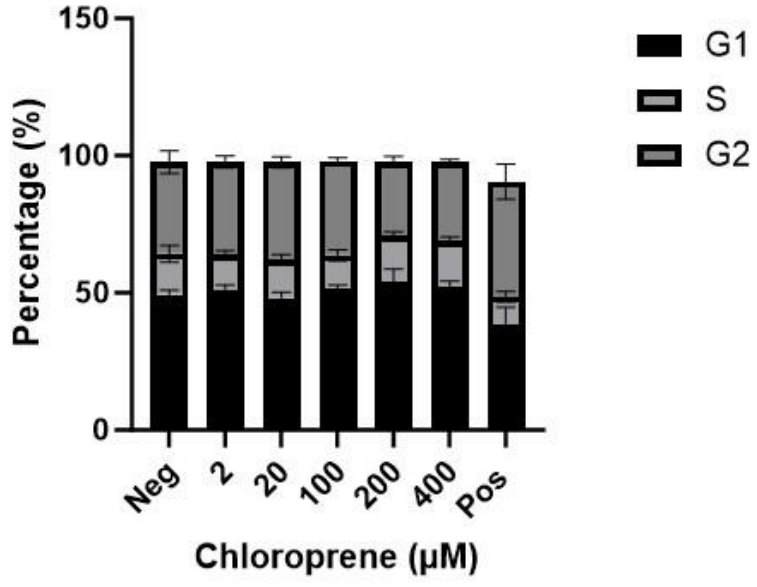

Figure 3.20: Cell cycle analysis of chloroprene at 48-hours without recovery. The cell cycle stages G1, S and G2 are represented using the flow cytometric method. n=3 was performed including 3 technical replicates and the average was plotted with error bars. The negative control used here was methanol and 10 µM MMS was used as the positive control here. The key is shown to the top right with different colours representing each cell cycle stage. No statistical significance shown here**.**

As apoptosis is affected by multiple other cellular processes, it was an important mechanism to consider in this multi-endpoint analysis. There does not seem to be any differences between the methanol solvent and the doses in **Figure 3.21**. However, overall there was a very limited apoptotic effect of all the chloroprene doses on TK6 cells.

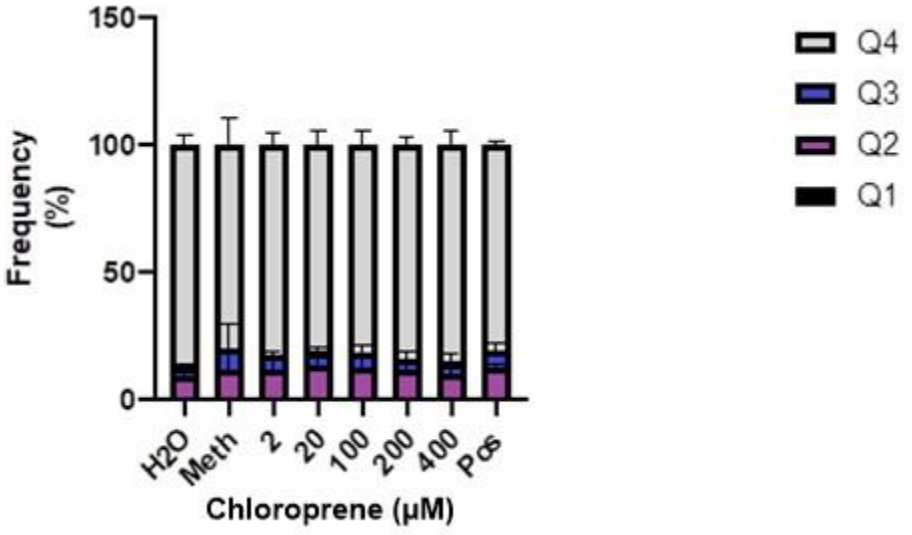

Figure 3.21: Apoptosis analysis of chloroprene on TK6 cells at 24-hours without recovery using the annexin V and 7-AAD dyes and the flow cytometry method. Q1 is the percentage of necrotic cells. Q2 is the percentage of late apoptotic cells. Q4 is the percentage of viable cells and Q3 is the percentage of early apoptotic cells. The negative control used here was methanol and the positive control was 0.1 µM staurosporine. n=3 was performed including 3 technical replicates and the average was plotted with error bars. The key indicates the stages Q1-Q4. There was no statistical significance observed here**.**

In order to understand if the cellular processes affect the mechanism(s) of action utilized by chloroprene, a PCR array of important cancer genes was carried out **(Figure 3.22)**. The PCR array can flag up any genes of interest which can help explain how chloroprene is capable of causing oncogenesis. *CCND1* is upregulated by >115 fold after chloroprene exposure at 400 µM, which suggests that cell cycle disruption could be a major mechanism used by chloroprene. As a result of the *CCND1* upregulation, 12-hour and 48-hour cell cycle analysis was also carried out **(Figure 3.19)** and **(Figure 3.20)**. This gene upregulation is so great that it masks the other biologically relevant genes also upregulated in **Figure 3.22** seem not important. The great upregulation of *CCND1* means something must be happening at a gene expression level as it is not reflected in the cell cycle analyses in **Figure 3.18**, **Figure 3.19** and **Figure 3.20**. Perhaps a full time course analysis would pick up a change at a specific timepoint.

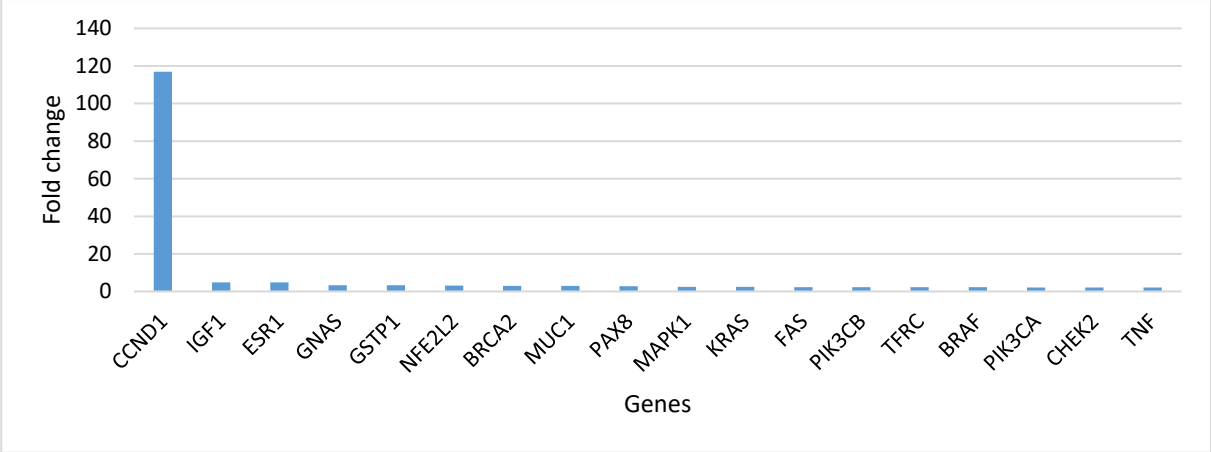

Figure 3.22: The general cancer panel of genes conducted as a PCR array for chloroprene when compared to its methanol negative control. Only biologically relevant (±2 fold change) genes are included in this graph. This work is n=1, therefore no statistical analysis was carried out. The TK6 cells were dosed with 400 µM chloroprene for 24-hours before the RNA was extracted for the PCR array. This PCR array was chosen as it included a range of different cancer related genes which could help unpick the MoA used by each chemical.

It was important to assess the mitochondrial health as mitochondria play a role in a number of cellular processes and mitochondrial stress often generates DNA damage. The addition of chloroprene only slightly reduces the bioenergetic flux when compared to its methanol solvent **(Figure 3.23)**. However, overall there is limited effect on the Seahorse trace as a result of chloroprene treatment, meaning it is not a significant mitochondrial stressor. The doses chosen for Seahorse are the same as those chosen for PCR array in order to keep consistency. It is the dose at which a response is first seen. The full Seahorse data breakdown can be found in **Figure 3.24 (A-H)** for chloroprene.

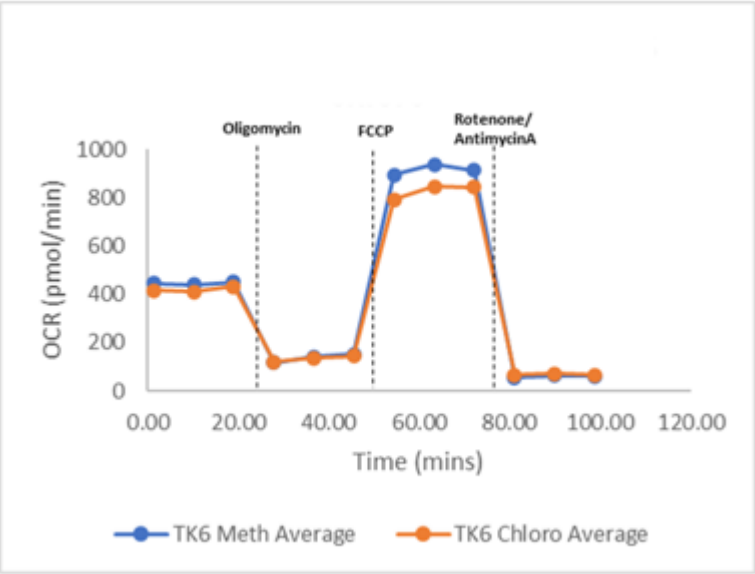

Figure 3.23: A Seahorse trace graph showing the bioenergetic flux profiles of 400 µM chloroprene compared to the methanol negative/solvent control. Oligomycin, FCCP and rotenone/antimycinA are chemical stressors added at different time points to investigate the mitochondrial stress reaction. The full name of FCCP is (carbonyl cyanide-p-trifluoromethoxy) phenylhydrazone and it acts as a mobile ion carrier. n=3 was performed here and the average was plotted.

The different output graphs from the sesahorse XF analyser, each represent a different parameter of respiration. There is no statistical significance observed with any of the graphs A through to H. Interestingly, although there is no significance, the non-mitochondrial respiration (**A**), however for chloroprene is slightly higher than methanol, the solvent control. In all other graphs, the solvent control is higher.

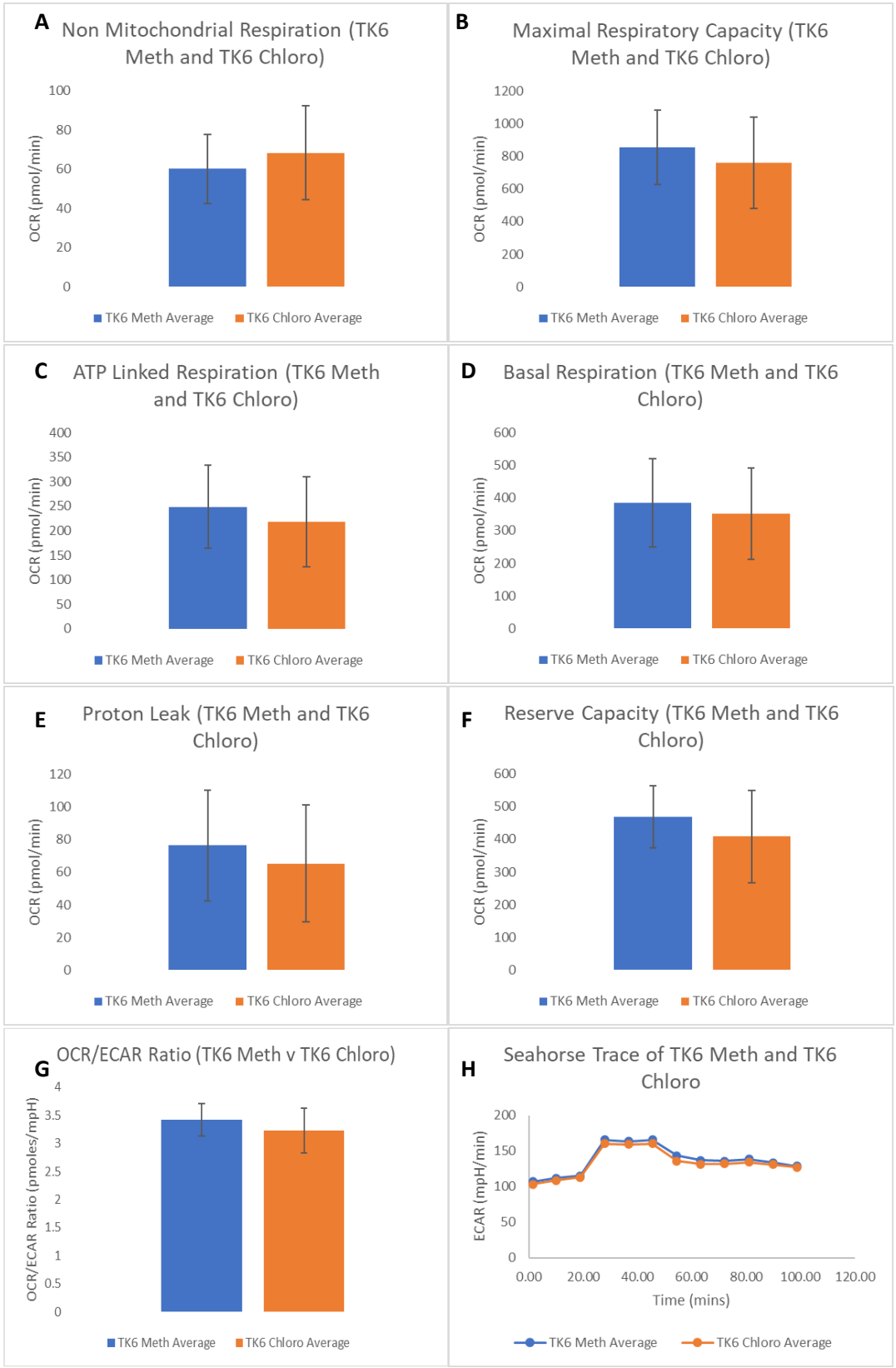

Figure 3.24 (A-H): Seahorse graphs for chloroprene indicating the different respiration parameters when compared to the methanol solvent control. **A** represents non mitochondrial respiration, **B** is the maximal respiratory capacity, **C** is the ATP linked respiration, **D** is basal respiration, **E** is proton leak, **F** is the reserve capacity, **G** demonstrates the OCR/ECAR ratio and **H** represents the ECAR graph. There was no statistical significance.

3.3.3 Rosuvastatin

In order to assess genotoxicity and cytotoxicity of rosuvastatin **(Figure 3.25)**, the mononucleate Mn was carried out alongside RPD. As the dose of rosuvastatin increases, the cytotoxicity decreases and at the top dose of 400 µM RPD drops to the maximum threshold of 40% (55%+/-5% (OECD 2012)). However, the 400 µM dose is still included in **Figure 3.25** because it can be compared to the chronic doses **(Figure 3.26)**. As the dose of rosuvastatin increases, there no change in Mn level, which is the response that is expected for a NGC.

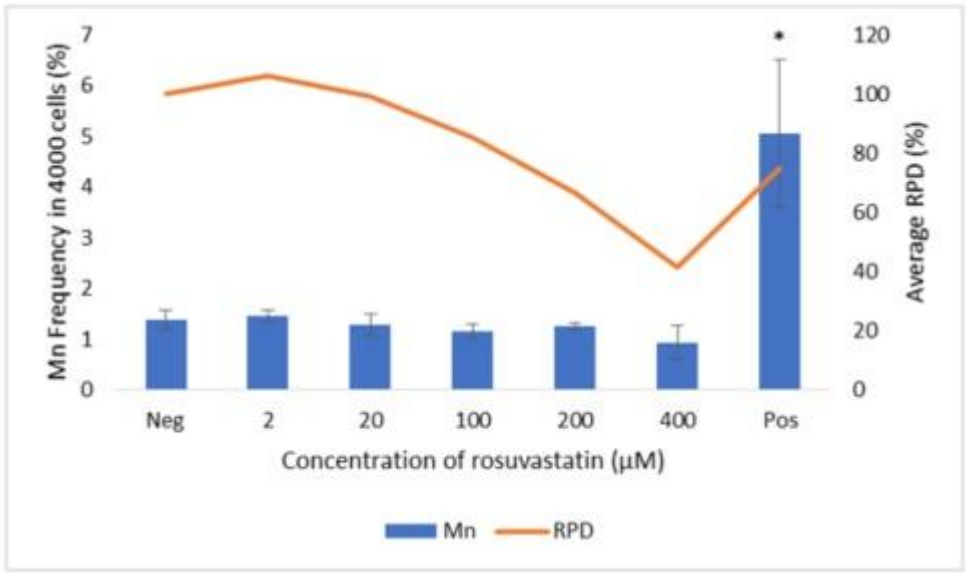

Figure 3.25: The acute mononucleate micronucleus (Mn) assay and relative population doubling (RPD) at 24-hour rosuvastatin exposure with 24-hours recovery in TK6 cells. n=3 was carried out for this work and the average was plotted with error bars. The negative control used here was DMSO and 10 µM MMS was used as the positive control. There was no statistical significance observed here with the addition of rosuvastatin. There was statistical significance seen with the positive control (MMS) giving a *P* value of 0.0123.

In order to compare the standard regulatory, acute dosing with a more real-life exposure scenario, chronic dosing was also carried out, where a fractionated dose was delivered each day for 5 days equating to the same total dose as in **Figure 3.25**. Interestingly, **Figure 3.26** shows that with a chronic dosing system, rosuvastatin is better tolerated in terms of cytotoxicity, unusually the RPD is actually increased with the addition of rosuvastatin. Rosuvastatin causes a consistent increase in Mn, even when increasing the dose, which is again a rare occurrence but typical of the complex nature of NGCs.

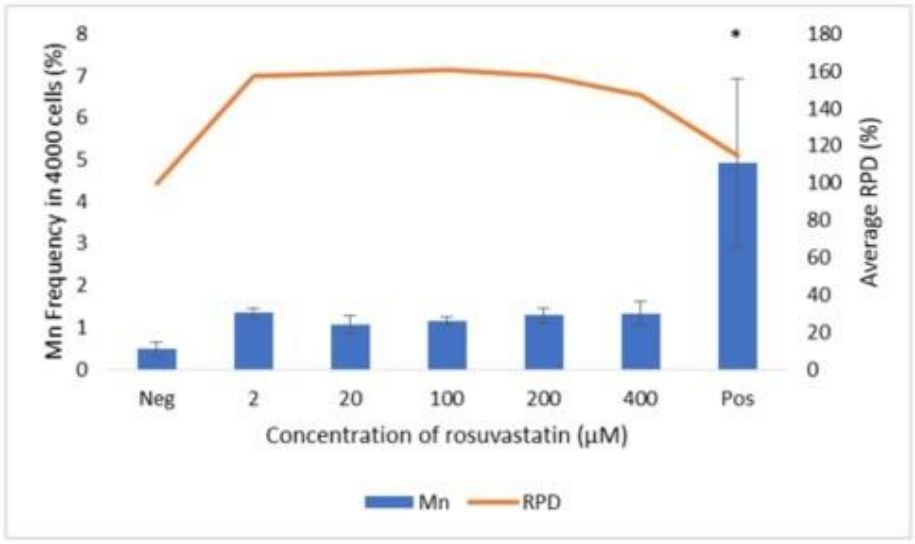

Figure 3.26: The chronic mononucleate micronucleus assay and relative population doubling at 5-day repeated exposure to fractionated rosuvastatin with 24-hours recovery in TK6 cells. The negative control used here was DMSO and 10 µM MMS was used as the positive control. n=3 was carried out for this work and the average was plotted with error bars. There was no statistical significance with the addition of rosuvastatin. There was statistical significance seen with the positive control (MMS) giving a *P* value of 0.0193.

ROS is an important mechanism to consider for NGCs as it can contribute to damaging the DNA as a secondary mechanism. The DCFDA fluorescence assay quantifies the total ROS produced by the cells for a series of time points after treatment with rosuvastatin **(Figure 3.27)**. There seems to be no ROS induction as a result of treatment with rosuvastatin, so this is not the MoA utilized by rosuvastatin.

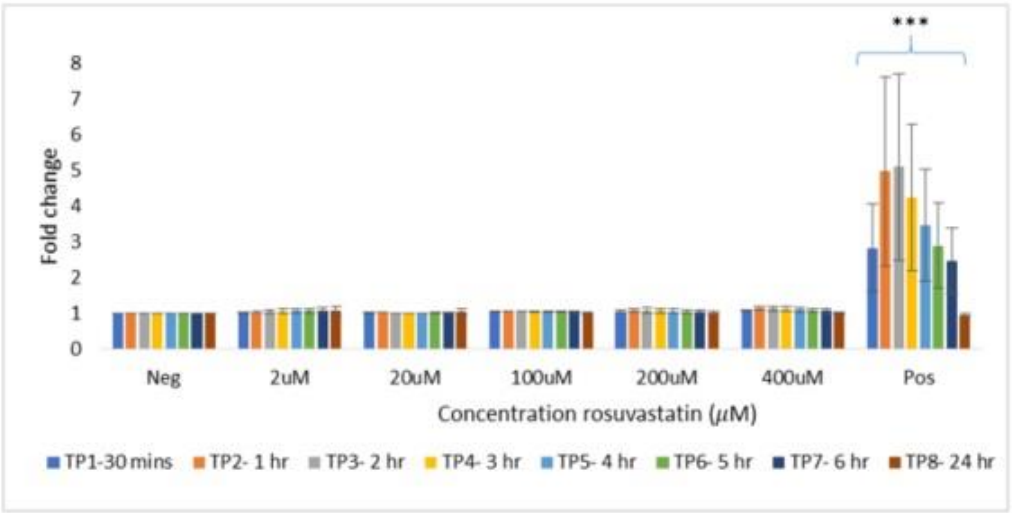

Figure 3.27: The reactive oxygen species (ROS) analysis with rosuvastatin as the test chemical. 30 minutes, 1 hour, 2 hours, 3 hours, 4 hours, 5 hours, 6 hours and 24-hours were all measured and plotted against fold change of total ROS produced. An n=3 was carried out here and the average was plotted with error bars included. The negative/solvent control used was DMSO and hydrogen peroxide at 100 µM is the positive control (indicated as pos on the graph). There was no statistical significance observed with the addition of rosuvastatin. The positive control (H_2O_2) returned a significant response with a *P* value of 0.00027.

Cell cycle abnormalities are proven to be an important mechanism when assessing mechanisms of carcinogenesis. A 24-hour rosuvastatin treatment was carried out prior to cell cycle analysis as can be seen in **Figure 3.28.** There seems to be no changes to the cell cycle with a 24-hour treatment. There are very subtle changes within the cell cycle stages but with no significance or trend when compared to the negative control.

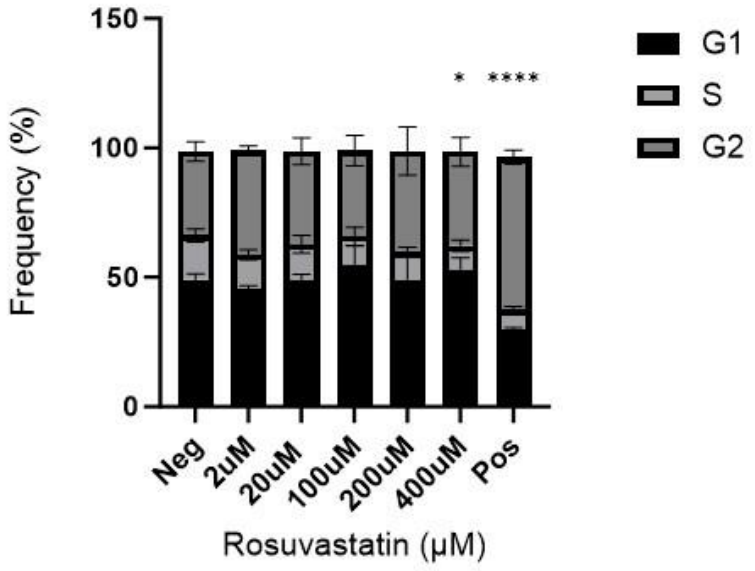

Figure 3.28: Cell cycle analysis of rosuvastatin at 24-hours without recovery. The cell cycle stages G1, S and G2 are represented using the flow cytometric method. n=3 was performed including 3 technical replicates and the average was plotted with error bars. The negative control used here was DMSO and 10 µM MMS (P = 0.00001) was used as the positive control here. The key is shown to the top right with different colours representing each cell cycle stage. A one-way ANOVA was performed, there was only significance in the reduction of size in the S phase of 400 µM (P = 0.0388) dose (* < 0.05).

Apoptosis goes hand in hand with DNA damage, cell cycle analysis and certain gene expression changes. The apoptotic analysis of rosuvastatin **(Figure 3.29)** at 24-hours post treatment, shows a very minor dose dependent increase of cell death from 2 µM – 200 µM. At 400 µM the level of apoptosis seems to drop slightly, which is not the expected result. However, the unusual behaviour seen in **(Figure 3.29)** is typical of NGCs due to their complex nature and utilising multiple overlapping MoAs.

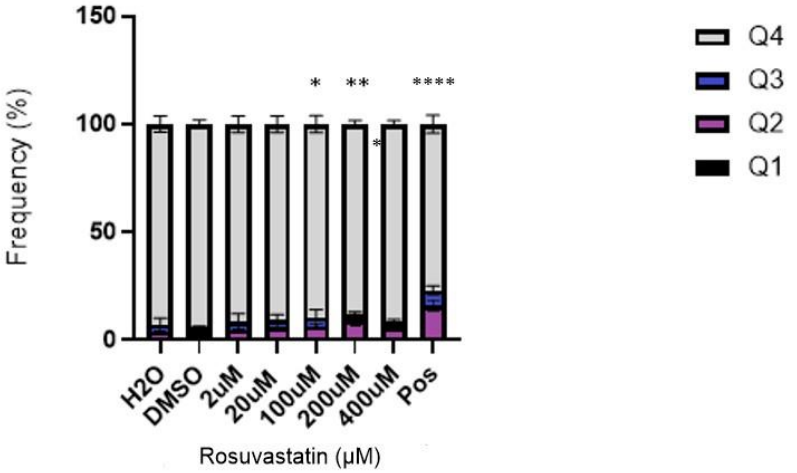

Figure 3.29: Apoptosis analysis of rosuvastatin at 24-hours without recovery using the annexin V and 7-AAD dyes and the flow cytometry method. Q1 is the percentage of necrotic cells. Q2 is the percentage of late apoptotic cells. Q4 is the percentage of viable cells and Q3 is the percentage of early apoptotic cells. The negative control used here was DMSO and the positive control was 0.1 µM staurosporine (P = 0.00003). n=3 was performed including 3 technical replicates and the average was plotted with error bars. The key indicates the stages Q1-Q4. A one-way ANOVA was performed and there is significance at Q4 for 100 µM (P = 0.0392) and 200 µM (P = 0.0013) (* < 0.05, **<0.005)

Understanding gene expression changes is vital in underpinning the mechanistic routes used by NGCs, in this case rosuvastatin **(Figure 3.30), (Figure 3.31)** and **(Figure 3.32)**. These PCR arrays provide the information necessary for any follow up PCR. The gene panel arrays available meant that the correct cell line and solvent could not always be directly compared for this chemical unfortunately. Rosuvastatin was treated in TK6 cells, as metabolic activation was not required and using DMSO as a solvent. However, comparisons have been made with the correct solvent, but incorrect cell line and alternatively the correct cell line but incorrect solvent. These graphs have then been compared and those genes up/downregulated in both scenarios have been logged and displayed in **(Figure 3.32)** to give the greatest confidence in the results. *CD44* and *TGFB1* are some examples of the most upregulated genes in **(Figure 3.32)**. CD44 has a role in the development and progression of cancer (Chen et al., 2018), so it is unsurprising it is highly upregulated in both graphs. However, the exact way in which it does this requires further investigation.

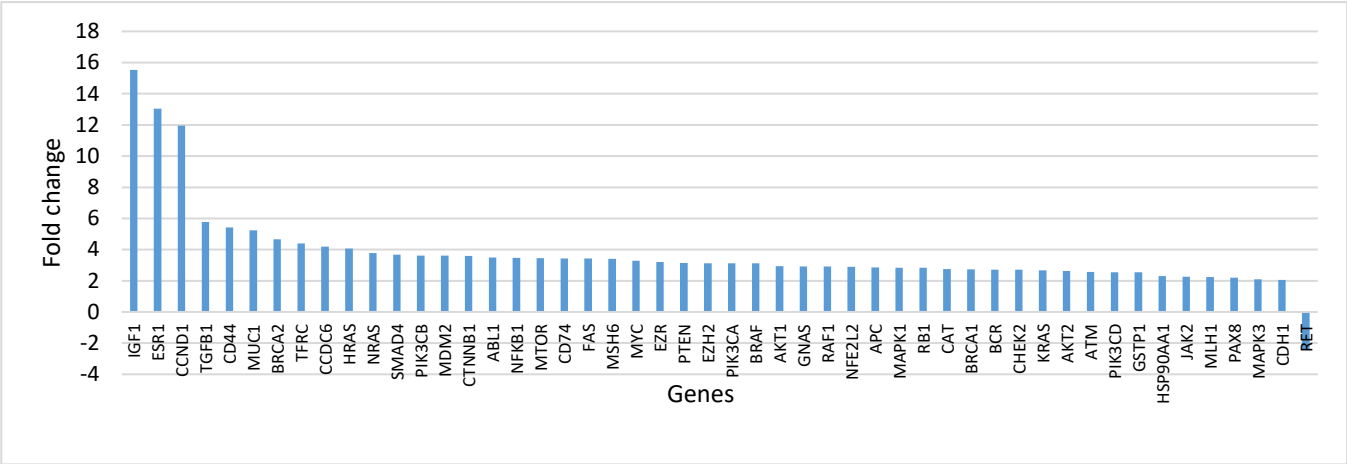

Figure 3.30: PCR array of rosuvastatin for a general panel of cancer genes. The biologically relevant (±2 fold change) downregulated genes are included in the graph. The TK6 cells were dosed with 200 µM rosuvastatin for 24-hours before the RNA was extracted for the PCR array. The PCR array was compared to the negative/solvent control which was DMSO. n=1 was performed here, therefore no statistical analysis was carried out. There was a positive control PCR array done with MMS to refer to.

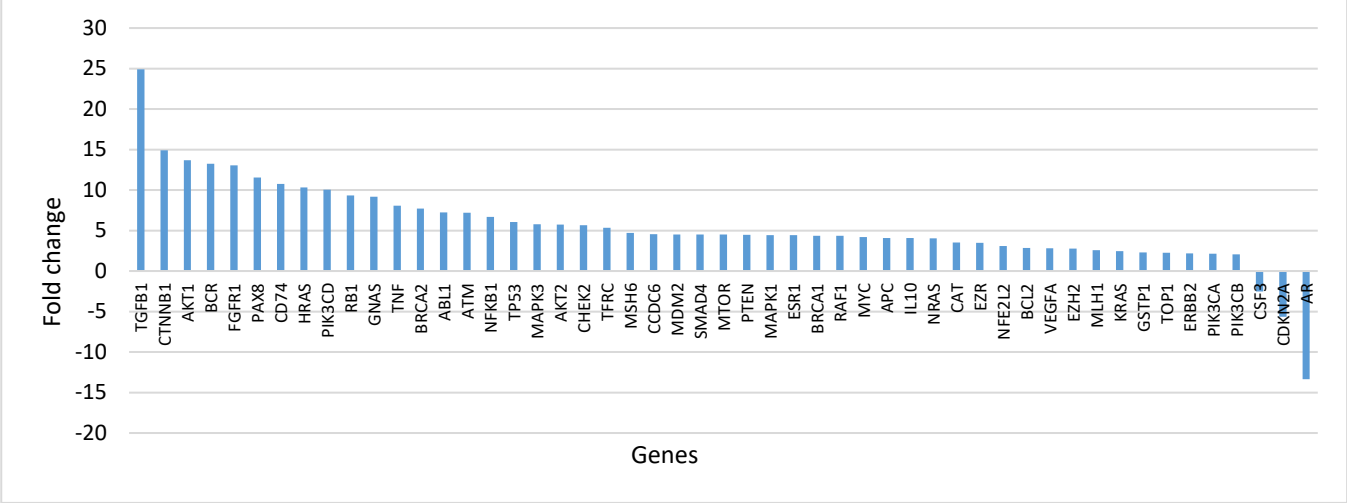

Figure 3.31: PCR array for a general panel of cancer genes. The biologically relevant (±2 fold change) downregulated genes are included in the graph. The TK6 cells were dosed with 200 µM rosuvastatin for 24-hours before the RNA was extracted for the PCR array. The PCR array was compared to the negative/solvent control which was DMSO. n=1 was performed here, therefore no statistical analysis was carried out. There was a positive control PCR array done with MMS to refer to.

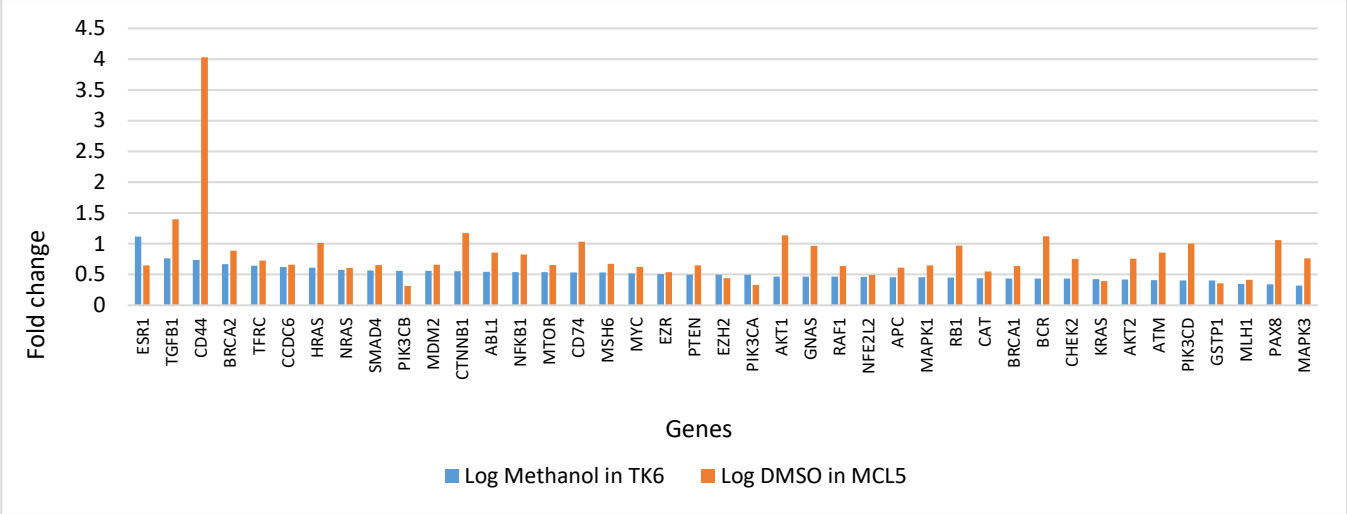

Figure 3.32: The PCR array general panel of cancer genes for rosuvastatin using a log overlap of both the correct cell line and correct solvent. All of the biologically relevant (±2 fold change) log values of the up and downregulated genes included in the graph. This work is n=1, therefore no statistical analysis was carried out. The TK6 cells were dosed with 200 µM rosuvastatin for 24-hours before the RNA was extracted for the PCR array. There was a positive control PCR array done with MMS to refer to.

As mitochondria are important in numerous cellular processes it is important to assess the function of the mitochondria as this could be part of the MoA used by rosuvastatin. **Figure 3.33** shows a large decrease in the Seahorse trace of rosuvastatin when compared to its DMSO solvent. This suggests a large amount of mitochondrial dysfunction, suggesting this could be a part of the mechanistic pathway responsible for carcinogenesis. The full Seahorse data breakdown can be found in **Figure 3.34 (A-H)** for rosuvastatin.

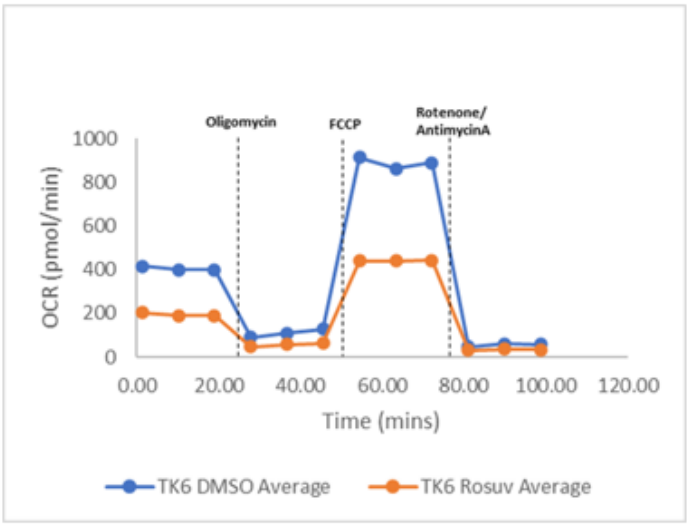

Figure 3.33: A Seahorse trace graph showing the bioenergetic flux profiles of rosuvastatin at 200 µM compared to the DMSO negative/solvent control. Oligomycin, FCCP and rotenone/antimycinA are chemical stressors added at different time points to investigate the mitochondrial stress reaction. The full name of FCCP is (carbonyl cyanide-p-trifluoromethoxy) phenylhydrazone and it acts as a mobile ion carrier. n=3 was performed here and the average was plotted.

There was a significant (* < 0.05) drop in the non-mitochondrial respiration (**A**) for rosuvastatin when compared to the DMSO solvent control. There was also a significant (** < 0.005) drop in the maximal respiratory capacity (**B**), ATP linked respiration (**C**), basal respiration (**D**), reserve capacity (**F**) and the OCR/ECAR ratio (**G**).

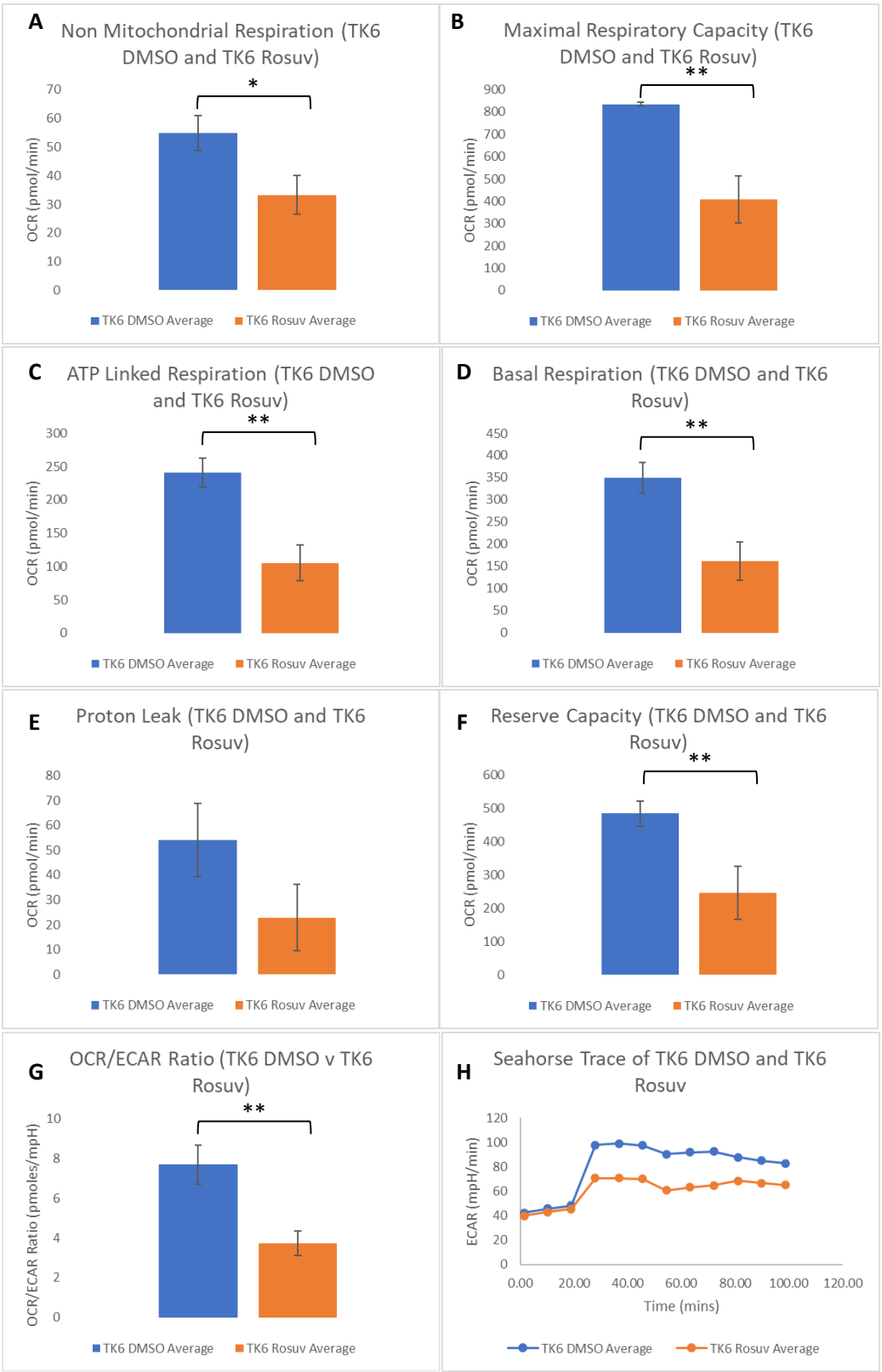

Figure 3.34 (A-H): Seahorse graphs indicating the different respiration parameters when compared to the DMSO solvent control. **A** represents non mitochondrial respiration ($P = 0.0147$), **B** is the maximal respiratory capacity ($P = 0.0023$),, **C** is the ATP linked respiration ($P = 0.0026$),, **D** is basal respiration ($P = 0.0041$),, **E** is proton leak (non-significant), **F** is the reserve capacity ($P = 0.0095$),, **G** demonstrates the OCR/ECAR ratio ($P = 0.0040$), and **H** represents the ECAR graph. Unpaired T tests were carried out for these analyses (* < 0.05, **<0.005).

3.3.4 Additional Data

After understanding that these chemicals produced a largely negative response to all endpoints tested, it was thought that they may benefit from 3D liver cell models. The HepG2 spheroids were treated for 24-hours with the same doses used in the acute data generated in TK6 cells. The data represented here (**Figure 3.35**, **Figure 3.36** and **Figure 3.37**) was completed with help from Dr Ume-Kulsoom Shah from the *In vitro* Toxicology group in Swansea University. These data show an interesting response as it appears that in this more physiological model, there seems to be more biphasic behaviour. For example, **Figure 3.35** shows a steady response until 2 µM where there seems to be a reduction in Mn at this dose and then a slight increase again at 3 µM. This could suggest Hormesis is prevalent at 2 µM with TCDD.

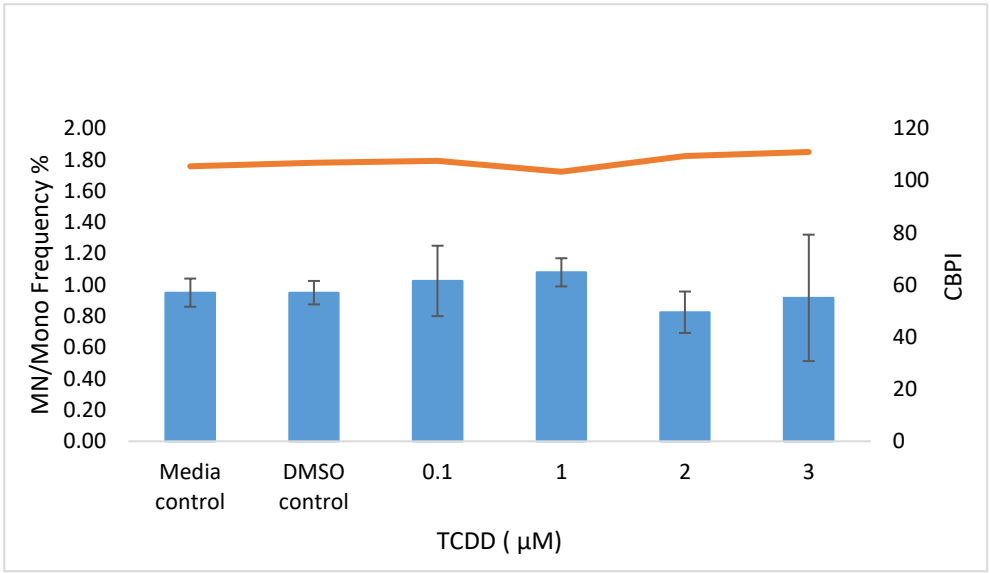

Figure 3.35: 3D HepG2 spheroids were treated with TCDD for 24-hours without recovery and assessed for cytotoxicity by CBPI and genotoxicity by Mn frequency. n=3 was conducted for this experiment and the average was plotted with error bars. Although the CBPI calculation has been performed on the data here, cytochalasin B was not added during this experiment. 1000 cells were counted in total. No statistical significance was shown.

A similar response is observed with chloroprene in **Figure 3.36**, as there is a slight reduction in Mn induction at 20 µM and then a dose dependent increase from 100 µM onwards.

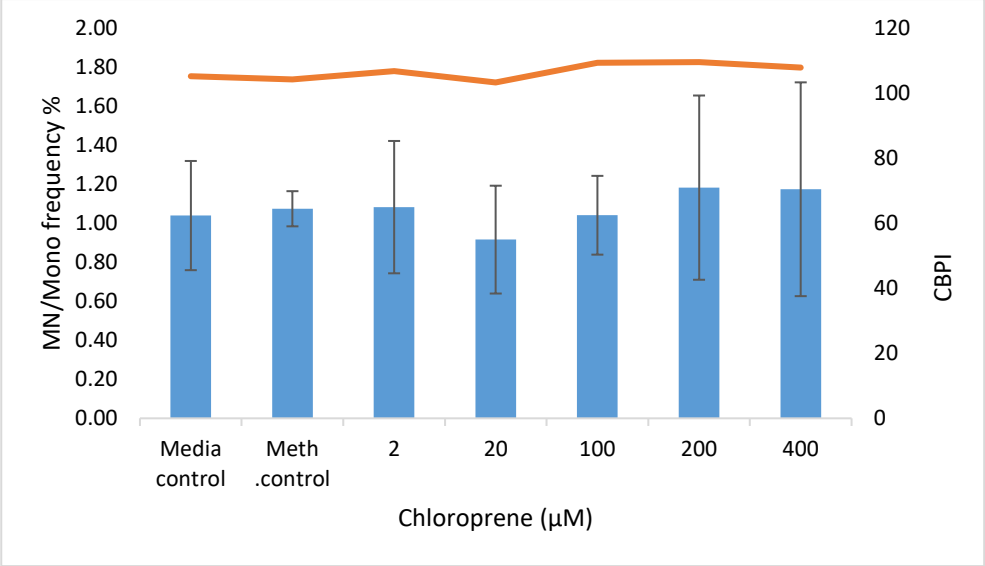

Figure 3.36: 3D HepG2 spheroids were treated with chloroprene for 24-hours without recovery and assessed for cytotoxicity by CBPI and genotoxicity by Mn frequency. n=3 was conducted for this experiment and the average was plotted with error bars. Although the CBPI calculation has been performed on the data here, cytochalasin B was not added during this experiment. 1000 cells were counted in total. No statistical significance was shown.

The HepG2 spheroid data showed a potential hormetic response at 2 µM in **Figure 3.37** and there is a slight reduction of Mn produced when compared to the negative control. From 20 µM there is an increase of Mn up to 100 µM before a gradual decrease to 400 µM. This response could also represent a biphasic response seen with NaMAr in **Figure 5.6**.

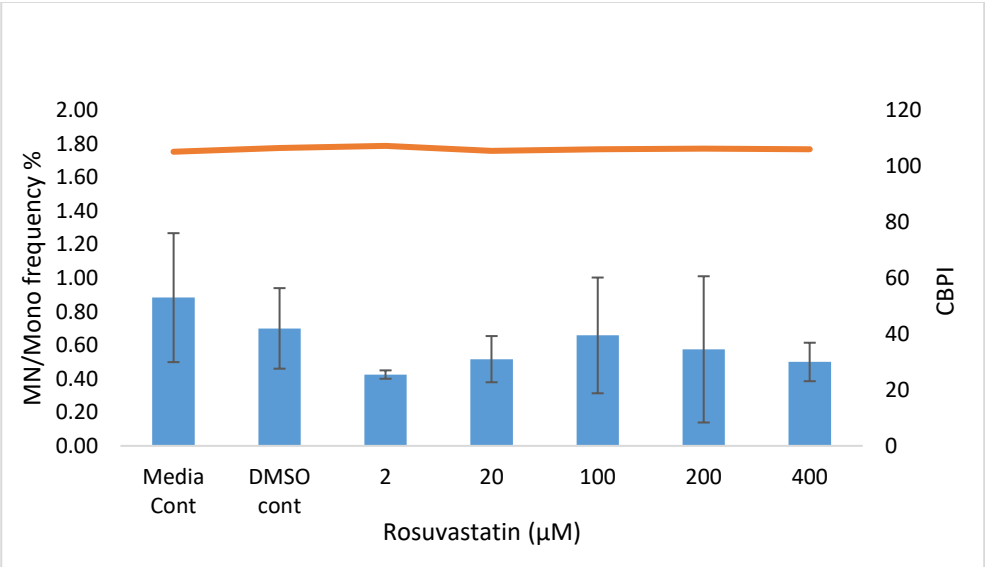

Figure 3.37: 3D HepG2 spheroids were treated with rosuvastatin for 24-hours without recovery and assessed for cytotoxicity by CBPI and genotoxicity by Mn frequency. n=3 was conducted for this experiment and the average plotted with error bars. Although the CBPI calculation has been performed on the data here, cytochalasin B was not added during this experiment. For consistency 10 µM MMS was used as a positive control with these experiments. 1000 cells were counted in total. No statistical significance was shown.

As cytoB was not added during the HepG2 spheroid work in order to mimic the rest of the Mn data. It was thought there may be some interesting results to be seen with the BN frequencies of TCDD (**Figure 3.38**), chloroprene (**Figure 3.39**) and rosuvastatin (**Figure 3.40**). The average BN frequency was calculated without the addition of cytoB, which gives an idea of the natural cell division or block in cytokinesis taking place. Both **Figure 3.38** and **Figure 3.39** showed a statistical significance increase or decrease in BN frequency. No statistical significance was seen in BN frequency in **Figure 3.40**.

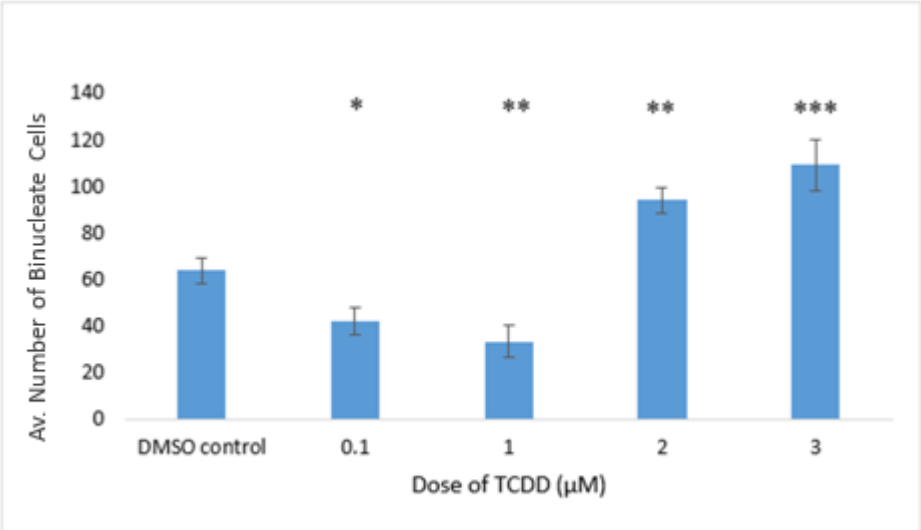

Figure 3.38: The average BN frequency of TCDD treated cells in the 3D HepG2 spheroids. n=3 was conducted for this work and the average was plotted with error bars. An unpaired T-test was carried out and statistical significance was shown (* < 0.05, **<0.005, ***<0.0005). Cells were disaggregated using trypsin. 1000 cells were counted in total. There was statistical significance seen with 0.1 µM TCDD with a *P* value of 0.0226, 1 µM TCDD (*P* = 0.0034), 2 µM TCDD (*P* = 0.0034) and 3 µM TCDD (*P* = 0.0002).

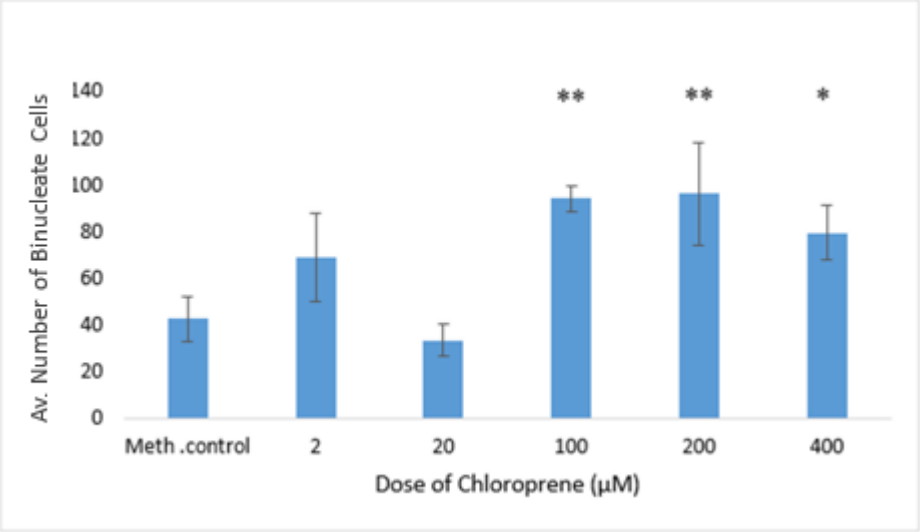

Figure 3.39: The average BN frequency of chloroprene treated cells in the 3D HepG2 spheroids. n=3 was conducted for this work and the average was plotted with error bars. An unpaired T-test was carried out and statistical significance was shown (* < 0.05, **<0.005). 1000 cells were counted in total. There was statistical significance seen with 100 µM chloroprene with a *P* value of 0.0055, 200 µM chloroprene (*P* = 0.0043) and 400 µM chloroprene (*P* = 0.0396).

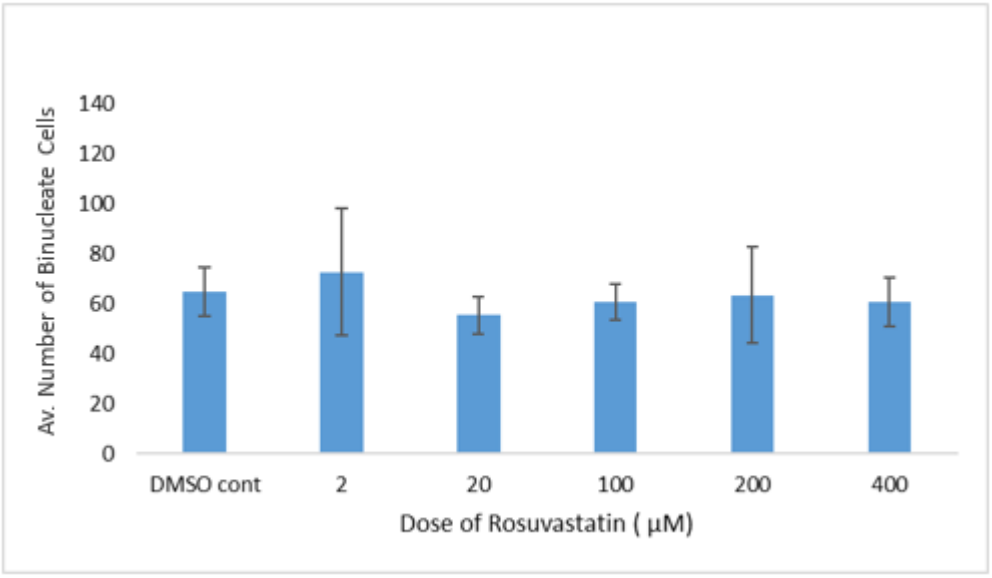

Figure 3.40: The average BN frequency of rosuvastatin treated cells in the 3D HepG2 spheroids. n=3 was conducted for this work and the average was added with error bars. No statistical significance was seen. 1000 cells were counted in total.

With TCDD in **Figure 3.38** it seemed as though there was a decrease of cellular proliferation up to 1 µM and an increase in proliferation in 2 and 3 µM respectively. Again **Figure 3.39** showed the BN frequency for chloroprene, which was interesting as there seems to be a fluctuation in the proliferation profile of this chemical. There seems to be an increase in proliferation at doses 2 µM, 100 µM, 200 µM and 400 µM. However, it looks as if there is a decrease of proliferation at

20 µM again maybe displaying a biphasic response. Rosuvastatin does not seem to show any changes in the BN frequency in **Figure 3.40** and it looks relatively stable throughout the dose range. It poses the question whether in some cases a natural cytokinesis block is acting as the BN frequency increases considerably when compared to the negative control.

3.4 Discussion

3.4.1 TCDD

TCDD is thought to disrupt cellular signaling, is an endocrine modifier and activates the AhR. TCDD forms a heterodimer complex with the aryl hydrocarbon receptor nuclear translocator which binds to regulatory sequences and is responsible for the receptor mediated modifications of expression (Hernández *et al*., 2009). TCDD is responsible for numerous cell signaling disruption events and alterations in order to induce carcinogenesis. This could explain the negative results for the other mechanistic investigation carried out in this research. Further exploration and unpicking of the pathways used by TCDD could potentially be determined with additional qPCR assessment.

The Mn for TCDD following the acute exposure in **Figure 3.7** shows no genotoxicity or cytotoxicity in MCL5 cells. The Mn for TCDD following the chronic exposure in **Figure 3.8** again shows no cytotoxicity or genotoxicity, there is a slight decrease in Mn induction when compared to the negative control, although it did not reach significance.

Figure 3.9a shows that MCL5 cells did not produce any ROS as a result of TCDD treatment. At 1 µM TCDD treatment, there was even a significant decrease in ROS produced at 2 hours and 3 hours post treatment. This could be demonstrating a slight AOX action at that dose and time points. It is known that metals such as nickel and chromium cause induction of ROS, but it is also thought that xenobiotics such as TCDD or benzopyrenes can also stimulate ROS production (Henkler *et al*., 2010). **Figure 3.9a** shows no ROS production *in vitro* and therefore disagrees with Henkler's, (2010) claims. It is thought that induced ROS can activate signaling pathways such as MAPK in order to initiate a signalling cascade and also trigger *NFKB* (Loeb, 2001). Although, there is no ROS produced in **Figure 3.9a**, there has been an upregulation of *MAPK1*, *MAPK3* and *NFKB1* which is in agreement with Loeb, (2001). **Figure 3.9b** shows there was significant ROS production with the H_2O_2 positive control.

TCDD did not induce any significant changes to cell cycle at 24-hours (**Figure 3.10**), the proportion of G1, S and G2 stayed constant throughout the dose range. Apoptosis was not induced by TCDD in MCL5 cells shown in **Figure 3.11**. The lack of a significant increase in apoptosis as a result of TCDD treatment could highlight a possible anti-apoptotic mechanism. It has been noted that TCDD is capable of altering cellular proliferation, cell cycle regulation and apoptosis (Henkler and Luch, 2010). However, **Figure 3.10** and **Figure 3.11** showed no cell cycle or apoptotic changes as a result of TCDD treatment. Data from Wilde *et al*., (2017) is in

agreement with the cell cycle data in **Figure 3.10**. However Xu *et al*., (2014) have shown that TCDD is capable of inducing apoptosis but with a long-term treatment of over 7 days, which was not demonstrated with the data here as the apoptosis experiment was a 24-hour treatment. **Figure 3.7** and **Figure 3.8** demonstrate the RPD which indicates cell viability and hence potential cytotoxicity, however, it does not give a measure of cellular proliferation, such as the MTT assay.

Mitochondrial stress is an important hallmark of cancer, but **Figure 3.13** showed very minimal change in the Seahorse trace, meaning it does not seem likely that the mitochondria are damaged as a result of TCDD treatment.

The most positive result that TCDD showed was its vast array of biologically relevant genes upregulated in the cancer panel PCR array demonstrated in **Figure 3.12**. The PCR array shows a total of 60 genes upregulated, this is the highest number of upregulated genes of all of the chemicals assessed. This indicates a lot of potential cell signaling disruption with this carcinogen. TCDD is related to the increased expression of RAS proteins which are responsible for cellular growth and death, the proto-oncogenes *c-fos, c-jun* and *erbA*, as well as cyclin dependent kinases (Knerr and Schrenk. 2006). **Figure 3.12** is in agreement with the increased expression of *RAS* proteins as it shows the upregulation of *KRAS*, *HRAS* and *NRAS*. The *CDKN2A* is also upregulated in the PCR array for TCDD seen in **Figure 3.12** which would indicate cell cycle disruption which was not seen. *FGFR2* is the highest upregulated gene in the TCDD PCR array and this gene is present several cancer types. This gene encourages the proliferation and migration of cancer cells (Szybowska *et al.,* 2019).

A systemic assessment of TCDD and cancer was carried out by Xu *et al*., (2016), indicating that high external exposure to TCDD is significantly associated with all cancer mortality assessed but not all cancer incidence (Xu *et al*., 2016). The strong toxicity of TCDD highlights the considerable epidemiologic public health threat. TCDD is associated with a wide range of cancer types such as oesophageal, lung and soft-tissue sarcoma. The human carcinogenic potential and mechanisms utilized by TCDD are still largely misunderstood (Xu *et al*., 2016).

Future work to enable an *in vitro* detection of TCDDs carcinogenicity would be to assess numerous time points, a larger dose range and further qPCR investigations. There were several limitations of working with the highly toxic TCDD. As the chemical was already dissolved in DMSO, it was difficult to choose any doses higher than 3 µM as the DMSO concentration would

have been too high for the *in vitro* system. Although DMSO is known as a universal solvent, it also has an effect on cellular systems. For example, DMSO can stimulate proliferation at low levels (<0.5%), induce apoptosis and ROS from levels as low as 0.009% and necrosis at 3.7% (Sangweni *et al*., 2021). DMSO also has an effect on the bioenergetic flux of MCF-7 cells (Sangweni *et al*., 2021). Both TCDD and rosuvastatin utilize DMSO as a solvent and both of these NGCs seem to give many negative results to the test battery chosen. DMSO could potentially be counteracting the effects of the NGCs assessed and exerting its own effects. Likewise, chloroprene uses methanol as the solvent, which could also exert its own effects. It has been shown that DMSO is capable of inactivating the cytotoxic effects of cisplatin (Madassery *et al*., 2015). DMSO was also tested for cytotoxic and genotoxic effects, which can be seen in the **Appendices Figures A4, A5, A6** and **A7.**

3.4.2 Chloroprene

The acute treatment of TK6 cells with chloroprene (**Figure 3.15**) had minimal effects on both cytotoxicity and genotoxicity with a stable RPD and an interesting Mn pattern. The Mn seemed to first increase at 2 µM and then decrease slightly at 100 µM before increasing again at 400 µM. However, there is no statistical significance observed with these data.

The chronic treatment with chloroprene in **Figure 3.16** again showed very stable RPD values across all doses and minimal changes to the Mn induction across the full dose range. There was a very slight reduction of Mn induction at 200 µM and 400 µM doses when compared to the negative control. Moreover, like **Figure 3.15**, there is no statistical significance observed with these data.

Figure 3.17 shows that ROS was not produced as a result of chloroprene exposure. However, it states in the literature that chloroprene is capable of producing ROS in the form of epoxides which are able to cause cytotoxicity and the formation of DNA adducts (Black, *et al*., 2015). This suggests that oxidative stress is a potential MoA of chloroprene. This is in contrast to **Figure 3.17,** where a possible AOX effect was observed instead of ROS production. The data here is conflicting when compared to the literature for chloroprenes ROS production. It is possible that DCFDA can undergo cell-free interactions with the compound tested (Tetz *et al*., 2013). It is also thought that DCFDA can be converted to DCF with increased serum concentrations (Tetz *et al*., 2013). A total ROS burden is detected by the DCFDA assay, carried out in a 96 well plate format and compatible with multiple ROS types and cell types (Oparka *et al*., 2016). Although, the data here disagrees with Oparka *et al*., (2016) as the data in **Figure 3.17**

does not show ROS production as stated a possible MoA in the literature. Follow up work for chloroprene could include AOX studies, to confirm whether the DCFDA result seen is actually an AOX effect.

Figure 3.18 shows slight changes in cell cycle distribution as a result of 24-hour chloroprene treatment. There seemed to be a similar pattern shown with cell cycle as there are in the acute Mn assessment. At dose 2 µM there is an increase in G1 before a decrease at 20 µM and 100 µM but then G1 increased again at 200 µM before a final decrease in G1 at 400 µM.

Due to the interesting results in **Figure 3.18** and the significant upregulation of *CCND1* in **Figure 3.22**, cell cycle was repeated again at an earlier time (12 hours-**Figure 3.19**) and a later time point (48 hours-**Figure 3.20**). However in both cases there seems to be no significant changes in the cell cycle at these time points.

There was a systemic biological review carried out for chloroprene gene expression and some key targets were identified such as *ANTXR2, HIP1, CFTR, TBL1X, EPHX1*. These genes are critical for carcinogenesis and are involved in inflammation, angiogenesis, cell transformation and gene transcription regulation (Guo and Xing. 2016). In my study using a general cancer panel, *CCND2* was also shown to be an important gene identified in the analysis. This gene is involved in cell cycle progression (G1 to S phase), which is in agreement with **Figure 3.18** and is analogous to *CCND1* which is significantly upregulated in **Figure 3.22** (Guo and Xing. 2016). This all highlights the importance of cell cycle perturbations and could be the responsible MoA for chloroprene induced carcinogenesis.

Chloroprene has minimal apoptotic changes in **Figure 3.21**, similar to TCDD in **Figure 3.11**, which could again indicate a possible anti-apoptotic effect, so this could potentially be a MoA used by chloroprene.

Figure 3.23 shows the Seahorse trace of chloroprene when compared with its solvent control methanol, indicating very minimal changes again similar to **Figure 3.13**. This suggests that there is minimal mitochondrial damage as a result of chloroprene addition.

In **Figure 3.23**, the PCR array of chloroprene is indicated, showing all of the biologically genes but focussing on the massive upregulation of *CCND1*. The upregulation of *CCND1* overshadows the other genes in this array and suggests that *CCND1* is of great importance when trying to understand the MoA of chloroprene.

It has been shown as a result of the 2-year rodent bioassay that the neoplasms formed are as a result of oncogene (*KRAS*) activation (Sills *et al*., 1999), which is mirrored by the PCR array data in **Figure 3.22.** The *KRAS* gene was upregulated by 2.3-fold, which is biologically relevant as it is above the 2 fold cut off. This is an oncogene and is often seen throughout the literature as a result of chloroprene exposure (Ton *et al*., 2007).

1-3 butadiene and chloroprene are multisite carcinogens in both rats and mice (Ton *et al*., 2007). However, chloroprene's genotoxicity has been questioned due to the largely negative *in vitro* tests (Ton *et al*., 2007). It is possible that chloroprene could use multiple different routes of carcinogenesis and it may be able to act as both a genotoxic and NGC. A recent occupational exposure study carried out in the U.S. showed that chloroprene did not increase the risk of death by cancer in the workplace (Marsh *et al*., 2020). Further mortality assessments via epidemiology studies are required to understand the full effects of long-term chloroprene exposure.

Chloroprene has numerous factors indicating a mutagenic MoA taking place such as influencing metabolism and toxicokinetics, the mutation spectra in rodent tumours and a structural similarity to carcinogens (Eastmond. 2012). Future work for chloroprene could be to further investigate the increased gene expression of *CCND1* and try to decipher what this means for the MoA of chloroprene. Perhaps exploring more time points would be beneficial when trying to understand cell cycle. Also, as methanol is the solvent used for chloroprene, this may also exert an adverse effect on the cells so requires more attention.

3.4.3 Rosuvastatin

Rosuvastatin is not widely studied in the literature, it appears in publications listed as a NGC (Kirkland *et al*., 2016) but it is largely misunderstood. There are also contradictions in the literature, for example Wang *et al*., (2010) suggests that rosuvastatin possesses some anti-tumour and anti-angiogenic effects in prostate cancer.

Figure 3.25 shows the acute Mn results for TK6 cells treated with rosuvastatin. The data demonstrates a strong dose dependent cytotoxic response however no genotoxicity was observed. The data by Berber *et al*., (2014) is in agreement with **Figure 3.25** that Rosuvastatin induces cytotoxicity however more investigation is needed to establish its genotoxic potential. An *in vivo* study on *Drosophila melanogaster* has showed that rosuvastatin induced cytotoxicity (Orsolin *et al*., 2015) which is in agreement with **Figure 3.25**. It is suggested that rosuvastatin is genotoxic in human peripheral lymphocytes and therefore a clastogen or aneugen, as it has

showed a significant increase in Mn induction and comet tail length (Berber *et al*., 2014). This is conflicting with the data in this study, although it is not in agreement with **Figure 3.25**, it is in agreement with **Figure 3.26**. Berber *et al*., (2014) conducted their study in human lymphocytes, which is similar to this study which utilized TK6 cells. Berber *et al*., (2014) also conducted acute studies of a 24-hour and a 48-hour time point, which again was done in this study. However, the acute genotoxic results differ from this work, while the genotoxicity is seen in the chronic studies.

Although, when dosed chronically in **Figure 3.26**, rosuvastatin looks to have induced a Mn response throughout the whole dose range, suggesting genotoxicity is induced, although not in a dose dependent manner. Though it looks as if a response is induced, the difference is not statistically significant. Cytotoxicity does not seem to be induced across all doses, suggesting that rosuvastatin is more tolerated by the cells with fractionated doses over time. In another study, rosuvastatin has found to be negative in the Ames test, the *in vitro* micronuclei, the *in vitro* chromosomal aberration and the MLA (Hwang *et al*., 2020).

Hwang *et al*., (2020), is in agreement with **Figure 3.25** as it is negative for Mn induction *in vitro.* **Figure 3.26** demonstrated a slight but constant Mn induction with chronic dosing which was not seen in the study by Hwang *et al*., (2020)**.** However, rosuvastatin had positive carcinogenicity results in both mice and rat studies and gave structural alerts in QSAR toolbox prediction as a NGC (Hwang *et al*., 2020). However, it has recently been shown that rosuvastatin has a cytotoxic and genotoxic potential as a result of evaluation in human lymphocytes. It showed that results of chromosomal aberration, comet assay and the Mn assay confirmed rosuvastatins genotoxicity (Ökçesiz and Ündeğer Bucurgat. 2021). This is in agreement with the chronic Mn results seen in **Figure 3.26** but not with the acute Mn data in **Figure 3.25**.

Rosuvastatin does not seem to produce ROS (**Figure 3.27**) as there is no fold change differences at the different time points and doses. Studies have shown that rosuvastatin possesses AOX action, which could explain why there is a lack of ROS produced in **Figure 3.27** (Orsolin *et al*., 2015).

There seems to be very minor changes with the cell cycle profile for rosuvastatin in **Figure 3.28**, which means this is most likely not a main MoA used by rosuvastatin.

Figure 3.29 represents a very slight dose dependent apoptotic induction by rosuvastatin, however at the top dose of 400 µM there is a slight decrease in apoptotic induction.

It has been shown that rosuvastatin is capable of inducing apoptosis in HUVEC cells and can also arrest HUVEC cells at the G1 cell cycle phase (Wang *et al*., 2010). Although, the cell type is different, these results were not mirrored in TK6 cells in **Figure 3.28** and **Figure 3.29** as both cell cycle and apoptosis remained largely unchanged as a result of rosuvastatin treatment.

Statin studies have shown an anti-cancer effect, leading to investigations of repurposing statins as a possible anti-cancer drug (Jiang *et al*., 2021). Due to the anti-cancer effect of statins it has been shown that they can cause cell cycle arrest, inhibition of tumour growth and they are able to supress angiogenesis (Demierre *et al*., 2005). **Figure 3.28** only shows cell cycle arrest at the S phase of the top dose of 400 µM, perhaps this could contribute to the MoA utilized by rosuvastatin. If there is DNA damage and progression through the cell cycle, this can lead to oncogenesis and could therefore be the MoA of oncogenesis. Statin studies have also shown an induction of apoptosis (Bardou *et al*., 2010). However, **Figure 3.29** shows very minimal changes in apoptosis except a statistically significant decrease of Q4 with 100 µM and 200 µM and therefore this could play a part in the NGC MoA of rosuvastatin. As there does not seem to be an induction of apoptosis, this could allow genetically damaged cells to divide and cause the initiation of cancer.

The bioenergetic flux of rosuvastatin in **Figure 3.33** is roughly 5 fold lower at maximal capacity than that of the DMSO solvent control. This means there is a reduction in mitochondrial function as a result of treatment with rosuvastatin.

The PCR array for rosuvastatin **Figure 3.32,** is comprised of **Figure 3.30** and **Figure 3.31** overlayed and logged. Limitations with the number of PCR arrays that could be carried out meant that unfortunately rosuvastatin could not be compared with its correct control. DMSO is the solvent control for rosuvastatin and TK6 cells were treated cells however the available PCR array controls were ‘DMSO in MCL5 cells’ and ‘Methanol in TK6’. Both of the plates used, had a correct aspect of the study (cell line or solvent) so by overlaying and only plotting the biologically relevant logged overlaps, hopefully this enables conclusions to be drawn from **Figure 3.32**. Most of the upregulated genes (when compared to both negatives) showed a higher response in MCL5 which could be due to the metabolic capacity. It is promising that there was a large number of overlaps between the two negative controls. Like TCDD in **Figure 3.12** there are a vast number of genes upregulated suggesting that there is a lot of cell signaling disruptions, so this is a possible MoA for rosuvastatin. In the overlapped graphs for rosuvastatin, there is only upregulation of genes, no downregulation.

Future work for rosuvastatin would include further investigation into *CD44* which is a non-kinase transmembrane glycoprotein as this gene showed the highest change in gene expression. This could potentially explain the MoA utilized by rosuvastatin. As mentioned, TCDD and rosuvastatin both have DMSO as a solvent which exerts its own effects on the cells, which could be masking/enhancing the effects seen from rosuvastatin alone. It has been shown that *CD44* plays an important role in cancer development and progression (Chen *et al*., 2018). Future work should also include a follow up of the chronic Mn data (**Figure 3.26**), although it was not statistically significant it is interesting data nevertheless.

Statins have numerous benefits as a result of inhibiting HMG-CoA reductase, in addition to reducing cholesterol levels and improving cardiovascular health. They are also capable of inducing anti-inflammatory effects, improving endothelial function, immunomodulation and antithrombosis effects to name a few (Buhaescu and Izzedine, 2007). Perhaps some of these beneficial effects of statins, are responsible for counteracting some of the negative NGC effects. This could potentially explain the lack of positive *in vitro* results for the testing battery.

3.4.4 The additional data

The additional HepG2 spheroid data in **Figure 3.35**, **Figure 3.36** and **Figure 3.37** for TCDD, chloroprene and rosuvastatin respectively did not show any genotoxicity or cytotoxicity across all three chemicals tested. This HepG2 3D model has increased liver-specific function when compared to a 2D monolayer and it has required the expression of both phase I and phase II metabolic enzymes, bile transport and the storage of glycogen (Ramaiahgari *et al.*, 2014). As a result, this model is more physiologically relevant and has increased metabolic capabilities however this has not given any further insights into the genotoxicity of these chemicals. The BN frequencies were calculated for each chemical tested indicated by **Figure 3.38**, **Figure 3.39** and **Figure 3.40.** The data here represented the natural cellular division and block of cytokinesis.

Section 3.3.4 was interesting, although the genotoxicity did not differ from the 2D cell culture data, it showed an interesting pattern of potential biphasic responses. It has been seen that NGCs in particular are thought to often act as a molecular switch representing a biphasic response (Fitzmaurice *et al.*, 2022).

In this 3D HepG2 work, spontaneous BNs were seen in the mononucleate Mn assay cultures. This could be as a result of the improved microenvironment and metabolic capabilities. However, BNs were not considered in the assessment of the 2D chronic and acute cultures. They

may have also been present there as they were in the previous collaborative work from Swansea university (Doherty *et al.*, 2014).

It has previously been shown in a collaborative study between AstraZeneca and Swansea University that BN cells can be formed during the mononuclear Mn assay (Doherty *et al.,* 2014). The elevated BN frequency was also seen after a 24-hour treatment in TK6 cells and in AHH-1 cells. This corresponds with the data seen in **Figure 3.35, Figure 3.36** and **Figure 3.37** completed in TK6 and MCL5 cells**.** It is stated in Doherty *et al.,* 2014 that the exact mechanism of BN induction is unknown, but it could be as a result of genotoxic stressors prior to the progression into cytokinesis. However, the chemicals assessed here were all NGCs, so they have induced a form of toxicity capable of causing cell cycle arrest. Another point to mention is that the cytotoxicity has been investigated in **Figure 3.35, Figure 3.36** and **Figure 3.37**, so the increased BN frequency is not as a result of cytotoxicity. It is also indicated in Doherty *et al.,* 2014 that micronuclei were seen in some of the spontaneous BN cells and if these micronuclei are counted as well as micronuclei in mononucleate cells then this demonstrates a significant induction of Mn in TK6 cells.

3.5 Conclusions

Due to the differences in MoA between genotoxic and NGCs, it is thought that the gene expression profiles for the different classes of carcinogens would also be distinct (van Delft *et al*., 2004). The genes controlling cellular functions such as DNA repair, cell cycle arrest and apoptosis include *MDM2* and *GADD45* for cell cycle arrest and *IGF-BP* and *BAX* for apoptotic induction (Levine, 1997). These genes are often associated with GCs, however NGCs are capable of using diverse and in some cases multiple mechanisms to elicit oncogenesis. The PCR arrays for TCDD (**Figure 3.12),** (**Figure 3.23**) and rosuvastatin (**Figure 3.32**) show the upregulation of some of these genes, suggesting they could be interfering with these cellular processes. TCDD shows the upregulation of both *MDM2* and *IGF1*, chloroprene indicated the upregulation of *IGF1* and rosuvastatin demonstrated the upregulation of *MDM2*. This could suggest that these increased gene expressions are linked with the mechanisms of action related to these processes.

These 3 chemicals were largely negative for most of the endpoints tested, which may be due to numerous factors including the complex mechanisms used by these NGCs. Appropriate dose

selection, time points chosen and cell model choice could also be responsible. Using a 3D liver cell model could be the answer to further understanding these NGCs, as a 2D test system may be too primitive to detect minor changes. A more physiologically relevant test environment could better mimic the *in vivo* conditions and ensure that the chemicals are fully metabolised. Future work could incorporate the optimised spheroid HepG2 cell model as described in (Llewellyn *et al*., 2020) established at this laboratory at Swansea university primarily for nanomaterials. Potentially even liver organoids could be a next step in the advancement of understanding these complex chemicals.

Chapter 4: Nickel Chloride ($NiCl_2$)

4.1 Introduction

$NiCl_2$ has a simple 2-dimensional structure as seen in **Figure 4.1**. It is water soluble and available as an anhydrous salt (yellow) or a hexahydrate crystal (green) (Stannard *et al*., 2016).

Figure 4.1: Chemical structure of $NiCl_2$ adapted from (PubChem, Nickel chloride). Colours are representative of each chemical (blue indicates chlorine, purple indicates nickel).

4.1.1 Environmental exposure

Nickel is a naturally occurring metallic element present in the earth's crust. Nickel can exist in a number of different mineral forms and is mainly found in soil but also in water supplies, in the air and within plants and animals. Volcanic eruptions are responsible for widespread release of nickel into the environment. Soluble nickel compounds are easily incorporated into soils causing problematic widespread environmental pollution (Rudel *et al*., 2013). Accumulation of nickel can lead to toxicity in the human body, which is associated with the metal ion concentration (Genchi *et al*., 2020). Nickel also has a number of uses in industry, these include alloy production, electroplating and in the production of stainless steel. Throughout the production of stainless steel etc., nickel is released into the atmosphere. This environmental and industrial release enables nickel to pose a threat to human health by allowing long-term repeated exposures. Lung inhalation is the main exposure route of nickel compounds however ingestion and skin absorption are alternative routes. The main health outcome to nickel is an allergic reaction however some research has also shown carcinogenic effects to humans (Cameron *et al*., 2011). Nickel can also cause neurotoxicity, hepatotoxicity, genetic toxicity and reproductive toxicity (Poonkothai and Vijayavathi, 2012). Nickel is able to bind to small dust particles which settle on the ground. When nickel is released via wastewater from industrial processes, it attaches to the iron or manganese particles in the soil or sediment. However, the presence of nickel in the environment, does not seem to affect marine animals (ATSDR, 2005). Human exposure of nickel comes from a range of sources such as food consumption, drinking water, breathing particles in the air and tobacco smoking (Cameron *et al*., 2011). In the general public, the greatest level of nickel and nickel compound exposure will come from dietary consumption (Coogan *et al*., 1989). Other forms of nickel interaction are direct contact with stainless steel, jewellery and also artificial body parts (Cameron *et al*., 2011).

Perhaps the most important source of human nickel exposure is to $NiCl_2$, as it has widespread use in electroplating onto other metals (National Toxicology Program, 2013). One major use of $NiCl_2$, is as a nickel catalyst for ammonia absorption in gas masks (Stannard *et al*., 2016). $NiCl_2$ is able to penetrate the skin with a 77% absorbance rate within a 24-hour period (ATSDR, 2005). It is well known that insoluble nickel compounds are more potent carcinogens than soluble nickel compounds. $NiCl_2$ is a water-soluble compound, so is deemed a weaker carcinogen. Nickel compounds are present in multiple forms in the environment, perhaps the most common is $NiCl_2$ (Guo *et al*., 2020). Carcinogenic activity is inversely correlated with the water solubility of nickel compounds (National Toxicology Program, 1996). It has been shown that soluble and insoluble nickel compounds act via different carcinogenic mechanisms of action. Soluble nickel compounds have been shown to arrest cell growth and are capable of degrading cyclin D1 (*CCND1*) whereas insoluble nickel compounds do not act this way (Ouyang *et al*., 2009). Some water insoluble nickel particles are taken up by phagocytosis *in vitro* (Abbracchio *et al*., 1981), which efficiently delivers nickel to target cells such as lysosomes for degradation (Sen and Costa, 1986). Water soluble nickel compounds are not readily phagocytosed (Abbracchio *et al*., 1981), soluble nickel undergoes dissolution instead (Hirano *et al*., 1994) which gives rise to nickel ions which can be transported into the cytoplasm via calcium (Ca^{2+}) channels for example (Refsvik and Andreassen, 1995).

4.1.2 Occupational Exposure

As nickel is widely used in industrial processes it is a source of occupational exposure for the workers. Some examples of occupational exposure to nickel consists of mining, refinery and fumes from welding (Alfhili *et al*., 2022). There is a major nickel refinery based in Clydach, Swansea which has operated since 1901 and has been the main focus of a number of research questions. Since 1920, there have been reports of 365 cases of respiratory cancer linked to nickel inhalation at this site (Clemens and Landolf, 2003). Nickel and its compounds have proven to be a hazard to living organisms as a result of the genotoxicity, carcinogenicity, mutagenicity and immunotoxicity it presents (Alarifi *et al*., 2014). The general public are exposed to low levels of nickel daily through tobacco smoke, air, food and water (Stannard *et al*., 2016). Occupational nickel exposure has shown an increase of breast, lung, head, neck, nasal, stomach and kidney cancers (Kasprzak *et al*., 2003a). Nickel compounds are classified as weakly mutagenic but are capable of causing epigenetic effects (Ke *et al*., 2006). Nickel has also demonstrated clear spermatotoxic results (Pandey and Srivastava, 2000). As nickel exposure is responsible for reproductive and developmental toxicity, it therefore affects fertility and can cause birth defects

(Beshir *et al*., 2016). High level nickel exposure is capable of affecting embryo development and trophoblast cells (Yao *et al*., 2014). Nickel significantly reduces the proliferative potential of the trophoblast's inner mass of cells, which means the embryo struggles to implant in the uterine lining (Forgacs *et al*., 2012).

In 1990, the international committee on nickel carcinogenicity issued an epidemiology report, that nickel salts and sulphuric nickel compounds are responsible for causing nasal and pulmonary cancers due to occupational exposure of refinery workers (Anttila *et al*., 1998). To add to this, a cohort was taken from a nickel refinery in Finland and it was a reported that there was an elevated incidence of nasal and lung cancers (Karjalainen *et al*., 1992). Refinery workers are often exposed to mixtures of nickel compounds as opposed to a specific or pure form of nickel. This means that the compounds may display a range of different properties when compared to pure nickel forms. It is important to assess the carcinogenic potential of each compound present as well as conducting research on mixtures of nickel compounds (Goodman *et al*., 2009).

4.1.3 Carcinogenicity of $NiCl_2$

The IARC classified all nickel compounds as human carcinogens, excluding metallic nickel (IARC, 1990). IARC classifies nickel and its alloys as group 2B carcinogens (possibly carcinogenic to humans) and nickel compounds as group 1 carcinogens (Kim *et al*., 2015). This means that $NiCl_2$ is classified as group 2B carcinogen as there is limited carcinogenicity data available in humans but there is appropriate experimental data available in animals (IARC, 1990).

There are numerous animal studies with positive carcinogenicity data for nickel salts, however $NiCl_2$ is considered to be a weaker carcinogen overall when compared to other nickel compounds such as nickel sulphate. For example, $NiCl_2$ did not produce tumours in rats as a result of intramuscular dosing and only few tumours in their lungs and stomachs, highlighting the weak carcinogenicity present (Stannard *et al*., 2016). Different nickel compounds have different carcinogenic and genotoxic potentials. It has been suggested that $NiCl_2$ can be both a carcinogen and an initiator meaning it has the potential to act as both a GC and a NGC (Diwan *et al*., 1992). A CTA carried out with $NiCl_2$, highlighted that it is a unique carcinogen as it does not display a dose-dependent linear relationship in respect to the average induction of foci detected. $NiCl_2$ was chosen in this CTA due to its indirect DNA damaging properties (Callegaro *et al*., 2016). There are several studies that highlight an increased cancer incidence after exposure

to $NiCl_2$. Synergistic effects have been reported between cigarette smoking and nickel exposure (Andersen *et al*., 1996) and UV radiation and $NiCl_2$ exposure (Uddin *et al*., 2007).

A feature of metallic compounds is their capability of increasing mutagenicity and carcinogenicity of genotoxic agents (Shen and Zhang, 1994). Nickel is able to bind to DNA and nuclear proteins and is also able to interrupt nucleotide and base-excision repair when subject to low, non-cytotoxic concentrations. Nickel is capable of impairing DNA adduct repair (Hartwig and Scwerdtle, 2002). It is suggested that metal compounds can alter gene expression, increasing cell proliferation by affecting tumour suppressor genes or proto-oncogenes (Beyersmann and Hartwig *et al*., 2008). It has been reported that the nickel ion is the crucial carcinogenic part of nickel compounds. A hypothesis suggests that nickel ions are able to inhibit magnesium binding to proteins within heterochromatin (Costa *et al*., 1994). Nickel ions have a high affinity for interacting with heterochromatin due its high protein content. Nickel ions also have an increased attraction towards amino acids rather than DNA (Costa *et al*., 1994). As nickel ions bind to the histone proteins within heterochromatin, oxygen radicals are produced which are DNA damaging (Kasprzak *et al*., 2003b).

Nickel is able to imitate hypoxic conditions, leading to the activation and accumulation of hypoxia inducible factor (HIF). This can then inhibit prolyl hydroxylase activity and therefore disturbing the degradation of HIF (Kang *et al*., 2006). Hypoxia is a common characteristic for carcinogenesis and encourages a number of tumour forming functions such as the inflammation, angiogenesis and glucose uptake (Kang *et al*., 2020).

4.1.4 Genotoxicity of $NiCl_2$

The genotoxicity of $NiCl_2$ is poorly understood with mixed positive and negative results published in the literature, which highlights that $NiCl_2$ is an interesting chemical to investigate. Here, numerous arguments for $NiCl_2$ acting as a GC are flagged. However,$NiCl_2$ was selected as a NGC in this study, despite some conflicting genotoxicity information in the literature (Dallas *et al.,* 2013). It highlights the complexities of NGCs, due to the results seen in the literature, meaning further investigation into the mechanism(s) of actions utilized is required. Dallas *et al.,* (2013) mentions that $NiCl_2$ is a weak genotoxin, which may explain some of the contradicting information available on this carcinogen. It is an interesting chemical due to its direct and indirect DNA interactions as well as potential epigenetic effects. A literature review has stated that nickel has the ability to damage the DNA strands, disrupt the covalent crosslinks and the DNA repair processes (Cameron *et al*., 2011). It is thought that nickel produces ROS as a result

of its ability to bind with amino acids, proteins and peptides (Cameron *et al*., 2011). It has been noted that some GCs are also capable of acting in a non-genotoxic manner and are able to also cause tumours by using both indirect and non-genotoxic mechanisms (Smith *et al*., 2016). Experiments in both rodents (*in vivo*) and human cells (*in vitro*) have shown that numerous nickel compounds are capable of inducing genetic damage such as DNA strand breaks, chromosomal damage, cell transformation, mutation and altered DNA repair (National Toxicology Program, 2013). This highlights the variations between different nickel compounds and the controversy in the literature regarding this carcinogen. An *in vivo* inhalation study in rats showed that nickel induced tumour formation (Ottolenghi *et al*., 1975). Nickel has shown genotoxicity *in vitro* with both the comet assay and the Mn assay in HepG2 and BALB/3T3 cells (Terpilowska and Siwicki, 2018).

$NiCl_2$ is classified as a known NGC, however a number of other nickel compounds are classified as GCs (IARC, 1990). There is a possibility that there could be overlaps with $NiCl_2$'s direct and indirect genotoxicity.

Nickel compounds soluble in water, such as $NiCl_2$ have been shown to cause oxidative stress and to cause DNA damage (Lynn *et al*., 1997). The genotoxic effects of soluble nickel compounds are reduced when compared with insoluble nickel forms as they are rapidly cleared by protective mechanisms from the lungs (Dunnick *et al*., 1995). In rodent studies, nickel is removed from the lungs which is not the case for *in vitro* studies as there is a lack of clearance mechanisms. This could mean that there are prolonged and non-physiological exposures *in vitro* which provides enough time for nickel ions to reach the nucleus and cause genotoxic effects (Dunnick *et al*., 1995).

$NiCl_2$ causes lipid peroxidation via malondialdehydye induced genotoxicity (Niedernhofer *et al*., 2003) however this does not have an effect on DNA strand breakage. The hydroxyl radical (OH^-) production is responsible for the DNA strand breakage caused by $NiCl_2$. Accelerated OH^- radical production plays an important role in the genotoxicity induced by Ni (Chen *et al*., 2003). Studies conducted in broiler chickens showed that the diets supplemented with 300 mg/kg or more nickel, demonstrated immunotoxicity, cytotoxicity and genotoxicity in locations such as the spleen, tonsil, kidney, intestine and the thymus (Yin *et al*., 2015).4.1.5 Possible mechanism of action of $NiCl_2$.

Long-term/chronic exposure to carcinogens such as nickel is a growing health concern (Yang, 2011) as nickel exposure has been documented to show an increased affinity with lung and nasal

cancers (Leonard *et al*., 2004). Carcinogenesis of heavy metals is known to be induced via a ROS action (Pan *et al*., 2011). It is thought that nickel's genotoxicity and carcinogenicity could also be due to the production of free radicals and the inhibition of DNA-repair processes (Hartwig and Schwerdtle, 2002). Alone, nickel does not show a strong mutagenic effect and is classified as a weak genotoxin. However, there are multiple reports of nickel working synergistically with a combined treatment e.g. in addition to gamma radiation, which could be explained by nickel's indirect genotoxicity and interference with DNA repair mechanisms (Carmona *et al*., 2011).

Nickel is known to induce oxidative stress in human lymphocytes *in vitro* (M'Bemba-Meka *et al*., 2006). Nickel does not cause effective free-radical production alone, instead it uses Nickel-thiol complexes to generate free radicals (Das and Büchner, 2007). A proposed MoA is that nickel enters the cell, via phagocytosis as $NiCl_2$ is water soluble (Cameron *et al*., 2011), and in turn activates the calcium sensing receptor (CaSR) receptor which triggers stimulation of intracellular Ca^{2+} therefore inducing Ca^{2+} and hypoxia-inducible factor pathways. Nickel can then enter the nucleus to bind directly with the DNA, reacts with H_2O_2 forming nickel-oxygen complexes which can oxidise thymine and cytosine residues and form the known oxidative stress marker 8-Hydroxy-2'-Deoxyguanosine (8-OhdG). This oxidative stress both damages the DNA and inhibits the DNA repair processes (Cameron *et al*., 2011). Nickel can also stimulate polymorphonuclear leukocytes which produce ROS and mediate inflammation therefore inducing indirect DNA damage. Additionally, nickel is able to downregulate the tumour suppressor p53, activate the proto-oncogene c-Myc and stimulate the transcription factor AP-1, all of which contribute to the increased cellular proliferation and tumour development (Cameron *et al*., 2011). $NiCl_2$ also increases stress on the endoplasmic reticulum and increases the production of the inflammation cytokine *IL-1B* (Guo *et al*., 2016). Nickel has shown to enhance the toxicity of genotoxic carcinogens by disrupting DNA repair and packaging by binding to fundamental proteins or effecting the protein expression (Arita *et al*., 2013). **Figure 4.2** below represents a range of the possible ways tumourigenesis can be initiated by $NiCl_2$. NGCs such as $NiCl_2$ could use 1 or more mechanisms of action in order to cause cancer.

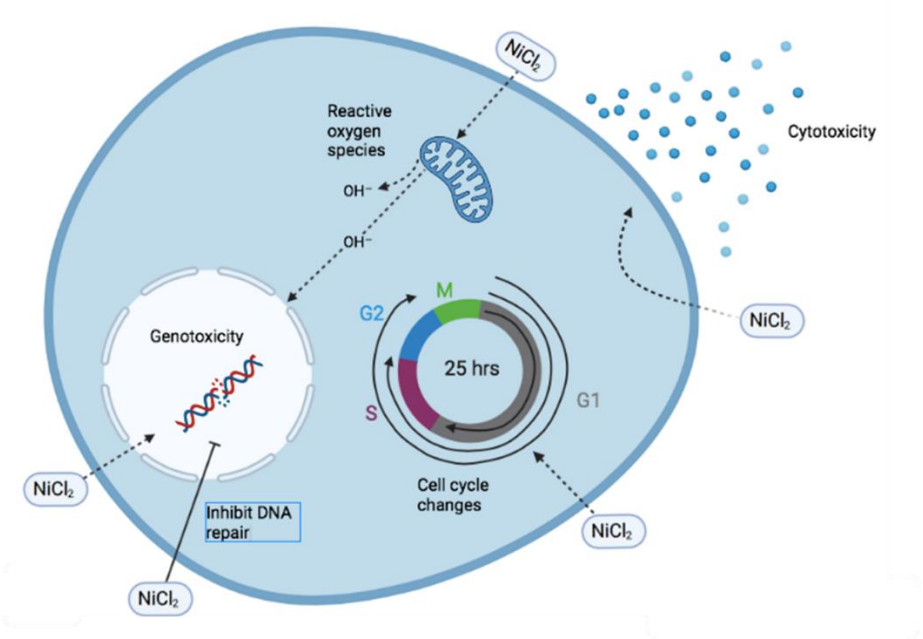

Figure 4.2 Schematic displaying some of the potential routes that have been assessed in this work, utilized by $NiCl_2$, to initiate tumourigenesis. These MoAs include ROS, cytotoxicity, genotoxicity and cell cycle but do not include some of the potential routes highlighted in the literature such as lipid peroxidation and protein oxidation

It has also been suggested that nickel exposure can cause a hypoxic environment due to iron depletion (Chen and Costa, 2009). Hypoxia is a condition exhibited by some tumours, this could be as a result of exposure to metal ions. It does this by disrupting iron levels and therefore disturbing homeostasis of iron transporters and the regulation enzymes (Cameron *et al*., 2011). Studies have shown that carcinogenic nickel compounds can stimulate the HIF-1 signalling pathway, which primarily mediates hypoxic conditions (Salnikow *et al*., 2003). A proposed pathway of Ni induced hypoxia is via the substitution of iron therefore inactivating the prolyl hydroxylase enzyme and changing the cell's metabolism to mimic a hypoxic environment (Salnikow *et al*., 2003). Hypoxia is a common state in many malignant tumours and is also thought to drive angiogenesis, cancer progression and occasionally therapy resistance (Muz *et al*., 2015). A hypoxic environment can also induce genetic damage (Mustafa *et al*., 2011; Mustafa *et al*., 2012; Mustafa *et al*., 2015)., which contributes to the weight of evidence in the literature stating that $NiCl_2$ is actually a GC, despite its classification as a NGC (Kirkland *et al*., 2016).

4.2 Methods

Methods utilised in this chapter were performed as detailed in the main methods.

4.2.1 $NiCl_2$ test chemical

$NiCl_2$ is available as a yellow powder which is water soluble and produces a green liquid once dissolved. It was sourced from Sigma Aldrich (Merck), Dorset. This chemical utiliseutilized H_2O as it's solvent as was weighed and diluted fresh before each use in **Chapter 2 in section 2.3.3.** The doses were selected based on the literature and an RPD experiment to determine the toxic top dose and these doses were used consistently throughout the different endpoints.

4.2.2 Anti-oxidant treatment

Pre-treatment with the antioxidant (AOX) N-acetyl cysteine (NAC) was carried out 1 hour prior to dosing with $NiCl_2$. The antioxidant AOX treatment was carried out in the same manner as the mononucleate Mn (**Chapter 2 in section 2.4.3)** alongside RPD analysis.

4.3 Results

$NiCl_2$ underwent multiple endpoint analysis including the acute and chronic treatment followed by the mononucleate Mn, RPD, ROS, NAC treatment with Mn and RPD, cell cycle analysis, apoptosis analysis, Seahorse analysis and a general cancer panel PCR array. The dose range (50, 100, 125 and 150 µM) was chosen based on previous work undertaken in the Swansea group (Stannard *et al*., 2016). This range was carried through to complete endpoint analysis.

The 24-hour (+ 24-hour recovery), acute Mn and RPD treatment for $NiCl_2$ **Figure 4.3** shows the concentration plotted against Mn frequency and the average RPD. There is a dose dependent drop in RPD however, it is not below the 55 ± 5% recommended cytotoxicity parameter in the OECD guidelines (TG487). The Mn data shows a dose dependent increase from 50 µM to 150 µM. When compared with to the negative control, there is a significant increase in the percentage of Mn induced at 125 µM and 150 µM $NiCl_2$. The positive control used in the Mn experiments was 10 µM MMS as stated in chapter 2 section 2.3.4.

Figure 4.4 shows equivalent data for the chronic exposures when doses are fractionated across 5 days. It is useful to compare acute data **Figure 4.3** with chronic data **Figure 4.4** for $NiCl_2$. It is evident that by fractionating the doses of $NiCl_2$ in the chronic exposure, the genotoxicity and cytotoxicity is reduced and the cells are able to better tolerate the exposure.

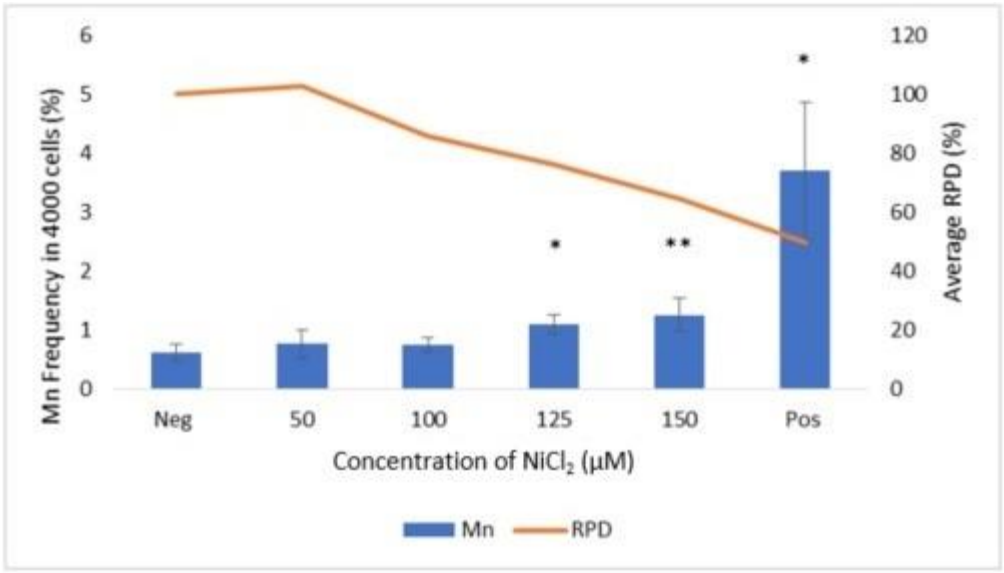

Figure 4.3: The acute mononucleate micronucleus (Mn) assay and relative population doubling (RPD) at 24-hour nickel chloride ($NiCl_2$) exposure with 24-hours recovery in TK6 cells. n=3 was carried out for this work and the average was plotted with error bars. The negative control used here was H_2O and 10 µM MMS was used as the positive control. A one-way ANOVA was performed (* < 0.05, ** <0.005). The *P* value for 125 µM was 0.0203, for 150 µM was 0.0027 and for MMS the *P* value was 0.0104.

The 5-day fractionated (+ 24-hour recovery), chronic treatment of $NiCl_2$ **Figure 4.4** shows both Mn and RPD data. There does not seem to be any major changes in RPD across the dose range, suggesting little cytotoxicity induced by the fractionated doses. There are also no significant changes in the Mn data across the dose range, in contrast to the acute data shown in **Figure 4.3**. Hence, the cytotoxicity and genotoxicity are ameliorated by chronic dosing.

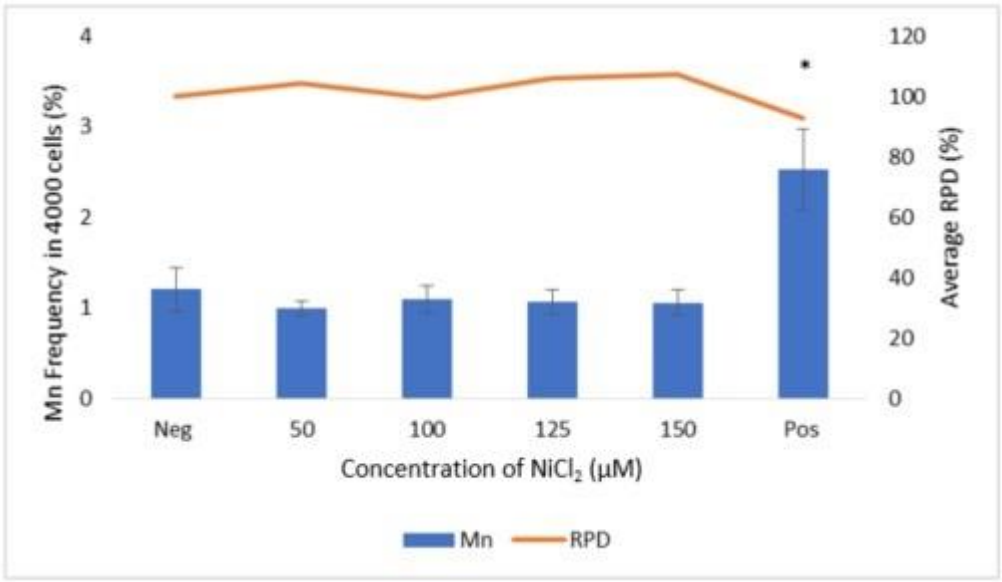

Figure 4.4: The chronic mononucleate micronucleus assay and relative population doubling at 5-day repeated exposure to fractionated $NiCl_2$ with 24-hours recovery in TK6 cells. The negative control used here was H_2O and 10 µM MMS was used as the positive control. n=3 was carried out for this work and the average was plotted with error bars. There was no statistical significance for $NiCl_2$, however, MMS showed statistical significance with a *P* value of 0.0107.

The significant acute Mn doses of 125 µM and 150 µM were repeated with the addition of the AOX NAC to confirm ROS production (**Appendix Figure A8**). The chronic Mn and RPD experiment was also conducted with $NiCl_2$ (**Appendix Figure A9**). There were slight reductions in the Mn values however there was no significance displayed.

In order to assess if ROS induction could be implicated as a mechanism in $NiCl_2$ induced DNA damage, total ROS was determined for each acute dose of $NiCl_2$ **Figure 4.5a** at a series of time points, using the DCFDA assay. Fold change was plotted against concentration. As with the Mn data (**Figure 4.3**), doses 125 µM and 150 µM show a significant increase in fold change ROS, when compared to the negative control, confirming ROS is produced with $NiCl_2$. There is a time dependent increase in ROS levels across the 24-hours period where the peak ROS levels at 6 hours. The positive control can be found in **Figure 4.5b** in a separate graph so not to mask the effects seen by $NiCl_2$.

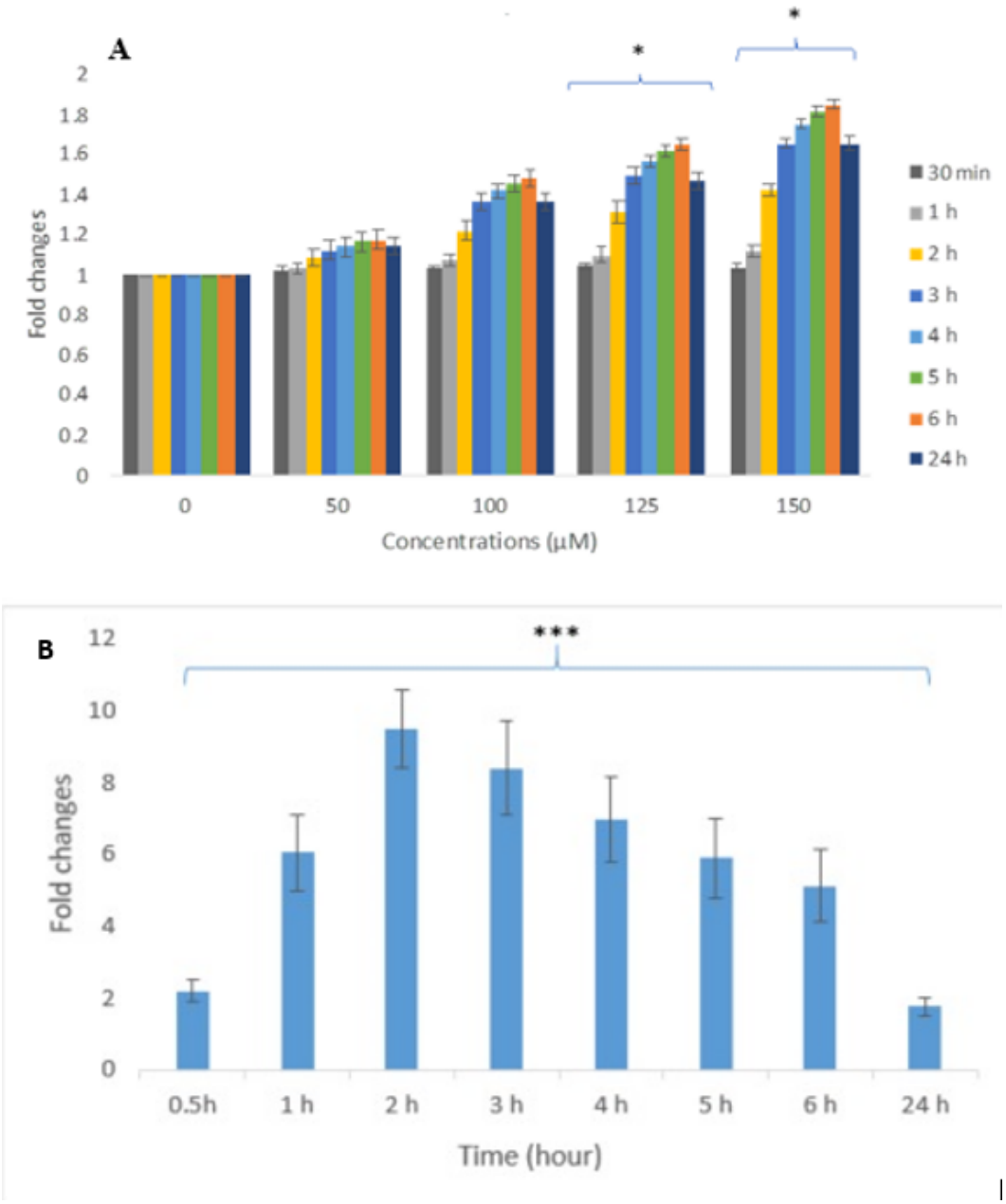

Figure 4.5 (a and b): Figure 4.5a represents the reactive oxygen species (ROS) analysis with nickel chloride ($NiCl_2$) treatment at a series of time points (30 minutes, 1 hour, 2 hours, 3 hours, 4 hours, 5 hours, 6 hours and 24-hours) plotted against fold change without recovery. A positive control of 100 µM H_2O_2 (P = 0.00024) was carried out in this experiment however, due to the high level of ROS produced, the $NiCl_2$ fold change would be masked if it was included in the same graph. The negative control used here was H_2O. **Figure 4.5b** shows the positive control displayed in the separate graph. n=3 was carried out for this work and the average was plotted with error bars. A Dunns test was performed (* < 0.05) showing that all time points treated with 125 µM (P = 0.0203) and 150 µM (P = 0.0201) were significantly increased when compared to the negative control.

As DNA damage was evident after $NiCl_2$ exposure (**Figure 4.3**) and given the impact of DNA damage on cell cycle checkpoints, cell cycle disruption was assessed across the same dose range in an acute setting. $NiCl_2$ induced impacts on the Cell cycle were analysed 24-hours after $NiCl_2$

exposure at the same dose range as previous endpoints (**Figure 4.6**). There are very subtle changes in cell cycle profile induced by $NiCl_2$. As the dose increased, the percentage of cells in G1 decreased, the percentage of cells in G2 increased and there were no noticeable changes in S phase. The changes in G1 and G2 interestingly occurred at doses which also produced DNA damage (**Figures 4.3/4.4**). Hence DNA damage induced cell cycle checkpoints may be activated, leading to accumulated G2 cells. There was no statistical significance in the cell cycle data for $NiCl_2$.

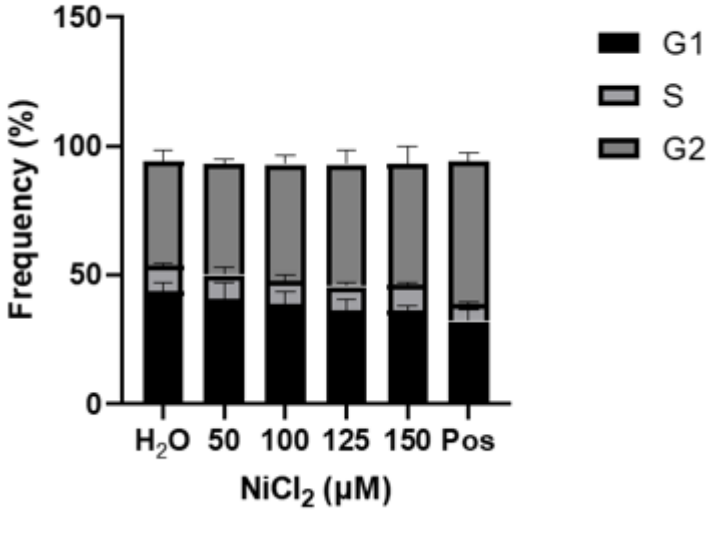

Figure 4.6: Cell cycle analysis of $NiCl_2$ at 24-hours without recovery. The cell cycle stages G1, S and G2 are represented using the flow cytometric method. n=3 was performed including 3 technical replicates and the average was plotted with error bars. The negative control used here was H_2O and 10 µM MMS was used as the positive control here. The key is shown to the top right with different colours representing each cell cycle stage. No statistical significance shown here.

As DNA damage and cell cycle disruption can trigger cells to undergo apoptosis, cell death was measured across the same dose range in an acute setting. Cell death was induced by both apoptosis and necrosis and was analysed after 24-hours $NiCl_2$ exposure (**Figure 4.7**) with the same defined dose range. Apoptosis was measured using the annexin V approach and necrotic cells were identified by facilitating 7-AAD staining. There were not any noticeable changes in apoptotic nor necrotic cell numbers induced by $NiCl_2$ (**Figure 4.7**) at this dose range. There was no statistical significance in the apoptosis data for $NiCl_2$.

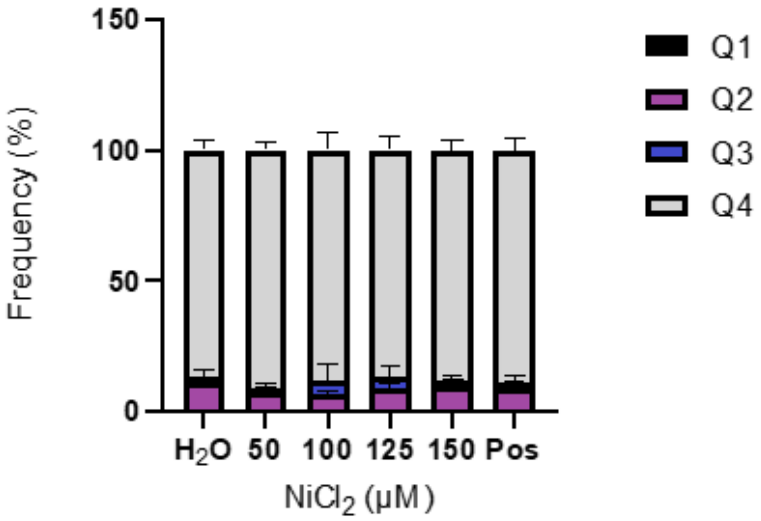

Figure 4.7: Apoptosis analysis of $NiCl_2$ at 24-hours without recovery using the annexin V and 7-AAD dyes and the flow cytometry method. Q1 is the percentage of necrotic cells. Q2 is the percentage of late apoptotic cells. Q4 is the percentage of viable cells and Q3 is the percentage of early apoptotic cells. The negative control used here was H_2O and the positive control was 0.1 µM staurosporine. n=3 was performed including 3 technical replicates and the average was plotted with error bars. The key indicates the stages Q1-Q4. There was no statistical significance observed here.

In order to try and further unpick the mechanism(s) of $NiCl_2$ induced carcinogenicity, a general cancer gene panel was assessed using a PCR array (**Figure 4.8**). Interestingly, all of the biologically relevant genes were downregulated by $NiCl_2$ with between 2- and 12-fold changes in gene expression. Substantial fold changes in gene expression were noted for *VEGF* (11.8), *TP53* (10.0), *TOP1* (9.7), *VHL* (7.1) and *PTEN* (6.10). These gene expression changes cover cancer relevant hallmarks such as angiogenesis (*VEGF*), cell cycle/apoptosis (p53), signaling (*PTEN*), signaling and tumour suppressor (*VHL*) and DNA repair (*TOP1*).

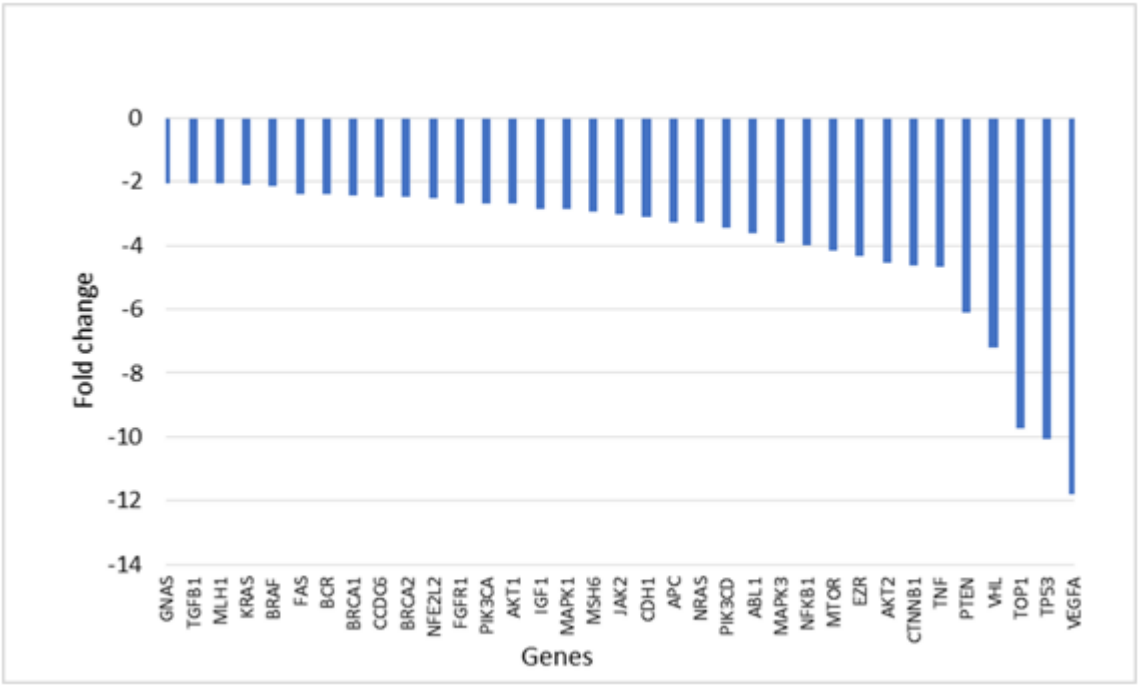

Figure 4.8: PCR array for a general panel of cancer genes. The biologically relevant (±2 fold change) downregulated genes are included in the graph. The TK6 cells were dosed with 150 µM $NiCl_2$ for 24-hours before the RNA was extracted for the PCR array. The PCR array was compared to the negative/solvent control which was H_2O. n=1 was performed here, therefore no statistical analysis was carried out.

As some of the biologically relevant genes downregulated are linked with metabolism and mitochondrial stresses bioenergetic analysis was investigated using a Seahorse bioanalyser. Some examples of the mitochondrial stresses are mitochondrial precursor over accumulation stress (mPOS) and unfolded protein response activated by mistargeting of proteins (UPRam) (Wang and Chen, 2015). Mitochondrial stress analysis was carried out as NGCs are capable of inducing stresses that can lead to potential mechanistic outcomes such as the production of ROS. The Seahorse trace observed in (**Figure 4.9**) shows the perturbations that present as a result of the addition of $NiCl_2$.

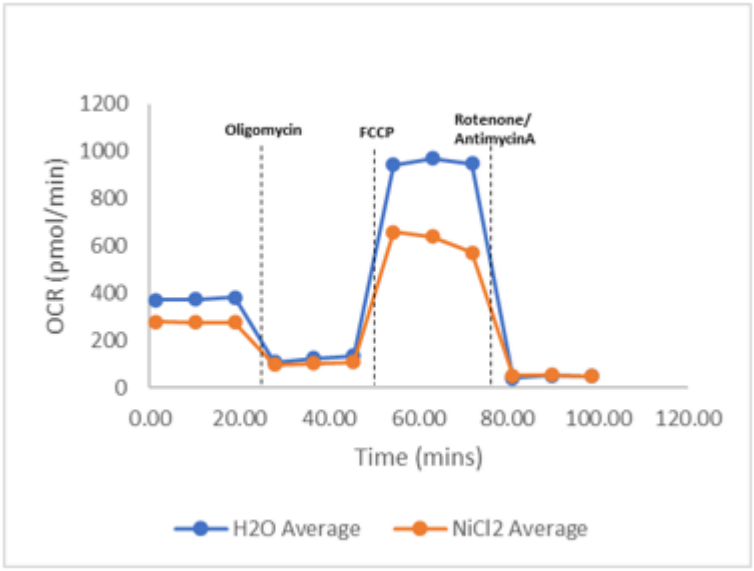

Figure 4.9: A Seahorse trace graph showing the bioenergetic flux profiles of $NiCl_2$ compared to the H_2O negative/solvent control. Oligomycin, FCCP and rotenone/antimycinA are chemical stressors added at different time points to investigate the mitochondrial stress reaction. The full name of FCCP is (carbonyl cyanide-p-trifluoromethoxy) phenylhydrazone and it acts as a mobile ion carrier. n=3 was performed here and the average was plotted.

Figure 4.9 shows that $NiCl_2$ reduced the OCR and the ECAR was also reduced (**Figure 4.10**). This means that when cells are treated with $NiCl_2$, less ATP is produced.

The Seahorse trace in **Figure 4.9** is coupled with the data shown in **Figure 4.10**. $NiCl_2$ has a reduced maximal capacity, ATP linked respiration, basal respiration, proton leak and reserve capacity when compared with H_2O. Meanwhile, the non-mitochondrial respiration and the OCR/ECAR ratio is largely unchanged by the addition of $NiCl_2$.

Figure 4.10 which represents a number of measurements that can be calculated from the Seahorse output data. The OCR is a quantitative measure of the mitochondrial electron transport rate which is crucial for understanding cellular metabolism (Mookerjee *et al*., 2015). **Figure 4.10 C and D** are often closely linked as basal respiration is often strongly controlled by ATP linked respiration (Brand and Nicholls, 2011). A large decrease in the maximal respiratory capacity, **B**, indicates a mitochondrial dysfunction potential (Brand and Nicholls, 2011). **H** represents the ECAR and therefore the rate of glycolysis (Mookerjee *et al*., 2015).

The basal respiration for $NiCl_2$ represents the energetic demand of the cell under normal conditions (before any mitochondrial stressors are added) is less than that of the H_2O control. ATP linked respiration is as a result of the ATP synthase inhibitor oligomycin exerting its effects, this shows the ATP produced by the mitochondria to meet the cell's energetic

requirements. For $NiCl_2$, this means that the cells requirements after treatment are less than that of the negative control. Suggesting that $NiCl_2$ reduces the cells energetic needs. Proton leak can represent mitochondrial damage or it can act as a regulator of mitochondrial ATP production. This does not seem to have any correlation with the cell death/apoptosis results for $NiCl_2$ assessment. $NiCl_2$ levels are lower than H_2O, suggesting there is not mitochondrial damage present with $NiCl_2$ treatment. Maximal respiration is measured after the addition of the uncoupler FCCP, which works by mimicking an energy demand therefore stimulating the respiratory chain to work at full capacity, which requires oxidation of sugars, fats and amino acids. This demonstrates the maximum rate of respiration the cell can reach, meaning that cells treated with $NiCl_2$ can achieve a much lower maximal respiratory capacity. The addition of $NiCl_2$ means the cells metabolic abilities have been lowered. The reserve capacity (or spare respiratory capacity) demonstrates the cells health, as already mentioned, after treatment with $NiCl_2$ the cells cannot respond as well as the negative control (cells treated with water only). The non-mitochondrial respiration is measured after the addition of rotenone/antimycin A. This is the persistent oxygen consumption after the block of ATP production from the mitochondria. This is very slightly increased with the addition of $NiCl_2$ and is an important measure of mitochondrial respiration (Agilent, 2022).

The Agilent Seahorse XF Analyzers can measure the OCR which indicated mitochondrial respiration and ECAR which measures glycolysis at approximately 5 minute intervals (Agilent, 2022).

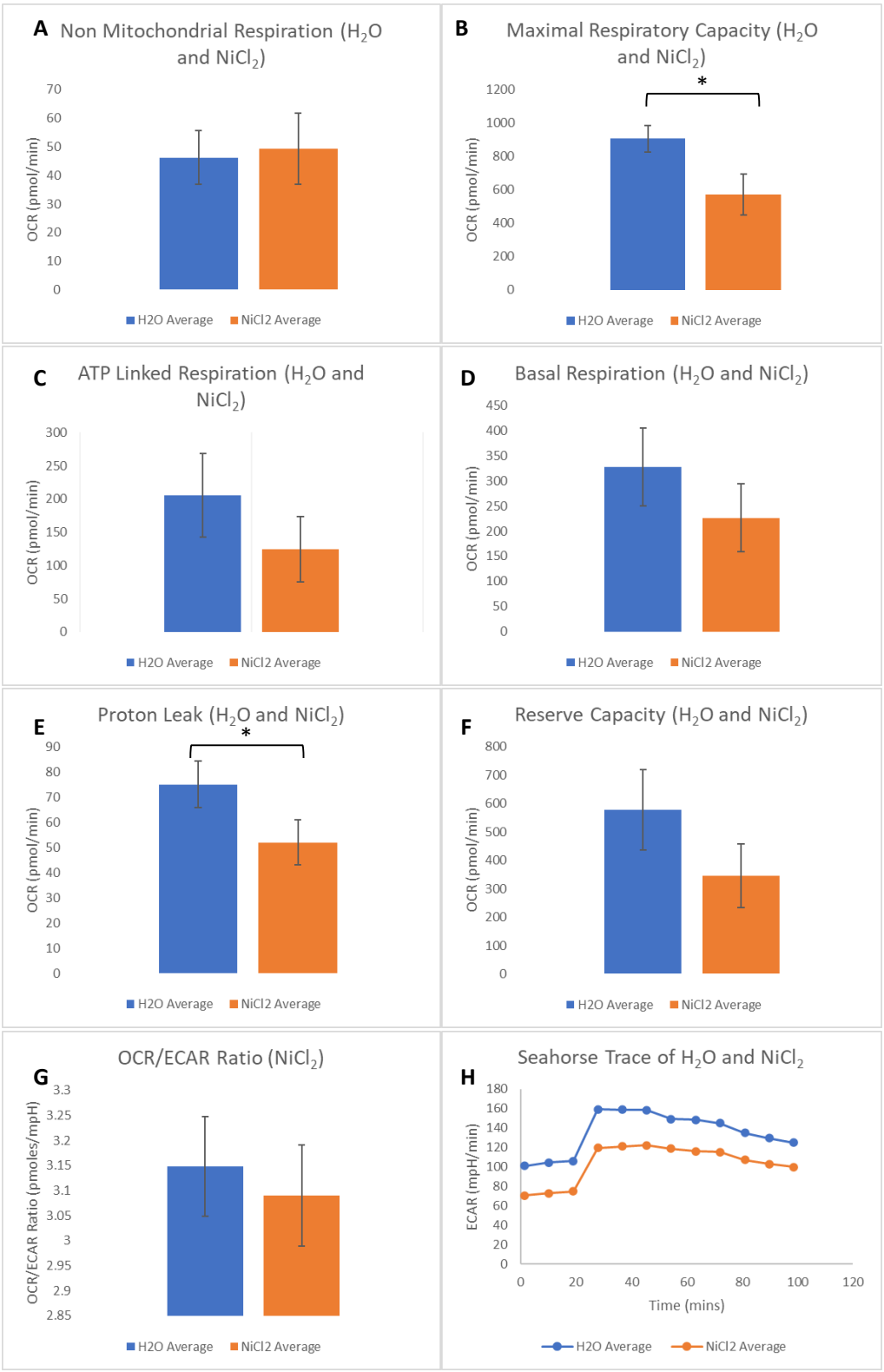

Figure 4.10 (A-H): Seahorse graphs indicating the different respiration parameters when compared to the H_2O solvent control. **A** represents non mitochondrial respiration , **B** is the maximal respiratory capacity (P = 0.0170), **C** is the ATP linked respiration, **D** is basal respiration, **E** is proton leak (P = 0.0356), **F** is the reserve capacity, **G** demonstrates the OCR/ECAR ratio and **H** represents the ECAR graph. Unpaired T tests were carried out for these analyses (* < 0.05). All graphs are compared to the negative/solvent control which is H_2O. This work was undertaken as n=3 and the averages were plotted with error bars included.

Figure 4.10 shows an overall decrease in most factors with the addition of $NiCl_2$. **A** shows a very slight increase in non-mitochondrial respiration whereas **B-F** all show a visibly larger drop with the addition of $NiCl_2$. **G** represents the OCR/ECAR ratio, demonstrating a very small decrease overall and **H** indicates the ECAR measurement which signifies glycolytic potential.

$NiCl_2$ has a negative effect on the mitochondria meaning that there is a decreased output as a result of each of the mitochondrial stressors added due to the Seahorse assay. This means that as a consequence of the $NiCl_2$ treatment, the cells have a lower energetic profile which is an added stress even before the Seahorse assay has started. The change to mitochondrial function could be linked to the ROS production in **Figure 4.5a**. The maximal respiratory capacity (**Figure 4.10 B**) and the proton leak (**Figure 4.10 E**) showed a significant reduction with $NiCl_2$ when compared with the H_2O control.

4.4 Discussion

It was shown here that exposure of TK6 cells to $NiCl_2$ caused cytotoxicity, genotoxicity, ROS induction, some cell cycle perturbations and a change in mitochondrial health represented by OCR/ECAR. Apoptosis was not significantly altered at the doses utilized throughout these experiments. There were a series of gene expression changes induced by $NiCl_2$ that require further investigation. **Figure 4.11** shows a diagrammatic summary of the MoAs relative effect levels with regard to increasing doses.

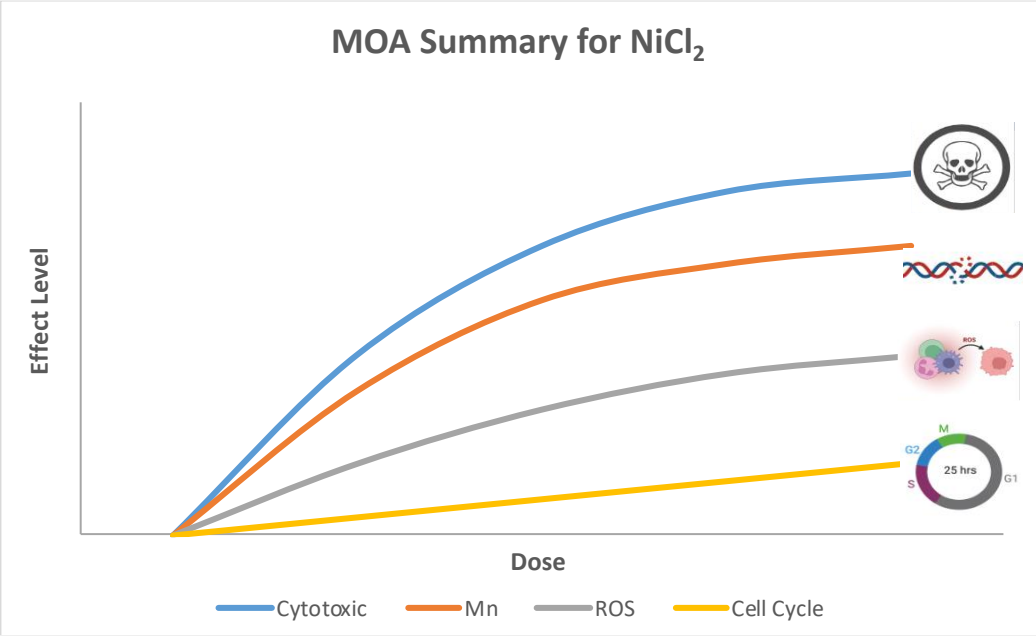

Figure 4.11 A qualitative summary of nickel chloride's ($NiCl_2$) responsible mechanism of action (MoAs) overall effect level. This figure used images of MoAs taken from biorender.com. There is a key at the bottom of the graph representing each end point.

4.4.1 $NiCl_2$ induced genotoxicity

There are a number of controversies in the literature regarding the genotoxicity of $NiCl_2$ and it is largely misunderstood. The acute data observed for $NiCl_2$ is an important finding and questions the classification of the compound. Even though $NiCl_2$ has previously been classified as a NGC, it behaved here like a GC, which further highlights the complex nature of NGCs. With the acute treatment of $NiCl_2$ (**Figure 4.3**), there was a statistically significant increase in micronuclei, suggesting clear DNA damage was induced. Genotoxicity and cytotoxicity can work together and should be considered together as well as with cell death as these endpoints are heavily linked. The cell viability was also reduced with the acute treatment, however it was not below the 50% toxicity threshold set by OCED. When the $NiCl_2$ treatment was carried out in a chronic manner (**Figure 4.4**), there was no statistically significant increase in micronuclei, suggesting

any DNA damage present has had the chance to be repaired and therefore the cells managed the effects of this exposure to $NiCl_2$. This could mean that at low levels of $NiCl_2$ administered daily, the DNA repair machinery is not inhibited so can manage that level of cell and DNA stress. This is in agreement with a study carried out by Gliga *et al.,* (2020) demonstrating the lack of genotoxicity with a chronic exposure.

A study carried out in Swiss albino mice also suggested that $NiCl_2$ is a GC (Danadevi *et al*., 2004), which would agree with the acute data results. The literature questioned the genotoxic potential of $NiCl_2$ as it showed minimal DNA protein cross links even at high concentrations in rat lymphocytes (Chakrabarti *et al*., 2001). It is suggested that it is the chemical ligands that are responsible for the DNA damage so other nickel compounds may be more DNA reactive due to this (Chakrabarti *et al*., 2001). A study in earthworms showed the genotoxicity and carcinogenicity potential of $NiCl_2$ (Reinecke and Reinecke, 2004). However most of the studies, that suggest $NiCl_2$ is a GC, are carried out in animal models which could explain the controversies in the results. *In vitro* studies such as (Chen *et al*., 2003) show $NiCl_2$ genotoxicity measured with the comet assay. It is thought that $NiCl_2$ induced DNA damage is as a result of the production of hydroxyl radicals via the Fenton reaction which can damage the DNA bases (Torreilles and Guerin, 1990). It has been stated in the literature that nickel is genotoxic as a result of the inhibition of DNA repair and the DNA-damaging ROS (Kasprzak *et al*., 2003). Another reason nickel is thought to be genotoxic is due to the activation of cell cycle checkpoints, double-stranded DNA breaks and in some cases can cause cellular death (Farkash and Prak, 2006).

Nevertheless, others still recognise $NiCl_2$ as a NGC (or also known as an epigenetic carcinogen) (Ke *et al*., 2006). The dispute among the different studies about the genotoxicity profile for $NiCl_2$ could be impacted by the ROS data (Stannard *et al*., 2016). ROS are often thought to be linked with GCs only however, it is possible for NGCs to also utilize ROS as a MoA (Åkerlund *et al*., 2018).

4.4.2 ROS induction

It is widely understood in the field, that $NiCl_2$ utilizes ROS production as its main MoA, echoed by data presented here (**Figure 4.5a**). As well as oxidative stress, mitochondrial dysfunction also plays an important role in nickel induced toxicity. Nickel can induce mitochondrial membrane potential impairment, destruction of mitochondrial DNA and can reduce the mitochondrial concentration of ATP. Oxidative stress and mitochondrial dysfunctions can

negatively impact each other, for example mitochondrial perturbations can interrupt the electron transport chain therefore increasing ROS (Genchi *et al*., 2020). In another study investigating the CTA, Chinese hamster ovary (CHO) cells were cultured and dosed with both $NiCl_2$ (water soluble) and nickel sulphide (Ni_3S_2) (relatively water soluble) (Xi *et al*., 1993). The differences in MoA of soluble and insoluble nickel compounds could be due to the fact that insoluble nickel is capable of acting more like a particle and having more impact in disrupting cellular processes. Whereas soluble nickel could pose less of a carcinogenic threat as it could be subject to natural homeostatic protection and be more readily excreted due to its soluble nature. Both nickel compounds produced an increase in the fluorescent oxidised DCF from DCFDA. There was a greater increase in ROS produced by Ni_3S_2 than $NiCl_2$, confirming that $NiCl_2$ is a weaker toxin/genotoxin/carcinogen. This suggests that oxygen radical intermediates may be facilitating nickel's genotoxicity (Xi *et al*., 1993). This is in agreement with the results produced in **Figure 4.5a**, suggesting that the main MoA of $NiCl_2$ is the induction of ROS.

In a study by (Huang *et al*., 1994) in Chinese hamster ovary cells it was shown that $NiCl_2$ did not cause lipid peroxidation like Ni_3S_2 and NiS. This again confirms that $NiCl_2$ is a weaker pro-oxidant and this could explain how it can behave as a NGC and uses more indirect methods of damaging DNA.

4.4.3 Cell cycle and Apoptosis

Both cell cycle and apoptosis, (**Figure 4.6**) and (**Figure 4.7**) do not show any significant changes respectively. However, $NiCl_2$ caused 7.6% decrease in G1 cells and 0.83% decrease in G2 cells at 150 µM. Some studies have shown that $NiCl_2$ can produce a block at the S phase, meaning cells will not go on to G2 phase (Costa *et al*., 1982) however, this was not seen with the cell cycle results in **Figure 4.6**. This could be due to the cell cycle analysis being carried out at a 24-hour time point, which may not have captured the potential block at S phase as it possibly occurred earlier. Future work could focus on a time course of cell cycle changes after exposure to $NiCl_2$. This could explain whether changes occur at an early time point but then cells have time to repair DNA damage and release the checkpoint in order to be pushed through the next phase of cell cycle so explaining the minimal changes at the 24-hour time point.

Studies have shown that $NiCl_2$ induces excess apoptosis in a number of different organs as one of its molecular mechanisms of toxicity (Guo *et al*., 2016). However, **Figure 4.7** does not show any significant induction of apoptosis therefore showing contradicting results to the literature. The doses chosen for the apoptosis analysis carried out in **Figure 4.7** were kept consistent

throughout all other analyses, whereas previous *in vitro* studies may have utilized higher doses where increased apoptotic levels would be observed. For instance (Peters *et al*., 2001) used doses of $NiCl_2$ at around 7-fold higher than those used in **Figure 4.7**.

It has been suggested that nickel is heterogeneous due to its random gene activation ability. It does not seem to induce apoptosis *in vitro* which is confirmed by **Figure 4.7**. In order to understand the $NiCl_2$-induced apoptosis (Guo *et al*., 2016) carried out messenger RNA (mRNA) expression analysis which showed that the Fas and ER stress-mediated apoptotic pathway was utilized. This is interesting because in (**Figure 4.8**) the PCR array shows a biologically relevant fold change in Fas levels. Again, slightly contradicting results to the literature as (Guo *et al*., 2016) reported an increase in Fas levels, however there was a 2.38-fold reduction. The studies conducted by (Guo *et al*., 2016) were carried out in broiler chickens, not humans, which may explain the conflicting results. Future work could include further investigation around the Fas pathway and B-Cell Lymphoma 2 (Bcl-2) and BCL-2 associated X protein (Bax) levels. Also, similar to cell cycle analysis, looking at different time points could potentially show changes in nickel induced apoptosis. Perhaps a later time point such as 48 hours would capture apoptotic changes.

$NiCl_2$ is a soluble nickel compound, which is known to have a less potent carcinogenic status than insoluble nickel. It was shown that soluble nickel caused G1/G0 cell cycle arrest and inhibited cell growth as well as the down regulation of *CCND1* which is responsible for controlling G1/S progression (Ouyang *et al*., 2009). **Figure 4.3** has increased cytotoxicity with the increased dose, which agrees with Ouyang *et al*., (2009). However when treated with $NiCl_2$ chronically, cytotoxicity does not seem to be induced, it appears to be better tolerated by the cells demonstrated in **Figure 4.4**. It is thought that *CCND1* is downregulated as a result of protein degradation as it is dependent on IKKα and there were no changes in *CCND1* mRNA expression. **Figure 4.6** shows as the dose of $NiCl_2$ increases there is a very slight decrease of the cells in G1, which does not agree with (Ouyang *et al*., 2009) because cells are not arrested in G1. This could be due to the 24-hour cell cycle time point, the lower doses of $NiCl_2$ used in this work and the fact that Ouyang used A549 cells. **Figure 4.8** does not demonstrate a significant downregulation of *CCND1* with TK6 cells, this could explain why there is not significant cell cycle arrests demonstrated.

4.4.4 Gene expression changes

The PCR array (**Figure 4.8**) data highlighted the biologically relevant genes which were all downregulated by $NiCl_2$. The vascular endothelial growth factor *VEGFA*, Tumour protein p53 *TP53*, DNA topoisomerase I *TOP1*, Von Hippel-Lindau *VHL* and phosphatase and tensin homolog *PTEN* are downregulated by the highest fold changes. Nickel is seen to promote the secretion of *VEGF* via the *ITGB3* pathway (Wu *et al*., 2019). *VEGF* is an important mediator of angiogenesis in cancer, it is enhanced by the expression of certain oncogenes, a selection of cytokines and hypoxia conditions. Angiogenesis cannot be modelled *in vitro*, however the altered gene expression of *VEGF* gives an indication of what may be happening *in vivo* (Carmeliet, 2005). Guo *et al*., (2016) suggest that $NiCl_2$ induces inflammation via the activation of the *NFKB* pathway. This corresponds with the PCR array data in (**Figure 4.8**) as there is a perturbation in the expression of *NFKB1*.

The PCR array results for $NiCl_2$ showed a greater than 6-fold down regulation of the tumour suppressor gene *PTEN*. The *PTEN* gene is frequently mutated in cancer cells (Di Cristofano and Pandolfi, 2000) and is responsible for the regulation of *PI3K*/*AKT* signaling pathway and controls cell growth, angiogenesis and proliferation (Carracedo and Pandolfi, 2008). Reduction in the function of *PTEN* and increased activity of the *PI3K* pathway links to increased *HIF-1a* expression during hypoxia (Emerling *et al*., 2008). *HIF-1a* links to the gene with the largest fold change *VEGF*, by activating its transcription. These both play crucial roles in the development and progression of cancer in humans (Rong *et al*., 2006) by stimulating angiogenesis (Forsythe *et al*., 1996). *VHL* is also a tumour suppressor, so its loss of function results in increased *HIF* activity (Kaelin Jr, 2008).

A study carried out on nude mice showed that $NiCl_2$ could potentially act as an anti-cancer agent which is a contrast to the majority of the literature. Mice had an implanted cancer cell model injected into their tongue and were given water containing 1 mM $NiCl_2$ for the following weeks. PCR analysis showed the reduced expression of, *VEGF*, in the presence of low-dose $NiCl_2$ treatment (Ota *et al*., 2018), which was also seen with **Figure 4.8**. *VEGF* is a known angiogenic factor, whose expression could be reduced in the presence of $NiCl_2$ as a result of *NFKB* inactivation (Ota *et al*., 2018). This could mean that $NiCl_2$ has potentially acted as an anti-cancer agent as it has downregulated *VEGF* expression, at a 150 µM dose for 24-hour time period. This is inconsistent with **Figure 4.3** because this is showing a statistically significant increase in Mn induction at 125 µM and 150 µM for a 24-hour period, indicating genotoxicity is present at these

doses. However, the anti-cancer effect has been observed in mice and at a higher dose, so this could also explain the contradictory results to the *in vitro* data.

PIK3CA was downregulated by $NiCl_2$ in (**Figure 4.8**) which was supported by (Pan *et al*., 2011) who found that the *PI3K/AKT* pathway was activated in nickel treated BEAS-2B cells. (Pan *et al*., 2011) also noted an upregulation of the anti-apoptotic Bcl-2 and Bcl-X, leading to apoptotic resistance and therefore contributing to nickel's carcinogenesis. This would agree with **Figure 4.7** as apoptotic levels are largely unchanged as a result of $NiCl_2$ 24-hour dosing.

DNA topoisomerase enzymes have a role in a number of processes in the nucleus as they can form a break in just one or in both strands of DNA. They are classified as important chemotherapy targets, they have roles in DNA transcription and replication (Gurumoorthy *et al*., 2016). This is interesting as in **Figure 4.8** *top1* is downregulated, so it may be responsible for interrupting these processes. If topoisomerase 1 is inhibited, it utilizes a MoA of disrupting DNA replication leading to cell death of cancer cells (Gurumoorthy *et al*., 2016). It is unclear, the exact role *top1* is playing in $NiCl_2$'s MoA. However, in combination with the other genes downregulated it is clear these perturbations are disrupting the normal cellular processes which can therefore lead to cancer initiation. This endpoint is very good at linking to other endpoints in order to create a holistic picture of the MoA taking place.

4.4.5 Mitochondrial perturbations

Mitochondrial function can be assessed by sequential injections of chemicals with different purposes (**Figures 4.9 and 4.10**). Oligomycin is an inhibitor of ATP synthase, FCCP is a mitochondrial uncoupler and a rotenone/antimycin A mixture acts as a mitochondrial inhibitor. The combination of these chemicals added at specific time points allow for the calculation of the OCR as well as a series of other functions (Kawalekar *et al*., 2016). The addition of $NiCl_2$ decreases the overall output from the mitochondria, the cells have a lower energetic demand as a result of $NiCl_2$ treatment. $NiCl_2$ causes the cells to have a lower energy which is a stress on the mitochondria before the various inhibitors are added. As there was decreased mitochondrial health once $NiCl_2$ was added, this means that the mitochondria are not working to their full potential. There was a significantly decreased maximal respiratory capacity and proton leak as a result of $NiCl_2$ treatment. Perhaps this mitochondrial stress could be linked with the increased ROS production (**Figure 4.5a**) as these end points can link to each other.

4.5 Conclusions

Nickel has been subject to several different carcinogenicity classifications based on the complexity of the mechanism(s) it uses to elicit oncogenesis. Epigenetic modulation can be caused by both genotoxic and NGCs, which adds to the difficulty of classifying these chemicals (Jacobs *et al*., 2016). It is suggested that $NiCl_2$ also has an epigenetic modifier potential, as well as being a NGC (Herceg *et al*., 2013). It is stated that nickel uses DNA methylation and the addition of histone markers as its epigenetic mechanisms. It is also stated that the recognised mechanisms of $NiCl_2$ are DNA repair disturbances, inflammation and genotoxicity (Herceg *et al*., 2013). It has been demonstrated that $NiCl_2$ is able to act in a genotoxic manner by activating p53 and inducing G2 cell-cycle arrest which are known genotoxic mechanisms (Wilde *et al*., 2017). It is clear that $NiCl_2$ is a complicated chemical that is capable of using multiple different MoA routes.

In conclusion, $NiCl_2$ induced cytotoxicity was observed with acute dosing but not observed with the chronic dosing of $NiCl_2$. There was a dose-dependent increase in Mn levels after acute exposure, suggesting a genotoxic MoA however there was no Mn dose response observed with the chronic Mn data implying that no genotoxicity was induced after dose fractionation. There was also a significant positive correlation observed with the ROS data, suggesting that oxidative stress is the main MoA utilized by $NiCl_2$, which is in agreement with the literature. The addition of NAC does seem to slightly reduce the level of genotoxicity present, however no significance was observed with these data (**Appendices Figures A8 and A9**). There are no significant changes in cell cycle and apoptosis for $NiCl_2$, which is unusual as the literature suggests cell cycle perturbations and apoptosis are both caused by $NiCl_2$. However, the lack of changes seen with cell cycle and apoptosis may be as a result of the single 24-hour time point chosen. The PCR array data highlighted biologically relevant changes in 34 genes in total. All of the changes in $NiCl_2$ gene expression showed downregulation, which is interesting as this is different to all other chemicals assessed in other chapters. The Seahorse data shows that $NiCl_2$ reduces the cells overall energetic requirement and means that the cells cannot work as hard as the untreated cells. The cells overall metabolic activities are reduced as a result of $NiCl_2$. It seems like $NiCl_2$ behaves more like a GC than a NGC. This could be dependent on the dose of $NiCl_2$ delivered and the dose regime (chronic or acute), meaning it could be capable of acting as both a GC and NGC, further highlighting the complexity of these chemicals. The test battery has definitely worked with certain endpoints from the multi-endpoint list, which is promising for the use of this proposed strategy.

Chapter 5: The Comparison of Two Arsenic Species; A Genotoxic and Non-Genotoxic Form

5.1 Arsenic general background

It is thought that As is one of the most significant threats in the environment (Tapio and Grosche, 2006). As has been well known as a toxic poison for centuries (Cullen, 2008). It is a naturally occurring environmental element, available in a number of different forms, each with unique chemical properties. As is present in the earth's crust and can therefore occur freely in nature or as a result of human activities (Hosseini *et al*., 2013). Inorganic As, commonly in trivalent form as an arsenite is one of the most abundant forms of As in nature, present in water soil and food products (Cohen *et al*., 2006).

As is capable of attaching to small airborne particles, to travel great distances and stay airborne for days at a time. It is primarily used as an insecticide, herbicide and wood preserver due to its resistance to decay (Chung *et al*., 2014). It is most commonly found in pesticides but can also be used in the production of paper and glass (Basu *et al*., 2001). As also has uses in medicine and industrial processes (Nriagu and Azcue, 1990). Furthermore, As is capable of interacting with oxygen and other air molecules, soil and bacteria which are all capable of causing As to change form and attach and detach from different particles (Fergusson, 1990). Both organic and inorganic As are readily absorbed into the blood stream and to the gastrointestinal tract. Organic As is often considered to be fairly harmless as it is not easily absorbed by cells. However, inorganic As is known to be much more bioavailable and reactive causing intracellular complications (Drobná *et al*., 2009). As, in both organic and inorganic forms, is widely dispersed in the air, soil and water as chemical compounds or as a metalloid.

As was one of the first chemicals to be identified as a carcinogen in ~1879. Miners in Saxony had high incidence of lung cancer which was caused by inhaled As (Neubauer, 1947). In 1887, it was reported that patients that had undergone As treatments such as for syphilis, psoriasis and epilepsy to name a few, developed skin cancer as a result (Hutchinson, 1887).

As was most commonly known as a poison up until the mid-1850s. It was a popular choice of poison due to its odourless and colourless properties, meaning it was often undetected in food and beverages (Bartrip, 1992). There was no reliable means of testing for and measuring As levels in tissues at postmortem examination. The first trial recorded to present forensic evidence, was of an As poisoning case, where it was examined based on appearance, texture and the way it behaved in water (Cullen, 2008). In 1832, James Marsh began developing a test method for

providing solid evidence of the presence of As. The test involved mixing the sample with zinc and acid before heating, leading to the production of a silver substance (Marsh, 1837). Marsh's method was first used in the 1840 trial in France of Marie LaFarge, where she poisoned her husband by including As in cakes (Cullen, 2008). As was also used in a prominent political assassination case of Napoleon Bonaparte in 1851 and was used by both Borgia and Medici families to eradicate enemies (Cullen, 2008). Symptoms of As poisoning included vomiting, diarrhoea and abdominal pain which could be the symptoms of many other illnesses and diseases, such as cholera (ATSDR, 2007).

As poisoning has 2 known antidotes which are Dimercaprol (BAL) and succimer (DMSA). Both dimercaprol and succimer work by forming an inert dimer with As. Dimercaprol should be administered by deep intramuscular injections and given in a dose of 2.5-5.0 mg/kg 4-hourly for 2 days and then 2.5 mg/kg intramuscularly twice daily for 1-2 weeks. Succimer is delivered orally in order to treat As poisoning (Bradberry and Vale, 2007).

As is a complex chemical because it has properties of both a metal and a non-metal and is therefore classified as a metalloid. Elemental As is a grey, solid, metal, whereas most organic and inorganic As is present as a white or colourless powder with no smell or taste, hence the use as a poison (ATSDR, 2007).

As a carcinogen, As seems to have the ability to act via both direct and indirect genotoxic mechanisms. As there is often a reported lack of mutagenesis, it is likely that the indirect genotoxic mechanisms are the primary route of oncogenesis (Klein *et al*., 2007).

Numerous chemicals such as veterinary drugs, pesticides and food additives are subject to toxicity testing before they can be included in society. The acceptable daily intake (ADI) is calculated based on the no observed adverse effect level (NOAEL) and the safety factor which takes into account the species difference between rodents and humans (Nohmi, 2018). The NOAEL is the highest dose in a toxicological assessment where no statistical significance is observed. The ADI is the level where no adverse effects are thought to occur. Chemical use in society is permitted if the level is below the ADI (Nohmi, 2018).

NGCs are thought to have a threshold, where the chemicals are thought to be safe. This means that NGCs can be used in products as long as they do not exceed the safe threshold. GCs, however, are thought to be toxic at even low doses (Nohmi, 2018) for the majority, however GCs can also have thresholds too (Batke *et al*., 2021). Therefore, it is important to be able to

distinguish between genotoxic and NGCs (Nohmi, 2018). Thresholds are a major consideration for NGCs and it is not currently playing a role in their risk assessment (Pratt and Barron, 2003).

It is well understood that even at low levels, As can still initiate154carcinogenesis (Mandal and Suzuki, 2002). As's abundance on land is approximately 1.5-3 mg/kg^{-1}, this includes organic (natural) and inorganic (pollutants) (Mandal and Suzuki, 2002). As can occur in over 200 different mineral forms, 60% of these are arsenates, 20% are sulphides and sulphosalts and 20% incorporates elemental As, arsenites, oxides, arsenides and silicates (Onishi, 1969).

5.1.1 Arsenic exposure through food and water

In the 1930s it was accepted that As contamination of drinking water caused skin cancer (IARC, 1980) as a result of the characteristic skin lesions caused by As exposure as seen in **Figure 5.1** (Saha, 2003).

As contaminated drinking water is the main exposure route, followed by As within the diet through the contamination of food sources. In the diet, As is often found in seafood, although this contamination is usually from the less toxic, organic origin (Tapio and Grosche, 2006). The exposure through drinking water is usually a chronic exposure as it is often the main water source utilized by the individuals (Mazumder, 2000).

There are several regions worldwide that have received attention due to the levels of As in drinking water supplies (Argos *et al*., 2010). The incidence of inorganic As contaminated ground water in Bangladesh is known as the largest mass poisoning in history (Smith *et al*., 2000). Elevated inorganic As exposure in the main drinking water supplies is still present in certain parts of the world such as China, Mexico, Bangladesh, India and Argentina to name a few (IARC, 2012).

Tobacco is closely regulated and tested for the presence of As, lead (Pb), cadmium (Cd) and nickel (Ni) (Campbell *et al*., 2014). Between 9-16% of the compounds released during tobacco combustion are As (Lugon-Moulin *et al*., 2008). It is suggested that although there are hundreds of ng of As in each cigarette, it is possible that <1 ng to 70 ng of As is transferred to the smoker (Behera *et al*., 2014). The main organic As species found in numerous different tobaccos was dimethylarsinic acid (DMA) otherwise known as cacodylic acid. Both organic and inorganic As species were found in the tobacco analysed but inorganic As is most prevalent. There are large geographical differences, for example China has a noticeably high level of As in its cigarette brands compared to the western world (Campbell *et al*., 2014).

Many As compounds are water soluble, and so are able to contaminate a series of water bodies. The contamination of drinking water supplies is a concerning threat to public health. Chronic As exposure through consumption of contaminated food and water has been shown to induce detrimental health outcomes such as vascular disease, keratosis and numerous forms of cancer (Gibb *et al*., 2011). As well as food and water exposure, other routes of concern are cigarette smoking, occupational exposure and through the use of cosmetics (Chung *et al*., 2014).

The main inorganic form of As is the trivalent meta arsenite which exists in ground water. Organic forms of As are a group known as the methylated metabolites such as monomethylarsonic acid (MMA) and DMA or Caco (Basu *et al*., 2001). Caco is the main metabolite formed post exposure to arsenite (trivalent) or arsenate (pentavalent) inorganic As. It is also thought that Caco has a set of unique toxic traits and is a complete carcinogen (Kenyon and Hughes, 2001). Caco is said to be more than 10-fold less toxic than inorganic As (Kaise *et al*., 1989).

As exposure through food products is one of the main routes of human exposure. In particular, rice is capable of absorbing inorganic As from both the soil and water. This is a major problem because rice is a staple food source for many (Williams *et al*., 2007), brown rice syrup is a sweetener for many snacks and rice flour is a common ingredient in processed food. This is a health concern as rice is 10 times more efficient than other crops at taking up As from the environment (Jackson *et al*., 2012). As As is naturally occurring, it can also enter the food chain via terrestrial animals and through marine organisms. There are a range of As concentrations in a wide range of food products (Jackson *et al*., 2012).

5.1.2 Arsenic Epidemiology studies

Epidemiological studies are responsible for classifying As as a human carcinogen (Bleyl, 1989). As can act via numerous mechanistic routes such as disruption of signal transduction pathways which can in turn interfere with cellular processes such as inhibiting growth, affecting apoptosis and the up/down-regulating of angiogenesis (Rossman, 2003).

There have been numerous epidemiological studies of As poisoning. However, As normally synergistically works alongside other carcinogens to induce tumourigenesis and chronic exposure is needed. Chronic As ingestion is linked with several cancers, such as lung and skin (Jager and Ostosky-Wegman, 1997) which agrees with the principle that NGCs work via long term exposure to these chemicals as detected by the 2-year rodent bioassay (Hernández *et al*., 2009).

Chronic As poisoning is associated with characteristic skin lesions as seen in **Figure 5.1** below, developing within several years of exposure (Saha, 2003). These skin lesions usually involve the hyper-pigmentation in areas such as the neck, chest and abdomen followed by hyperkeratosis of palms and soles (Saha, 2003).

Figure 5.1: Taken with permission from DermNet, displaying the symptoms of chronic As poison and shows some of the skin lesions that develop.

An example of an As epidemiology incident was the As contaminated well water in the south-west of Taiwan between 1961 and 1985 (Thornton and Farago, 1997). Trivalent arsenite is the most abundant species in well waters, with As levels ranging from 0.01-1.82 mg/L^{-1} (Mandal and Suzuki, 2002). This concentration is high considering the well waters are concentrated areas of water and these sources were used for drinking water (Mandal and Suzuki, 2002). As is usually found in natural water sources at low concentrations, with the maximum value of 50 $\mu g/L^{-1}$ and the World Health Organisation (WHO) recommended less than 10 $\mu g/L^{-1}$ (WHO, 2001). There were multiple cases of different cancers (including liver, bladder and kidney), keratosis, black foot disease and hyperpigmentation (Chen *et al*., 1988). The Taiwanese government put a water treatment plan in place in order to remove the As in the groundwater before consumption (Mandal and Suzuki, 2002).

Epidemiological incidents of As contaminated ground water are well reported worldwide. There are many countries affected including: Chile, several parts of the USA, Canada, Hungary, New Zealand, Poland, Spain, Japan and Vietnam (Mandal and Suzuki, 2002). There are reports in many areas of industrial As pollution for example, as a result of the construction of a geothermal power plant in the Philippines, wastewater from a factory contaminating well water in Japan and air pollution from copper smelters in the USA to name a few (Mandal and Suzuki, 2002). There was also contamination of food and beverages with As and its derivatives such as soya sauce in Japan and wine in Germany (Mandal and Suzuki, 2002).

5.1.3 Occupational exposure

Occupational As exposure has been reported in a wide range of professions such as the use and manufacture of agricultural products, wood preservatives and animal feed. As exposure is also described in the mining and smelting of metallic ore and in the production of glass and pigment factories and electronic semiconductors (ATSDR, 2007).

Mining is a common cause of health problems due to the inhalation of dust particles. The inhalation of As, its compounds and As contaminated dust is prevalent in gold, tin and uranium mines (Tomásek and Darby, 1995; Chen and Chen, 2002; Kusiak *et al*., 1991). Another environmental source of As exposure is through the air because of smelting activities and from coal-fired power stations (EFSA and CONTAM, 2009).

Occupational exposure to As and its compounds is mainly as a result of non-ferrous metal processing and specifically copper ore refining (Järup *et al*., 1989). In the process of copper ore refining, workers are exposed to As and its compounds via an inhalation route, which is a differing exposure route to the general public whereby the main exposure route is ingestion through food or water (Halatek *et al*., 2009). This exposure to gas and fine dusts can lead to pro-inflammatory changes and irritation of the respiratory system mainly due to the production of ROS, leading to lung cancer. This resultant ROS can alter brain function with long term exposure to As and its compounds (Chattopadhyay *et al*., 2002).

5.1.4 Sodium meta arsenite (inorganic arsenic – non-genotoxic form)

The chemical structure of NaMAr can be seen in **Figure 5.2** below and can be compared with that of Caco in **Figure 5.3**. Although, the structures of NaMAr and Caco are similar, they are responsible for two different forms of As, inorganic and organic and NGC and GC respectively.

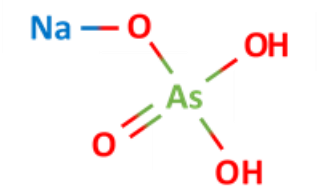

Figure 5.2: Sodium meta arsenite, the chemical structure adapted from (Pubchem, 2022). Colours are representative of each chemical (blue indicates sodium, red indicates a carbonyl group, hydroxide group or an oxygen bond and green indicates arsenic).

Sodium arsenite or NaMAr as it is also known, is an inorganic arsenical (Li and Rossman, 1991). Cohen *et al*., (2016) stated that inorganic As does not interact with DNA directly so therefore is a

NGC. However, a publication by Roy *et al*., (2018) notes that sodium arsenite shows genotoxic potential both *in vitro* and *in vivo* as it gives positive results in both test systems. This highlights the complexity of so-called NGCs as there are controversies in the literature related to whether they induce DNA damage or not.

Some of the non-genotoxic processes that arsenite may use could involve inhibited DNA repair, apoptosis changes, and alterations to cell proliferation (Klein *et al*., 2007). Arsenite has the ability to interfere with DNA repair, so can work well as a cocarcinogen. With a low arsenite concentration, there is a reduction in the activity of DNA ligase and interruption of p53 function (Vogt and Rossman, 2001). Wu *et al*., (2005) showed that at low doses of arsenite, UV induced apoptosis was inhibited, allowing the survival of damaged cells, which demonstrates the cocarcinogenic properties (Klein *et al*., 2007).

Risk assessments for inorganic As compounds are usually conducted as a group rather than as individual species. This is because within the human body, As compounds are often converted between forms (ECHA, 2022). The relationship between inorganic As and cancer was first declared in those individuals who were given As as a therapeutic agent. Arsenicals were given as a treatment of the sexually transmitted infection, syphilis. This treatment was developed by Ehrlich and this work received a Nobel Prize (Cullen, 2008).

Sodium arsenite is a trivalent arsenical which can react with sulphhydryl groups and therefore cause indirect genotoxicity (Cohen *et al*., 2013). Trivalent arsenicals are also capable of reacting with tubulin which can cause mitotic spindle arrest and therefore chromosomal segregation. These arsenicals are also able to react with the cilia, potentially inducing toxicity within the bronchial epithelium. This means that cytotoxicity is a more likely result than genotoxicity (Cohen *et al*., 2016).

NaMAr, like all NGCs, is extremely complicated to understand. It has shown to be a tumour promoter and maintain the progression of prostate cancer as well as having the ability to act as an anti-cancer drug for prostate cancer. NaMAr seems to act inhormetic fashion by increased cellular proliferation at lower concentrations but then decreasing proliferation as the NaMAr concentration increases (Lundqvist *et al*., 2019). It has also been stated that NaMAr could act via the inhibition of DNA repair, specifically the inhibition of ligase enzymes (Jha *et al*., 1992; Raisuddin and Jha, 2004; Nilsson *et al*., 1993).

Inorganic As does not induce tumourigenesis (especially skin tumours) in animal models; however tumours are induced in a mouse model, again agreeing that inorganic As is a NGC. Synergistic interactions with other environmental contaminants such as tobacco smoke and radon, is important when understanding the MoA of inorganic As (Ferreccio *et al*., 2000). It is proven that sun exposure works synergistically with As exposed populations to promote skin tumours (Chen *et al*., 2003). NGC mechanisms include oxidative stress, inhibition of DNA repair and induction of aneuploidy. Aneuploidy in particular can be observed at lower concentrations of As (Ochi *et al*., 2004) and may be related to spindle disruption.

5.1.5 Cacodylic acid (or Dimethylarsinic acid) (Genotoxic form)

The chemical structure of Caco can be seen in **Figure 5.3** below. Both structures, **Figure 5.2** and **Figure 5.3** have the central As symbol with a covalently bonded oxygen (O) molecule and a single hydroxide (OH). However, Caco has two methyl groups (CH_3) while NaMAr has one oxygen bound to sodium and another single hydroxide.

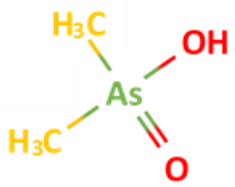

Figure 5.3: Cacodylic acid, the chemical structure adapted from (Pubchem, 2022). Colours are representative of each chemical (yellow indicates a methyl group, red indicates a carbonyl group or hydroxide group and green indicates arsenic).

DMA is more commonly known as Caco and it is the most common form of As in the environment, it is also used as both herbicides and pesticides (Wagner and Westwig, 1974).

Although most As compounds show negative results for mutagenicity, it has been shown that Caco is a potent clastogen and induces CAs, single strand breaks (Dong and Luo, 1993) and DNA adduct formation (Yamamoto *et al*., 1995). A study carried out by (Yamamoto *et al*., 1995) demonstrated that Caco-initiated carcinogenesis in the liver, kidneys, urinary bladder and thyroid gland of the rats tested. The lowest concentration of 50 ppm (or 50 mg/L^{-1}) was capable of causing carcinogenesis in the urinary bladder. There is a much higher As concentration used in the *in vivo* studies when compared to the contaminated well waters in Taiwan.

Caco can cause cytotoxicity and regenerative hyperplasia, is a mitogen and tumour promotor, causes hyper and hypomethylation and inhibition of GJIC (Hernández *et al*., 2009). It has been

shown that low DMA concentrations induce apoptosis in human cells after 48 hours, therefore highlighting the importance of evaluating longer term dosing (Hernández *et al*., 2009). Factors that may increase the carcinogenic potential of As exposure include UV exposure, chronic liver disease and a poor nutritional status (Hsueh *et al*., 2003).

It is known that Caco is a complete carcinogen and a tumour promoter, which can be seen in the bladder of rats (Li *et al*., 1998). The bladders treated with Caco showed many small tumours, whereas the control group did not display tumours (Li *et al*., 1998). Arsenate is reduced to give arsenite which is then methylated into the two forms of MMA and DMA (Thompson, 1993). Caco is the main metabolite of inorganic As for human beings (Buchet and Lauwerys, 1987). It acts as a mitotic poison leading to mitotic arrest and the formation of tetraploids (Eguchi *et al*., 1997).

The genotoxic form of As is known to be Caco, which acts by directly damaging the DNA through processes such as biomethylation. The organic forms of As are more potent genotoxins than the non-genotoxic inorganic forms (Nesnow *et al*., 2002). However, organic As in food for example is much less toxic than inorganic As (Uneyama *et al*., 2007). ROS have been shown to be important mediators of As's DNA damaging potential (Nesnow *et al*., 2002). As induces the production of numerous different types of ROS such as the superoxide radical anion, the hydroxyl radical, hydrogen peroxide, peroxyl radical and a singlet oxygen. These different forms of ROS are induced by As exposure to different organism cell lines including human vascular smooth muscle cells (VSMC) (Shi *et al*., 2004). It has been shown that As can encourage mitochondrial toxicity. It does this by uncoupling oxidative phosphorylation and inhibiting succinic dehydrogenase which both contribute to the production of the superoxide radical anion and this can give rise to other ROS forms (Corsini *et al*., 1999).

Caco is capable of causing single strand breaks in DNA, which can be seen *in vitro* for rodents and human lung cells. The proposed MoA for Caco is due to ROS. Caco has also shown it can act as a tumour promoter in both rats and mice (Kenyon and Hughes, 2001).

5.1.6 Possible mechanisms of action

The main MoA suggested for the different As compounds is ROS generation, this is supported with the use of AOX studies (Tapio and Grosche, 2006). *In vivo* studies have shown that AOXs such as zinc, folic acid and vitamins A, C and E all contribute to the protection of As induced oxidative injury and also lipid peroxidation (Rabbani *et al*., 2003).

Another genotoxic mechanism utilized by As is sustaining increased proliferation, which is vital for tumourigenesis (Hanahan and Weinberg, 2001). Exposure to low As concentrations has shown an increase in human cellular proliferation and the comutagenic properties of arsenicals can also be seen (Vega *et al*., 2001; Rossman *et al*., 1997; Li and Rossman, 1989).

Caco is mutagenic, cytotoxic and genotoxic via a clastogenic mechanism (Kenyon and Hughes, 2001). DNA single strand breaks, protein cross-links (Yamanaka *et al*., 1997) and ROS in the form of a peroxyl radicals are some of the main ways it is suggested that Caco acts mechanistically (Tezuka *et al*., 1993).

5.2 Methods

Methods utilised in this chapter were performed as detailed in the main methods.

5.2.1 Sodium meta arsenite and cacodylic acid test chemicals

NaMAr is available as a white powder which is water soluble and produces a clear liquid once dissolved. It was sourced from Sigma Aldrich (Merck), Dorset. This chemical utilized H_2O as its solvent and was weighed and diluted fresh before each use. Caco acid (Sigma Aldrich (Merck), Dorset) is also a white powder in appearance producing a clear liquid once dissolved in its H_2O solvent in **Chapter 2 section 2.3.3.** The doses for both test chemicals were selected based on individual RPD experiments to determine the cytotoxic top dose of NaMAr and Caco and then these doses were used consistently throughout the different endpoints.

5.3 Results

Both the genotoxic and non-genotoxic forms of As, NaMAr and Caco, respectively, underwent the same multi-endpoint analysis. These included (acute and chronic) mononucleate Mn , RPD, ROS analysis, cell cycle analysis, apoptosis analysis, a general cancer panel qPCR array and a mitochondrial stress test. The dose ranges of the two As forms used in this study are very different; NaMAr has a dose range of 2-10 µM and Caco has a dose range of 500-5000 µM before a genotoxic response is observed. The acute treatment with NaMAr (**Figure 5.4**) can be compared with the acute treatment for Caco (**Figure 5.5**). The shape of the two graphs are analogous with some suggestions of Mn induction as doses increase, coupled to a steep decline in RPD, indicating cytotoxicity. As mentioned above, it is interesting to note the different dose ranges that cause genotoxicity and cytotoxicity. NaMAr seems more potent by comparison as it causes genotoxicity and cytotoxicity at 500-fold lower concentrations than Caco.

It is important to note that with **Figure 5.4** and **Figure 5.5** the top doses (10 µM and 5000 µM) respectively are below the 55 ± 5% recommended maximum cytotoxicity parameter in the OECD guidelines (TG487). Therefore, these doses would normally not be included in the figures, however they are included to show the complete dose range and to allow comparison with the same doses in the chronic approach.

Figure 5.4 shows the 24-hour (+ 24-hour recovery) (Doherty *et al*., 2014), acute Mn and RPD treatment for NaMAr. There was a significant increase in Mn production at doses 8 µM and 10 µM but at very low RPD levels. **Figure 5.5** shows the 24-hour (+ 24-hour recovery), acute Mn and RPD with Caco treatment. Although there seems to be an overall positive correlation, there was no statistical significance observed.

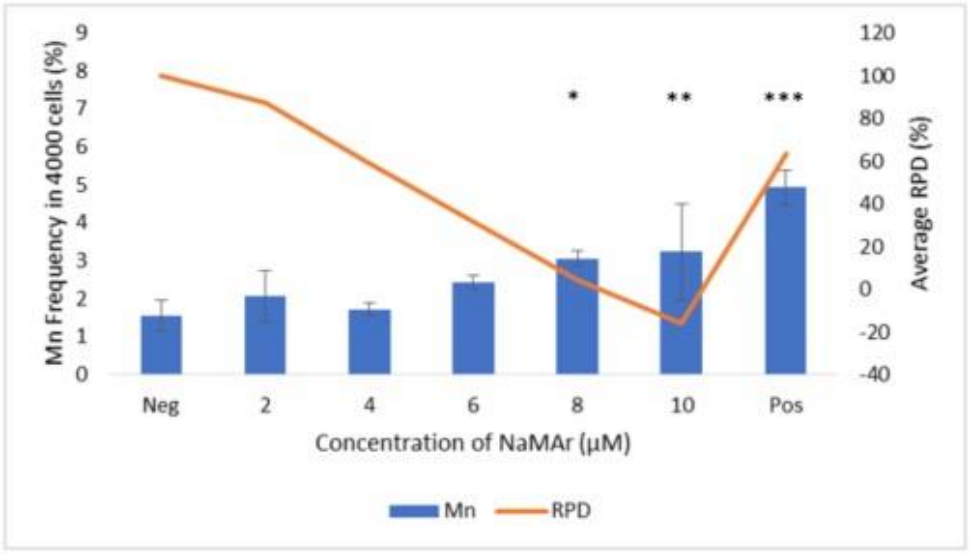

Figure 5.4: The acute mononucleate micronucleus assay and relative population doubling graph at 24-hour sodium meta arsenite exposure with 24-hours recovery in TK6 cells. n=3 was carried out for this work and an average was plotted with error bars. There was statistical significance at 8 µM (P = 0.0391) and 10 µM (P = 0.0049) for Mn induction when compared to the negative control, as indicated by asterisks (* <0.05, **<0.005). The negative/solvent control used here was H_2O and the positive control was 10 µM MMS (P = 0.00026).

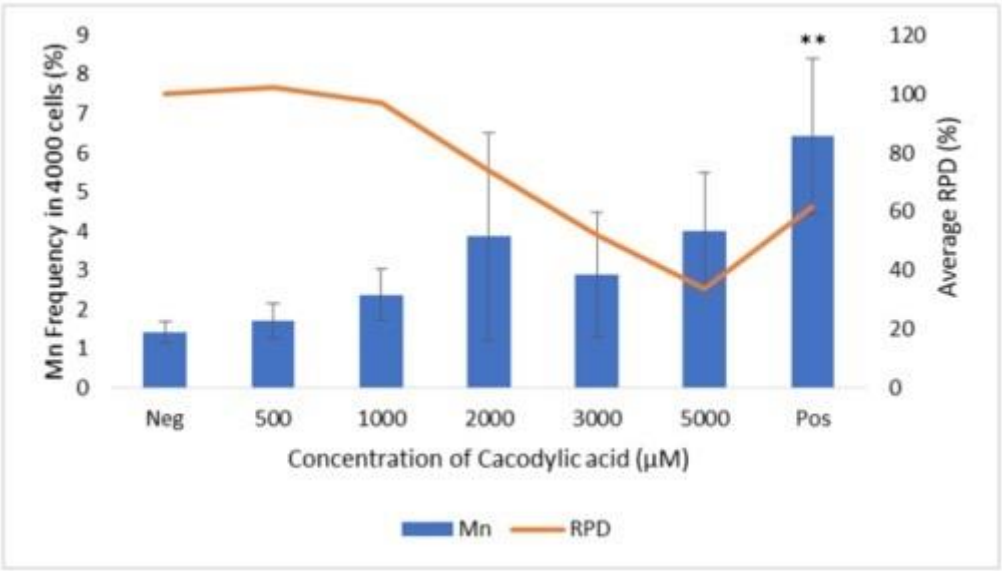

Figure 5.5: The acute mononucleate micronucleus and relative population doubling data at 24-hour cacodylic acid exposure with 24-hours recovery in TK6 cells. n=3 was carried out for this work and an average was plotted with error bars. There was no statistical significance with the addition of cacodylic acid. The negative/solvent control used here was H_2O and the positive control was 10 µM MMS (P = 0.00123).

Comparisons can also be made between **Figure 5.4** and **Figure 5.6** as these are the acute and chronic results of NaMAr. There are some differences between these two graphs, the acute NaMAr graph in **Figure 5.4** showed a positive correlation however doses 8 µM and 10 µM were not counted as these are beyond the RPD cytotoxicity threshold. Whereas the chronic graph in

Figure 5.6 demonstrates a statistically significant response from 4 µM. The same comparisons can be made with **Figure 5.5** and **Figure 5.7** as these are the acute and chronic results for Caco. In **Figure 5.5** there is a non-significant induction of Mn, whereas in **Figure 5.7** there is a clear dose dependent Mn induction from 2000 µM. Here, with the chronic dosing we saw genotoxicity (Mn induction) by both the non-genotoxic form (NaMAr) and the genotoxic (Caco) form of As.

Figure 5.6 represents the chronic data for NaMAr where the doses were fractioned over 5 days but represent the same total doses as the acute treatment seen in **Figure 5.4**. A statistically significant increase in Mn induction was observed from dose 4 µM to dose 10 µM maintaining a consistently high Mn induction level, these effects were mostly noted in a low toxicity background as measured by RPD. **Figure 5.7** is the 5-day repeated exposure using the fractionated acute total doses. There was an increase in Mn induction with statistical significance from dose 2000 µM to 5000 µM, these effects were mostly noted (2000, 3000 µM) in a low toxicity background as measured by RPD.

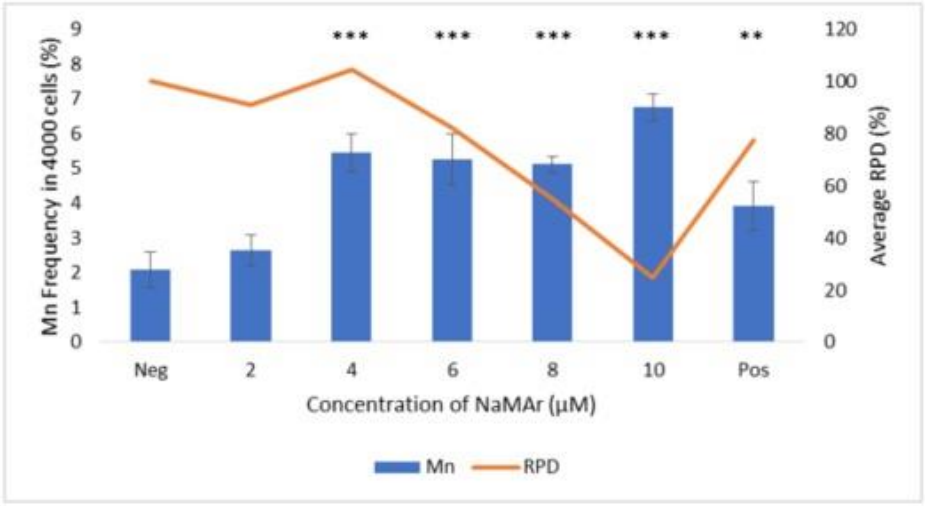

Figure 5.6: The chronic mononucleate micronucleus assay and relative population doubling at 5-day repeated, fractionated exposure with sodium meta arsenite and 24-hours recovery in TK6 cells. n=3 was carried out for this work and an average was plotted with error bars. The negative/solvent control used here was H_2O and the positive control was 10 µM MMS (P = 0.0043),. There was statistical significance at 4 µM (P = 0.0001), 6 µM (P = 0.0001),, 8 µM (P = 0.0001), and 10 µM (P = 0.0001), for Mn induction as indicated by asterisks (* <0.05, **<0.005, ***<0.0005).

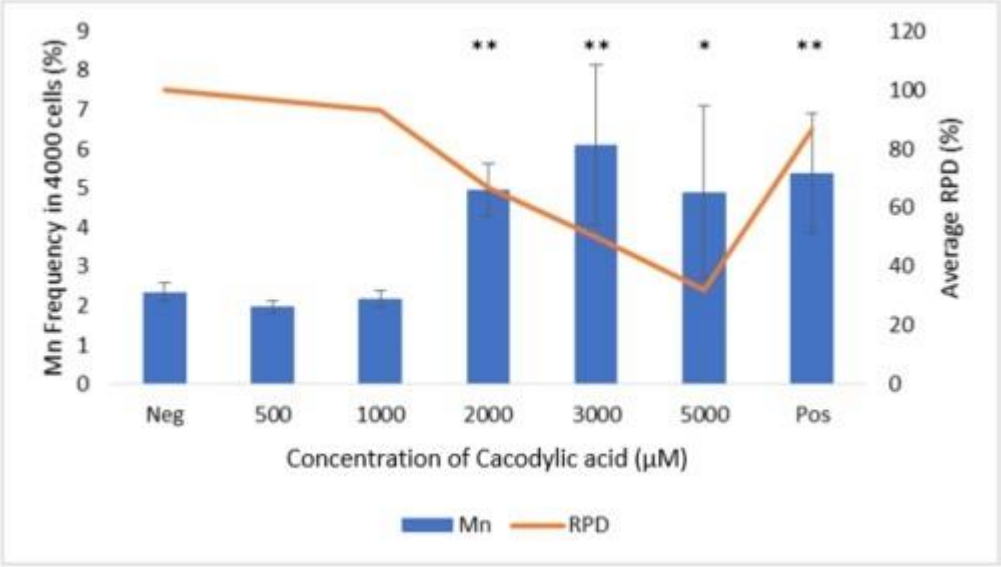

Figure 5.7: The chronic mononucleate micronucleus assay and relative population doubling at 5-day repeated, fractionated exposure with cacodylic acid and 24-hours recovery in TK6 cells. n=3 was carried out for this work and an average was plotted with error bars. The negative/solvent control used here was H_2O and the positive control was 10 µM MMS (P = 0.0027). There was statistical significance at 2000 µM (P = 0.0033),, 3000 µM (P = 0.0034), and 5000 µM (P = 0.0219), for Mn induction as indicated by asterisks (* <0.05, **<0.005).

As ROS are believed to be an important MoA of many NGCs and As in particular, it was part of this testing battery. A series of time points from 30 minutes to 24-hours without recovery assessed total ROS production for NaMAr (**Figure 5.8**) and Caco (**Figure 5.9**).

There does not seem to be ROS produced by NaMAr, **Figure 5.8** shows there is a very slight increase in trend, however it is only slight and there is no statistical significance. **Figure 5.9** shows that ROS is not produced with the addition of Caco, even with the increasing doses and increasing time points.

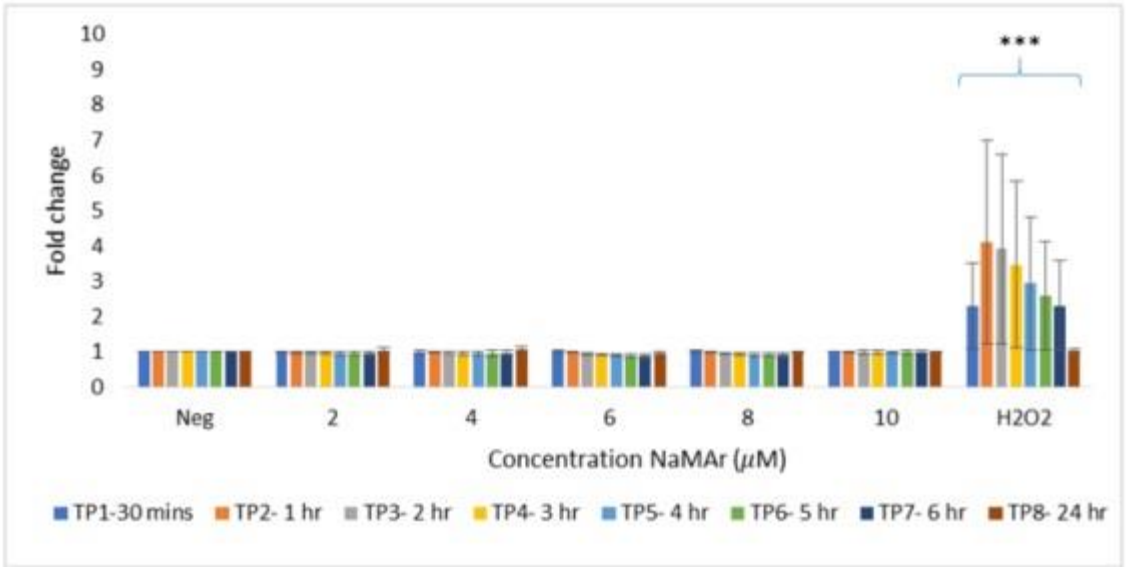

Figure 5.8: The reactive oxygen species (ROS) analysis with sodium meta arsenite treatment at a series of time points against fold change without recovery. 30 minutes, 1 hour, 2 hours, 3 hours, 4 hours, 5 hours, 6 hours and 24-hours were all measured. An n=3 was carried out here and the average was plotted with error bars included. The negative/solvent control used was H_2O and hydrogen peroxide at 100 µM is the positive control (indicated as pos on the graph). There was no statistical significance observed with the addition of NaMAr, however, significance was seen with the positive control (H_2O_2) giving a *P* value of 0.0002.

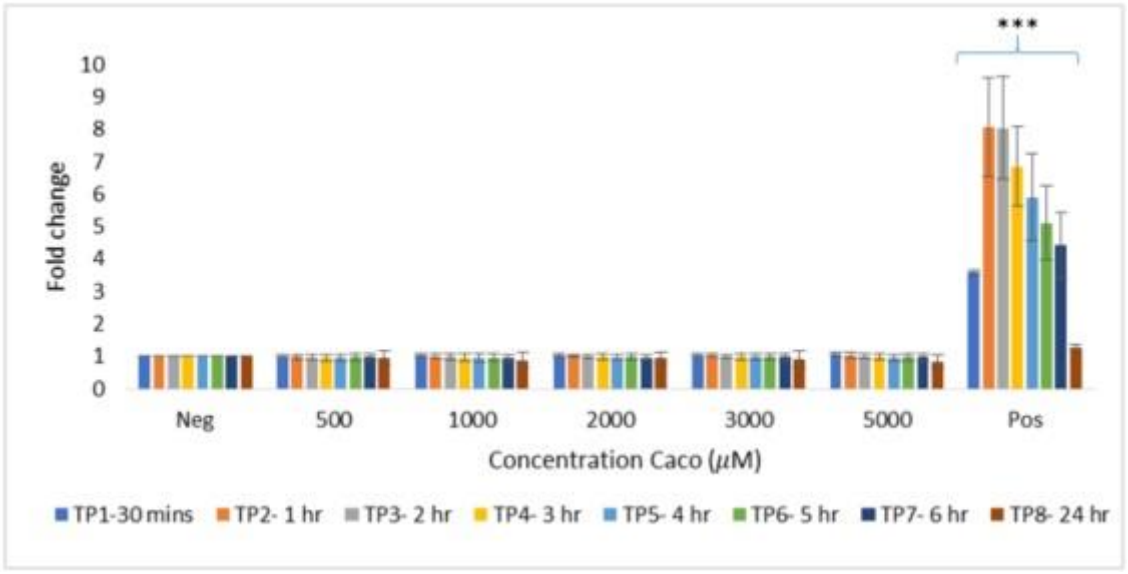

Figure 5.9: The reactive oxygen species (ROS) analysis with cacodylic acid as the test chemical. 30 minutes, 1 hour, 2 hours, 3 hours, 4 hours, 5 hours, 6 hours and 24-hours were all measured and plotted against fold change of total ROS produced. An n=3 was carried out here and the average was plotted with error bars included. The negative/solvent control used was H_2O and hydrogen peroxide at 100 µM is the positive control (indicated as pos on the graph). There was no statistical significance observed with the addition of cacodylic acid, however, significance was observed with the positive control (H_2O_2) giving a *P* value of 0.0001.

The impact of the observed DNA damage by As compounds on cell cycle checkpoints is an important mechanism to assess, therefore cell cycle disruption was investigated across the same dose ranges for both As compounds in an acute setting. For NaMAr there was obvious DNA damage in both an acute (**Figure 5.4**) and chronic setting (**Figure 5.6**). **Figure 5.10** shows the dose dependent changes in cell cycle distribution following exposure to NaMAr. The data seems to display a biphasic response where there is an increase in G1 arrest between 2 µM and 4 µM. However, from 4 µM there is a decrease of cells in G1 and there seems to be a plateau between 8 µM and 10 µM. This is an interesting cell cycle response and there is a possible link with Mn induction occurring at the 2 µM to 4 µM dose with the chronic data (**Figure 5.6**).

Figure 5.11 demonstrates that Caco had a dose dependent decrease of cells in the G1 checkpoint from 2000 µM to 5000 µM. The lower doses of 500 µM and 1000 µM seem to have little effect on the cell cycle checkpoints. As per **Figure 5.11**, these cell cycle changes link to the Mn induction in **Figure 5.7** (i.e. 2000 µM and above).

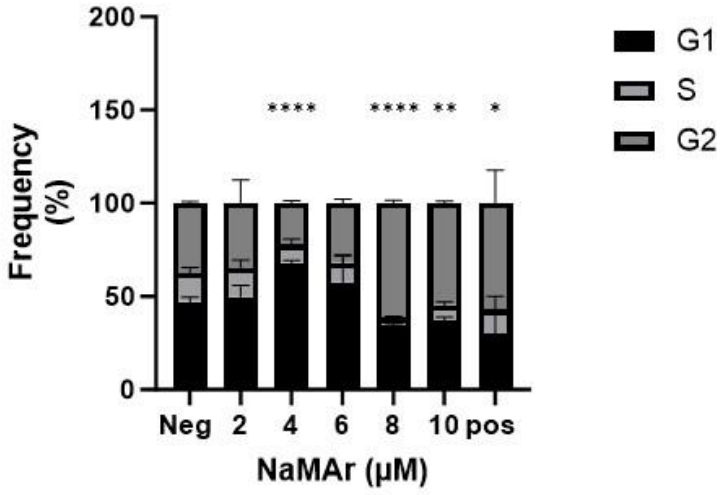

Figure 5.10: Cell cycle analysis of sodium meta arsenite at 24-hours without recovery. The cell cycle stages G1, S and G2 are represented using the flow cytometric method. n=3 was carried out for this work including 3 technical replicates and the average was plotted with error bars. The negative control used here was H_2O and 10 µM MMS was used as the positive control here (P = 0.04291). The key is shown to the top right with different colours representing each cell cycle stage. There was statistical significance at 4 µM (P = 0.00002), 8 µM (P = 0.00004), and 10 µM (P = 0.00451), with a two-way ANOVA. Statistical significance as indicated by asterisks (* <0.05, **<0.005, ***<0.0005, ****<0.00005).

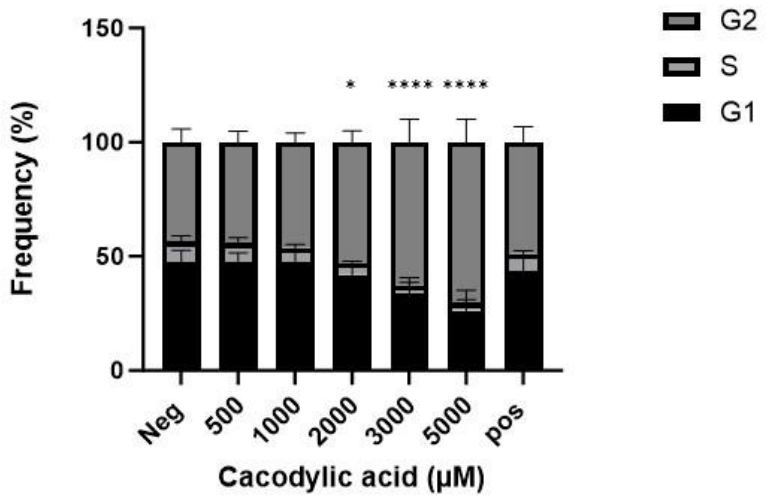

Figure 5.11: Cell cycle analysis of cacodylic acid at 24-hours without recovery. The cell cycle stages G1, S and G2 are displayed along with the standard deviation error bars. n=3 was carried out for this work and the average was plotted. The negative control used here was H_2O and 10 µM MMS was used as the positive control here. The key is shown to the top right with different colours representing each cell cycle stage. There was statistical significance at 2000 µM (P = 0.04981), 3000 µM (P = 0.00004), and 5000 µM (P = 0.00002), using a two-way ANOVA. Statistical significance as indicated by asterisks (* <0.05, **<0.005, ***<0.0005, ****<0.00005).

Both DNA damage and changes to cell cycle can initiate apoptosis in cells, hence this was assessed in a 24-hour setting after exposure to the As compounds. Only the acute 24-hour time-point was assessed because it is thought that cell cycle is a fast-acting endpoint. Annexin V and 7-AAD staining allow for evaluation of early and late apoptotic cells, necrotic cells and live cells. The data shown in **Figure 5.12 and 5.13** seems to display a dose dependent increase in apoptosis in cells exposed to both NaMAr (**Figure 5.12**) and Caco (**Figure 5.13**) which is to be expected. Although for NaMAr, again there seems to be a slight biphasic response between 2 µM and 4 µM in **Figure 5.12**, which is in agreement with the cell cycle and Mn data. **Figure 5.13** shows that Caco is inducing apoptosis in a dose dependent manner, acting in a similar pattern to the Mn and cell cycle data for Caco. As a general rule for Caco, at doses increase above 2000 µM, the apoptotic frequency also increases.

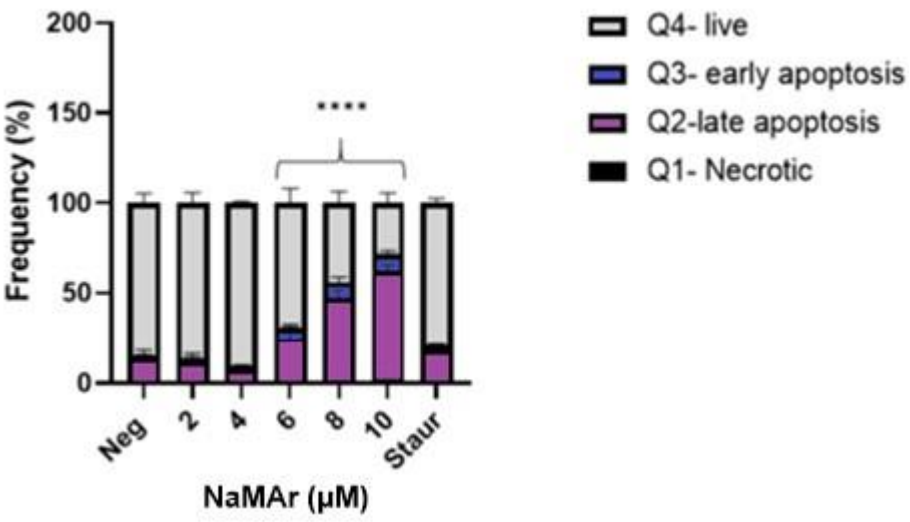

Figure 5.12: Apoptosis and necrosis analysis of sodium meta arsenite at 24-hours without recovery. The different quartiles represent the different stages of apoptosis, necrosis and live cells. n=3 was carried out for this work and the average was plotted with error bars. The negative control used here was H_2O and 0.1 µM staurosporine was used as the positive control. The key is shown to the top right with different colours representing each of the four stages (Q1-Q4). There was statistical significance at 6 µM (P = 0.00003), 8 µM (P = 0.00002) and 10 µM (P = 0.00001) from a two-way ANOVA. Statistical significance as indicated by asterisks (* <0.05, **<0.005, ***<0.0005, ****<0.00005).

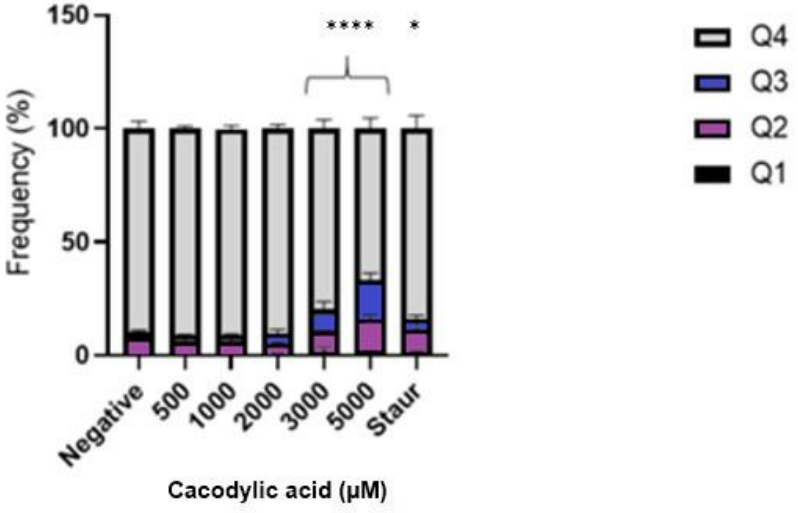

Figure 5.13: Apoptosis and necrosis analysis of cacodylic acid at 24-hours without recovery. The quartiles represent the different percentages of cells at the different apoptotic and necrotic stages as well as live cells. n=3 was carried out for this work and the average was plotted with error bars. The negative control used here was H_2O and 0.1 µM staurosporine (P = 0.0124) was used as the positive control. The key is shown to the top right with different colours representing each of the four stages (Q1-Q4). There was statistical significance for Q2 and Q3 at 3000 µM (P = 0.00004) and 5000 µM (P = 0.00003) using a two-way ANOVA. Statistical significance as indicated by asterisks (* <0.05, **<0.005, ***<0.0005, ****<0.00005).

In a further attempt to understand the mechanisms utilized by both types of As, a panel of cancer genes were investigated by means of a Bio-Rad general cancer panel PCR array (**Figure 5.14 and Figure 5.15**). The genes cluster of differentiation 4 (*CD4*) and interleukin 4 (*IL4)* (both work with the *TGFB* pathway) and transferrin (*TF)* (iron binding and stimulating cell proliferation) are some of the main genes upregulated by both NaMAr and Caco. For **Figure 5.14**, *RET* (the proto-oncogene) is also an important gene as it is the most upregulated within the PCR array. The two forms of As upregulate different genes, this further adds to the fact that the two forms behave in different ways in order to initiate oncogenesis. *FAS* was upregulated by both forms of As which is interesting because both forms induced significant levels of apoptosis and *FAS* is linked to the apoptotic pathway (Guo *et al*., 2016).

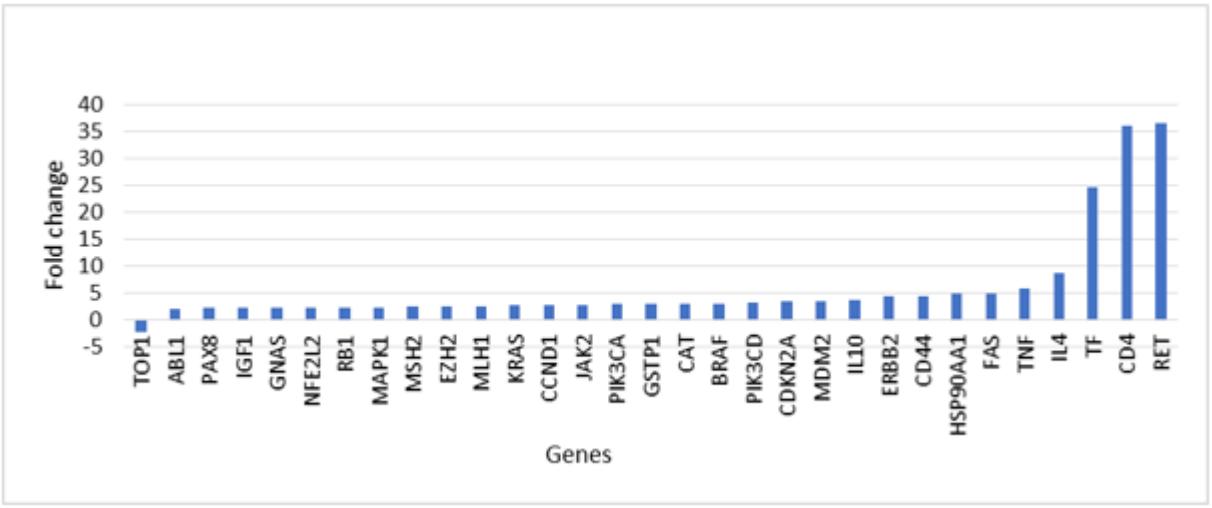

Figure 5.14: PCR array general cancer gene panel for sodium meta arsenite. All of the biologically relevant (±2-fold change) up/downregulated genes are included. The TK6 cells were dosed with 6 µM NaMAr for 24-hours before the RNA was extracted for the PCR array. The PCR array was compared to the negative/solvent control which was H_2O. This work is n=1, therefore no statistical analysis was carried out.

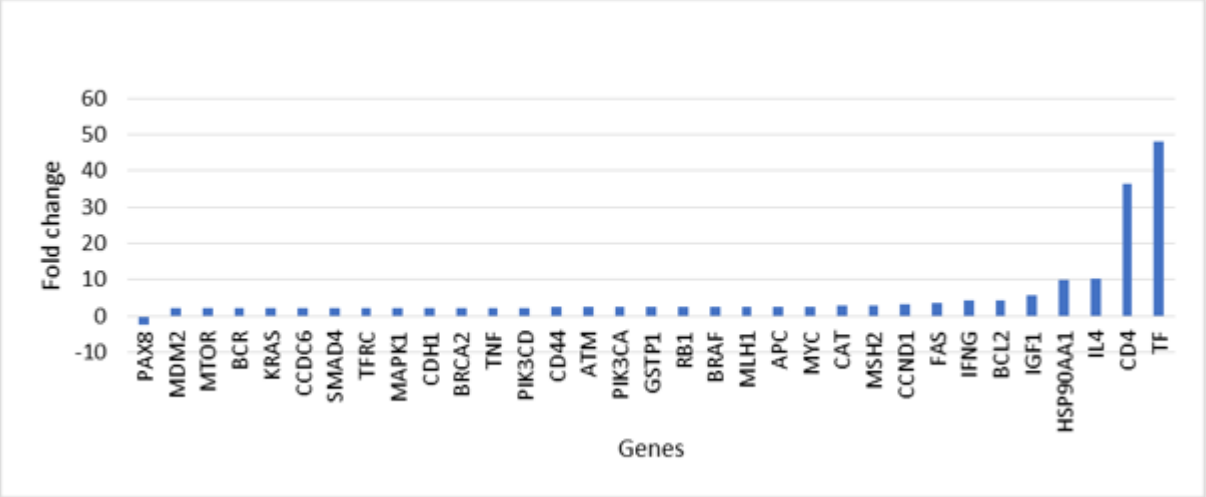

Figure 5.15: PCR array general panel of cancer genes for cacodylic acid. All of the biologically relevant (±2-fold change) downregulated genes are included in the graph. The TK6 cells were dosed with 5000 µM cacodylic acid for 24-hours before the RNA was extracted for the PCR array. The PCR array was compared to the negative/solvent control which was H_2O. This work is n=1, therefore no statistical analysis was carried out.

Mitochondrial stress is an important factor to consider as this can be a cause of DNA damage therefore leading to oncogenesis. **Figure 5.16** shows the Seahorse Analyzer trace graph for NaMAr compared to a water solvent control. The OCR for NaMAr is reduced when compared with the negative. **Figure 5.17** shows that the Seahorse Analyzer trace of Caco has completely destroyed the mitochondrial function with an approximate 9-fold decrease, therefore meaning there is limited function remaining. Even the baseline level is significantly reduced and there are only very minor changes from the baseline level throughout the bioenergetic flux. The doses chosen for Seahorse analysis were the lowest doses to show an effect (4 µM for NaMAr and 2000 µM for Caco) which was kept consistent with the PCR array. The full Seahorse data breakdown can be found in **Figure 5.18 (A-H)** for NaMAr and **Figure 5.19 (A-H)** for Caco.

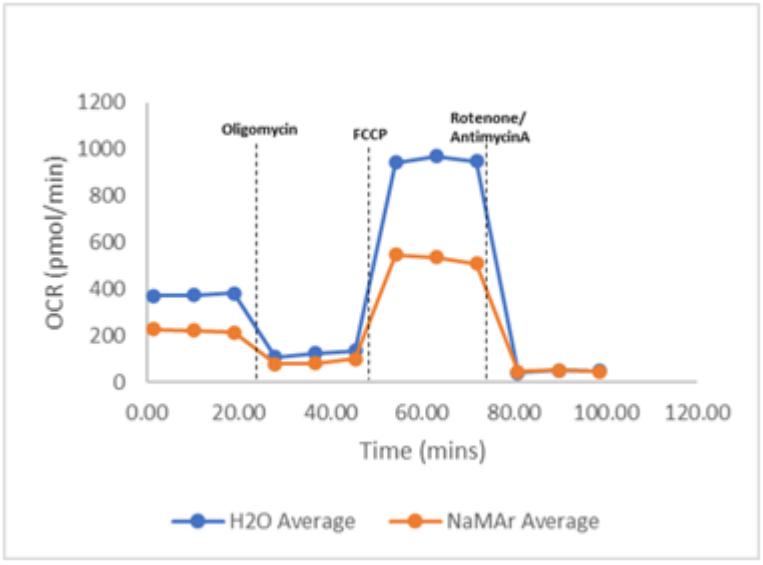

Figure 5.16: The bioenergetic flux profile of a 24-hour sodium meta arsenite treatment when compared to a H_2O negative/solvent control. Oligomycin, FCCP and rotenone/antimycinA are chemical stressors added at different time points to investigate the mitochondrial stress reaction. The full name of FCCP is (carbonyl cyanide-p-trifluoromethoxy) phenylhydrazone and it acts as a mobile ion carrier. n=3 was performed here and the average was plotted.

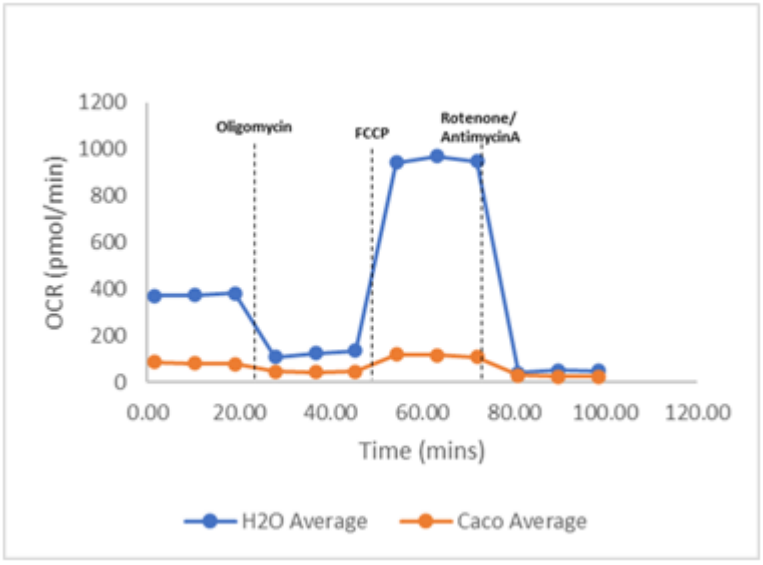

Figure 5.17: The bioenergetic flux profile of a 24-hour cacodylic acid treatment when compared to a H_2O negative/solvent control. Oligomycin, FCCP and rotenone/antimycinA are chemical stressors added at different time points to investigate the mitochondrial stress reaction. The full name of FCCP is (carbonyl cyanide-p-trifluoromethoxy) phenylhydrazone and it acts as a mobile ion carrier. n=3 was performed here and the average was plotted.

Figure 5.18 (A-H) and **Figure 5.19 (A-H)** for NaMAr and Caco respectively, represent all individual graphs of the different outputs from the Seahorse mitochondrial stress test analysis. **Figure 5.18** has no change for non-mitochondrial respiration **(A)** and the OCR/ECAR ratio **(G)**. There are statistically significant changes in the maximal respiration capacity between NaMAr

and the H_2O control **(B)** and the proton leak **(E)**. There seems to be a considerable drop in ATP linked respiration **(C)**, basal respiration **(D)** and reserve capacity **(F)** between NaMAr and the H_2O control. However there is no statistical significance observed as the error bars for all are large. There is a slight reduction of around 50 mpH/min in the ECAR of NaMAr when compared to the H_2O control.

Figure 5.19 showed significance throughout each of the Seahorse output graphs. The OCR/ECAR ratio **(G)** showed no significance at all as there was considerable variation between repeats for this output. The non-mitochondrial respiration **(A)** had the lowest level of significance of all of the graphs, with a p value of less than 0.05. There is a significant drop in ATP linked respiration **(C)**, basal respiration **(D)**, reserve capacity **(F)** and proton leak **(E)** between Caco and the H_2O control. Each of these graphs had a p value of less than 0.005. There are statistically significant changes in the maximal respiration capacity between Caco and the H_2O control (B) with a p value of less than 0.0005. There is a slight reduction of around 90 mpH/min in the ECAR of Caco when compared to the H_2O control.

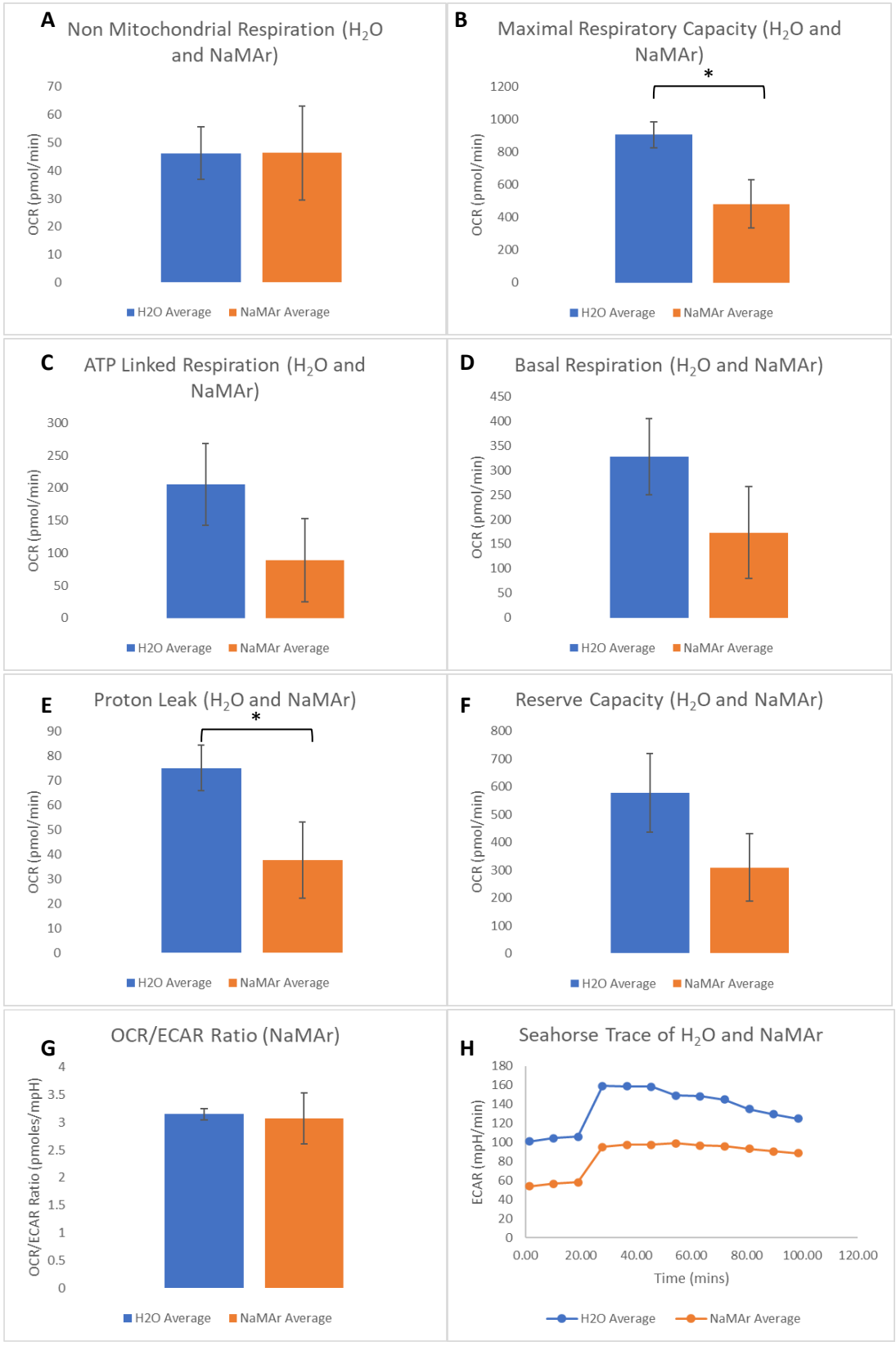

Figure 5.18 (A-H): Seahorse graphs for NaMAr indicating the different respiration parameters when compared to the H_2O solvent control. **A** represents non mitochondrial respiration, **B** is the maximal respiratory capacity ($P = 0.0019$),, **C** is the ATP linked respiration, **D** is basal respiration, **E** is proton leak ($P = 0.0228$),, **F** is the reserve capacity, **G** demonstrates the OCR/ECAR ratio and **H** represents the ECAR graph. Unpaired T tests were carried out for these analyses (* < 0.05).

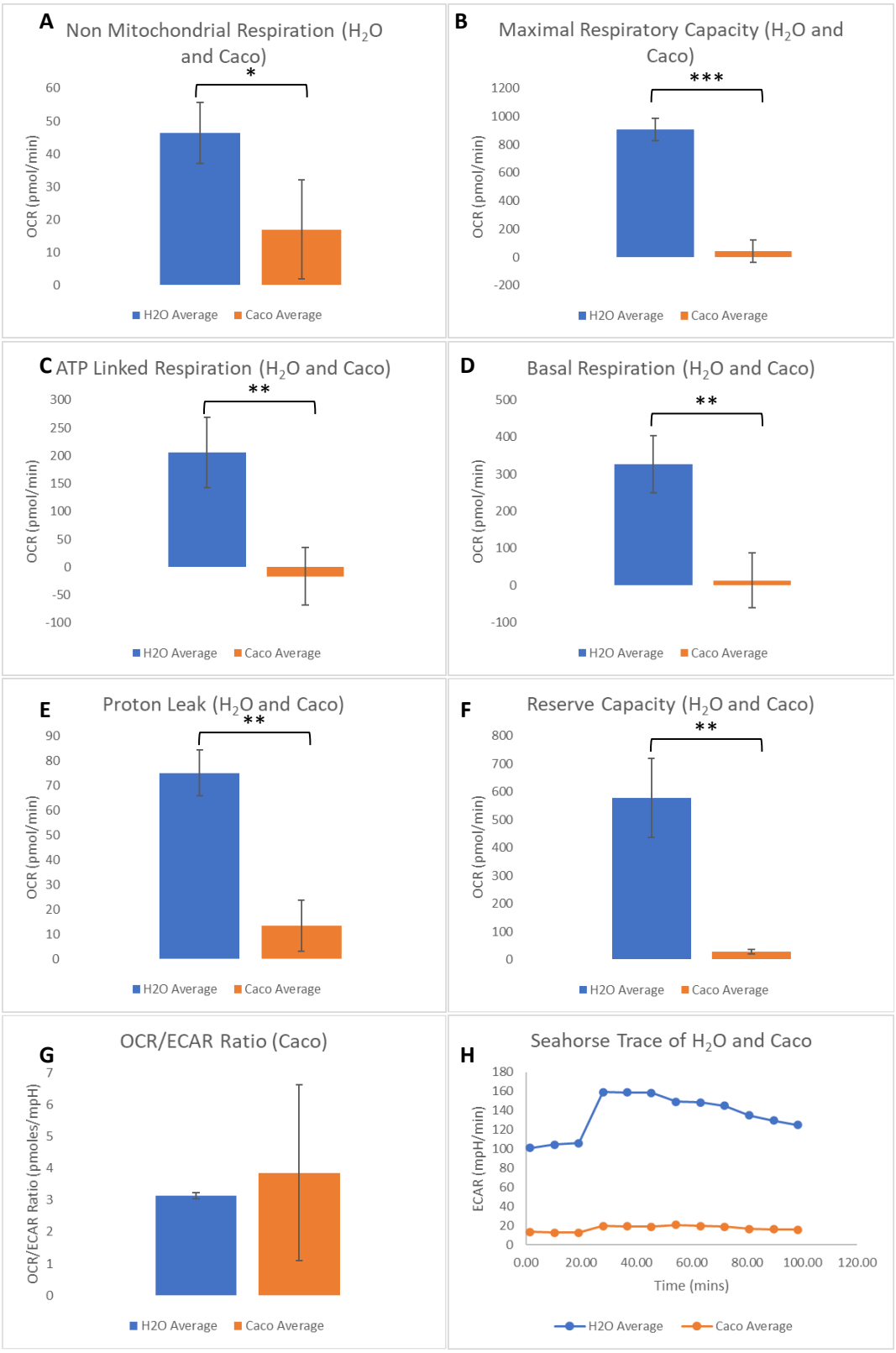

Figure 5.19 (A-H): Seahorse graphs for cacodylic acid indicating the different respiration parameters when compared to the H_2O solvent control. **A** represents non mitochondrial respiration (P = 0.0456),, **B** is the maximal respiratory capacity (P = 0.0002),, **C** is the ATP linked respiration (P = 0.0091),, **D** is basal respiration (P = 0.0070),, **E** is proton leak (P = 0.0015),, **F** is the reserve capacity (P = 0.0025),, **G** demonstrates the OCR/ECAR ratio and **H** represents the ECAR graph. Unpaired T tests were carried out for these analyses (* < 0.05, **<0.005, ***<0.0005).

5.4 Discussion

The Mn induction in **Figure 5.4** shows a concentration-dependent response with NaMAr, suggesting that there may be genotoxicity in an acute testing system. This is unexpected considering NaMAr is classified as a NGC but could potentially produce genotoxic metabolites under certain conditions. There is clear cytotoxicity displayed as a result of treatment with this form of As. Note that the statistical significance for Mn induction demonstrated at doses 8 µM and 10 µM should not be considered as they exceed the cytotoxicity threshold of 50% set by the OECD guidelines for Mn analysis (OECD, 2012). The doses 8 µM and 10 µM are included in order to form a comparison with the chronic data (**Figure 5.6**).

Caco (**Figure 5.5**) also showed a dose-dependent response, however Mn induction did not reach statistical significance. Cytotoxicity was induced in a dose dependent fashion and exceeds the 50% threshold at the top dose of 5000 µM. When comparisons are made between **Figure 5.4** and **Figure 5.5** there are noteworthy differences in dose ranges required in order to observe a response. Caco has a dose range of 500-5000 µM whereas NaMAr has a dose range of 2-10 µM meaning there is a 250-500-fold difference between the dose ranges. The literature is in agreement with the data here, showing that much higher concentrations of Caco are required when compared to NaMAr (Kenyon and Hughes, 2001). It is a possibility that the difference in structure between the two compounds could be responsible for the potency of the two chemicals as seen in **Figure 5.2** and **Figure 5.3**. There seems to be a slight decrease in Mn induction at 4 µM which is subtle, however it proves to be in accordance with **Figures 5.6, 5.10 and 5.12** as it suggests a biphasic response.

The chronic dosing of NaMAr is portrayed in **Figure 5.6** which demonstrates a typical GC response. From dose 4 µM there is a significant increase in Mn induction for every dose thereafter. Again, it should be noted that the 10 µM dose is producing excessive cytotoxicity (>50%). The data here are in agreement with the hypothesis that chronic dosing may be more useful in identifying NGCs *in vitro*. There is a potential benefit of utilising a chronic dosing approach as this may lead to an accumulation of toxicity which could be seen in the Mn assessment (Wills *et al*., 2017).

The fractionated doses for Caco can be seen in **Figure 5.7**. From the 2000 µM dose onwards Mn were induced, however the 5000 µM has cytotoxicity above the 50% threshold. There seems to be a large increase in Mn induction at 2000 µM. This could potentially be due to a NGC mechanism also taking place or further investigation of the dose range between 1000 µM and

2000 µM is required. With both **Figure 5.6** and **Figure 5.7** it looks as if a molecular switch has been activated between doses 2 µM and 4 µM for NaMAr and between 1000 and 2000 for Caco.

NaMAr was capable of inducing Mn after chronic dosing was utilized, even though it is classified as a NGC. This is also seen in Dural *et al*., (2020) with potassium bromate (KBr), even though this is a GC, when chronic dosing was employed it was shown that there was a better tolerance of cytotoxicity but increased genotoxicity with increased doses.

ROS do not seem to be produced by NaMAr nor Caco **Figure 5.8** or **Figure 5.9** respectively using the DCFDA approach. This is a surprising result considering the literature suggests that ROS are the main MoA of As toxicity (Hu *et al*., 2020). Throughout the literature it is heavily cited that As is a known ROS producer, so here it must be due to the assay used. Although it is widely used, the DCFDA assay is often criticized as it has several problems such as only detecting H_2O_2 (Degli Esposti, 2002) and interference from different proteins (Burkitt and Wardman, 2001). Looking at the ROS graphs, both **Figures 5.8 and 5.9** show a flat response or even with a slight downward trend, suggesting that neither of the arsenic compounds utilize a ROS MoA. Certain molecules have been known to auto fluoresce in the DCFDA assay (Billi, 2009) or whether the As test chemicals somehow interfered with the fluorescence and therefore produced false negatives. This is also surprising when you consider that both compounds affect mitochondrial function (**Figure 5.16, Figure 5.17**). This could mean that a more specific ROS assay is required to look at individual radicals, as total ROS does not seem to be affected but this area definitely warrants further investigation. The assay was validated by including 100 µM H_2O_2 as a positive control which showed ROS production in each assay. Also, the assay showed ROS production with $NiCl_2$ further proving that the assay worked.

As is thought to be a ROS inducer so it is interesting to note there was no ROS induction with either As compound (**Figure 5.8, Figure 5.9**) as a result of the DCFDA assay. However, both **Figure 5.14** and **Figure 5.15** demonstrate that ROS-induced signaling factors, such as map kinases (*MAPK1)* are upregulated (Hu *et al*., 2020). Tapio and Grosche, (2006) showed numerous studies that highlighted an activated MAPK pathway after As exposure both *in vitro* and *in vivo*. Although, *MAPK1* was upregulated in **Figure 5.14** and **Figure 5.15**, the fact there is no ROS induction in **Figure 5.8** and **Figure 5.9** does not provide a complete picture of the MoA of these compounds.

The lack of ROS production seen in **Figure 5.8** and **Figure 5.9** could be explained by the type of ROS assay chosen. It is thought that As primarily produces hydroxyl radicals (HO•) or

superoxide radicals ($O_2 \cdot^-$) (Tapio and Grosche 2006). However, the DCFDA assay used in this work, predominantly measures H_2O_2 production (Black and Brandt, 1974) therefore choosing this chemical as the positive control. The DCFDA assay is one of the most widely used probes for measuring H_2O_2 production (Degli Esposti, 2002). There are some criticisms of using the DCFDA assay such as cell leakage (Royall and Ischiropoulos, 1993) and interference from iron proteins such as cytochrome c (Burkitt and Wardman, 2001). Future work could include performing a more suitable assay, such as using reduced ethidium bromide (EthBr), dihydroethidine (DHE) as this is a frequently used fluorescent probe which measures superoxides (Rothe and Valet, 1990).

The cell cycle analysis of NaMAr (**Figure 5.10**) seems to demonstrate a biphasic effect which mirrors the effect seen with the Mn data, highlighting the complex effect seen with this agent (Kakehashi *et al*., 2013). It is also stated that NGCs can exert a variety of epigenetic effects such as causing post-translational modifications and targeting nuclear receptors to trigger cellular carcinogenesis (Kakehashi *et al*., 2013). A biphasic dose response seems to be present with the cell cycle analysis results after the addition of NaMAr. Certain NGCs such as TCDD for instance have been described as a molecular switch. The more nonlinear the response, the more likely it is to be a molecular switch. These molecular switches respond to stimuli and undergo reversible changes when they are activated (Fitzmaurice *et al*., 2022).

These molecular switches act in a very sudden way causing fundamental changes in the function of cellular processes (Andersen *et al*., 2002). It looks as if a molecular switch is activated between 2 µM and 4 µM NaMAr treatment as there is a sudden change in the response and every concentration thereafter seems to show a regular dose response. At 4 µM, there seems to be an increase of cells arrested in G1 however from 6 µM onwards it can be observed that the cells are being pushed into the G2 phase. This molecular switch effect can be seen more clearly in **Figure 5.20** below.

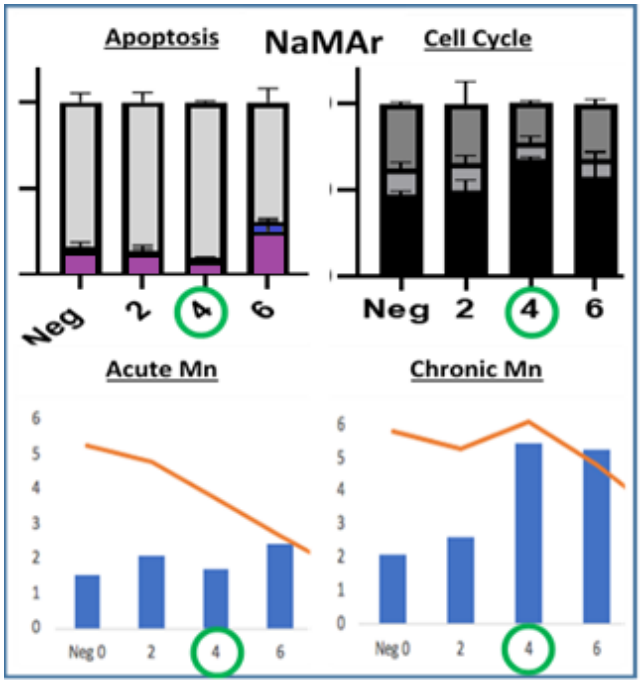

Figure 5.20: The molecular switch at 4 µM for sodium meta arsenite is represented by the four different endpoints; apoptosis, cell cycle and acute and chronic micronucleus. There is a clear effect observed at the highlighted dose. With most of the doses after 4 µM showing statistical significance.

The acute Mn data show a decrease at 4 µM before an increase at 6 µM which is comparable to the pattern seen in apoptosis assay. In the apoptosis data there is a decrease of live cells and an increase of the apoptotic cells after the 4 µM dose. Whereas the cell cycle data and chronic Mn results show a similar pattern where there is an increase at 4 µM and a slight drop at 6 µM. This is an interesting effect and should be followed up with future work.

Other As studies observed a similar cell cycle pattern (after 4 µM) where the cells are pushed into the G2 phase of cell cycle (Hassani *et al*., 2017). It is thought that this is as a result of the upregulation of certain cyclins such as *CCND1* and cyclin dependent kinase inhibitor 2A (*CDKN2A)* which are capable of promoting cellular progression from G1 to S and then from S to G2 respectively (Vermeulen *et al*., 2003). This is in agreement with **Figure 5.14** as both *CCND1* and *CDKN2A* are among the upregulated genes in the qPCR arrays. The accumulation of cells in G2 phase could be due to the spindle or mitosis aberrations (Chang *et al*., 2010).

In the majority of tumours, trivalent arsenicals such as NaMAr can induce a G1 or G2 cell cycle arrest but not induce apoptosis (Li *et al*., 2009) which agrees with **Figure 5.10** and **Figure 5.12**.

Caco shows dose dependent changes in cell cycle, **Figure 5.11** shows that as the dose increases, the cells are moved into the G2 phase. Similar to **Figure 5.10**, this perturbation in the cell cycle could relate to the upregulation of *CCND1* and *CCDC6*. There is evidence to support that

CCDC6 is capable of maintaining genomic stability, cell survival and control over the cell cycle (Cerrato *et al*., 2017).

The apoptotic data for NaMAr shown **in Figure 5.12** mimics the same biphasic behaviour shown in **Figure 5.6** and **Figure 5.10.** The biphasic hormetic responses seen with NaMAr from 2-4 µM in **Figure 5.4, Figure 5.6, Figure 5.10** and **Figure 5.12** has also been noted in the literature (Lundqvist *et al*., 2019). From 4 µM, the results show a dose dependent increase in apoptosis. When **Figure 5.12** is compared to **Figure 5.13,** it can be seen that even though the NaMAr dose range is much lower, it has a much greater apoptotic effect. Arsenite is capable of inducing apoptosis (Chen *et al*., 1998) as seen in **Figure 5.12** hence its use in chemotherapy (Mead, 2005). Zhao *et al*., (2002) highlighted the strong relationship between As -induced apoptosis and a G2/M cell cycle arrest which can be seen in **Figure 5.10**.

The effect of Caco on cell death (**Figure 5.13**) shows there is limited apoptotic induction up to 2000 µM, which is in agreement with both **Figure 5.5** and **Figure 5.7**. Caco produces a limited apoptotic induction with doses 3000 µM and 5000 µM, however this is still a small induction when compared to **Figure 5.12**.

The general panel of cancer genes assessed for NaMAr can be seen in **Figure 5.14**. There is a 36-fold upregulation of both *RET* and *CD4*. Interestingly, this 36-fold upregulation of *CD4* is synonymous with Caco (**Figure 5.15**). There are some overlaps between **Figure 5.14** and **Figure 5.15**, which is expected as they are both As compounds.

The gene expression changes for Caco (**Figure 5.15**) show a substantial upregulation of *TF* and *CD4* with fold changes of 48- and 36-fold increases respectively. The main role of *TF* in humans is to allow the entry of iron into all cells and it is expressed at low levels in the majority of normal tissues. *TF* is upregulated in most cancer cells but is most prevalent in malignant cells. The *TF* receptor is a potential target for cancer therapies due to the cancer cells dependence of iron for cell proliferation, the function of internalising iron and the increased expression in malignant cells (Daniels *et al*., 2012). Therefore, the large upregulation of *TF* in **Figure 5.15** is a common occurrence in a number of cancers. Future work could have looked further into iron related processes such as ferroptosis. This is interesting because As is a metal like iron, so could use similar mechanisms of action.

Changes to the tumour microenvironment could be responsible for changes to immune metabolism and can alter the anti-tumour immunity profiles by either promoting or impairing its function (Sugiura and Rathmell, 2018). This may explain the otherwise confusing upregulation

of *CD4* in **Figure 5.15** as the anti-tumour immunity may be impaired. A study by Ma *et al*., (2016) demonstrated that increased linoleic acid in the liver altered the CD4+ T cells leading to increased apoptosis. This is in agreement with **Figure 5.13**, where apoptosis has been increased.

Figure 5.16 shows a large decline in the bioenergetic flux profile with the addition of NaMAr. This suggests the mitochondrial function is decreased. There is a difference of around 200-fold between the water negative control and NaMAr. Dysfunctional mitochondria are capable of modifying a series of cellular processes that can lead to tumourigenesis such as changes in metabolism, gene expression, cell cycle, cell viability as well as cell growth (Boland *et al*., 2013).

Mitochondria are an important organelle in numerous cellular processes and are heavily involved in As -induced apoptosis (Woo *et al*., 2002). The mitochondria are both a target and source of excessive ROS production (Chen *et al*., 2001). The Seahorse Analyzer trace of cells treated with Caco (**Figure 5.17**) was very interesting because it appears that the mitochondrial function is completely reduced and mitochondrial toxicity has occurred. If there is dysfunction in the electron transport chain specifically this can produce increased ROS (Naranmandura *et al*., 2011), however this is not synonymous with the ROS induction data (**Figure 5.15**). It has also been shown that Caco produces a lower level of ROS when compared to other arsenicals (Naranmandura *et al*., 2011). The ROS produced as a result of Caco treatment stimulates ROS production in organelles other than the mitochondria such as ribosomes, the Golgi apparatus and the endoplasmic reticulum (Naranmandura *et al*., 2011). It is well known that As causes a decrease of mitochondrial membrane potential as a result of depolarisation, therefore initiating lipid peroxidation and ROS production (Han *et al*., 2008). It has also been shown that Caco initiates cell death cascades by altering the function of mitochondrial proteins such Bcl-2 (Yen *et al*., 2012), which can be seen in **Figure 5.15**.

Jiang *et al*., (2013) produced data in agreement with the data seen here, that NaMAr is capable of causing genotoxicity (as seen in **Figure 5.5, Figure 5.7**), cytotoxicity (as seen in **Figure 5.5, Figure 5.7**), cell cycle arrest (**Figure 5.11**), and apoptosis (**Figure 5.13**), however there is a contradiction about the production of ROS (**Figure 5.9**). ROS was not observed above negative control concentrations produced with the DCFDA assay however (Jiang *et al*., 2013) used an assay based on the DCFDA method but it was a different kit from Applygen Technologies Inc, Beijing, China.

It seems as though the multiple endpoints are inter supporting in this chapter as seen in **Figure 5.20**. It is also interesting to note that the mechanisms of the two forms of As are broadly similar despite their different classifications as GC and NGC. There were controversies in the classification of the two chemicals, so perhaps there has been incorrect labelling of one of these chemicals.

5.5 Conclusion

As is a very complex chemical, it is present in both genotoxic and non-genotoxic forms, it exists in both organic and inorganic forms and it also has both metal and non-metal properties. As has been known for centuries for its poisoning properties and its use was common practice in homicide (Mead, 2005). Chronic exposure to As has been associated with numerous human diseases (Martinez *et al*., 2011). There are a number of As -related diseases such as skin lesions, ischemia, hypertension, diabetes and numerous types of cancer (Chen *et al*., 1995). However, interestingly As trioxide is used as an anti-cancer treatment against acute promyeloid leukaemia (APL), for relapse patients or patients unresponsive to other chemotherapy (Mead, 2005). This means that As is capable of causing instant mortality, short and long-term medical conditions and is also able to act as a chemotherapeutic agent. These opposing behaviours of As and its compounds suggest that is it a very difficult and complicated chemical to explore.

The two forms of As studied in this work are NaMAr (NaMAr) and Caco , which are the non-genotoxic and genotoxic forms respectively. NaMAr showed cytotoxicity in both an acute and toxic setting, likewise Caco displayed cytotoxicity in both acute and chronic exposures. Both NaMAr and Caco displayed a significant increase in Mn induction with a chronic exposure, i.e. genotoxicity. This highlights the importance of chronic dosing in order to more closely mimic a real-life exposure. The ROS data conflicts with what is seen in the literature. As is thought to be a ROS inducer, however the results do not indicate ROS production with either form of As and Caco actually shows a very slight AOX action. Future work would include more mechanistic investigation surrounding ROS. Cell cycle perturbations displayed an important mechanistic pathway for both As forms. NaMAr shows a biphasic cell cycle response around 4 µM and thereafter a dose dependent G2 arrest can be seen. Caco shows a clear dose dependent G2 arrest similar to NaMAr, showing the importance of cell cycle as part of the MoA for both As forms. Apoptosis proved to be important for both As forms, again NaMAr showed the same biphasic response seen with cell cycle analysis. Both NaMAr and Caco showed a dose dependent

increase in apoptosis, with NaMAr showing the strongest apoptotic induction. There are some overlaps with the PCR array data for both As forms. There are 31 biologically relevant genes for NaMAr and 33 biologically relevant genes for Caco. There are links with ROS, apoptosis, cell cycle and other potential mechanisms by some of the genes highlighted in these arrays. There is a lot of future work that can be carried out using the PCR array data and further investigating some of the important genes. The bioenergetic flux profiles of the two As forms are quite different, however they both show a reduction in mitochondrial function. NaMAr reduces the Seahorse Analyzer trace around 200 pmol/min whereas Caco completely diminishes mitochondrial function. It has been noted that Caco is capable of decreasing mitochondrial membrane potential and affecting mitochondrial function proteins leading to increased cell death.

Overall, the multiple endpoint analysis has proven useful, except for the contradicting ROS results. NaMAr behaves as is expected of a NGC and shows promise of detecting this NGC *in vitro* with chronic dosing. Caco seems to behave in both genotoxic and non-genotoxic ways with its acute and chronic Mn results, highlighting the convolutions with these chemicals. The multiple endpoints assessed help to create a holistic picture of the mechanisms utilized. Some future work including further investigation into oxidative stress assays and follow up gene expression analysis via qPCR, could add to robustness of this *in vitro* testing approach.

Chapter 6: Discussion

6.1 GC v NGC

Carcinogens are classified into two main groups, GCGC and NGCs . GCs are capable of causing cancer as a result of altering the genetic material directly whereas NGCs are able to cause cancer via secondary mechanisms (Hayashi, 1992). It is thought that NGCs often use multiple mechanisms in order to cause the initiation of cancer. A difficulty with NGCs is their species and tissue specificity. The carcinogenicity testing strategy is a series of *in vitro* and *in vivo* genotoxicity tests, which NGCs often do not affect (Hernández *et al*., 2009). NGCs are generally negative in *in vitro* and *in vivo* mutagenicity tests and do not facilitate DNA repair (Pérez at al., 2016).

Carcinogens can behave in a series of complex ways, for example GCs can also utilize alternative mechanisms in order to contribute to carcinogenesis (Jacobs *et al*., 2020). The NTP devised the term 'genotoxic carcinogen' in the 1980s, after testing 222 chemicals. Of the chemicals tested, 115 were carcinogens however 62% were DNA reactive GC but 38% were non-DNA reactive carcinogens (NGCs) (Nohmi, 2018). There is also some evidence to show that NGCs often require multiple alternative mechanisms in order to initiate oncogenesis (Hernández *et al*., 2009). NGCs are increasingly difficult to test for as they do not have one unifying feature, despite being grouped together (Hernández *et al*., 2009). As the 2 year-rodent bioassay is the way in which NGCs are detected currently, there is a growing concern as a result of the reduction of the 2-year rodent bioassay, meaning these carcinogens could go undetected. CTAs are also recommended to detect NGCs, however there are several problems with these assays. For example, they do not agree with the 3R's ideals as these assays are quite unethical and are not considered fully *in vitro* (Meyer, 1983). This represents the importance of creating an *in vitro* test system for NGCs due to their prevalence, complexity and reduction of the 2-year bioassay.

6.2 Current testing limitations

Traditional carcinogenicity testing is comprised of short term *in vitro* and *in vivo* assays and in some cases chemicals are recommended to undergo the 2-year rodent bioassay which confirms if a chemical is a NGC. However, there is currently no *in vitro* test system for NGCs and this is becoming of increasing importance (Kirkland *et al*., 2005). This is the basis for my PhD work, to

assess if an *in vitro* battery could detect NGCs thus preventing the automatic use of animals in testing.

There are several sub-chronic and chronic *in vivo* toxicity tests carried out currently, with the gold standard being the 2-year rodent bioassay (Chan *et al*., 1992). The long-term exposures are costly and use large numbers of animals which mean that not all chemicals are subject to this testing. There are also concerns around using animal data to report on human health. There is a growing need to develop long term *in vitro* testing alternatives (Macko *et al*., 2021).

Jacobs *et al*., (2020) highlights the many limitations with the 2 year rodent bioassay including the lack of human relevance and MoA information. It is explained that there are a number of ongoing approaches aiming to reduce the use of the 2 year rodent bioassay and instead replace this highly criticized assay with *in vitro*, *in silico* and shorter *in vivo* studies. It is not yet at the stage where *in vivo* studies are completely replaced but the new alternative approaches will aim to better understand NGCs and comply with the 3Rs (Jacobs *et al*., 2020).

6.3 Chemicals assessed

Here, the mechanisms associated with 6 chemicals were studied; 5 NGCs; $NiCl_2$, NaMAr, rosuvastatin, chloroprene and 2,3,7,8-tetrachlorodibenzo-p-dioxin and a GC; Caco. The 6 chemicals were chosen after a thorough literature search and utilising already formulated lists of NGCs (Kirkland *et al*., 2016; Hernández *et al*., 2009; Vinken *et al*., 2008; Hwang *et al*., 2020). Numerous factors were considered when conducting the literature search. The chemicals were picked due to interesting and varying suggested mechanisms of action, with a range of different uses in society as well as largely understudied or unknown chemicals. Caco is actually a GC and organic form of As. This chemical was chosen to form contrasts and comparisons with NaMAr, the NGC inorganic form of As (Dong and Luo, 1993).

$NiCl_2$ is a heavy metal and a known ROS producer (Cameron *et al*., 2011). The most important use of $NiCl_2$ is the electroplating onto other metals (National Toxicology Program, 2013). $NiCl_2$ is readily absorbed dermally, potentially causing health risks for industrial workers (ATSDR, 2005). Nickel compounds are proven to be carcinogenic but only possesses a weak genotoxic potential in animals and humans (Hartwig *et al*., 1994). Nevertheless, $NiCl_2$ has been classified as a NGC.

NaMAr is an inorganic form of As and possible MoAs behind its carcinogenicity include repair inhibition or a possible ROS producer (Kirkland *et al*., 2016). NaMAr is used as an insecticide, herbicide and antibacterial agent (PubChem, 2023). There is much controversy in the literature surrounding NaMAr highlighting the complexity of this chemical. Kirkland *et al*., (2016) has classified NaMAr as a NGC, whereas others such as (Guilamet *et al*., 2004) suggest that it is a GC.

Caco is an organic form of As and is the most common form of As in the environment. Like NaMAr, it is also used in pesticides and herbicides (Wagner and Westwig, 1974). It works via a genotoxic MoA, causing DNA single strand breaks and ROS (Tezuka *et al*., 1993). Even though Caco is not a NGC, it was chosen because it can be directly compared and contrasted to NaMAr as they are both carcinogenic forms of As.

Rosuvastatin is a type of statin drug and is used to lower cholesterol, it acts via a mechanism of inhibiting HMG-CoA (AstraZeneca, 2022). There are opposing views on rosuvastatin, as Kirkland *et al*., (2016) classifies it as a NGC. Although, some studies have demonstrated that rosuvastatin can act as an anti-cancer drug, specifically with prostate cancer (Lustman *et al*., 2013).

The MoA utilized by chloroprene is largely unknown but it is believed to potentially have a link to chronic cytotoxicity (Shelby, 1990). This chemical was chosen as it has an interesting link to 'cancer alley' (Randolph, 2021), where chloroprene is used to produce neoprene, a synthetic rubber (Valentine and Himmelstein, 2001). There are controversies about the carcinogenic nature of chloroprene, though it is classified as a NGC (Vinken *et al*., 2008).

TCDD is the most common type of NGC studied to date, it has been recognised to utilize the AhR as part of the MoA, although the MoA is largely unknown (Bock and Köhle, 2006). TCDD is often used as a herbicide (Schecter *et al*., 2006). TCDD is a very commonly studied dioxin and NGC due to the high potency and unknown MoA of carcinogenesis (Van den Berg *et al*., 2006). TCDD is largely negative in all of the *in vitro* genotoxicity tests (Hwang *et al*., 2020).

More NGCs were considered during the PhD and 2 more chemicals were tested but were abandoned due to problems with dissolution and precipitation. Two NGCs that were tested but not followed-up were cholic acid (Hwang *et al*., 2020) and DEA(Kirkland *et al*., 2016). Some of the preliminary data for these chemicals can be found in the Appendix (**Appendices Figures A1, A2 and A3**). Cholic acid is a bile acid that occurs naturally and is commonly used to treat patients with deficiencies of bile acid synthesis (Liver Tox, 2012). A suggested MoA for cholic

acid is xenobiotic metabolizing enzyme inhibitors (Hwang *et al*., 2020). Nevertheless, cholic acid caused pH changes and precipitation of the chemical out of solution. As a result, cholic acid was only assessed for cytotoxicity and was taken no further. There were many questions regarding whether any effect seen could be as a result of the pH changes induced by cholic acid. It is also interesting to note that a related bile acid, deoxycholic acid, is classified as a GC (Jenkins *et al*., 2007) which means the two bile acids could have been compared if carried forward.

DEA has many uses in society such as a component of soaps, surfactants, laundry detergents, shampoo, conditioner and cosmetics (IARC, 2013). It is also used in industry as a corrosion inhibitor as well as many other uses (IARC, 2013). DEA is thought to be carcinogenic via a MoA of choline deficiency which in turn leads to hepatocyte proliferation, apoptosis and transformation (Zeisel, 1996). However, in this study, DEA was not taken further than the initial cytotoxicity studies as the NGC was difficult to work with mainly due to the viscosity of the chemical. There is very preliminary data showing that there is no real response until 10 mM.

6.4 Limitations of Cell lines

This work has focused solely on the individual cell lines; TK6 and MCL5. Cell lines are the primary *in vitro* model systems that are used in medical research such as drug discovery and cancer research as well as many other disease types. Due to the fact that cell lines can keep dividing, it provides a great biological model to carry out experiments. Cell lines are also capable of mimicking the tumour microenvironment in a 3D manor and being incorporated into a more sophisticated co-culture format (Mirabelli *et al*., 2019). It has been shown that human cell lines can effectively retain genomic information and diversity of the origin cancer and therefore provide a good model system for the disease in which they were derived (Mirabelli *et al*., 2019).

Although cell lines can provide an insight into understanding the NGCs, they have a number of limitations in cancer research. The 2D culture of cell lines used in this work weakly resembles the tumour microenvironment. The first cultured cell line was HeLa cells, derived from the cervical cancer of Henrietta Lacks in 1951 (Scherer *et al*., 1953) from which a number of different cell lines originated. It was demonstrated that there are only a finite number of passages a cell can undergo before modifications mean that the cells are behaving differently to the tumour it was derived from (Nelson-Rees *et al*., 1976). Cell lines derived from human cancer are the most extensively studied *in vitro* models in the field. Although primary clinical

samples are available, it is still necessary to test therapeutic strategies on preclinical *in vitro* models as this gives a basic understanding of any effects seen (Gillet *et al*., 2013). However, questions remain as to whether simple 2D cell models can adequately represent the complex biology of cancer. Both intrinsic and expressed toxicity needs to be measured using *in vitro* and *in vivo* systems. Tumours have been recognised as very complex organs, even more so than healthy tissues. Both the specialised cell types involved and the tumour microenvironment as a whole need to be studied to understand the complete tumour biology. The tumour is much more than just a collection of dividing homogenous cancer cells. It is understood that an array of different cell types contribute to the tumour microenvironment. Some examples of the cells present within a tumour are endothelial cells, cancer cells, cancer associated fibroblasts, pericytes and tumour promoting inflammatory cells (Hanahan and Weinberg, 2011).

It is possible that the TK6 and MCL5 cell lines mainly used here, were not a strong enough *in vitro* model alone. TCDD has shown the induction of both phase I and II metabolising enzymes such as CYP1A1, which is present in MCL5 cells (Dere *et al*., 2006). There are several limitations with respect to the metabolic competency of MCL5 cells. Although, this cell line has proved to be proficient in phase I metabolism of chemicals such as benzo [a] pyrene (BaP) it has shown deficient phase II metabolism. MCL5 cells may not have been the best cell type to investigate TCDD and perhaps this NGC would benefit from a stronger *in vitro* model (David *et al*., 2016). However, Crepsi *et al*., (1991) suggested that MCL5 cells show promise as a carcinogen screening system.

The 3 NGCs in **chapter 3** (rosuvastatin, chloroprene and TCDD) were further investigated in **Section 3.4.4** as they had negative results in most endpoints tested. The additional data, shows promise for further understanding with these chemicals as a result of a more sophisticated model. These chemicals could further benefit from a more complex systems such as organoids for example, which are very advanced models of whole organs. Alternatively, a co-culture model comprised of multiple different cell types present in the tumour microenvironment may prove to be a better *in vitro* model of these complex NGCs. However, it has been shown that TK6 cells *in vitro* are able to differentiate between GC and NGCs (Wilde *et al*., 2017). These cells have shown promise as a result of the gene set they possess which are involved in numerous mechanisms of carcinogenesis (Ellinger-Ziegelbauer *et al*., 2009). The multiple endpoint approach in the TK6/MCL5 cell lines allow for a holistic response to the different NGCs tested which agrees with the data produced in Wilde *et al*., (2017).

6.5 Strengths and Weaknesses of this work

A strength of this work was the integration of multiple cancer-specific endpoints to study wider cancer-related MoAs. It is accepted that by integrating a series of endpoints in conjunction with traditional genotoxicity testing it will provide additional mechanistic understanding (Wilde *et al*., 2017). The multi-endpoint approach is beneficial particularly in the case of NGCs, as NGCs are complex and capable of utilising diverse and multiple mechanisms in parallel (Guyton *et al*., 2009).

Ellinger-Ziegelbauer *et al*., (2009) reported similar endpoints included in the NGC *in vitro* testing battery used here. Using gene expression profiles, numerous mechanism(s) of action were investigated, such as regulation of the cell cycle, apoptosis, oxidative DNA damage and a mitochondrial function and stress response. All of these mechanisms were also focused on within the *in vitro* testing battery carried out in this work. This is promising as it suggests that the endpoints picked in this battery are also being considered in terms of NGC detection throughout the literature.

Only 6 chemicals were assessed fully with the 8 endpoints, if time permitted more chemicals would have been assessed with the full testing battery and the battery itself would have been extended further. For example, follow-up PCR on a few selected interesting genes could have been carried out. Further time point analyses could also have been investigated, both cell cycle and apoptosis could have benefitted from this. There were 2 more NGCs assessed at early stages but not taken forward due to dissolution and dosage problems. If more NGCs with varying MoAs were assessed, it could provide a more complete understanding of the success of this multi endpoint *in vitro* test battery for NGCs.

Another main limitation of this work was the time taken to conduct the battery of tests for each chemical. This screening battery is not a high-throughput approach, so in order to implement an effective *in vitro* testing system, it should be a faster approach. For example, the data is always conducted as n=3 and takes 4 days to complete 1 replicate. In order to have true biological replicates the acute Mn data is conducted over 3 weeks and can take a further 2 weeks to complete the scoring. Likewise, the chronic data takes 8 days to complete one replicate alone, so can take over a month to complete this work and again a further 2 weeks to score. Each of the other endpoints are slightly faster to complete but still taking roughly 1 week per replicate. However, taking into account the analysis times. For example, with the flow cytometry, ROS, Seahorse and PCR endpoints there is additional data analysis required which is time consuming.

If the toxicogenomics systems could use comparable mechanistic focuses to give a similar set of results, this may improve the output. There are other systems that are comprised of a multiple endpoint approach such as AstraZeneca's multi-end point genotoxicity assessment (MEGA) screen (Elloway *et al*., 2016). This work could benefit from analytical techniques such as gas chromatography mass spectroscopy (GC-MS) and inductively coupled plasma mass spectroscopy (ICP-MS) in order to investigate the metabolites of the carcinogens (Baron *et al*., 2017).

In line with Rosefort *et al.,* (2004), perhaps using the mononucleate version of the Mn assay to assess potential genotoxicity in a chronic setting is not the best approach. Rosefort suggests that clastogenic MoAs would be missed with this methodology, which may explain an underestimation of 'genotoxicity' detected in a chronic setting. Although it is thought that NGCs are not detected with *in vitro* genotoxicity approaches, a main hypothesis of this work was that chronic dosing could facilitate their identification.

6.6 Acute and Chronic dosing

Both acute and chronic dosing were utilized in this work to form a direct comparison between the two dosing types. The acute dosing employed a traditional one-off spiked dose with 24-hour exposure as used in regulatory toxicity testing (Kopp-Schneider *et al*., 2013). The chronic dosing used in this work was a 5-day fractionated treatment previously carried out in this laboratory (Chapman *et al*., 2015) whereby each acute dose was fractionated and delivered over 5 days. In order to compare directly between the acute and chronic exposures, the same total doses were matched. For example, with $NiCl_2$, where an acute total dose of 150 µM was used. The fractionated chronic dose was 30 µM per day for 5 days giving a total of 150 µM delivered to the system. Acute toxicity remains an important primary aspect of regulatory toxicology. Nevertheless, chronic dosing is useful to understand the longer-term implications of the chemicals (Macko *et al*., 2021).

Most human exposures such as occupational and environmental are due to long term low dose exposures. Alternatively, acute higher dose exposures dominate regulatory *in vitro* testing (Blakey *et al*., 2008). A publication from our laboratory in Swansea university indicated that chronic dosing could lead to a reduced genotoxic response when compared with acute dosing of MMS and N-methyl-N-nitrosourea (MNU) on TK6 cells. It is thought that acute dosing can overwhelm the cellular systems whereas chronic dosing allows the cellular system to tolerate the

exposure better which is more in line with real-life exposures (Chapman *et al*., 2015). This may be true for DNA reactive genotoxic agents which are subject to DNA repair, the case for NGCs may prove to be more complicated.

This means that it is plausible that much of the published acute genotoxicity data is an over-estimate of the genotoxic potential of the chemical (Dural *et al*., 2020). This work demonstrates that $NiCl_2$ agrees with this statement as chronic treatment has less of a genotoxic response than the acute treatment of. On the other hand, the As work disagrees with this statement because the chronic treatments of NaMAr and Caco show more genotoxicity than the acute treatments. TCDD is a complex chemical and is negative for genotoxicity both acute and chronic. Therefore, it neither agrees nor disagrees with the statement that acute dosing over-estimates genotoxicity. Likewise, chloroprene is also negative for genotoxicity in both an acute and chronic setting. Finally, like As, rosuvastatin disagrees with the statement because the chronic treatment shows more genotoxicity than the acutetreatment. The variety of responses to the acute and chronic dose regimens could be explained by the complexity of mechanisms utilized by NGCs.

When focussing on cytotoxicity effects, it is a general statement that toxicity is better tolerated in a chronic setting as there has been time for DNA repair machinery to elicit a response. This can first be seen with $NiCl_2$ where there is greater cytotoxicity than with the chronic treatment. With the As compounds this is not true as the cytotoxic effect seen in the acute data for NaMAr and Caco mirrors that of the chronic data for NaMAr and Caco. There is a strong cytotoxic response with both acute and chronic treatments. TCDD seems fairly unaffected by cytotoxicity both in an acute and chronic setting, both tolerating toxicity in a similar manor. It seems as if chloroprene can be equally tolerated by both acute dosing with chloroprene and chronic treatment. Lastly, rosuvastatin showed that it agreed with the statement ‘cytotoxicity is better tolerated in a chronic system’. There is a drastic difference in the levels of cytotoxicity as a result of rosuvastatin treatment as the acute dosing had a low of 41% RPD which is lower than the recommended OECD guideline but is included to form a comparison with the chronic work. Whereas with the chronic treatment of rosuvastatin, the RPD has actually reached levels above 100% suggesting chronic rosuvastatin is encouraging cellular proliferation.

Dural *et al*., (2020) also showed that by employing chronic dosing with pro-oxidants, it can highlight different results to the standard acute treatments. Chronic dosing can also flag possible mechanistic differences, which may not be apparent with acute dosing alone. This was seen with

both As treatments, where chronic dosing revealed genotoxicity that was not seen with acute dosing.

6.7 Doses and time points

The doses for each chemical were determined using a combination of previously published data in the literature and acute cytotoxicity dose finding studies (OECD, 2010a). The dose finding studies are based on the OECD guidelines for the testing of chemicals, highlighting that the top dose should produce 55±5% cytotoxicity (OECD, 2010b).

The time points utilized in this work were mostly 24-hours treatment with 24-hours recovery for acute dosing. The chronic dosing was 5-day fractionated treatment with 24-hours recovery and reaching the same total doses as acute dosing. Recovery was utilised with the Mn assays only as per Doherty *et al*., 2014. It has been shown that chronic, low dose exposures can reduce the level of damage induced. This could be a result of the low doses allowing time for DNA repair mechanisms to take place (Chapman *et al*., 2015). Low-dose tolerance is in agreement with certain chemicals such as $NiCl_2$, TCDD and rosuvastatin. In Chapman *et al.*, (2015) both 5-day and 10-day low dose chronic treatment studies were tested and compared. It showed that there was not a significant difference between 5- and 10-day treatments, so 5 day chronic treatments were taken forward in this work.

For the examination of other cancer-relevant endpoints, an acute dosing approach was used to capture the impact on these endpoints more easily. This work however may have benefitted from a range of different acute and chronic time points. As an example, the cell cycle endpoint was carried out at 24-hours however, certain NGCs may have an earlier affect so could show cell cycle perturbations at 6 or 12 hours. For instance, the 5- and 10-day treatment comparison carried out in (Chapman *et al*., 2015) was carried out using genotoxic test chemicals. Perhaps NGCs would show a difference in their tolerance of longer chronic studies.

6.8 Cell cycle

Cell cycle dysfunction is of increasing importance when considering the contributors of tumourigenesis. Many cancer detection batteries will include cell cycle as a target and for therapies to include regulating cell cycle progression (Stewart *et al*., 2003). **Figure 6.1** Shows stages of progression of a healthy cell within the cell cycle. A statement from a biology textbook

(Curtis, 1983) states that ‘dividing cells pass through a regular sequence of cell growth and division.’

In a normal cell cycle, there is a gap phase at the end of mitosis and before the start of a new DNA replication. A neuron is an example of a cell type that does not undergo cell division and are in a quiescent state within the nervous systems of adults (Frade and Ovejero-Benito, 2015). There is an important transition between G1 and S phase as this is considered a ‘point of no return’ checkpoint in the cell cycle (Hunt *et al.*, 2011). Checkpoints are in place as they have the ability to prevent progression through the cell cycle if DNA damage is not repaired (Hunt *et al.*, 2011). Cyclin-dependent kinases (CDKs) are responsible for driving the progression through the cell cycle (Hunt *et al.*, 2011).

It has been shown that for human somatic cells such as epithelial cells, the cell cycle process can take between 16 and 24h. G1 phase is thought to take between 6-12h, S phase takes approximately 6-8h and G2/M takes around 3-4h. However, each cell type can take different timeframes to complete these stages for example, pluripotent stem cells take around 32-38h to complete a full cell cycle (Dalton, 2009). There are 3 main checkpoints in the cell cycle which are G1/S, G2/M and the spindle checkpoint (Molinari, 2000). These checkpoints are important in this work as cells can be arrested in different stages of the cell cycle so therefore affecting the distribution of cells at different doses of the studied carcinogens.

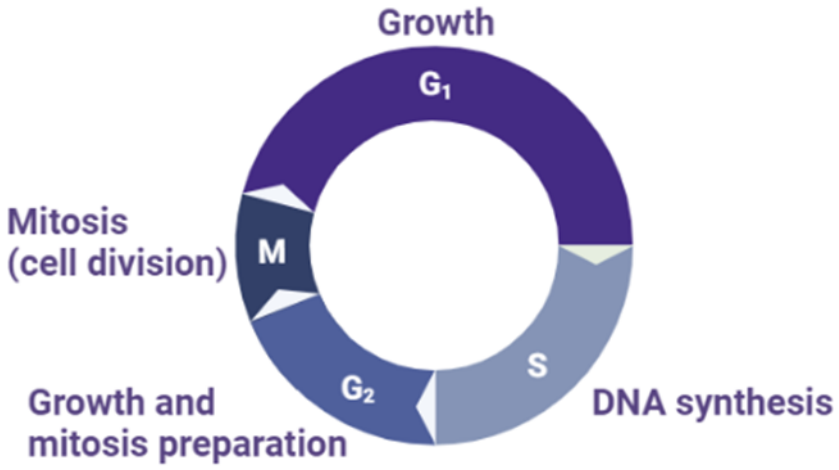

Figure 6.1: Represents the stages of cell cycle (G1, S, G2 and M) with a simplified description of what happens in each period. Made on biorender.com.

The stimulation of cell cycle progression when there is an error in the cell means it is likely for DNA damage to be passed on to the daughter cells, such as with As. Therefore, cell cycle perturbations can be affected by both genotoxic and NGCs (Salnikow and Zhitkovich, 2008). It has been shown that As compounds in particular are successful tumour promotors and that the different forms of As are capable of acting in a genotoxic and non-genotoxic manner. This also means that As could be capable of acting via a dual mechanism of tumour promotion and cytotoxicity (Kenyon and Hughes, 2001).

Both **Figure 5.10** and **Figure 5.11** agree with the fact that As can allow progression through the cell cycle and could be using this mechanism as part of their tumour promotion ability. $NiCl_2$ (**Figure 4.6**), TCDD (**Figure 3.10**) and chloroprene (**Figure 3.18, 3.16, 3.17**) all have no effect on cell cycle changes. Rosuvastatin (**Figure 3.28**) has a slight change in the S phase of cell cycle but otherwise it remains relatively stable throughout. This highlights the fact that each NGC has a different MoA with only As here altering the cell cycle.

Gene expression changes in the cancer panel PCR array represent numerous cell cycle perturbations which can be responsible for cancer initiation. It has been shown that cell cycle progression and DNA replication are forms of cancer promotion that NGCs can be responsible for (Hernández *et al*., 2009).

6.9 Misclassification/mislabelling of NGC

There may be a problem with the classification of carcinogens as there is often conflicting literature around where certain chemicals belong. NGCs are more difficult to test for than GCs as they do not have a singular defining feature that can be tested for using a single test (Hernández *et al*., 2009). It is understood that NGCs require a battery of tests in order to detect them *in vitro* (Hwang *et al*., 2020).

There is an increasing drive to move away from methods such as the 2-year rodent bioassay and make use of both *in vitro* and *in vivo* NAMs (Cohen *et al*., 2019). It has been suggested that dose, exposure duration and exposure route should all be considered when categorizing carcinogens. Chemical carcinogenesis is not just a property possessed by the molecule but is a result of the species exposed, the exposure scenario and the chemical function (Doe *et al*., 2022). It is thought that the question of carcinogenesis categorization has been over simplified, leading to often incorrect classifications, especially when considering the complexity of NGCs (Doe *et al*., 2022). The determination of carcinogen classification should encompass MoAs at least, in

order to form a complete picture of the NGC (Doe *et al*., 2022). Certainly, it has been shown that several NGCs ($NiCl_2$, As) can induce genotoxicity and so therefore the label "NGC" may not be appropriate.

6.10 Future work

The investigation into more physiologically relevant microenvironments such as a 3D spheroid model as a component of the *in vitro* test battery could prove to be beneficial (Astashkina and Grainger, 2014). A multiple cell line co-culture or a primary cell model may also provide more human relevant answers to standard dose response studies for NGCs (Astashkina and Grainger, 2014). A deeper understanding of the gene expression changes because of NGC treatment would be beneficial in trying to unpick the MoA utilized by different chemicals. Perhaps using an approach such as RNA sequencing would be useful to incorporate into the battery, however there are cost restrictions with this approach. If time permitted, follow up qPCR for some of the highly upregulated genes (such as *CCND1*, *TF* and *CD44*) would improve understanding. Exploration of multiple time points and recovery times would provide further insight for some chemicals as each chemical can act at different times (Mathijs *et al*., 2009), some being very instant and some having a greater effect over a prolonged period of time. If time course studies were implemented for each NGC with certain endpoints such as genotoxicity, cytotoxicity, gene expression and cell cycle for instance.

Some NGCs could benefit from further chronic Mn studies. Both As compounds, NaMAr and Caco and rosuvastatin show interesting chronic dosing results. Perhaps different length chronic dosing regimens could be tested, and different dose combinations delivered in order to further understand the MoAs of these chemicals. Dose selection has been based on previous data from the Swansea laboratory, data published in the literature and acute toxicity studies such as RPD. It is possible to calculate *in vitro* doses by using *in vivo* study data, which although it is performed in rodents, it may be possible to extrapolate to understand the human equivalent doses (Bouhaddou *et al*., 2020). *In vitro* findings are often extrapolated in order to translate the cell data to humans (Mattes, 2020).

The importance of a multi-endpoint approach has been highlighted, especially when investigating NGCs (Chapman *et al*., 2021). Although, there is a question of which endpoints are most important to assess. A relative ranking of the endpoints could begin with assessment of Mn after chronic treatment as this closely mimics the real-life exposure. This would be followed

by the gene expression understanding, then cell cycle changes and finally mitochondrial health evaluation. Other endpoints could be included and/or different approaches could be taken to unpick the MoAs used by these complex carcinogens. After a thorough literature search, multiple endpoints most commonly mentioned as possible NGC MoAs were selected in this study. More of a focus on epigenetic effects such as histone modifications could also be incorporated into the testing battery (Hernández *et al*., 2009).

The results of the mitochondrial stress tests look promising across multiple NGCs. Further investigation of the mitochondrial health could provide an additional mechanistic understanding. $NiCl_2$ (**Figure 4.9**), NaMAr (**Figure 5.16**), Caco (**Figure 5.17**) and rosuvastatin (**Figure 3.33**) all show a large drop in the OCR after treatment.

6.11 Reactive oxygen species detection

ROS is an important endpoint as it is thought to be utilized by numerous NGCs (Fukushima *et al*., 2005). For instance, both NaMAr and Caco were believed to operate via a ROS MoA (Nesnow *et al*., 2002), however neither chemical showed significant ROS induction. This could be due to the DCFDA assay used, which has been highly criticized (Royall and Ischiropoulos, 1993). It is possible that the DCFDA assay is not a very sensitive assay which means it might only detect ROS when a certain threshold is passed. This could mean that perhaps the As compounds are ROS producing, but below the threshold of detection with DCFDA. The assay showed ROS production for $NiCl_2$ (**Figure 4.5a**) and consistently shows ROS production as a result of the positive control treatment of 100 µM H_2O_2. This proves that the assay does work however it does not answer a question about the threshold that is required to display a positive response. There was validation work carried out within the laboratory with this assay and the detection of H_2O_2 as a positive control, as there was a significant induction of ROS detected using just 10 µM H_2O_2 (Dural *et al.*, 2020). There could have been further assay validation carried out, such as conducting western blot analysis using antibodies against the anti-oxidant transcription factor, nuclear factor erythroid- related factor (Nrf2) (Oommen *et al.*, 2016 (a); Oommen *et al.*, 2016 (b)). There are numerous other ROS detection assays commercially available so future work could test other kits to see whether they have a lower detection threshold.

The DCFDA assay is a commonly used method and readily available product (Roesslein *et al*., 2013). Other commercial ROS detection kits include the $NO^{\bullet}$ assay, electron spin resonance (ESR), GSH peroxidase and lipid peroxidation (Roesslein *et al*., 2013). A problem with the

chemiluminogenic/fluorogenic assays such as DCFDA, is that they can only detect the peroxides in the presence of a peroxidase such as horseradish peroxidase (HRP) or a transition metal (Gasser *et al*., 2012). HRP/transition metals are capable of decomposing the peroxides to give radicals which can react with the dye in the assay. Although, HRP can affect the results as it is capable of quenching the signal (Ruch *et al*., 1983). This could explain why there was a positive ROS result in **Figure 4.5a** with $NiCl_2$ as it is a transition metal. However there was a negative result with NaMAr (**Figure 5.8**) and Caco (**Figure 5.9**) which has been documented as strong ROS producers in the literature. A further limitation of the ROS detection assays such as DCFDA is that they utilize organic solvents such as DMSO or ethanol which are powerful hydroxyl scavengers leading to an underestimation of ROS produced (van Acker *et al*., 1996).

Unfortunately, all of the ROS assays have some limitations. For example, dihydrorhodamine (DHR) or otherwise known as the $NO^{\bullet}$ assay, converts DHR to rhodamine mediated by a DHR radical. This intermediate is often oxidised further producing a fluorescent product which can induce an additional signal giving an enhanced result (Rothe and Valet, 1990). The ESR technique only allows the measurement of unreactive radicals as the highly reactive radicals do not accumulate to detectable levels (Tarpey *et al*., 2004). The GSH peroxidase assay relies on the levels of GSH or the oxidised form glutathione disulphide (GSSG). Though, GSH can be regenerated from the oxidised form meaning the GSSG concentration could be underestimated (Roesslein *et al*., 2013). The lipid peroxidation assay works slightly differently, it measures the quantity of oxidised fatty acids such as malondialdehyde (MDA) which correlates to the level of radicals released. While it is a different approach, this method is not MDA specific (Byrdwell *et al*., 2002) and compounds with a similar absorption are taken into account meaning there is likely an overestimation with this method (Buerki-Thurnherr *et al*., 2013).

6.12 Solvents

It is important to consider the solvents used to dissolve each NGC as in some cases the solvent itself could have an effect on the cells. There were three solvents used throughout this PhD; double distilled water (d_2H_2O); DMSO and methanol. Firstly, wherever possible d_2H_2O was used as it would have the least additional effect on the cells. Secondly, DMSO is known as the universal solvent and is suggested as a solvent for numerous chemicals (Galvao *et al*., 2013). DMSO has an amphipathic nature so is often used as a solvent for hydrophobic molecules despite the toxicity (Szmant, 1975). It is also often used for cryopreservation, due to the water displacing property (Julien *et al*., 2012). Throughout this work, the concentration of DMSO was kept at a constant per experiment. In most cases the recommended 1% DMSO was used, the

only exception was with TCDD, where a 2% DMSO concentration was used in order to reach the highest dose.

Finally, methanol is only used where necessary, as it is thought to be the most toxic to the cells. $NiCl_2$, NaMAr and Caco all use d_2H_2O as the solvent. TCDD and rosuvastatin require DMSO as the solvent, as they are insoluble in water and both NGCs were purchased already dissolved in DMSO. Chloroprene proved difficult to dissolve, it was insoluble in both water and DMSO so had to be dissolved in methanol, after testing and also searching the literature for suggestions.

Solvents are essential for dissolving chemicals and agents that are not water soluble. It is important to understand the effects of the solvents, especially in cancer research, as the added toxicity from the solvents is problematic. It is necessary to understand the effect of the solvents alone, so the combined effect with the chemical can be understood (Nguyen *et al*., 2020). Methanol has also proven to be a good solvent and have a minimal toxic effect on cell lines such as MCF-7, HepG2 and VNBCRA1. It has been found in the literature that as long as both DMSO and methanol are kept 1% or below then the toxic effect seen is minimal (Nguyen *et al*., 2020). The solvents were always kept at 1% throughout this PhD, so complied with the literature to minimise unwanted side-effects.

6.13 Apoptosis

The apoptosis results have been largely negative throughout, this could be as a result of cell lines having cancer cell properties and therefore have the ability to evade apoptosis. Although TK6 and MCL5 cells are not derived from cancer cells, they have been Epstein-Barr virus (EBV)-immortalised (Robles *et al*., 2001) and perhaps this could have an effect on the apoptotic results. Apoptosis is a debated MoA, as it can be utilized by both genotoxic and NGCs (van Delft *et al*., 2004). However, the fact that the apoptosis mechanism is widely used could prove to be helpful as some chemicals can act via multiple mechanisms, so apoptosis could be a first step in the battery.

It is interesting to note that $NiCl_2$ (**Figure 4.7**), TCDD (**Figure 3.11**) and chloroprene (**Figure 3.21**) all show very little apoptotic induction. However, both As compounds; NaMAr (**Figure 5.12**) and Caco (**Figure 5.13**) show a significant increase of apoptosis. Also, rosuvastatin (**Figure 3.29**) demonstrates a slight significant increase in apoptotic induction.

As has been used in the treatment of several different conditions such as leukaemia for instance as it was capable of inducing apoptosis (Hughes *et al*., 2011). This As -induced apoptosis has been mirrored in the data produced here in **Figure 5.12** and **Figure 5.13**. Numerous genes

assessed in the cancer panel PCR array, were also linked to apoptosis and evading apoptosis is a feature of cancers in general making it an important endpoint to consider in an *in vitro* testing battery (Santibáñez-Andrade *et al*., 2023). Apoptosis is often linked to elevated ROS levels and this is turn can modulate numerous pathways such as inhibiting apoptosis and increased cellular proliferation etc. (Santibáñez-Andrade *et al*., 2023). Yet, within this work ROS and apoptosis do not seem to be linked with any of the NGCs tested.

6.14 Seahorse

It has been shown that mitochondrial stress is linked to a number of other mechanistic pathways. The mitochondrial dysfunction can be mediated by cytotoxicity, linked to ROS, apoptosis and lipid peroxidation (Chen *et al*., 1990). This is encouraging in terms of the endpoints chosen for the test battery. One negative with the data produced in this work is the disparity between ROS and mitochondrial function as they are heavily linked processes (Wadgaonkar and Chen, 2021).

There was a decreased OCR with most of the chemicals assessed including $NiCl_2$ (**Figure 4.9**), NaMAr (**Figure 5.16**), Caco (**Figure 5.17**), rosuvastatin (**Figure 3.33**). It has been documented that As is capable of disturbing the integrity of the mitochondrial membrane, which explains the response in **Figure 5.17**. Although, these chemicals all produced a mitochondrial stress related response, Caco seemed to completely diminish the OCR and the others only reduced it. These chemicals likely utilize mitochondrial stress as part of the MoA in order to initiate oncogenesis. Both TCDD (**Figure 3.13**) and chloroprene (**Figure 3.23**) had minimal changes to its OCR when compared to the solvent control.

The positive controls, MMS (a historical positive control) and EthBr (a mitochondrial positive control) have also undergone Seahorse analysis as seen in the **Appendices Figures A10, A11, A12 and A13** for completeness.

6.15 Gene expression changes

The general cancer panel PCR array has proven to be one of the most positive endpoints assessed and works nicely with some of the other endpoints assessed within the test battery. There is a lot of interest and promise in toxicogenomics in relation to NGCs (Hernández *et al*., 2009). All chemicals investigated showed an interesting gene expression profile which compliments the other endpoints assessed. Future work could include follow-up PCR to further assess the different time points and doses against different genes. A gene that was upregulated as a result of all except one PCR arrays was *FAS*, which is a member of the tumour necrosis factor (*TNF*) superfamily (**Figure 6.2**). This gene has a regulatory role in programmed cellular death

(Genecards (FAS), 2023), which is interesting as only both As (**Figures 5.12 and 5.13**) compounds and rosuvastatin (**Figure 3.29**) showed a significant increase in apoptosis. Another gene upregulated in most of the PCR arrays carried out was *KRAS*, which is an oncogene and is upregulated in many cancers and responsible for regulating cell proliferation (Genecards (KRAS), 2023). Both *FAS* and *KRAS* work together by evading apoptosis and increasing proliferation to cause cancer. It seems as if these mechanisms are working in the background of all the chemicals assessed even if it is not seen in the main endpoints assessed. More of the common gene occurrences can be seen in **Figure 6.2** below.

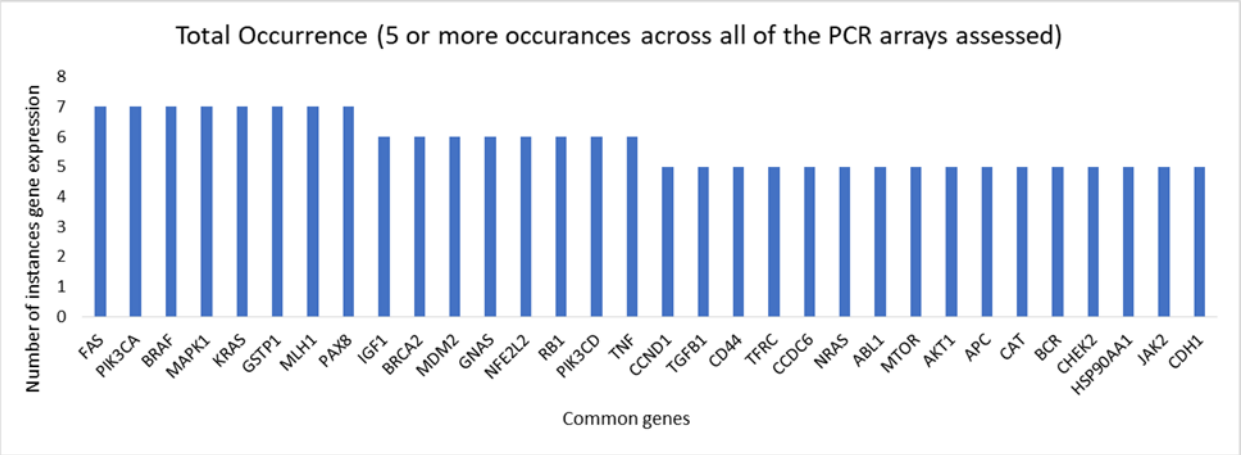

Figure 6.2: The most commonly upregulated genes across all of the PCR arrays carried out. These genes have all had changed expression in 5 or more instances. All gene names including housekeeping genes and the controls are as found in the general cancer panel, also seen in **Figure 2.5**.

Toxicogenomics is an approach that can use expression patterns of NGCs and take a MoA-based method to detect these complex chemicals in an *in vitro*, high throughput manner (Schaap *et al*., 2015). Toxicogenomics can be used to predict the genotoxicity of chemicals including NGCs, there has been a study conducted in rat livers which identified 6 genes expressed in 24 NGCs (Nie *et al*., 2006). There were a selection of NGCs chosen (including phenobarbital, rotenone and WY-14643) to evaluate and this highlighted the 6 selected NGC gene signatures (Nie *et al*., 2006).

6.16 New techniques

Techniques such as toxicogenomics are proving to be a positive candidate to detect NGCs using clustering methods flagging structural alerts. It can, not only detect NGCs but also distinguish between direct genotoxins, aneugens and clastogens (Hernández *et al*., 2009). Classifier genes were able to identify some main mechanisms of action such as cell cycle control, nucleic acid binding, apoptosis and transcription regulation activity to name a few (Hernández *et al*., 2009).

The AstraZeneca MEGA) is a high content high throughput system which has many benefits such as permitting the identification of numerous genotoxicity phenotypes and simultaneously allows for limited mechanistic understanding (Elloway *et al*., 2016). This modern technology could be a beneficial way of testing NGCs as a first step, it would still be part of a battery of tests if the mechanistic route is not determined. If these high throughput approaches were used as well as *in silico* models, this could provide a holistic approach to understanding NGCs.

6.17 Conclusion

As mentioned, NGCs are very complex chemicals and can act via numerous different mechanism(s) of action. The main aim of this work was to develop an *in vitro* testing system to detect NGCs, primarily utilising a chronic dosing approach. This was due to previous promising chronic data from our laboratory (Chapman *et al*., 2015; Stannard *et al*., 2016). While numerous nickel compounds are GCs, $NiCl_2$ is classified as a NGC (IARC, 1990). $NiCl_2$ showed genotoxicity in an acute setting however tolerated it better with a chronic exposure. The second aim of this PhD was to understand the MoAs utilized by the NGCs. It primarily utilized a ROS MoA and had little effect on cell cycle and apoptosis. There was a widespread downregulation of genes in the PCR array and the mitochondrial stress test represented a drop in OCR as a result of $NiCl_2$ treatment.

There is some promise in the hypothesis that chronic dosing may reveal NGCs, when NaMAr is considered, it is true that genotoxicity is observed with a chronic exposure but not with an acute exposure. However, the same pattern is seen with the genotoxic form of As, Caco. This could mean that either one of the As compounds could have potentially been mislabelled or just that they are behaving in a similar way despite their genotoxicity differences. As is thought to be a ROS producer (Nesnow *et al*., 2002), however the results of this work disagree with the literature as neither form of As produces ROS. Both As compounds have a significant effect on cell cycle, meaning it is likely that this is a MoA utilized by NaMAr and Caco (Hassani *et al*., 2017). Similarly, both As compounds had a significant effect on apoptosis which is in agreement with the information in the literature (Chen *et al*., 1998). One main difference between the two As compounds is that NaMAr works in an interesting biphasic manner, whereas Caco does not. The two forms of As both induce a similar gene expression response with some overlaps but also many differences. The bioenergetic flux of Caco is more dramatic than in NaMAr however they both cause a drop in the OCR as a result of chemical exposure.

NGCs also come in the form of drugs such as rosuvastatin, which is contradictory as statins are used as cholesterol lowering drugs and have also been shown to have anti-cancer properties (Wang *et al*., 2010). Rosuvastatin performed negatively in some of the *in vitro* test battery. Genotoxicity was not induced in an acute or chronic setting and there was no ROS produced. There was a significant reduction of cells in the S phase of the cell cycle at the top dose (400 µM) of rosuvastatin. Rosuvastatin also induced apoptosis, gene expression changes and increased mitochondrial stress after exposure. The MoA of rosuvastatin is still largely unknown but could be a combination of mechanisms taking place. Gene expression changes could further explain the mechanism(s) utilized by rosuvastatin.

TCDD is widely studied throughout the literature but the MoA is still an unknown (Van den Berg *et al*., 2006). This is further confirmed as it displayed a negative result in most of the test battery, with the only promising endpoint being the PCR array. TCDD displayed the highest number of genes upregulated out of the chemicals tested which is in agreement with the literature as it states that TCDD alters numerous cellular processes (Henkler and Luch, 2010). This suggests that TCDD is likely to act through cell signaling disruption in order to cause cancer. Unfortunately, TCDD did not benefit greatly from the *in vitro* battery of tests proposed.

Again, chloroprene is largely negative in the *in vitro* test battery endpoints and Black, *et al*., (2015) states that chloroprene can produce ROS, cytotoxicity and DNA-adducts however this data all disagrees with the literature as none of these mechanisms seem prevalent. There was no genotoxicity and only minimal cytotoxicity induced as a result of chloroprene exposure. ROS was not induced, there was a slight reduction in ROS levels suggesting a possible AOX mechanism. There were minimal changes in the cell cycle at 24-, 48- and 12-hour exposures. There were not any significant changes in the levels of apoptosis or serious changes in the OCR as a result of chloroprene exposure. There was a 120-fold increase in *CCND1*, which encouraged further investigation into the cell cycle. Which could mean that cell cycle perturbations could be the MoA utilized by chloroprene. However, after further cell cycle investigation, there was not any evident cell cycle changes. Perhaps a full time-course study would have been beneficial here. All NGCs tested behaved differently within the multi-endpoint approach, but it allowed the formation of a proposed strategy for the *in vitro* testing of NGCs which can be seen in **Figure 6.3** below. This proposed strategy is based on the COM guidelines for GCs (**Figure 1.3**).

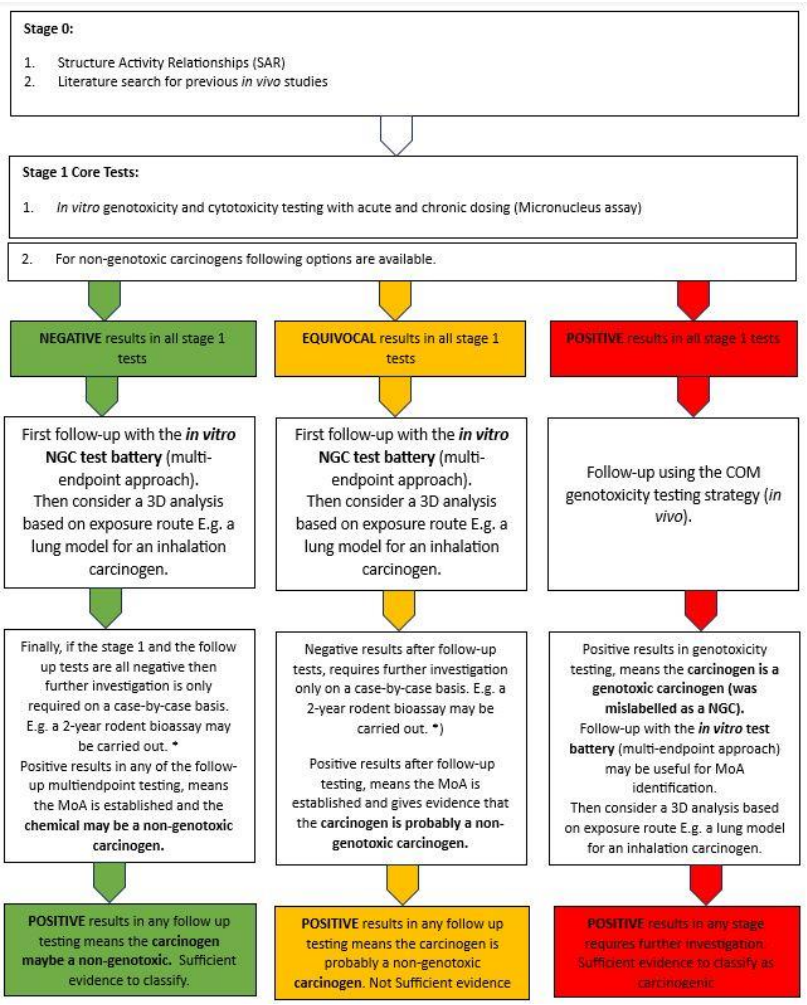

Figure 6.3: This flow chart represents a potential strategy for NGCs based on the current GC strategy from the COM guidelines (as seen in **Figure 1.3**). The *in vitro* test battery includes further investigation into cell cycle, apoptosis, ROS, mitochondrial health and a basic toxicogenomics assessment (PCR array) to determine certain up/downregulated genes, highlighting a potential MoA used. The * denotes a sector-specific regulation, where the 2-year rodent bioassay can only be performed if the carcinogen is from certain sectors such as pharmaceuticals.

Overall, the *in vitro* testing battery was promising for some NGCs although does not show an across-the-board success so may still require further investigation. Some NGCs behave in such a complex manor that they did not show a positive result for any of the tests within the battery other than some gene expression changes. NGCs are difficult chemicals because there is not a 'one test fits all' approach due to the diversity of mechanism(s) of action. It is also important to understand that these endpoints assessed are all linked so they should not be viewed as a stand-alone MoA but as part of the whole picture. Although, with most of the NGCs there was an indication of which MoA(s) were utilized as a result of the *in vitro* multi-endpoint testing battery. Future work is required to ensure the reduction in use of the 2-year rodent bioassay but

hopefully the proposed strategy in **Figure 6.3** would help reduce the numbers of rodents subject to this test. It has been shown that a combination approach which encompasses many different methodologies is the most beneficial approach.

Consequently, this work does succeed in detecting NGCs using the *in vitro* test battery and establishing the MoAs used by the carcinogens. Chronic dosing did not allow for the detection of NGCs (other than NaMAr). However, this is still an important principle that should be optimised and utilised as part of the *in vitro* test battery.

Appendices

These two chemicals, cholic acid (**Figure A1**) and DEA (**Figure A2**) were taken no further than initial studies due to problems with dissolution and precipitation out of solution. **Figure A1** and **Figure A2** show a broad range of doses tested however, there seems to be no cytotoxicity induced with either chemical. This may be due to the problems experienced when working with these NGCs.

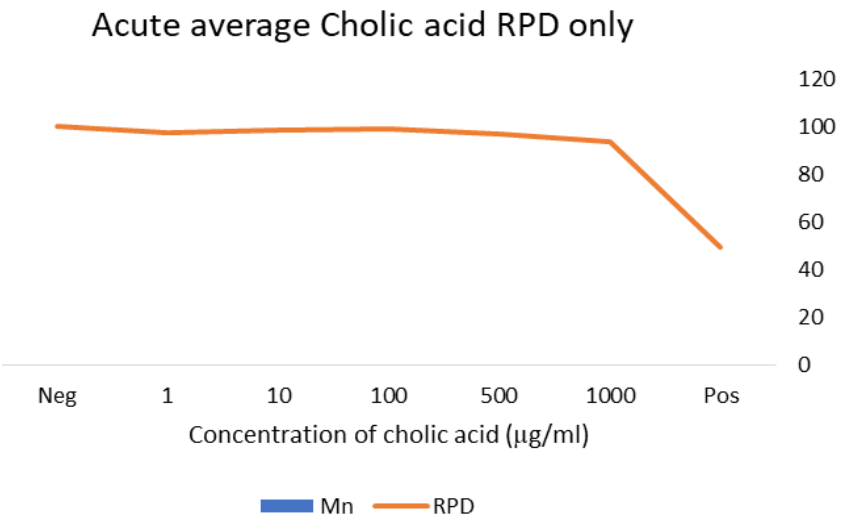

Figure A1: The RPD dose range finding study was conducted for cholic acid at n=3. Cholic acid was not taken further as it was affecting the pH and causing precipitation out of solution.

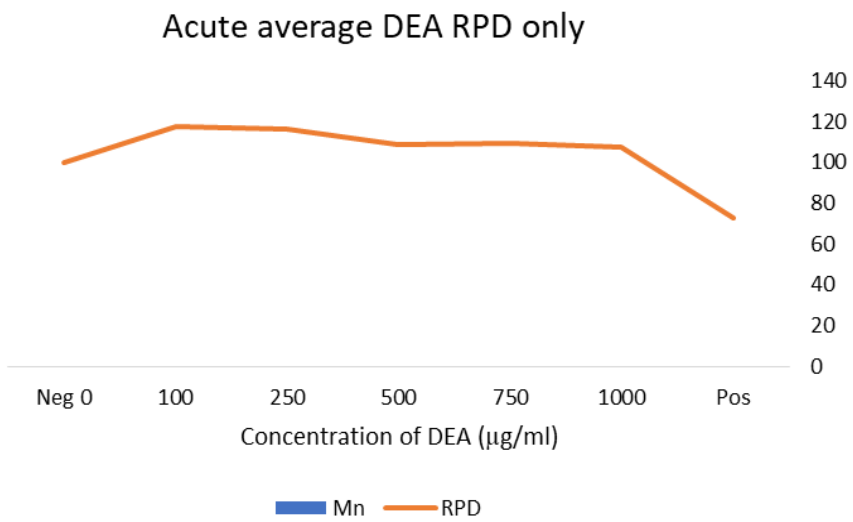

Figure A2: The RPD dose range finding study was conducted for diethanolamine (DEA) at n=3. DEA was not taken further in this work as it was not dissolving in the solute very well, maybe due to the viscosity.

A singular dose of 10,000 µM / 10 mM DEA was taken onto genotoxicity assessment as seen in **Figure A3** below. However, there is no significance increase in Mn as a result of 24-hour 10,000 µM DEA treatment.

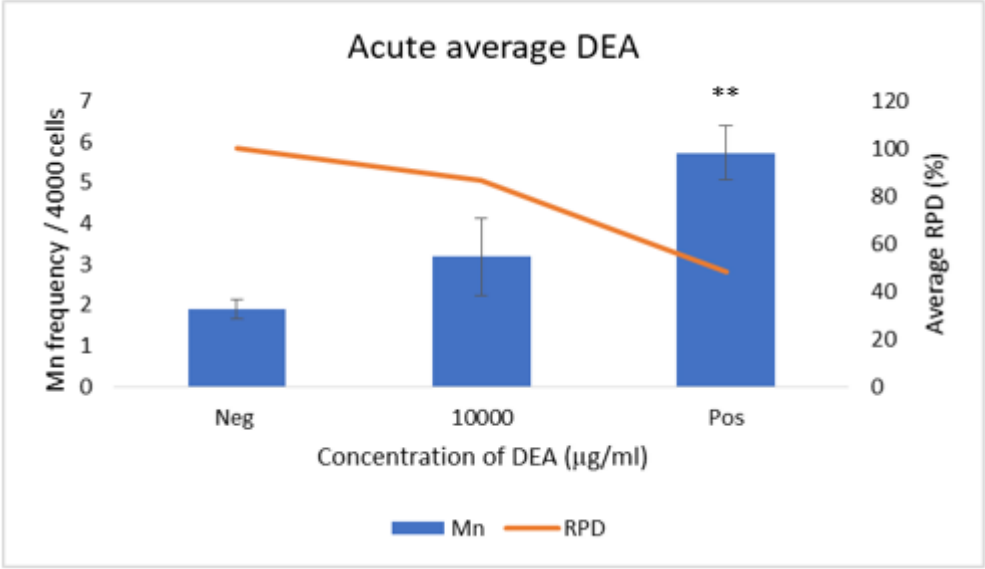

Figure A3: A limited Mn study was carried out with diethanolamine (DEA) with a dose of 10 mM (10,000 µM) which is the maximum range of *in vitro* studies. This work was conducted before the decision was made to not continue with this chemical due to dissolution problems. The positive control was MMS and showed significance with a *P* value of 0.0029.

DMSO studies were carried out both acutely and chronically in TK6 and MCL5 cell lines in order to assess cytotoxicity and genotoxicity of the universal solvent. It shows that DMSO is more cytotoxic when delivered in an acute experiment. It seems as if DMSO is better tolerated in a chronic system. There is no increase in genotoxicity induction in **Figure A4** or **Figure A5** as a result of DMSO treatment in TK6 cells. There is also no increase in genotoxicity induction in **Figure A6** or **Figure A7** as a result of DMSO treatment in MCL5 cells.

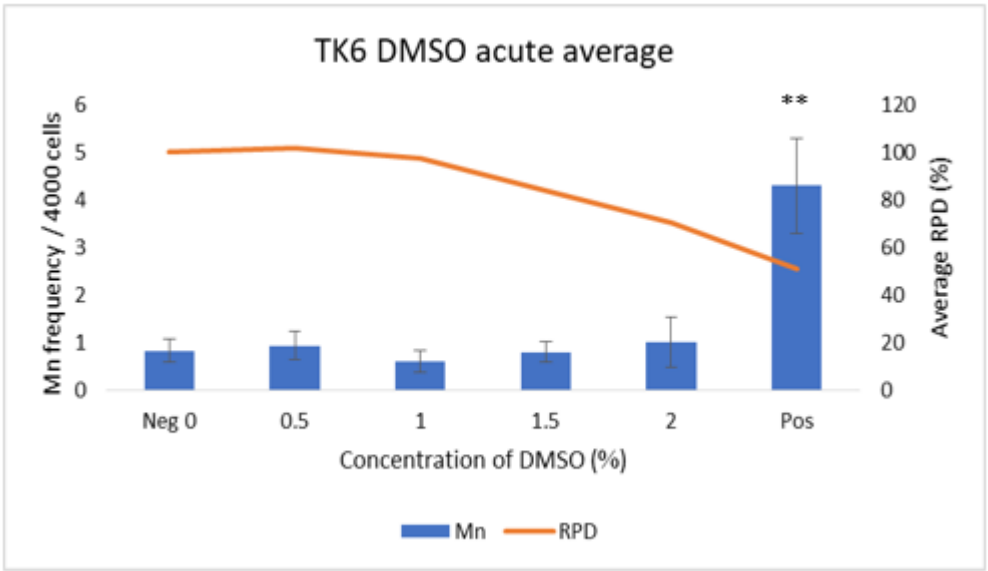

Figure A4: A test experiment of different percentages of DMSO added to TK6 cells in an acute 24-hour treatment. n=3 was carried out. There was no significance as a result of DMSO. The positive control was MMS and showed significance with a *P* value of 0.0059.

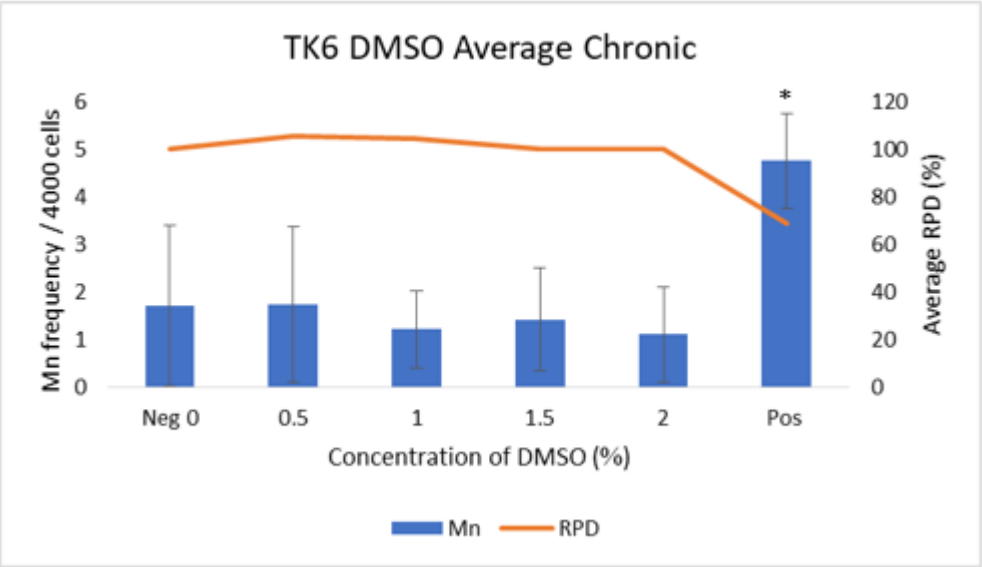

Figure A5: A test experiment of different percentages of DMSO added to TK6 cells in a 5-day fractionated treatment. n=3 was carried out. There was no significance as a result of DMSO. The positive control was MMS and showed significance with a *P* value of 0.0550.

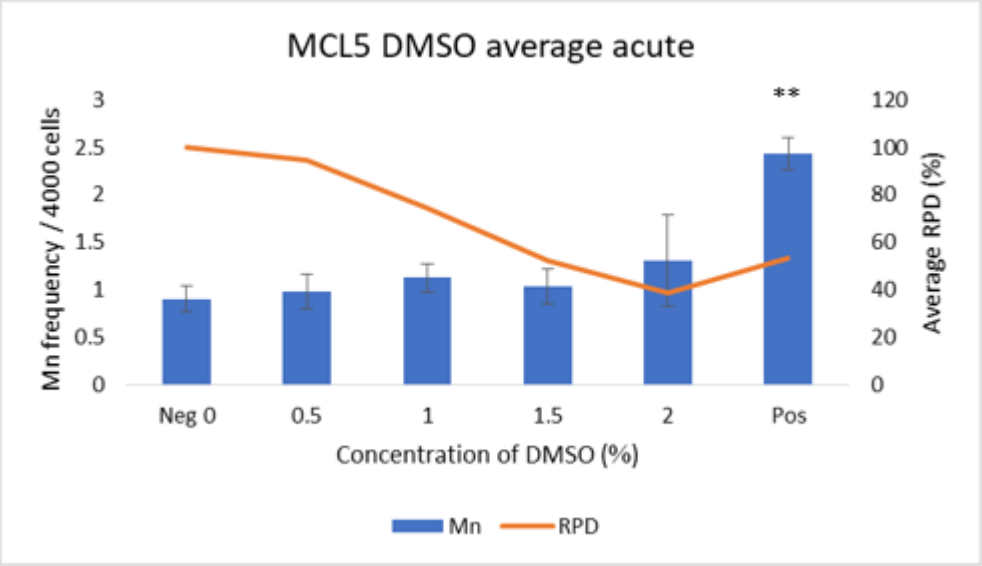

Figure A6: A test experiment of different percentages of DMSO added to MCL5 cells in an acute 24-hour treatment. n=3 was carried out. There was no significance as a result of DMSO. The positive control was MMS and showed significance with a *P* value of 0.0006.

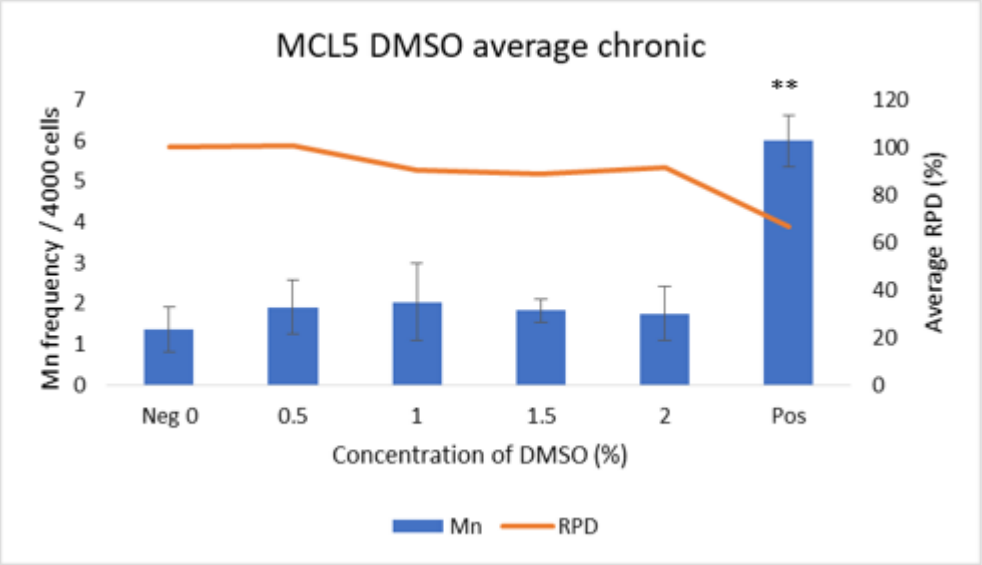

Figure A7: A test experiment of different percentages of DMSO added to MCL5 cells in a 5-day fractionated treatment. n=3 was carried out. There was no significance as a result of DMSO. The positive control was MMS and showed significance with a *P* value of 0.0011.

The use of AOXs such as NAC can reduce the cytotoxicity and genotoxicity caused by Nickel treatment (Song *et al*., 2017) which is highlighted by **Figure A8** and **Figure A9**. Both **Figure A8** and **Figure A9** seem to slightly reduce the level of genotoxicity (although not to a statistically significant level) by a comparable level, suggesting that AOX action has worked in both an acute and chronic setting.

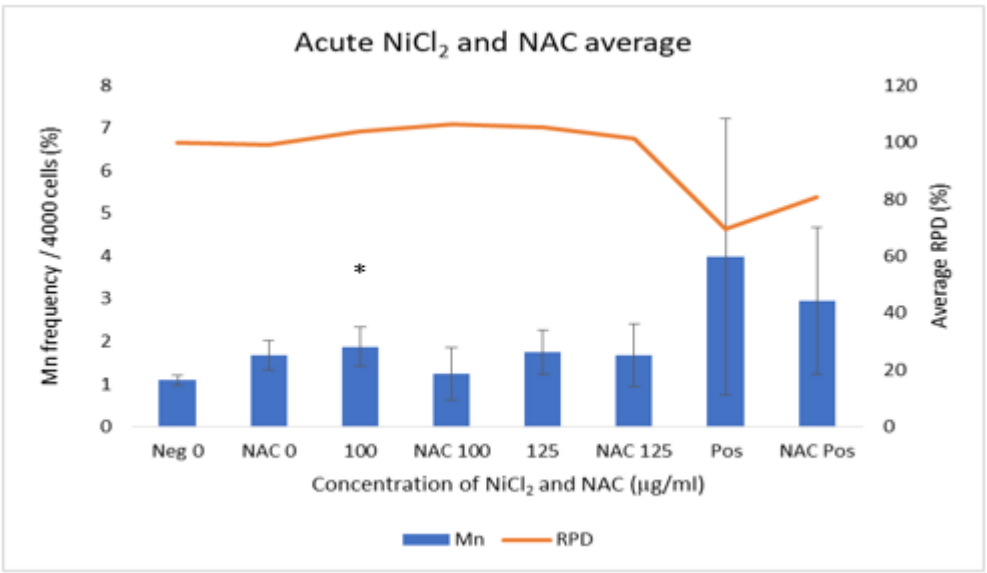

Figure A8: Mononucleate micronucleus assay and relative population doubling at 24-hours with $NiCl_2$ only and $NiCl_2$ with the addition of the AOX N-acetyl cysteine at 100 and 125 µM concentrations with 24-hours recovery in TK6 cells. n=3 was carried out. Statistical significance was seen when 100 µM was compared to the negative control with a *P* value of 0.0460.

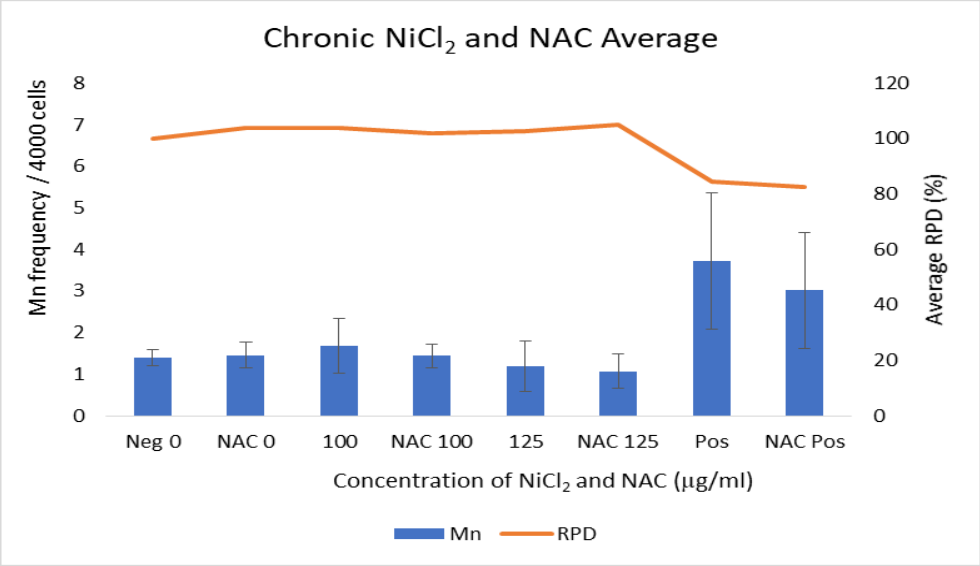

Figure A9: Mononucleate micronucleus assay and relative population doubling at 5-day chronic, fractioned treatment with $NiCl_2$ only and $NiCl_2$ with the addition of the AOX N-acetyl cysteine at 100 and 125 µM concentrations with 24-hours recovery in TK6 cells. n=3 was carried out. There was no statistical significance.

MMS as represented by **Figure A10** did not show significant changes in any of the data. EthBr is classed as Seahorse positive control so the graphs are shown in **Figure A11**. There were significant changes in the maximal respiratory capacity, ATP linked respiration, basal respiration, proton leak and the OCR/ECAR ratio.

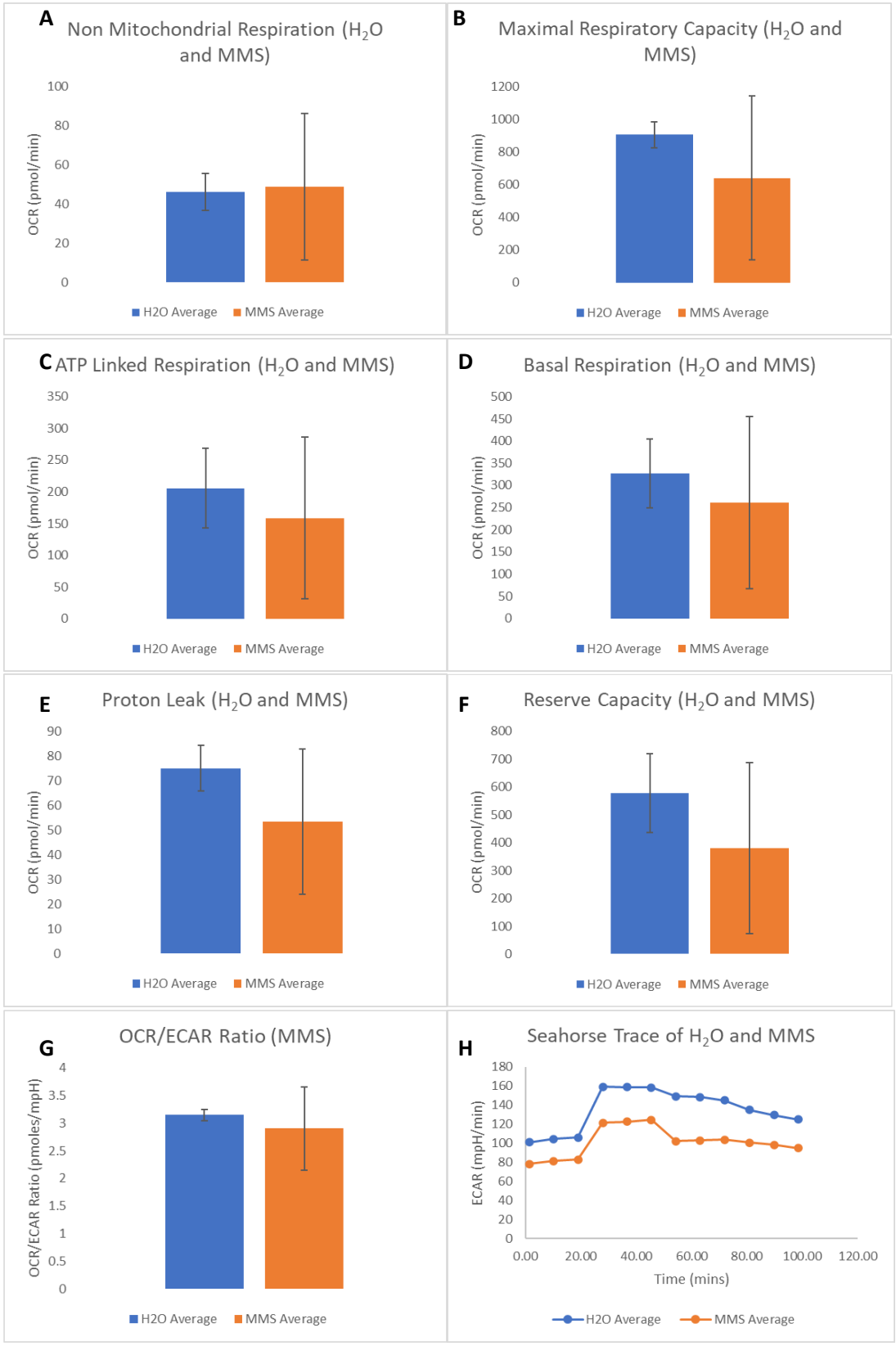

Figure A10 (A-H): Seahorse graphs for MMS indicating the different respiration parameters when compared to the H_2O solvent control. **A** represents non mitochondrial respiration, **B** is the maximal respiratory capacity, **C** is the ATP linked respiration, **D** is basal respiration, **E** is proton leak, **F** is the reserve capacity, **G** demonstrates the OCR/ECAR ratio and **H** represents the ECAR graph. There was no statistical significance.

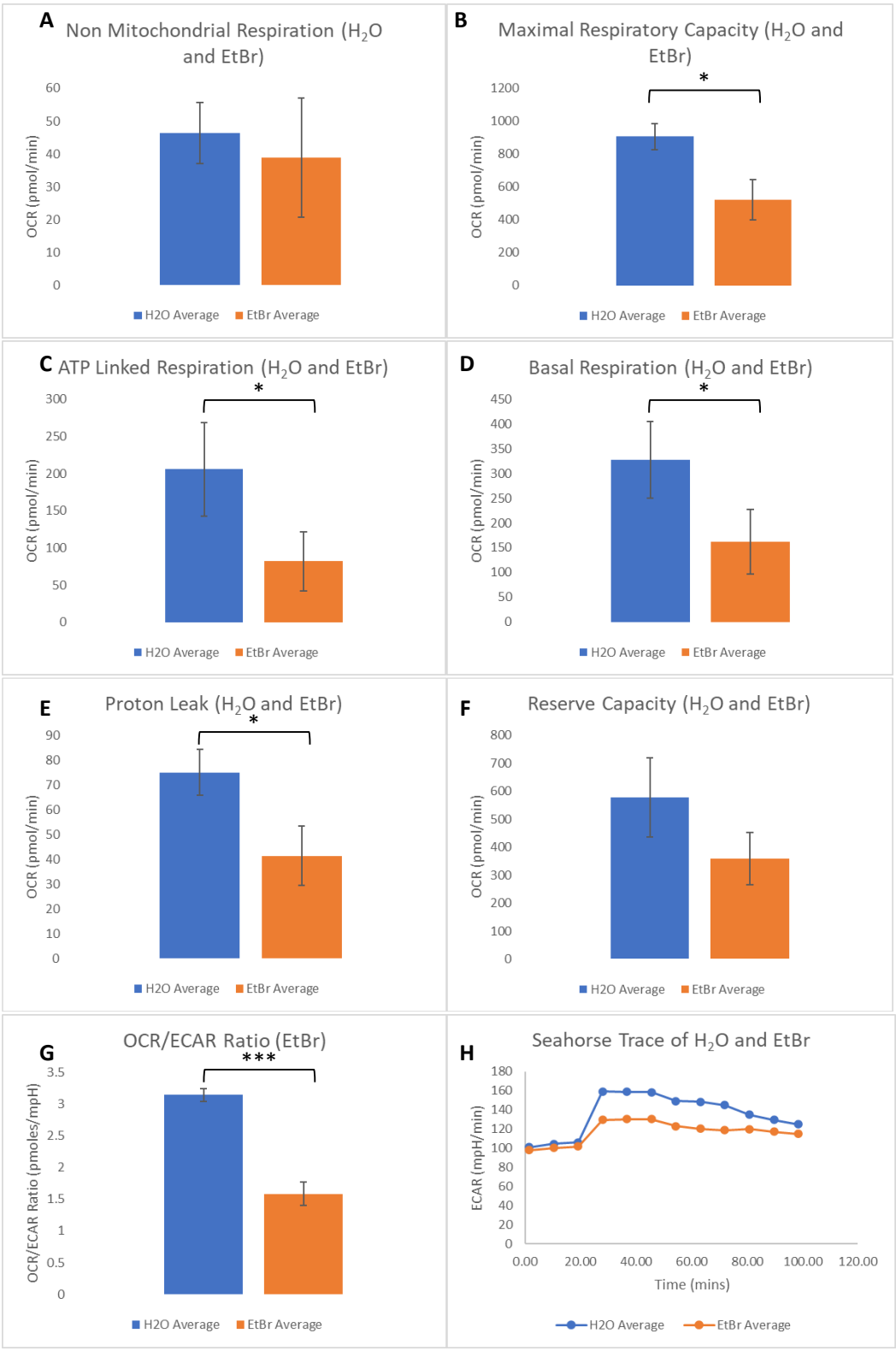

Figure A11 (A-H): Seahorse graphs for Ethidium Bromide indicating the different respiration parameters when compared to the H_2O solvent control. **A** represents non mitochondrial respiration, **B** is the maximal respiratory capacity ($P = 0.0103$),, **C** is the ATP linked respiration ($P = 0.0448$),, **D** is basal respiration ($P = 0.0478$),, **E** is proton leak ($P = 0.0187$),, **F** is the reserve capacity, **G** demonstrates the OCR/ECAR ($P = 0.0002$), ratio and **H** represents the ECAR graph. Unpaired T tests were carried out for these analyses (* < 0.05, **<0.005, ***<0.0005).

The Seahorse traces for MMS **(Figure A12)** and EthBr **(Figure A13)** are included below. MMS was included for consistency as it was used as a positive control for most other endpoints. EthBr was considered a Seahorse positive control so was included to provide an example of a chemical that disturbs mitochondrial function.

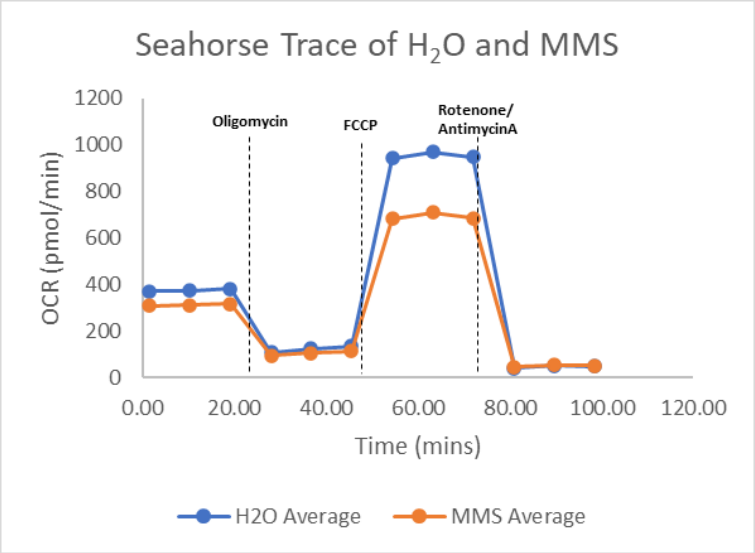

Figure A12: A Seahorse trace graph showing the bioenergetic flux profiles of MMS compared to the H_2O solvent control.

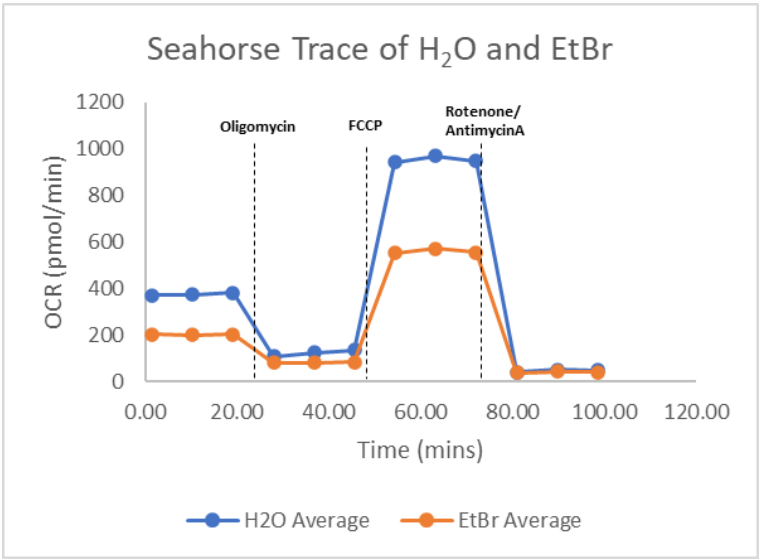

Figure A13: A Seahorse trace graph showing the bioenergetic flux profiles of EthBr compared to the H_2O solvent control.

Glossary

Acute exposure: The exposure of cells to a single total dose of test chemical over a short period of time, which in this case 24-hours.

Apoptosis: A type of programmed and controlled cellular death, which is actioned as part of an organism's normal development, removing any abnormal cells.

Binucleate: A cell that has two nuclei due to the inhibition of cellular division, which forms as a result of cytochalasin B treatment.

Chronic exposure: The exposure of cells to fractionated doses of test chemicals over a set period, which in this case 5 days.

Dimethyl sulphoxide (DMSO): A chemical capable of dissolving both organic and inorganic substances, it is known widely as the universal solvent.

Genotoxic carcinogen: An agent that acts directly and damages the cellular DNA in order to lead to the initiation of a cancer.

Mechanism of action: This refers to the biochemical process or processes by which a chemical produces an effect.

Micronucleus: A small DNA-containing extracellular body removed from the main nucleus and present in the cytoplasm. The micronuclei morphologically mirrors the main nucleus.

Micronucleus assay: It is used to assess the genotoxic potential of chemical agents.

Mononucleate: A cell that has a single nucleus and has undergone normal cellular division.

Non-genotoxic carcinogen: An agent that acts indirectly and uses alternative mechanisms to cause cancer.

Reactive oxygen species: Highly reactive chemical encompassing different oxygen containing species. An accumulation of ROS can lead to genomic damage.

Relative population doubling: A proliferation calculation comparing the number of PDs of a treated cell population to an untreated control.

Seahorse trace: A Seahorse XF Analyzer measures key indicators of mitochondrial respiration via the OCR and produces a unique graph shape as a result of different injections.

Spheroid: A simple 3D cell aggregate capable of showing cell-cell adhesion and can retain their extracellular matrix in order to better mimic the *in vivo* environment.

Bibliography

Andersen, M., Yang, R., French, C., Chubb, L. and Dennison, J., 2002. Molecular circuits, biological switches, and nonlinear dose-response relationships. *Environmental Health Perspectives* **110:** 971-978.

Aardema, M. and MacGregor, J. 2003. Toxicology and Genetic Toxicology in the New Era of "Toxicogenomics": Impact of "-omics" Technologies. In: Inoue, T., Pennie, W.D. (eds) Toxicogenomics. Springer, Tokyo.

Abbracchio, M., Heck, J., and Costa, M. 1981. Differences in surface properties of amorphous and crystalline metal sulfides may explain their toxicological potency. *Chemosphere* **10**: 897–908.

Abcam. 2023. *DCFDA / H2DCFDA - cellular Ros Assay Kit (AB113851), Abcam*. Available at: https://www.abcam.com/products/assay-kits/dcfda--h2dcfda-cellular-ros-assay-kit-ab113851.html#description_images_2.

Acquavella, J. and Leonard, R. 2001. A review of the epidemiology of 1,3-butadiene and chloroprene. *Chemico-Biological Interactions* **135-136**: 43-52.

Aden, D., Fogel, A., Plotkin, S., Damjanov, I. and Knowles, B. 1979. Controlled Synthesis of HBsAg in a Differentiated Human Liver Carcinoma-Derived Cell Line. *Nature*. **282**: 615–616.

Agency for Toxic Substances and Disease Registry (ATSDR). 2005. *Toxicological Profile for Nickel (Update)*Atlanta, GA: U.S. Department of Public Health and Human Services, Public Health Service.

Agilent. 2023a. Cell Mito Stress Test. Available at: https://www.agilent.com/en/product/cell-analysis/real-time-cell-metabolic-analysis/xf-assay-kits-reagents-cell-assay-media/seahorse-xf-cell-mito-stress-test-kit-740885.

Agilent. 2022. *How Agilent Seahorse XF Analyzer*. Available at: https://www.agilent.com/en/products/cell-analysis/how-seahorse-xf-analyzers-work.

Agilent. 2023b. *Immobilization of Non-Adherent Cells with Cell-Tak.* Available at: https://www.agilent.com/cs/library/technicaloverviews/public/5991-7157EN.pdf

Ahmadzai, A., Trevisan, J., Fullwood, N., Carmichael, P., Scott, A. and Martin, F. 2011. The Syrian hamster embryo (SHE) assay (pH 6.7): mechanisms of cell transformation and application of vibrational spectroscopy to objectively score endpoint alterations. *Mutagenesis.* **27:** 257-266.

Åkerlund, E., Cappellini, F., Di Bucchianico, S., Islam, S., Skoglund, S., Derr, R., Wallinder, I., Hendriks, G. and Karlsson, H. 2018. Genotoxic and mutagenic properties of Ni and NiO nanoparticles investigated by comet assay, *gamma*-H2AX staining, Hprt mutation assay and ToxTracker reporter cell lines. *Environ Mol Mutagen*. **59**: 211–22.

Alarifi, S., Ali, D., Alakhtani, S., Al Suhaibani, E. and Al- Qahtani, A. 2014. Reactive oxygen species-mediated DNA damage and apoptosis in human skin epidermal cells after exposure to nickel nanoparticles. Biol Trace Elem Res. **157**: 84-93.

Albertini, R., Clewell, H., Himmelstein, M., Morinello, E., Olin, S., Preston, J., Scarano, L., Smith, M., Swenberg, J., Tice, R. and Travis, C. 2003. The use of non-tumour data in cancer risk assessment: reflections on butadiene, vinyl chloride, and benzene. *Regulatory Toxicology and Pharmacology* **37:** 105-132.

Alberts, B., Johnson, A., Lewis, J., Raff, M., Roberts, K. and Walter, P. Molecular Biology of the Cell. 4th edition. New York: Garland Science; 2002. Cancer as a Microevolutionary Process. Available from: https://www.ncbi.nlm.nih.gov/books/NBK26891/

Alfhili, M., Alamri, H., Alsughayyir, J. and Basudan, A., 2022. Induction of hemolysis and eryptosis by occupational pollutant $NiCl_2$ is mediated through calcium influx and p38 MAP kinase signaling. *International Journal of Occupational Medicine and Environmental Health* **35:** 1-11.

Allemang, A., De Abrew, N., Shan, Y., Krailler, J. and Pfuhler, S. 2020. A comparison of classical and 21st century genotoxicity tools: A proof of concept study of 18 chemicals comparing in vitro micronucleus, ToxTracker and genomics-based methods (TGx-DDI, whole genome clustering and connectivity mapping)', *Environmental and Molecular Mutagenesis* **62:** 92–107.

Alvarez, M. and Doné, S. 2014. SYBR® Green and TaqMan® quantitative PCR arrays: expression profile of genes relevant to a pathway or a disease state. *Methods Mol Biol.* **1182:** 321-59.

Andersen, A, Berge, S., Engeland, A. and Norseth, T. 1996. Exposure to nickel compounds and smoking in relation to incidence of lung and nasal cancer among nickel refinery workers. *Occupational Environmental Medicine* **53:**708-13.

Anderson, J., Knowlton, K., May, H., Bair, T., Armstrong, S., Lappé, D. and Muhlestein, J. 2018. Temporal changes in statin prescription and intensity at discharge and impact on outcomes in patients with newly diagnosed atherosclerotic cardiovascular disease—Real-world experience within a large integrated health care system: The IMPRES study. *Journal of Clinical Lipidology* **12:** 1008-1018.

Anttila, A., Pukkala, E., Aitio, A., Rantanen, T. and Karjalainen, S. 1998. Update of cancer incidence among workers at a copper/nickel smelter and nickel refinery. *International Archives of Occupational and Environmental Health* **71:** 245-250.

Argos, M., Kalra, T., Rathouzetal, P. 2010. Arsenicexposurefrom drinking water, and all-cause and chronic-disease mortalities in Bangladesh (HEALS): a prospective cohort study, *The Lancet* **376:** 252–258.

Arita, A., Muñoz, A., Chervona, Y., Niu, J., Qu, Q., Zhao, N., Ruan, Y., Kiok, K., Kluz, T., Sun, H., Clancy, H., Shamy, M., & Costa, M. 2013. Gene expression profiles in peripheral blood mononuclear cells of Chinese nickel refinery workers with high exposures to nickel and control subjects. *Cancer epidemiology, biomarkers & prevention : a publication of the American Association for Cancer Research, cosponsored by the American Society of Preventive Oncology **22*****:*** 261–269.

Arome, D., and Chinedu, E. 2013. The importance of toxicity testing. *J. Pharm. BioSci*. ***4*****:** 146-148.

Arzumanian, V., Kiseleva, O. and Poverennaya, E. 2021. The Curious Case of the HepG2 Cell Line: 40 Years of Expertise. Int J Mol Sci. **22**: 13135.

Ashby, J. 1986. The prospects for a simplified and internationally harmonized approach to the detection of possible human carcinogens and mutagens. *Mutagenesis* **1:** 3–16.

Ashby, J. 1995. Druckrey's definition of "genotoxic", *Mutation Research/Fundamental and Molecular Mechanisms of Mutagenesis* **329:** 225.

Ashby, J. and Tennant, R. 1988. Chemical structure, Salmonella mutagenicity and extent of carcinogenicity as indicators of genotoxic carcinogenesis among 222 chemicals tested in rodents by the U.S. NCI/NTP. *Mutat. Res.* **204:** 17- 115.

Ashfaq, M., Ahmad, H., Khan, I. and Mustafa, G. 2013. LC determination of rosuvastatin and ezetimibe in human plasma. *Journal of the Chilean Chemical Society* **58**: 2177–2181.

Astashkina, A. and Grainger, D. 2014. Critical analysis of 3-D organoid *in vitro* cell culture models for high-throughput drug candidate toxicity assessments. *Advanced Drug Delivery Reviews* **69-70:** 1–18.

Astrazeneca.ca. 2022. [online] Available at: https://www.astrazeneca.ca/content/dam/az-ca/downloads/productinformation/crestor-product-monograph-en.pdf Cambridge, UK.

ATSDR. 1998. Toxicological Profile for Chlorinated Dibenzo-p-dioxins. Update. (Final Report). NTIS Accession. No. PB99-121998. Atlanta, GA: Agency for Toxic Substances and Disease Registry. 729.

ATSDR (Agency for toxic substances and disease registry). 2007. Toxicological profile for arsenic. Atlanta, GA: Agency for Toxic Substances and Disease Registry, U.S. Department of Health and Human Services, Public Health Service.

ATSDR (Agency for toxic substances and disease registry). 2005. Toxicological profile for Nickel, Atlanta, GA: US Public Health Service, Agency for Toxic Substances and Disease Registry.

Auerbach, C., Robson, J. and Carr, J. 1947. The chemical production of mutations. *Science* **105:** 243–247.

Barbalata, C., Tefas, L., Achim, M., Tomuta, I. and Porfire, A. 2020. Statins in risk-reduction and treatment of cancer. *World Journal of Clinical Oncology* **11:** 573–588.

Bardou, M., Barkun, A. and Martel, M. 2010. Effect of statin therapy on colorectal cancer. *Gut* **59:** 1572-1585.

Baron, M., Mintram, K., Owen, S., Hetheridge, M., Moody, A., Purcell, W., Jackson, S. and Jha, A. 2017. Pharmaceutical metabolism in fish: using a 3-D hepatic in vitro model to assess clearance. *PLoS ONE* **12**: e0168837.

Bartrip, P. 1992. A "pennurth of arsenic for rat poison": The Arsenic Act, 1851 and the prevention of secret poisoning. *Medical History* **36:** 53-69.

Bartsch, H. and Malaveille C. 1989. Prevalence of genotoxic chemicals among animal and human carcinogens evaluated in the IARC Monograph series. *Cell Biol Toxicol* **5:** 115–127

Basu, A., Mahata, J., Gupta, S. and Giri, A. 2001. Genetic toxicology of a paradoxical human carcinogen, arsenic: a review. *Mutation Research/Reviews in Mutation Research* **488:** 171-194.

Begley, C. and Ellis, L. 2012. Raise standards for preclinical cancer research. *Nature* **483:** 531-533.

Behera, S., Xian, H. and Balasubramanian R. 2014. Human health risk associated with exposure to toxic elements in mainstream and sidestream cigarette smoke. *Sci Total Environ.* **472:** 947–956.

Belini, V., Wiedemann, P. and Suhr, H. 2013. In situ microscopy: a perspective for industrial bioethanol production monitoring. J Microbiol Methods. **93**: 224–232.

Benigni, R., Bossa, C. and Tcheremenskaia, O. 2013. Nongenotoxic carcinogenicity of chemicals: mechanisms of action and early recognition through a new set of structural alerts. Chem Rev. **113:** 2940–2957.

Berber, A., Celik, M. and Aksoy, H. 2014. Genotoxicity evaluation of HMG CoA reductase inhibitor rosuvastatin. *Drug and Chemical Toxicology* **37:** 316–21.

Beshir, S., Ibrahim, K., Shaheen, W. and Shahy, E. 2016. Hormonal Perturbations in Occupationally Exposed Nickel Workers. *Open Access Macedonian Journal of Medical Sciences* **4:** 307-311.

Beyersmann, D. and Hartwig, A. 2008. Carcinogenic metal compounds: recent insight into molecular and cellular mechanisms. *Arch Toxicol.* **82:** 493–512.

Bianconi E, Piovesan A, Facchin F, Beraudi A, Casadei R, Frabetti F, Vitale L, Pelleri MC, Tassani S, Piva F, Perez-Amodio S, Strippoli P, Canaider S. 2013. An estimation of the number of cells in the human body. *Ann Hum Biol.* **40**: 463-71.

Billi, D. 2009. Subcellular integrities in *Chroococcidiopsis* sp. CCMEE 029 survivors after prolonged desiccation revealed by molecular probes and genome stability assays. *Extremophiles* **13**: 49–57.

BioLegend. 2023. Propidium iodide solution, BioLegend. Available at: https://www.biolegend.com/en-us/products/propidium-iodide-solution-2651?GroupID=BLG2181.

Bio-Rad. 2023. *Fluorescent compensation - flow cytometry guide: Bio-rad*, *Bio*. Available at: https://www.bio-rad-antibodies.com/flow-cytometry-fluorescence-compensation.html.

Black, M. and Brandt, R. 1974. Spectrofluorometric analysis of hydrogen peroxide. *Analytical Biochemistry* **58:** 246-254.

Black, M., Dodd, D., McMullen, P., Pendse, S., MacGregor, J., Gollapudi, B. and Andersen, M. 2015. Using gene expression profiling to evaluate cellular responses in mouse lungs exposed to V2O5 and a group of other mouse lung tumourigens and non-tumourigens. *Regulatory Toxicology and Pharmacology* **73:** 339–347.

Blakey, D., Galloway, S., Kirkland, D. and MacGregor, J. 2008. Regulatory aspects of genotoxicity testing: from hazard identification to risk assessment. *Mutat. Res.* **657:** 84–90.

Blasi, T., Hennig, H., Summers, H. Theis, F., Cerveira, J., Patterson, J., Davies, D., Filby, A., Carpenter, A. and Rees, P. 2016. Label-free cell cycle analysis for high-throughput imaging flow cytometry. *Nat Commun* **7**: 10256.

Bleyl, D., 1989. IARC Monographs on the Evaluation of Carcinogenic Risks to Humans. Overall Evaluations of Carcinogenicity: An Updating of IARC Monographs vol. 1 to 42.

Supplement 7. 440 Seiten. International Agency for Research on Cancer, Lyon 1987. **33:** 462-462.

Blodgett, A. D. (2006). An Analysis of Pollution and Community Advocacy in 'Cancer Alley': Setting an Example for the Environmental Justice Movement in St James Parish, Louisiana. *Local Environ* **11:** 647–661.

Bock, K. and Köhle, C. 2006. Ah receptor: Dioxin-mediated toxic responses as hints to deregulated physiologic functions. *Biochemical Pharmacology* **72:** 393-404.

Boffetta, P., Mundt, K., Adami, H., Cole, P. and Mandel, J. 2011. TCDD and cancer: A critical review of epidemiologic studies. *Critical Reviews in Toxicology* **41:** 622-636.

Boland, M., Chourasia, A. and Macleod, K. 2013. Mitochondrial Dysfunction in Cancer. *Frontiers in Oncology*, 3.

Bouhaddou, M., Yu, L., Lunardi, S., Stamatelos, S., Mack, F., Gallo, J., Birtwistle, M. and Walz, A. 2020. Predicting *in vivo* efficacy from *in vitro* data: Quantitative Systems Pharmacology Modeling for an epigenetic modifier drug in cancer. *Clinical and Translational Science* **13:** 419–429.

Braakhuis, H., Slob, W., Olthof, E., Wolterink, G., Zwart, E., Gremmer, E., Rorije, E., van Benthem, J., Woutersen, R., van der Laan, J. and Luijten, M. 2018. Is current risk assessment of non-genotoxic carcinogens protective?. *Critical Reviews in Toxicology* **48:** 500-511.

Bradberry, S. and Vale, A. 2007. Management of poisoning: antidotes. *Medicine* **35:** 562-564.

Brand, M. and Nicholls, D. 2011. Assessing mitochondrial dysfunction in cells. *Biochemical Journal*, **435**: 297-312.

Bridges, B. 1974. The three-tier approach to mutagenicity screening and the concept of radiation-equivalent dose. *Mutation Research/Fundamental and Molecular Mechanisms of Mutagenesis* **26:** 335–340.

Bridges, B. 1976. Evaluation of mutagenicity and carcinogenicity using three-tier system. *Mutation Research/Fundamental and Molecular Mechanisms of Mutagenesis* **41:** 71–72.

Bridges, B. 1984. Use of the terms mutagenicity and genotoxicity. *Mutation Research/DNA Repair Reports* **132:** 139–140.

Brüsehafer, K., Manshian, B., Doherty, A., Zair, Z., Johnson, G., Doak, S. and Jenkins, G. 2015. The clastogenicity of 4NQO is cell-type dependent and linked to cytotoxicity, length of exposure and p53 proficiency. *Mutagenesis* **31:** 171–180.

Buerki-Thurnherr, T., Xiao, L., Diener, L., Arslan, O., Hirsch, C., Maeder-Althaus, X., Grieder, K., Wampfler, B., Mathur, S., Wick, P. and Krug, H. 2013. *In vitro* mechanistic study towards a better understanding of ZnO nanoparticle toxicity. *Nanotoxicology* **7:** 402–416.

Buhaescu, I. and Izzedine, H. 2007. Mevalonate Pathway: A review of clinical and therapeutical implications. *Clinical Biochemistry* **40:** 575–584.

Bulbulyan, M., Margaryan, A., Ilychova, S., Astashevsky, S., Uloyan, S., Cogan, V., Colin, D., Boffetta, P. and Zaridze, D. 1999. Cancer incidence and mortality in a cohort of chloroprene workers from Armenia. International *Journal of Cancer* **81:** 31-33.

Burkitt, M. and Wardman, P. 2001. Cytochrome c Is a Potent Catalyst of Dichlorofluorescin Oxidation: Implications for the Role of Reactive Oxygen Species in Apoptosis. *Biochemical and Biophysical Research Communications* **282:** 329-333.

Byrdwell, W. and Neff, W. 2002. Dual parallel electrospray ionization and atmospheric pressure chemical ionization mass spectrometry (MS), MS/MS and MS/MS/MS for the analysis of triacylglycerols and triacylglycerol oxidation products. *Rapid Commun. Mass Spectrom*. **16:** 300–319.

Calabrese, E. 2002. Hormesis: changing view of the dose-response, a personal account of the history and current status. Mutat Res. **511:** 181-189.

Callegaro, G., Corvi, R., Salovaara, S., Urani, C. and Stefanini, F., 2016. Relationship between increasing concentrations of two carcinogens and statistical image descriptors offocimorphology in the cell transformation assay. *Journal of Applied Toxicology* **37:** 709-720.

Cameron, K., Buchner, V. and Tchounwou, P. 2011. Exploring the molecular mechanisms of nickel-induced genotoxicity and carcinogenicity: a literature review. *Reviews on Environmental Health* **26**.

Campbell, R., Stephens, W. and Meharg, A. 2014. Consistency of arsenic speciation in global tobacco products with implications for health and regulation. *Tobacco Induced Diseases* **12:** 24.

Campbell, R., Stephens, W., Finch, A. and Geraki, K. 2014. Controls on the valence species of arsenic in tobacco smoke: XANES investigation with implications for health and regulation. *Environ Sci Technol.* **6:** 3449–3456.

Cancer Research UK (CRUK). Cancer statistics for the UK. 2022. Available at: https://www.cancerresearchuk.org/health-professional/cancer-statistics-for-the-uk.

Carmeliet, P. 2005. VEGF as a key mediator of angiogenesis in cancer. *Oncology* **69:** 4–10.

Carmona, E., Creus, A. and Marcos, R., 2011. Genotoxic effects of two nickel-compounds in somatic cells of *Drosophila melanogaster*. *Mutation Research/Genetic Toxicology and Environmental Mutagenesis* **718:** 33-37.

Carracedo, A. and Pandolfi, P., 2008. The PTEN–PI3K pathway: of feedbacks and cross-talks. *Oncogene* **27:** 5527-5541.

Caspari, R. and Lee, S. 2004. Older age becomes common late in human evolution. *Proc. Natl Acad. Sci.* USA **101**: 10895–10900.

Centers for disease control and prevention (CDC) 2022. NIOSH Pocket Guide to Chemical Hazards: beta-Chloroprene. [online] Available at: <https://www.cdc.gov/niosh/npg/npgd0133.html>.

Cerrato, A., Merolla, F., Morra, F. and Celetti, A. 2017. CCDC6: the identity of a protein known to be partner in fusion. *International Journal of Cancer* **142:** 1300-1308.

Chakrabarti, S., Bai, C. and Subramanian, K. 2001. DNA–Protein Crosslinks Induced by Nickel Compounds in Isolated Rat Lymphocytes: Role of Reactive Oxygen Species and Specific Amino Acids. *Toxicology and Applied Pharmacology* **170**: 153-165.

Chan, L., Kuksin, D., Laverty, D., Saldi, S. and Qiu, J. 2015. Morphological observation and analysis using automated image cytometry for the comparison of trypan blue and fluorescence-based viability detection method. Cytotechnology. **67**: 461–473.

Chang, C-H., Yu., F., Wu., T-S., Wang, L-T. and Liu, B-H. 2010. Mycotoxin citrinin induced cell cycle G2/M arrest and numerical chromosomal aberration associated with disruption of microtubule formation in human cells. *Toxicological Sciences* **119**: 84–92.

Channarayappa, Nath, J. and Ong, T. 1990. Micronuclei assay in cytokinesis-blocked binucleated and conventional mononucleated methods in human peripheral lymphocytes. *Teratogenesis, Carcinogenesis, and Mutagenesis* **10:** 273–279.

Chapman, K., Doak, S. and Jenkins, G. 2015. Acute Dosing and p53-Deficiency Promote Cellular Sensitivity to DNA Methylating Agents, *Toxicological Sciences* **144:** 357–365.

Chapman, K., Thomas, A., Wills, J., Pfuhler, S., Doak, S. and Jenkins, G. 2014. Automation and validation of micronucleus detection in the 3D EPIDERM™ human reconstructed skin assay and correlation with 2D dose responses. *Mutagenesis* **29:** 165–175.

Chapman, K., Wilde, E., Chapman, F., Verma, J., Shah, U., Stannard, L., Seager, A., Tonkin, J., Brown, M., Doherty, A., Johnson, G., Doak, S. and Jenkins, G. 2021. Multiple-endpoint *in vitro* carcinogenicity test in human cell line TK6 distinguishes carcinogens from non-carcinogens and highlights mechanisms of action. *Archives of Toxicology* **95:** 321–336.

Chattopadhyay, S., Bhaumik, S., Purkayastha, M., Basu, S., Nag Chaudhuri, A. and Das Gupta, S. 2002. Apoptosis and necrosis in developing brain cells due to arsenic toxicity and protection with antioxidants. *Toxicology Letters* **136:** 65-76.

Chen, C., Hsueh, Y., Lai, M., Shyu, M., Chen, S., Wu, M., Kuo, T. and Tai, T. 1995. Increased Prevalence of Hypertension and Long-term Arsenic Exposure. *Hypertension* **25:** 53-60.

Chen, C., Kuo, T. and Wu, M. 1988. ARSENIC AND CANCERS. *The Lancet* **331:** 414-415.

Chen, C., Wang, Y., Huang, W. and Huang, Y., 2003. Nickel induces oxidative stress and genotoxicity in human lymphocytes. *Toxicology and Applied Pharmacology* **189:** 153-159.

Chen, C., Zhao, S., Karnad, A. and Freeman, J. 2018. The biology and role of CD44 in cancer progression: Therapeutic implications. *Journal of Hematology & Oncology* **11:** 64.

Chen, H. and Costa, M. 2009. Iron-and 2-oxoglutarate-dependent dioxygenases: an emerging group of molecular targets for nickel toxicity and carcinogenicity. *Biometals.* **22**:191–6.

Chen, Q., Jones, T., Brown, P. and Stevens, J. 1990. The mechanism of cysteine conjugate cytotoxicity in renal epithelial cells. Covalent binding leads to thiol depletion and lipid peroxidation. *J Biol Chem* **265:** 21603–21611.

Chen, W. and Chen, J. 2002. Nested case-control study of lung cancer in four Chinese tin mines. *Occupational and Environmental Medicine* **59:** 113-118.

Chen, Y., Guo, Y., Su, H., Hsueh, Y., Smith, T., Ryan, L., Lee, M., Chao, S., Lee, J. and Christiani, D. 2003. Arsenic Methylation and Skin Cancer Risk in Southwestern Taiwan. *Journal of Occupational and Environmental Medicine* **45:** 241-248.

Chen, Y., Lin-Shiau, S. and Lin, J. 1998. Involvement of reactive oxygen species and caspase 3 activation in arsenite-induced apoptosis. *Journal of Cellular Physiology* 177: 324-333.

Chen, F., Vallyathan, V., Castranova, V. and Shi, X. 2001. Cell apoptosis induced by carcinogenic metals. *Molecular and Cellular Biochemistry* **222**: 183-188.

Chiba, M. and Masironi, R. 1992. Toxic and trace elements in tobacco and tobacco smoke. *Bull World Health Organ*. **70**: 269-75.

Children with cancer UK. 2023. *Childhood cancer facts and statistics 2021, Children with Cancer*. Available at: https://www.childrenwithcancer.org.uk/childhood-cancer-info/understanding-cancer/childhood-cancer-facts-figures/?gclid=EAIaIQobChMIr7mVwZubgQMVDdHtCh2XtwXUEAAYASAAEgI2Z_D_BwE.

Chronic arsenic poisoning. 2022. DermNet. Available at: https://dermnetnz.org/topics/chronic-arsenic-poisoning.

Chung, J., Yu, S. and Hong, Y., 2014. Environmental Source of Arsenic Exposure. *Journal of Preventive Medicine and Public Health* **47:** 253-257.

Cimino, M. 2006. Comparative overview of current international strategies and guidelines for genetic toxicology testing for regulatory purposes. *Environ. Mol. Mutagen*. **47**: 362-390.

Clare, M., Lorenzon, G., Akhurst, L., Marzin, D., van Delft, J., Montero, R., Botta, A., Bertens, A., Cinelli, S., Thybaud, V. and Lorge, E. 2006. SFTG international collaborative study on *in vitro* micronucleus test. *Mutation Research/Genetic Toxicology and Environmental Mutagenesis* **607:** 37–60.

Clemens, F. and Landolf, J. 2003. Genotoxicity of Samples of Nickel Refinery Dust. *Toxicological Sciences* **73:** 114-123.

Cohen, L. and Jefferies, A. 2019. Environmental exposures and cancer: using the precautionary principle. *Ecancermedicalscience*. **13**: ed91.

Cohen, S., Arnold, L., Beck, B., Lewis, A. and Eldan, M. 2013. Evaluation of the carcinogenicity of inorganic arsenic. *Critical Reviews in Toxicology* **43**: 711-752.

Cohen, S., Arnold, L., Eldan, M., Lewis, A. and Beck, B., 2006. Methylated Arsenicals: The Implications of Metabolism and Carcinogenicity Studies in Rodents to Human Risk Assessment. *Critical Reviews in Toxicology* **36:** 99-133.

Cohen, S., Boobis, A., Dellarco, V., Doe, J., Fenner-Crisp, P., Moretto, A., Pastoor, T., Schoeny, R., Seed, J. and Wolf, D. 2019. Chemical carcinogenicity revisited 3: risk assessment of carcinogenic potential based on the current state of knowledge of carcinogenesis in humans. *Regulat Toxicol Pharmacol* **103:**100-105.

Cohen, S., Chowdhury, A. and Arnold, L. 2016. Inorganic arsenic: A non-genotoxic carcinogen. *Journal of Environmental Sciences* **49**: 28-37.

Collaborative on Health and the Environment. 2016. Pesticides — The Collaborative on Health and the Environment. [online] www.healthandenvironment.org. Available at: https://www.healthandenvironment.org/environmental-health/environmental-risks/chemical-environment-overview/pesticides.

COM. 2010. *Committee on mutagenicity of chemicals in food, consumer products and the environment, GOV.UK*. Available at:

https://www.gov.uk/government/organisations/committee-on-mutagenicity-of-chemicals-in-food-consumer-products-and-the-environment.

Coogan, T., Latta, D., Snow, E., Costa, M. 1989. Toxicity and carcinogencity of nickel compounds. *Critical Review Toxicology*.**19:** 341–84.

Cooper, Geoffrey. 2000. The Cell: A Molecular Approach. 2nd Edition. : Sinauer Associates, Chicago.

Corsini, E., Asti, L., Viviani, B., Marinovich, M., Galli, C. 1999. Sodium arsenate induces overproduction of interleukin-1alpha in murine keratinocytes: Role of mitochondria. *J. Investig. Dermatol.* **113**: 760–765.

Costa, M., Cantoni, O., de Mars, M., Swartzendruber, D. 1982. Toxic metals produce an S-phase-specific cell cycle block. *Research Communications in Chemical Pathology and Pharmacology* **38** :405-19.

Costa, M., Zhuang, Z., Huang, X., Cosentino, S., Klein, C. B., and Salnikow, K. 1994. Molecular mechanisms of nickel carcinogenesis. *Sci. Total Environ*. **148:** 191–199.

Crespi, C., Gonzalez, F., Steimel, D., Turner, T., Gelboin, H., Penman, B. and Langenbach, R. 1991. A metabolically competent human cell line expressing five cDNAs encoding procarcinogen-activating enzymes: application to mutagenicity testing. *Chemical Research in Toxicology* **4**: 566-572.

Crofton-Sleigh, C., Doherty, A., Ellard, S., Parry, E. and Venitt, S. 1993. Micronucleus assays using cytochalasin-blocked MCL-5 cells, a proprietary human cell line expressing five human cytochromes P-450 and microsomal epoxide hydrolase. *Mutagenesis* **8:** 363–372.

Cullen, W. 2008. *Is arsenic an aphrodisiac?: the sociochemistry of an element*. Cambridge, Royal Society of Chemistry.

Curtis, G. 1983. Biology, 4th edn. New York, NY: Worth; ISBN **13:** 9780879011864.

Dallas, L., Bean, T., Turner, A., Lyons, B. and Jha, A. 2013. Oxidative DNA damage may not mediate Ni-induced genotoxicity in marine mussels: Assessment of genotoxic biomarkers and

transcriptional responses of key stress genes. *Mutation Research/Genetic Toxicology and Environmental Mutagenesis* **754:** 22-31.

Dalton, S. 2009. The molecular basis of embryonic stem cells self-renewal. Rajasekhar, V., Vemuri, M. editors. Regulatory networks in stem cells. Totowa, N. Humana Press. 3-12.

Danadevi, K., Rozati, R., Saleha Banu, B. and Grover, P. 2004. *In vivo* genotoxic effect of nickel chloride in mice leukocytes using comet assay. *Food and Chemical Toxicology* **42:** 751-757.

Daniels, T., Bernabeu, E., Rodríguez, J., Patel, S., Kozman, M., Chiappetta, D., Holler, E., Ljubimova, J., Helguera, G. and Penichet, M. 2012. The transferrin receptor and the targeted delivery of therapeutic agents against cancer. *Biochimica et Biophysica Acta (BBA) - General Subjects* **1820:** 291-317.

David, R., Ebbels, T. and Gooderham, N. 2016. Synergistic and Antagonistic Mutation Responses of Human MCL-5 Cells to Mixtures of Benzo[a]pyrene and 2-Amino-1-Methyl-6-Phenylimidazo[4,5-b]pyridine: Dose-Related Variation in the Joint Effects of Common Dietary Carcinogens. Environ Health Perspect. **124:** 88-96.

Degli Esposti, M. 2002. Measuring mitochondrial reactive oxygen species. *Methods* **26**: 335-340.

Demierre, M., Higgins, P., Gruber, S., Hawk, E. and Lippman, S. 2005. Statins and cancer prevention**.** *Nature Reviews Cancer* **5:** 930-942.

Dere, E., Boverhof, D., Burgoon, L. and Zacharewski, T. 2006. *In vivo – in vitro* toxicogenomic comparison of TCDD-elicited gene expression in Hepa1c1c7 mouse hepatoma cells and C57BL/6 hepatic tissue. *BMC Genomics* **7**: 80.

Dhawan, A. and Bajpayee, M. 2019. *Genotoxicity assessment: Methods and protocols*. New York, NY: Humana Press.

Di Bucchianico, S., Gliga, A., Åkerlund, E., Skoglund, S., Wallinder, I., Fadeel, B. and Karlsson, H. 2018. Calcium-dependent cyto- and genotoxicity of nickel metal and nickel oxide nanoparticles in human lung cells. *Particle and Fibre Toxicology* **15**.

Di Cristofano, A. and Pandolfi, P. 2000. The Multiple Roles of PTEN in Tumour Suppression. *Cell* **100:** 387-390.

Diwan, B., Kasprzak, K, Rice, J. 1992. Transplacental carcinogenic effects of nickel(II) acetate in the renal cortex, renal pelvis and adenohypophysis in F344/NCr rats. *Carcinogenesis* **13**: 1351– 7.

Doe, J., Boobis, A., Cohen, S., Dellarco, V., Fenner-Crisp, P., Moretto, A., Pastoor, T., Schoeny, R., Seed, J., Wolf, D. 2022. A new approach to the classification of Carcinogenicity. *Archives of Toxicology* **96**: 2419–2428.

Doherty, A., Wilson, A., Chocian, K., Molloy, J., Clatworthy, M., Doak, S., Jenkins, G. and O'Donovan, M. 2014. Genotoxins induce binucleation in L5178Y and TK6 cells. *Mutation Research/Genetic Toxicology and Environmental Mutagenesis* **770**: 29-34.

Dong, H., Holth, A., Kleinberg, L., Ruud, M., Elstrand, M., Tropé, C., Davidson, B. and Risberg, B. 2009. Evaluation of Cell Surface Expression of Phosphatidylserine in Ovarian Carcinoma Effusions Using the Annexin-V/7-AAD Assay: Clinical Relevance and Comparison With Other Apoptosis Parameters. *American Journal of Clinical Pathology* **132:** 756–762.

Dong, J. and Luo, X. 1993. Arsenic-induced DNA-strand breaks associated with DNA—protein crosslinks in human fetal lung fibroblasts. *Mutation Research Letters* **302:** 97-102.

Drobná, Z., Walton, F., Paul, D., Xing, W., Thomas, D. and Stýblo, M. 2009. Metabolism of arsenic in human liver: the role of membrane transporters. *Archives of Toxicology* **84:** 3-16.

Druckrey, H. 1973. Specific Carcinogenic and Teratogenic Effects of "Indirect" Alkylating Methyl and Ethyl compounds, and their Dependency on Stages of Ontogenic Developments. *Xenobiotica* **3**: 271–303.

Dunnick, J., Elwell, M., Radovsky, A., Benson, J., Hahn, F., Nikula, K., Barr, E., and Hobbs, C. 1995. Comparative carcinogenic effects of nickel subsulfide, nickel oxide, or nickel sulfate hexahydrate on chronic exposures in the lung. *Cancer Research* **55:** 5251–5256.

Dural, E., Shah, U., Pritchard, D., Chapman, K., Doak, S. and Jenkins, G. 2020. The effect of chronic dosing and p53 status on the genotoxicity of pro-oxidant chemicals *in vitro*. *Mutagenesis* **35:** 479–489.

Eastmond, D. 2012. Factors influencing mutagenic mode of action determinations of regulatory and advisory agencies. *Mutation Research/Reviews in Mutation Research* **751:** 49–63.

EcoEnclose. 2020. *Plastic Production, Cancer Alley and Environmental Justice*. [online] EcoEnclose. Available at: https://www.ecoenclose.com/blog/plastic-production-cancer-alley-and-environmental-justice/.

Elhajouji, A. 2010. Mitomycin C, 5-fluoruracil, colchicine and etoposide tested in the in vitro mammalian cell micronucleus test (MNvit) in the human lymphoblastoid cell line TK6 at Novartis in support of OECD draft Test Guideline 487. *Mutat. Res.* **702**, 157–162.

Ellinger-Ziegelbauer, H., Fostel, J., Aruga, C., Bauer, D., Boitier, E., Deng, S., Dickinson, D., Le Fevre, A., Fornace, A Jr., Grenet, O., Gu, Y., Hoflack, J., Shiiyama, M., Smith, R., Snyder, R., Spire, C., Tanaka, G. and Aubrecht, J. 2009. Characterization and interlaboratory comparison of a gene expression signature for differentiating genotoxic mechanisms. *Toxicol Sci.* **110**: 341-52.

Ellinger-Ziegelbauer, H., Stuart, B., Wahle, B., Bomann, W. and Ahr, H. J. 2004. Characteristic expression profiles induced by genotoxic carcinogens in rat liver. *Toxicol Sci* **77:** 19–34.

Elloway, J., Ling, S., David, .R and Doherty, A. 2016. Development of a multi-end point genotoxicity assessment screen (MEGA-Screen). *Toxicology Letters* **258:** S236-237.

Emerling, B., Weinberg, F., Liu, J., Mak, T. and Chandel, N. 2008. PTEN regulates p300-dependent hypoxia-inducible factor 1 transcriptional activity through Forkhead transcription factor 3a (FOXO3a). *Proceedings of the National Academy of Sciences* **105:** 2622-2627.

Environmental Protection Agency (EPA) . 2010. Toxicological review of chloroprene (CAS No. 126-99-8) In support of summary information on the Integrated Risk information System (IRIS). (EPA/635/R-09/010F). Washington, DC: National Center for Environmental

Assessment. Office of Research and Development. Available at: https://cfpub.epa.gov/ncea/iris/iris_documents/documents/toxreviews/1021tr.pdf.

Eruslanov, E. and Kusmartsev, S. 2010. Identification of ROS Using Oxidized DCFDA and Flow-Cytometry. In: Armstrong, D. (eds) Advanced Protocols in Oxidative Stress II. Methods in Molecular Biology, vol 594. Humana Press, Totowa, NJ.

European chemicals agency (ECHA) Echa.europa.eu. 2022. *Registration Dossier - ECHA*. [online] Available at: <https://echa.europa.eu/registration-dossier/-/registered-dossier/14857/7/7/1>

European commission (2012) *Cell transformation assay based on the bhas 42 cell line, TSAR*. Available at: https://tsar.jrc.ec.europa.eu/test-method/tm2012-06.

European council (EC). 2008. Council Regulation (EC) No 440/2008 of 30 May 2008 laying down test methods pursuant to Regulation (EC) No 1907/2006 of the European Parliament and of the Council on the Registration, Evaluation, Authorisation and Restriction of Chemicals (REACH). OJ L **142**:1.

European Food Safety Authority (EFSA) and EFSA Panel on Contaminants in the Food Chain (CONTAM) 2009. Scientific opinion on arsenic in food. *EFSA Journal* **7:** 1351, 199.

European Medicines Agency (EMA). 2013. *Ich S2 (R1) genotoxicity testing and data interpretation for pharmaceuticals intended human use - scientific guideline European Medicines Agency, European Medicines Agency*. Available at: https://www.ema.europa.eu/en/ich-s2-r1-genotoxicity-testing-data-interpretation-pharmaceuticals-intended-human-use-scientific.

Fadeel, B. and Orrenius, S. 2005. Apoptosis: a basic biological phenomenon with wide-ranging implications in human disease. *J Intern Med.* **258:** 479–517.

Farkash, E. and Prak, E. 2006. DNA damage and L1 retrotransposition. J Biomed Biotechnol.**2006** : 37285.

Fenech, M. 1993. The cytokinesis-block micronucleus technique and its application to genotoxicity studies in human populations. *Environ. Health Perspect.* **101:** 101–107.

Fenech, M. 2000. The *in vitro* micronucleus technique. *Mutation Research/Fundamental and Molecular Mechanisms of Mutagenesis* **455:** 81–95.

Fenech, M. 2007. Cytokinesis-block micronucleus cytome assay. *Nat Protoc* **2**: 1084–1104.

Fenech, M. and Morley, A. 1985. Measurement of micronuclei in human lymphocytes. *Mutat. Res.***148**: 29-36.

Fenech, M., Chang, W., Kirsch-Volders, M., Holland, N., Bonassi, S. and Zeiger, E. 2003. HUman MicronNucleus project. HUMN project: detailed description of the scoring criteria for the cytokinesis-block micronucleus assay using isolated human lymphocyte cultures. *Mutat Res*. **534**: 65-75.

Fergusson, J. 1990. The heavy elements: chemistry, environmental impact, and health effects. New York: Pergamon Press; 362-365.

Ferreccio, C., González, C., Milosavjlevic, V., Marshall, G., Sancha, A. and Smith, A. 2000. Lung Cancer and Arsenic Concentrations in Drinking Water in Chile. *Epidemiology* **11:** 673-679.

Figueroa, D., Asaduzzaman, M. and Young, F. 2018. Real time monitoring and quantification of reactive oxygen species in breast cancer cell line MCF-7 by 2′,7′–dichlorofluorescin diacetate (DCFDA) assay. *Journal of Pharmacological and Toxicological Methods* **94:** 26–33.

Finkel, T. 2011. Signal transduction by reactive oxygen species. *J Cell Biol.* **194:** 7–15.

Fitzmaurice, O., Bartkowski, M. and Giordani, S. 2022. Molecular switches—tools for imparting control in Drug Delivery Systems. *Frontiers in Chemistry*, 10.

Florentinus, S., Heerdink, E., Klungel, O. and de Boer, A. 2004. Should rosuvastatin be withdrawn from the market? *The Lancet* **364:** 1577

Forgacs, Z., Massanyi, P., Lukac, N. and Somosy, Z. 2012. Reproductive toxicology of nickel - review. *J Environ Sci Health A Tox Hazard Subst Environ Eng* **47:** 1249–1260.

Forkink, M., Smeitink, J., Brock, R., Willems, P. and Koopman, W. 2010. Detection and manipulation of mitochondrial reactive oxygen species in mammalian cells. *Biochimica et Biophysica acta (BBa)-Bioenergetics* **1797:** 1034-1044.

Forsythe, J., Jiang, B., Iyer, N., Agani, F., Leung, S., Koos, R. and Semenza, G. 1996. Activation of vascular endothelial growth factor gene transcription by hypoxia-inducible factor 1. *Molecular and Cellular Biology* **16:** 4604-4613.

Fowler, P., Smith, R., Smith, K., Young, J., Jeffrey, L., Carmichael, P., Kirkland, D. and Pfuhler, S. 2014. Reduction of misleading ("false") positive results in mammalian cell genotoxicity assays. III: Sensitivity of human cell types to known genotoxic agents. *Mutation Research/Genetic Toxicology and Environmental Mutagenesis* **767:** 28-36.

Fowler, P., Whitwell, J., Jeffrey, L., Young, J., Smith, K. and Kirkland, D. 2010. Cadmium chloride, benzo[a]pyrene and cyclophosphamide tested in the *in vitro* mammalian cell micronucleus test (MNvit) in the human lymphoblastoid cell line TK6 at Covance laboratories, Harrogate UK in support of OECD draft Test Guideline 487. *Mutation Research/Genetic Toxicology and Environmental Mutagenesis* **702:** 171-174.

Frade, J. and Ovejero-Benito, M. 2015. Neuronal cell cycle: the neuron itself and its circumstances. Cell Cycle. **14**: 712-20.

Fukushima, S., Kinoshita, A., Puatanachokchai, R., Kushida, M., Wanibuchi, H. and Morimura, K. 2005. Hormesis and dose–response-mediated mechanisms in carcinogenesis: Evidence for a threshold in carcinogenicity of non-genotoxic carcinogens. *Carcinogenesis* **26**: 1835–1845.

Galvao, J., Davis, B., Tilley, M., Normando, E., Duchen, M. and Cordeiro, M. 2013. Unexpected low-dose toxicity of the universal solvent DMSO *The FASEB Journal* **28:** 1317–1330.

Gasser, M., Wick, P., Clift, M., Blank, F., Diener, L., Yan, B., Gehr, P., Krug, H. and Rothen-Rutishauser, B. 2012. Pulmonary surfactant coating of multi-walled carbon nanotubes (MWCNTs) influences their oxidative and pro-inflammatory potential *in vitro*. *Part. Fibre Toxicol.* **9:** 17.

Genchi, G., Carocci, A., Lauria, G., Sinicropi, M. and Catalano, A. 2020. Nickel: Human Health and Environmental Toxicology. *International Journal of Environmental Research and Public Health* **17**: p.679.

Genecards (FAS). 2023. *FAS, GeneCards is a searchable, integrative database that provides comprehensive, user-friendly information on all annotated and predicted human genes*. Available at: https://www.genecards.org/cgi-bin/carddisp.pl?gene=FAS

Genecards (KRAS). 2023. *Kras, GeneCards is a searchable, integrative database that provides comprehensive, user-friendly information on all annotated and predicted human genes*. Available at: https://www.genecards.org/cgi-bin/carddisp.pl?gene=KRAS

Gibb, H., Haver, C., Gaylor, D., Ramasamy, S., Lee, J., Lobdell, D., Wade, T., Chen, C., White, P. and Sams, R. 2011. Utility of Recent Studies to Assess the National Research Council 2001 Estimates of Cancer Risk from Ingested Arsenic. *Environmental Health Perspectives* **119:** 284-290.

Gillet, J., Varma, S. and Gottesman, M. 2013. The clinical rlevance of cancer cell lines. *JNCI Journal of the National Cancer Institute* **105:** 452–458.

Gliga, A., Bucchianico, S., Akerlund, E. and Karlsson, H. 2020. Transcriptome profiling and toxicity following long-term, low dose exposure of human lung cells to ni and nio nanoparticles—comparison with NICL2. *Nanomaterials* **10:** 649.

GmbH, M.S.H.& S. 2023. *Metafer, MetaSystems*. Available at: https://metasystems-international.com/en/products/metafer/

Goodman, J. 2018. Goodbye to the bioassay. *Toxicol Res (Camb).* **7:** 558-564.

Goodman, J., Prueitt, R., Dodge, D. and Thakali, S. 2009. Carcinogenicity assessment of water-soluble nickel compounds. *Critical Reviews in Toxicology* **39:** 365-417.

Grandjean, P. 2016. Paracelsus Revisited: The Dose Concept in a Complex World. *Basic Clin Pharmacol Toxicol.* **119:** 126-32.

Groff, K., Evans, S., Doak, S., Pfuhler, S., Corvi, R., Saunders, S. and Stoddart, G. 2021. *In vitro* and integrated *in vivo* strategies to reduce animal use in genotoxicity testing, *Mutagenesis* **36:** 389–400.

Grosjean, D. 1990. Atmospheric Chemistry of Toxic Contaminants 1. Reaction Rates and Atmospheric Persistence. *Journal of the Air & Waste Management Association* **40:** 1397-140.

Guengerich, F. 2019. Cytochrome P450 Research and The Journal of Biological Chemistry. *J. Biol. Chem.* **294**: 1671–1680.

Guest R. and Parry J. 1999. P53 integrity in the genetically engineered mammalian cell lines AHH-1 and MCL-5. *Mutat. Res*. **423:** 39–46.

Guillamet, E., Creus, A., Ponti, J., Sabbioni, E., Fortaner, S. and Marcos, R. 2004. *In vitro* DNA damage by arsenic compounds in a human lymphoblastoid cell line (TK6) assessed by the alkaline Comet Assay. *Mutagenesis* **19:** 129–135.

Guo, H., Cui, H., Peng, X., Fang, J., Zuo, Z., Deng, J., Wang, X., Wu, B., Chen, K. and Deng, J. 2016. Nickel chloride ($NiCl_2$) induces endoplasmic reticulum (ER) stress by activating UPR pathways in the kidney of broiler chickens. *Oncotarget* **7:** 17508-17519.

Guo, H., Liu, H., Jian, Z., Cui, H., Fang, J., Zuo, Z., Deng, J., Li, Y., Wang, X., Zhao, L., He, R. and Tang, H. 2020. Immunotoxicity of nickel: Pathological and toxicological effects. *Ecotoxicology and Environmental Safety* **203:** 111006.

Guo, Y. and Xing, Y. 2016. Weighted gene co-expression network analysis of pneumocytes under exposure to a carcinogenic dose of chloroprene. *Life Sciences* **151:** 339-347.

Gurumoorthy, P., Mahendiran, D. and Kalilur Rahiman, A., 2016. Theoretical calculations, DNA interaction, topoisomerase I and phosphatidylinositol-3-kinase studies of water soluble mixed-ligand nickel(II) complexes. *Chemico-Biological Interactions* **248:** 21-35.

Gutschner, T. and Diederichs, S. 2012. The hallmarks of cancer. *RNA Biology* **9:** 703–719.

Guyton, K., Kyle, A., Aubrecht, J., Cogliano, V., Eastmond, D., Jackson, M., Keshava, N., Sandy, M., Sonawane, B., Zhang, L., Waters, M. and Smith, M. 2009. Improving prediction of

chemical carcinogenicity by considering multiple mechanisms and applying toxicogenomic approaches. *Mutation Research/Reviews in Mutation Research* **681**: 230-240.

Hajar, R., 2011. Statins: Past and Present. *Heart Views* **12:** 121.

Halatek, T., Sinczuk-Walczak, H., Rabieh, S. and Wasowicz, W. 2009. Association between occupational exposure to arsenic and neurological, respiratory and renal effects. *Toxicology and Applied Pharmacology* **239:** 193-199.

Han, Y., Kim, S., Kim, S. and Park, W. 2008. Arsenic trioxide inhibits the growth of Calu-6 cells via inducing a G2 arrest of the cell cycle and apoptosis accompanied with the depletion of GSH. *Cancer Letters* **270:** 40-55.

Hanahan, D. and Weinberg, R. 2000. The hallmarks of cancer. *Cell* **100:** 57–70.

Hanahan, D. and Weinberg, R. 2011. Hallmarks of Cancer: The Next Generation. *Cell* **144**: 646-674.

Hanahn, D. 2022. Hallmarks of cancer: New dimensions. *Cancer Discovery* **12:** 31–46.

Hartwig, A. and Schwerdtle, T., 2002. Interactions by carcinogenic metal compounds with DNA repair processes: toxicological implications. *Toxicology Letters* **127:** 47-54.

Hartwig, A., Krüger, I., Beyersmann, D. 1994. Mechanisms in nickel genotoxicity: the significance of interactions with DNA repair. *Toxicology letters* **72:** 353-358.

Hashimoto, K., Nakajima, Y., Matsumura, S. and Chatani, F. 2011 Comparison of four different treatment conditions of extended exposure in the in vitro micronucleus assay using TK6 lymphoblastoid cells. *Regul. Toxicol. Pharmacol.* **59**, 28–36

Hayashi, M.; Kojima, H.; Corvi, R.; Stokes, W.; Jacobs, A.; Morita, T.; Schechtman, L.; Suzuki, A. 2012. *The Validation Management Team Report on the Bhas 42 CTA*; EURL ECVAM Recommendations; EU Reference Laboratory for Alternatives to Animal Testing: Ispra, Italy.

Hayashi, Y. 1992. Overview of genotoxic carcinogens and non-genotoxic carcinogens. *Experimental and Toxicologic Pathology* **44:** 465–471.

Henkler, F., Brinkmann, J. and Luch, A. 2010. The Role of Oxidative Stress in Carcinogenesis Induced by Metals and Xenobiotics. *Cancers* **2**: 376-396.

Herceg, Z., Lambert, M., van Veldhoven, K., Demetriou, C., Vineis, P., Smith, M., Straif, K. and Wild, C. 2013. Towards incorporating epigenetic mechanisms into carcinogen identification and evaluation. *Carcinogenesis* **34:** 1955-1967.

Hernández, L., van Steeg, H., Luijten, M. and van Benthem, J. 2009. Mechanisms of non-genotoxic carcinogens and importance of a weight of evidence approach. *Mutation Research/Reviews in Mutation Research* **682:** 94-109.

Higuchi, Y., Kawai, K., Kanaki, T., Yamazaki, H., Chesné, C., Guguen-Guillouzo, C. and Suemizu, H. 2016. Functional polymer-dependent 3D culture accelerates the differentiation of HepaRG cells into mature hepatocytes. *Hepatol Res.* **46:** 1045-1057.

Himmelstein, M., Acquavella, J., Recio, L., Medinsky, M. and Bond, J. 1997. Toxicology and Epidemiology of 1,3-Butadiene. *Critical Reviews in Toxicology* **27:** 1-108.

Himmelstein, M., Capenter, S., Evans, M., Hinderliter, P. and Kenyon, E. 2004. Kinetic modeling of β-chloroprene metabolism: II. the application of physiologically based modeling for cancer dose response analysis. (Portions of this research were conducted at the National Health and Environmental Effects Laboratory (NHEERL). the research in this article has been reviewed by NHEERL and approved for publication. approval does not signify that the contents necessarily reflect the views and policies of the agency, nor does mention of a trade name or commercial products constitute endorsement or recommendation for use). *Toxicological Sciences* **79**: 28–37.

Hirano, S., Shimada, T., Osubi, J., Kodama, N., and Suzuki, K. 1994. Pulmonary clearance and inflammatory potency of intratracheally instilled or acutely inhaled nickel sulfate in rats. *Arch. Toxicol*. **68**: 548–554.

Holmes, T. and Rainsford, K., 2001. Differential effects of non-genotoxic carcinogens and proliferating agents on cell growth, survival and apoptosis in hepatic cells *in vitro*. *Life Sciences* **69:** 2975-2992.

Home office (2023) *Statistics of scientific procedures on Living Animals, Great Britain: 2022, GOV.UK*. Available at: https://www.gov.uk/government/statistics/statistics-of-scientific-procedures-on-living-animals-great-britain-2022/statistics-of-scientific-procedures-on-living-animals-great-britain-2022.

Hosseini, M., Shaki, F., Ghazi-Khansari, M. and Pourahmad, J., 2013. Toxicity of vanadium on isolated rat liver mitochondria: a new mechanistic approach. *Metallomics* **5:** 152.

Hosseinimehr, S., Izakmehri, M. and Ghasemi, A. 2015. *In vitro* protective effect of atorvastatin against ionizing radiation induced genotoxicity in human lymphocytes. *Cell Mol Biol* **61:** 68–71.

Hsu, K. H., Su, B. H., Tu, Y. S., Lin, O. and Tseng, Y. 2016. Mutagenicity in a Molecule: Identification of Core Structural Features of Mutagenicity Using a Scaffold Analysis. PLoS One. **11:** e0148900.

Hsueh, Y., Ko, Y., Huang, Y., Chen, H., Chiou, H., Huang, Y., Yang, M. and Chen, C. 2003. Determinants of inorganic arsenic methylation capability among residents of the Lanyang Basin, Taiwan: arsenic and selenium exposure and alcohol consumption. *Toxicology Letters* **137:** 49-63.

Hu, Y., Li, J., Lou, B., Wu, R., Wang, G., Lu, C., Wang, H., Pi, J. and Xu, Y. 2020. The Role of Reactive Oxygen Species in Arsenic Toxicity. *Biomolecules* **10:** 240.

Huang, X., Zhuang, Z., Frenkel, K., Klein, C. and Costa, M. 1994. The Role of Nickel and Nickel-Mediated Reactive Oxygen Species in the Mechanism of Nickel Carcinogenesis. *Environmental Health Perspectives* **102:** 281.

Huff, J., Melnick, R., Solleveld, H., Haseman, J., Powers, M. and Miller, R. 1985. Multiple Organ Carcinogenicity of 1,3-Butadiene in B6C3F 1 Mice After 60 Weeks of Inhalation Exposure. Science, **227:** 548-549.

Hughes, M., Beck, B., Chen, Y., Lewis, A. and Thomas, D. 2011. Arsenic exposure and toxicology: A historical perspective. *Toxicological Sciences* **123**: 305–332.

Hunt, T, Nasmyth, K and Novák, B. 2011. The cell cycle. Philos Trans R Soc Lond B Biol Sci. **366:** 3494-7.

Hutchinson, J. 1887. A Protest. *BMJ* **1**: 541-541.

Hwang, S., Yeom, H., Han, B., Ham, B., Lee, Y., Han, M. and Lee, M. 2020. Predicting Carcinogenic Mechanisms of Non-Genotoxic Carcinogens via Combined Analysis of Global DNA Methylation and *In Vitro* Cell Transformation. *International Journal of Molecular Sciences* **21:** 5387.

Interantional Agency for Research on Cancer (IARC). 1990. IARC Monograph on the Evaluation of Carcinogenic Risks to Humans. Chromium, Nickel and Welding. *Lyon, Paris.* International Agency for Research on Cancer.

International Agency for Research on Cancer (IARC). 2012. Arsenic, metals, fibres, and dusts. *IARC monographs on the evaluation of carcinogenic risks to humans* **100:** 41-93.

International Agency for Research on Cancer (IARC). 1980. Some Metals and Metallic Compounds. *Monographs on the Evaluation of the Carcinogenic Risk of Chemicals to Man* (IARC, Lyon, France).

International Agency for Research on Cancer (IARC). 1997. Polychlorinated dibenzo-*para*-dioxins IARC Monographs on the Evaluation of Carcinogenic Risks to Humans. *Polychlorinated Dibenzo-para-dioxins and Polychlorinated Dibenzofurans.* Lyon: IARC. **69:** 33–343.

Irigaray, P., Newby, J., Clapp, R., Hardell, L., Howard, V., Montagnier, L., Epstein, S. and Belpmme, D. 2007. Lifestyle-related factors and environmental agents causing cancer: An overview. *Biomedicine & Pharmacotherapy* **61:** 640–658.

Jackson, B., Taylor, V., Karagas, M., Punshon, T. and Cottingham, K., 2012. Arsenic, Organic Foods, and Brown Rice Syrup. *Environmental Health Perspectives* **120:** 623-626.

Jacobs, M., Colacci, A., Corvi, R., Vaccari, M., Aguila, M., Corvaro, M., Delrue, N., Desaulniers, D., Ertych, N., Jacobs, A., Luijten, M., Madia, F., Nishikawa, A., Ogawa, K., Ohmori, K., Paparella, M., Sharma, A. and Vasseur, P. 2020. Chemical Carcinogen Safety

Testing: OECD Expert Group International Consensus on the development of an integrated approach for the testing and assessment of chemical non-genotoxic carcinogens. *Archives of Toxicology* **94:** 2899–2923.

Jacobs, M., Colacci, A., Louekari, K., Luijten, M., Hakkert, B., Paparella, M. and Vasseur, P., 2016. International regulatory needs for development ofan IATA for non-genotoxic carcinogenic chemical substances. *Altex* **33**: 359-392.

Jager, J. and Ostosky-Wegman, P. 1997. Arsenic: a paradoxical human carcinogen, *Mutation Research* **386:** 181–184.

Järup, L., Pershagen, G. and Wall, S. 1989. Cumulative arsenic exposure and lung cancer in smelter workers: A dose-response study. *American Journal of Industrial Medicine* **15**: 31-41.

Jenkins, G., Souza, F., Suzen, S., Eltahir, Z., James, S., Parry, J., Griffiths, P. and Baxter, J. 2007. Deoxycholic acid at neutral and acid ph, is genotoxic to oesophageal cells through the induction of ROS: The potential role of anti-oxidants in Barrett's oesophagus. *Carcinogenesis* **28:** 136–142.

Jha, A., Noditi, M., Nilsson, R. and Natarajan, A. 1992. Genotoxic effects of sodium arsenite on human cells. *Mutation Research (Fundamental and Molecular Mechanisms of Mutagenesis)* **284:** 215-221.

Jiang, W., Hu, J-W, He, X-R, Jin, W-L, He, X-Y. 2021. Statins: A repurposed drug to fight cancer. *Journal of Experimental & Clinical Cancer Research* **40:** 241.

Jiang, X., Chen, C., Zhao, W. and Zhang, Z., 2013. Sodium arsenite and arsenic trioxide differently affect the oxidative stress, genotoxicity and apoptosis in A549 cells: An implication for the paradoxical mechanism. *Environmental toxicology and pharmacology* **36:** 891-902.

Jones, J. 2017. Americans hold record liberal views on most moral issues. Gallup. Available at https://news.gallup.com/poll/210542/americans-hold-record-liberal-views-moral-issues.aspx.

Jossé, R., Rogue, A., Lorge, E. and Guillouzo, A. 2012. An adaptation of the human HepaRG cells to the *in vitro* micronucleus assay. *Mutagenesis* **27:** 295–304.

Julien, C., Marcouiller, F., Bretteville, A., El Khoury, N., Baillargeon, J., Hebert, S. and Planel, E. 2012. Dimethyl sulfoxide induces both direct and indirect tau hyperphosphorylation. PLos One **7:** e40020.

Kaelin Jr, W., 2008. The von Hippel–Lindau tumour suppressor protein: O2 sensing and cancer. *Nature Reviews Cancer* **8:** 865-873.

Kaise, T., Yamauchi, H., Horiguchi, Y., Tani, T., Watanabe, S., Hirayama, T. and Fukui, S. 1989. A comparative study on acute toxicity of methylarsonic acid, dimethylarsinic acid and trimethylarsine oxide in mice. *Applied Organometallic Chemistry* 3: 273-277.

Kakehashi, A., Wei, M., Fukushima, S. and Wanibuchi, H. 2013. Oxidative Stress in the Carcinogenicity of Chemical Carcinogens. *Cancers* **5:** 1332-1354.

Kakiuchi-Kiyota, S., Crabbs, T., Arnold, L., Pennington, K., Cook, J., Malarkey, D. and Cohen, S., 2012. Evaluation of Expression Profiles of Hematopoietic Stem Cell, Endothelial Cell, and Myeloid Cell Antigens in Spontaneous and Chemically Induced Hemangiosarcomas and Hemangiomas in Mice. *Toxicologic Pathology* **41:** 709-721.

Kang, G., Li, Q., Chen, H. and Costa, M. 2006. Effect of metal ions on HIF-1α and Fe homeostasis in human A549 cells. *Mutation Research/Genetic Toxicology and Environmental Mutagenesis* **610:** 48-55.

Kang, Y., Hsu, W., Ou, C., Tai, H., Hsu, H., Yeh, K. and Ko, J., 2020. Metformin Mitigates Nickel-Elicited Angiopoietin-Like Protein 4 Expression via HIF-1α for Lung Tumourigenesis. *International Journal of Molecular Sciences* **21:** 619.

Karjalainen, S., Kerttula, R. and Pukkala, E. 1992. Cancer risk among workers at a copper/nickel smelter and nickel refinery in Finland. *International Archives of Occupational and Environmental Health* **63:** 547-551.

Karman, B., Basavarajappa, M., Craig, Z. and Flaws, J. 2012. 2,3,7,8-tetrachlorodibenzo-p-dioxin activates the aryl hydrocarbon receptor and alters sex steroid hormone secretion without affecting growth of mouse antral follicles *in vitro*. *Toxicology and Applied Pharmacology* **261:** 88–96.

Kasprzak, K. S., Sunderman, F. W., and Salnikow, K. 2003b. Nickel carcinogenesis. *Mutat. Res*. **533**: 67–97.

Kasprzak, K., Bal, W. and Karaczyn, A. 2003a. The role of chromatin damage in nickel-induced carcinogenesis. A review of recent developments. *Journal of Environmental Monitoring* **5:** 183-187.

Ke, Q., Davidson, T., Chen, H., Kluz, T. and Costa, M. 2006. Alterations of histone modifications and transgene silencing by nickel chloride. *Carcinogenesis* **27:** 1481-1488.

Kenyon, E. and Hughes, M. 2001. A concise review of the toxicity and carcinogenicity of dimethylarsinic acid. *Toxicology* **160:** 227-236.

Kermanizadeh, A., Berthing, T., Guzniczak, E., Wheeldon, M., Whyte, G., Vogel U., Moritz, W. and Stone, V. 2019. Assessment of nanomaterial-induced hepatotoxicity using a 3D human primary multi-cellular microtissue exposed repeatedly over 21 days—the suitability of the *in vitro* system as an *in vivo* surrogate. *Particle Fibre Toxicol* **16**: 42.

Kim, H., Kim, Y. and Seo, Y. 2015. An Overview of Carcinogenic Heavy Metal: Molecular Toxicity Mechanism and Prevention. *Journal of Cancer Prevention* **20:** 232-240.

Kinoshita, A., Wanibuchi, H., Wei, M. and Fukushima, S. 2006. Hormesis in carcinogenicity of non-genotoxic carcinogens. *Journal of Toxicologic Pathology* **19:** 111–122.

Kirkland, D., Aardema, M., Henderson, L. and Müller, L. 2005. Evaluation of the ability of a battery of three *in vitro* genotoxicity tests to discriminate rodent carcinogens and non-carcinogens I. Sensitivity, specificity and relative predictivity. *Mutat Res.* **584**: 1-256.

Kirkland, D., Kasper, P., Martus, H., Müller, L., van Benthem, J., Madia, F. and Corvi, R. 2016. Updated recommended lists of genotoxic and non-genotoxic chemicals for assessment of the performance of new or improved genotoxicity tests. *Mutation Research/Genetic Toxicology and Environmental Mutagenesis* **795:** 7-30.

Kirkland, D., Pfuhler, S., Tweats, D., Aardema, M., Corvi, R., Darroudi, F., Elhajouji, A., Glatt, H., Hastwell, P., Hayashi, M., Kasper, P., Kirchner, S., Lynch, A., Marzin, D., Maurici, D., Meunier, J., Müller, L., Nohynek, G., Parry, J., Parry, E., Thybaud, V., Tice, R., van

Benthem, J., Vanparys, P. and White, P. 2007. How to reduce false positive results when undertaking *in vitro* genotoxicity testing and thus avoid unnecessary follow-up animal tests: Report of an ECVAM Workshop. *Mutation Research/Genetic Toxicology and Environmental Mutagenesis* **628**: 31-55.

Kirsch-Volders, M. 1997. Towards a validation of the micronuclei test. *Mutation Res.* **392:** 1-4.

Kirsch-Volders, M. and Fenech, M. 2001. Inclusion of micronuclei in non-divided mononuclear lymphocytes and necrosis/apoptosis may provide a more comprehensive cytokinesis block micronucleus assay for biomonitoring purposes. *Mutagenesis* **16:** 51–58.

Klein, C., Leszczynska, J., Hickey, C. and Rossman, T. 2007. Further evidence against a direct genotoxic mode of action for arsenic-induced cancer. *Toxicology and Applied Pharmacology* **222:** 289-297.

Knerr, S. and Schrenk, D. 2006. Carcinogenicity of 2,3,7,8-tetrachlorodibenzo-p-dioxin in experimental models. *Molecular Nutrition & amp; Food Research* **50:** 897-907.

Koibuchi, N. 2006. Thyroid hormone action in developing brain and its modulation by polyhalogenated aromatic hydrocarbons. *International Congress Series* **1287:** 190–194.

Kopp-Schneider, A., Prieto, P., Kinsner-Ovaskainen, A. and Stanzel., S. 2013. Design of a testing strategy using non-animal based test methods: Lessons learnt from the Acutetox Project. *Toxicology in Vitro* **27:** 1395–1401.

Kusiak, R., Springer, J., Ritchie, A. and Muller, J. 1991. Carcinoma of the lung in Ontario gold miners: possible aetiological factors. *Occupational and Environmental Medicine* **48:** 808-817.

Laconi, E., Marongiu, F. and DeGregori, J. 2020. Cancer as a disease of old age: Changing Mutational and Microenvironmental Landscapes. *British Journal of Cancer* **122:** 943–952.

Lautraite, S., Bigot-Lasserre, D., Bars, R. and Carmichael, N. 2003. Optimisation of cell-based assays for medium throughput screening of oxidative stress. *Toxicology In Vitro* **17:** 207-220.

Lee, S., Yum, Y., Kim, S., Kim, Y., Lim, J., Lee, W.J., Koo, K., Kim, J.H., Kim, J.E., Lee, W.S., Sohn, S., Park, S., Park., J., Lee, J. and Kwon, S. 2013. Distinguishing between genotoxic and non-genotoxic hepatocarcinogens by gene expression profiling and bioinformatic pathway analysis. *Scientific Reports* 3: 2783.

Leonard, S.S., Bower, J.J. and Shi, X., 2004. Metal-induced toxicity, carcinogenesis, mechanisms and cellular responses. *Molecular and cellular biochemistry **255*:** 3-10.

Lesage, G. 2015. Persistent organic pollutant. In: Giorno L, Drioli E (eds) Encyclopedia of membranes. Springer, Berlin 1-2.

Levine, A. 1997. p53, the Cellular Gatekeeper for Growth and Division. *Cell* **88:** 323-331.

Li, J. and Rossman, T. 1989. Inhibition of DNA ligase activity by arsenite: a possible mechanism of its comutagenesis. *Molecular Toxicology* **2:** 1-9.

Li, J. and Rossman, T. 1991. Comutagenesis of sodium arsenite with ultraviolet radiation in Chinese hamster V79 cells. *Biology of Metals* **4**: 197-200.

Li, W., Wanibuchi, H., Salim, E., Yamamoto, S., Yoshida, K., Endo, G. and Fukushima, S., 1998. Promotion of NCI-Black-Reiter male rat bladder carcinogenesis by dimethylarsinic acid an organic arsenic compound. *Cancer Letters* **134:** 29-36.

Li, X., Chen, S., Guo, X., Wu, Q., Seo, J., Guo, L., Manjanatha, M., Zhou, T., Witt, K. and Mei, N. 2020. Development and Application of TK6-derived Cells Expressing Human Cytochrome P450s for Genotoxicity Testing. *Toxicological Sciences* **175:** 251-265.

Li, Y., Qu, X., Qu, J., Zhang, Y., Liu, J., Teng, Y., Hu, X., Hou, K. and Liu, Y. 2009. Arsenic trioxide induces apoptosis and G2/M phase arrest by inducing CBL to inhibit PI3K/akt signaling and thereby regulate p53 activation. *Cancer Letters* **284:** 208–215.

Lichtenstein, P., Holm, N., Verkasalo, P., Iliadou, A., Kaprio, J., Koskenvua, M., Pukkala, E., Skytthe, A. and Hemminki, K. *2000.* Environmental and heritable factors in the causation of cancer-analyses of cohorts of twins from Sweden, Denmark and Finland. *N Engl J Med* **342:** 78-85.

Liu, C., Wright, C., McAdam, K., Taebunpakul, S., Heroult, J., Braybrook, J. and Goenaga-Infante, H. 2012. Arsenic speciation in tobacco and cigarette smoke. *Beiträge zur Tabakforschung Int Contrib Tob Res.* **25:** 375–380

Liu, Y., Lv, X., Xie, N., Fang, Z., Ren, W., Gong, Y., Jin, Y. and Zhang, J. 2020. Time trends analysis of statin prescription prevalence, therapy initiation, dose intensity, and utilization from the hospital information system of Jinshan Hospital, Shanghai (2012–2018). *BMC Cardiovascular Disorders* **20:** .201.

Llewellyn, S., Conway, G., Shah, U.-K., Evans, S., Jenkins, G., Clift, M. and Doak, S. 2020. Advanced 3D Liver Models for *In vitro* Genotoxicity Testing Following Long-Term Nanomaterial Exposure. *Journal of Visualized Experiments* **5**(160).

Loeb, L. 2001. A mutator phenotype in cancer. Cancer Research **61**: 3230-3239.

Lorge, E. 2010. Comparison of different cytotoxicity measurements for the in vitro micronucleus assay using L5178Y and TK6 cells in support of OECD draft Test Guideline 487. *Mutat. Res.* **702**, 199–207.

Lorge, E., Moore, M., Clements, J., O'Donovan, M., Fellows, M., Honma, M., Kohara, A., Galloway, S., Armstrong, M., Thybaud, V., Gollapudi, B., Aardema, M. and Tanir, J. 2016. Standardized cell sources and recommendations for good cell culture practices in genotoxicity testing. *Mutation Research/Genetic Toxicology and Environmental Mutagenesis* **809:** 1-15.

Luechtefeld, T., Maertens, A., Russo, D. P., Rovida, C., Zhu, H. and Hartung, T. 2016. Analysis of Draize eye irritation testing and its prediction by mining publicly available 2008–2014 REACH data. *ALTEX* **33:** 123–134.

Lugon-Moulin, N., Martin, F., Krauss, M., Ramey, P. and Rossi, L. 2008. Arsenic concentration in tobacco leaves: a study on three commercially important tobacco (nicotiana tabacum L.) types. *Water Air Soil Pollut.* **192**: 315–319.

Lukamowicz, M., Woodward, K., Kirsch-Volders, M., Suter, W. and Elhajouji, A. 2011. A flow cytometry based *in vitro* micronucleus assay in TK6 cells—Validation using early stage pharmaceutical development compounds. *Environ. Mol. Mutagen.* **52**: 363-372.

Lundqvist, J., Helmersson, E. and Oskarsson, A. 2019. Hormetic Dose Response of NaAsO2 on Cell Proliferation of Prostate Cells *in Vitro*: Implications for Prostate Cancer Initiation and Therapy. *Dose-Response* **17:** 155932581984337.

Lustman, A., Nakar, S., Cohen, A. and Vinker, S., 2013. Statin use and incident prostate cancer risk: does the statin brand matter? A population-based cohort study. *Prostate Cancer and Prostatic Diseases* **17**: 6-9.

Luvai, A., Mbagaya, W., Hall, A. and Barth, J. 2012. Rosuvastatin: A Review of the Pharmacology and Clinical Effectiveness in Cardiovascular Disease. Clinical Medicine Insights: Cardiology **6:** 17–33.

Lynn, S., Yew, F., Chen, K. and Jan, K., 1997. Reactive oxygen species are involved in nickel inhibition of DNA repair. *Environmental and Molecular Mutagenesis* **29:** 208-216.

Ma, C., Kesarwala, A., Eggert, T., Medina-Echeverz, J., Kleiner, D., Jin, P., Stroncek, D., Terabe, M., Kapoor, V., ElGindi, M., Han, M., Thornton, A., Zhang, H., Egger, M., Luo, J., Felsher, D., McVicar, D., Weber, A., Heikenwalder, M. and Greten, T. 2016. NAFLD causes selective CD4+ T lymphocyte loss and promotes hepatocarcinogenesis. *Nature* **531:** 253-257.

Macaluso, M., Larson, R., Delzell, E., Sathiakumar, N., Hovinga, M., Julian, J., Muir, D., Cole, P. 1996. Leukemia and cumulative exposure to butadiene, styrene and benzene among workers in the synthetic rubber industry. *Toxicology* **113:** 190-202.

Macko, P., Palosaari, T. and Whelan, M. 2021. Extrapolating from acute to chronic toxicity *in vitro*. *Toxicology in Vitro* **76**: 105206.

Madassery, J., Raghavan, R. and Cheriyamundath, S. 2015. Dimethyl sulfoxide inactivates the anticancer effect of cisplatin against human myelogenous leukemia cell lines in *in vitro* assays. *Indian Journal of Pharmacology* **47:** 322.

Mahadevan, B., Snyder, R., Waters, M., Benz, R., Kemper, R., Tice, R. and Richard, A. 2011. Genetic toxicology in the 21st century: Reflections and future directions. *Environ. Mol. Mutagen*. **52:** 339-354.

Mandal, B. and Suzuki, K. 2002. Arsenic round the world: a review. *Talanta* **58:** 201-235.

Mandal, P. 2005. Dioxin: a review of its environmental effects and its aryl hydrocarbon receptor biology. *Journal of Comparative Physiology B* **175:** 221-230.

Mansoury, M., Hamed, M., Karmustaji, R., Al Hannan, F., Safrany, S. 2021. The edge effect: A global problem. The trouble with culturing cells in 96-well plates. Biochem Biophys Rep. **26**: 100987.

Manuppello, J. and Willett, C. 2008. Longer Rodent Bioassay fails to address 2-year bioassay's flaws. *Environmental Health Perspectives* **116:** A516-A517.

Maqbool, F., Mostafalou, S., Bahadar, H., Abdollahi, M. 2016. Review of endocrine disorders associated with environmental toxicants and possible involved mechanisms. *Life Sci.* ***145*****:** 265–273.

Marone, P., Hall, W. and Hayes, A. 2014. Reassessing the two-year rodent carcinogenicity bioassay: A review of the applicability to human risk and current perspectives. *Regulatory Toxicology and Pharmacology* **68:** 108–118.

Marsh, G., Kruchten, A. and Buchanich, J. 2020. Mortality patterns among industrial workers exposed to chloroprene and other substances. *Journal of Occupational & Environmental Medicine* **63**: 126–138.

Marsh, J. 1837. Separation of arsenic. In: Carson J, editor. *The American Journal of Pharmacy.* Vol. II. Philadelphia, PA: Merriew and Gunn. 307–314.

Martinez, V., Vucic, E., Becker-Santos, D., Gil, L. and Lam, W. 2011. Arsenic Exposure and the Induction of Human Cancers. *Journal of Toxicology* **2011:** 1-13.

Martins, C., Dreij, K. and Costa, P. 2019. The state-of-the art of environmental toxicogenomics: Challenges and perspectives of "OMICS" approaches directed to toxicant mixtures. *International Journal of Environmental Research and Public Health* **16:** 4718.

Mathijs, K.,Brauers, K., Jennen, D., Boorsma, A., Herwijnen, M., Gottschalk, R., Kleinjans, J. and van Delft, J. 2009. Discrimination for genotoxic and nongenotoxic carcinogens by gene expression profiling in primary mouse hepatocytes improves with exposure time. *Toxicological Sciences* **112:** 374–384.

Mattes, W. 2020. *In vitro* to *in vivo* translation. *Current Opinion in Toxicology* **23-24:** 114–118.

Mazumder, D. 2000. Diagnosis and treatment of chronic arsenic poisoning. *United Nations Synthesis Report on Arsenic in Drinking Water*, WHO, Geneva, Switzerland.

McTaggart, F. 2003. Comparative pharmacology of rosuvastatin. *Atherosclerosis Supplements* **4:** 9–14.

McTaggart, F., Buckett, L., Davidson, R., Holdgate, G., McCormick, A., Schneck, D., Smith, G. and Warwick, M. 2001. Preclinical and clinical pharmacology of rosuvastatin, a new 3-hydroxy- 3-methylglutaryl coenzyme A reductase inhibitor11CRESTOR is a trademark, the property of AstraZeneca PLC. Research discussed in this article was supported by AstraZeneca. *The American Journal of Cardiology* **87:** 28-32.

Melnick, R., Elwell, M., Roycroft, J., Chou, B., Ragan, H. and Miller, R. 1996. Toxicity of inhaled chloroprene (2-chloro-1,3-butadiene) in F344 rats and B6C3F(1) mice. *Toxicology* **108**: 79–91.

Meyer, A. 1983. *In vitro* transformation assays for chemical carcinogens. *Mutation Research/Reviews in Genetic Toxicology* **115:** 323-338.

Michaleas, S., Laios, K., Tsoucalas, G. and Androutsos, G. 2021. Theophrastus Bombastus von Hohenheim (Paracelsus) (1493–1541): The eminent physician and pioneer of toxicology. *Toxicology Reports* **8:** 411–414.

Michaleas, S., Veskoukis, A., Samonis, G., Pantos, C., Androutsos, G., Karamanou, M. 2022. Mathieu Joseph Bonaventure Orfila (1787-1853): The Founder of Modern Toxicology. *Maedica (Bucur).* **17:** 532-537.

Mirabelli, P., Coppola, L. and Salvatore, M. 2019. Cancer cell lines are useful model systems for Medical Research. *Cancers* **11:** 1098.

Molinari, M. 2000. Cell cycle checkpoints and their inactivation in human cancer. *Cell Prolif.* **33:** 261-74.

Mookerjee, S., Goncalves, R., Gerencser, A., Nicholls, D. and Brand, M. 2015. The contributions of respiration and glycolysis to extracellular acid production. *Biochimica et Biophysica Acta* **1847:** 171-181.

Muller, H. 1927. Artificial transmutation of the Gene. *Science* **66:** 84–87.

Murphy, M. 2009. How mitochondria produce reactive oxygen species. *Biochem J.* **417:** 1–13.

Mustafa, S., Al-Subiai, S., Davies, S. and Jha, A. 2011. Hypoxia-induced oxidative DNA damage links with higher level biological effects including specific growth rate in common carp, *Cyprinus carpio* L. *Ecotoxicology* **20**: 1455-1466. https://DOI 10.1007/s10646-011-0702-5.

Mustafa, S., Davies, S. and Jha, A. 2012. Determination of hypoxia and dietary copper mediated sub-lethal toxicity in carp, *Cyprinus carpio*, at different levels of biological organisation. *Chemosphere* **87:** 413-422. http://doi:10.1016/j.chemosphere.2011.12.037.

Mustafa, S., Karieb, S., Davies, S. and Jha, A. 2015. Assessment of oxidative damage to DNA, transcriptional expression of key genes, lipid peroxidation and histopathological changes in carp *Cyprinus carpio* L. following exposure to chronic hypoxic and subsequent recovery in normoxic conditions. *Mutagenesis* **30:** 107-116. https://doi.org/10.1093/mutage/geu048.

Muz, B. de la Puente, P., Azab, F., Azab, A. 2015. The role of hypoxia in cancer progression, angiogenesis, metastasis, and resistance to therapy. *Hypoxia* **11:** 83-92.

Nacif-Pimenta, R., da Silva Orfanó, A., Mosley, I., Karinshak, S., Ishida, K., Mann, V., Coelho, P., da Costa, J., Hsieh, M., Brindley, P. and Rinaldi, G. 2019. Differential responses of epithelial cells from urinary and biliary tract to eggs of *Schistosoma haematobium* and *S. mansoni*. *Sci Rep* **9**, 10731.

Nagarathna, P., Wesley, M., Reddy, P. and Reena, K. 2013. Review on genotoxicity, its molecular mechanisms and prevention. *Int J Pharm Sci Rev Res*. **22:** 236–43.

Naranmandura, H., Xu, S., Sawata, T., Hao, W., Liu, H., Bu, N., Ogra, Y., Lou, Y. and Suzuki, N. 2011. Mitochondria Are the Main Target Organelle for Trivalent

Monomethylarsonous Acid (MMAIII)-Induced Cytotoxicity. *Chemical Research in Toxicology* **24:** 1094-1103.

National Toxicology Program (NTP). 1998. Toxicology and carcinogenesis studies of chloroprene (CAS No 126-99-8) in F344/N rats and B6C3F1 mice (inhalation studies). Report No. NTP TR 467 (pp. 1–372). Research Triangle Park, NC: *National Toxicology Program Technical Report Series* **467:** 1-379.

National Toxicology Program (U.S.) 2013. Report on Carcinogens. Monograph on. Research Triangle Park, NC: National Toxicology Program, U.S. Department of Health and Human Services http://ntp.niehs.nih.gov/pubhealth/roc/candidates/index.html

National toxicology Program. 1996. NTP Toxicology and Carcinogenesis Studies of Nickel Oxide (CAS No. 1313-99-1) in F344 Rats and B6C3F1 Mice (Inhalation Studies). *National Toxicology Program Tech Rep Ser. **451**: 1—381.*

National Toxicology Programme (NTP). 2000. Ninth Report on Carcinogens, US DHHS, Research Triangle Park, NC.

NC3Rs. 2022. The 3Rs, NC3Rs. Available at: https://nc3rs.org.uk/who-we-are/3rs.

Nelson-Rees, W., Owens, R., Arnstein, P. and Kniazeff, A, 1976. Source, alterations, characteristics and use of a new dog cell line (Cf2Th). *In Vitro*. **12:** 665–669.

Nesnow, S., Roop, B., Lambert, G., Kadiiska, M., Mason, R., Cullen, W. and Mass, M. 2002. DNA Damage Induced by Methylated Trivalent Arsenicals Is Mediated by Reactive Oxygen Species. *Chemical Research in Toxicology* **15:** 1627-1634.

Neubauer, O. 1947. Arsenical Cancer: A Review. *British Journal of Cancer* **1:** 192-251.

Ng, N. and Ooi, L. 2021. A Simple Microplate Assay for Reactive Oxygen Species Generation and Rapid Cellular Protein Normalization. Bio Protoc.**11:** e3877.

Nguyen, S., Nguyen, H. and Truong, K. 2020 Comparative cytotoxic effects of methanol, ethanol and DMSO on human cancer cell lines. *Biomedical Research and Therapy* **7:** 3855–3859.

Nicholas, D., Proctor, E., Raval, F., Ip, B., Habib, C., Ritou, E., Grammatopoulos, T., Steenkamp, D., Dooms, H., Apovian, C., Lauffenburger, D. and Nikolajczyk, B. 2017. Advances in the quantification of mitochondrial function in primary human immune cells through extracellular flux analysis. *PLoS One.* **12:** e0170975.

Nie, A., McMillian, M., Parker, J., Leone, A., Bryant, S., Yieh, L., Bittner, A., Nelson, J., Carmen, A., Wan, J. and Lord, P. 2006. Predictive toxicogenomics approaches reveal underlying molecular mechanisms of nongenotoxic carcinogenicity *Mol. Carcinog*. **45**: 914–933.

Niedernhofer, L., Daniels, J., Rouzer, C., Greene, R. and Marnett, L. 2003. Malondialdehyde, a product of lipid peroxidation, is mutagenic in human cells. *Journal of Biological Chemistry* **278:** 31426–31433.

NIH. 2023. *Toxicology, National Institute of Environmental Health Sciences*. U.S. Department of Health and Human Services. Available at: https://www.niehs.nih.gov/health/topics/science/toxicology/index.cfm#:~:text=What%20is%20toxicology%3F,%2C%20animals%2C%20and%20the%20environment.

Nilsson, R., Jha, A., Zaprianov, Z. and Natarajan, A. 1993. Chromosomal aberrations in humans exposed to arsenic in the Srednogorie area, Bulgaria. *Fresenius Environ. Bull.* **2:** 59-64.

Nohmi, T. 2018. Thresholds of Genotoxic and Non-Genotoxic Carcinogens. *Toxicological Research* **34:** 281–290.

Nriagu, J. and Azcue, J. 1990. Arsenic in the environment. Part I. Cycling and characterization. New York: Wiley; 1-15.

Nurse, P., Masui, Y. and Hartwell, L. 1998. Understanding the cell cycle. *Nat. Med.* **4:** 1103–1106.

OECD. 2010a. OECD guideline for the testing of Chemicals. Proposal for updating Test Guideline 487. Available at: https://www.oecd.org/chemicalsafety/testing/50108793.pdf

OECD. *2010b. Guidelines for the Testing of chemicals*. Available at: https://www.oecd.org/chemicalsafety/testing/.

OECD. 2016a. *In Vitro* Mammalian Cell Micronucleus Test (MNvit). OECD Guideline for Testing of Chemicals No. 487, OECD, Paris. Available at: [http://www.oecd.org/env/testguidelines].

OECD. 2016b. Organisation for Economic and Cooperative Development. Guidance Document on the *in vitro* Bhas 42 cell transformation assay. Series on Testing and Assessment. No. 231. Paris. Available online: https://www.oecd.org/env/ehs/testing/ENV_JM_MONO(2016)1.pdf

Oecd.org. 2012. [online] Available at: <https://www.oecd.org/env/ehs/testing/TG487%20Oct%202012%20updated%2029oct.pdf> .

Ökçesiz, A. and Ündeğer Bucurgat, Ü. 2021. Evaluation of toxic effects of statins and their possible role in treatment of cancer. *İstanbul Journal of Pharmacy* **51:** 154-160.

Olsson, A., Pears, J., McKellar, J., Mizan, J. and Raza, A. 2001. Effect of rosuvastatin on low-density lipoprotein cholesterol in patients with hypercholesterolemia. *The American Journal of Cardiology* **88:** 504–508.

Onishi, H. 1969. Arsenic, in: K.H. Wedepohl (Ed.), Handbook of Geochemistry, Springer-Verlag, New York. Vol. II-2, Chapter 33.

(b) Oommen, D, Dodd, N., Yiannakis, D., Moyeed, R. and Jha, A. 2016. Linking genotoxicity and cytotoxicity with membrane fluidity: a comparative study in ovarian cancer cell lines following exposure to auranofin. *Mutation Research- Genetic Toxicology and Environmental Mutagenesis* **809**: 43-49.

(a) Oommen, D., Yiannakis, D. and Jha, A. 2016. BRCA1 deficiency increases the sensitivity of ovarian cancer cells to auranofin. *Mutation Research (Fundamental Mol. Mech. of Mutagenesis)* ***784-785:*** 8–15.

Oparka, M., Walczak, J., Malinska, D., van Oppen, L., Szczepanowska, J., Koopman, W., Wieckowski, M. 2016. Quantifying ROS levels using CM-H2DCFDA and HyPer. *Methods* **109:** 3-11.

Orsolin, P., Silva-Oliveira, R. and Nepomuceno, J. 2015. Modulating effect of synthetic statins against damage induced by doxorubicin in somatic cells of *drosophila melanogaster*. *Food and Chemical Toxicology* **81:** 111–119.

Ota, H., Shionome, T., Suguro, H., Saito, S., Ueki, K., Arai, Y. and Asano, M. 2018. Nickel chloride administration prevents the growth of oral squamous cell carcinoma. *Oncotarget* **9**: 24109-24121.

Ottolenghi, A., Haseman, J., Payne, W., Falk, H. and MacFarland, H. 1975.Inhalation studies of nickel sulfide in pulmonary carcinogenesis of rats. *Journal of National Cancer Institute **54**: 1165-72.*

Ouyang, W., Zhang, D., Li, J., Verma, U., Costa, M. and Huang, C. 2009. Soluble and insoluble nickel compounds exert a differential inhibitory effect on cell growth through IKKα-dependent cyclin D1 down-regulation. *Journal of Cellular Physiology* **218:** 205-214.

Ozden, S., Kara, N., Sezerman, O., Durasi, İ., Chen, T., Demirel, G., Alpertunga, B., Chipman, J. and Mally, A. 2015. Assessment of global and gene-specific DNA methylation in rat liver and kidney in response to non-genotoxic carcinogen exposure. *Toxicology and Applied Pharmacology* **289:** 203-212.

Pamphilon, D., Selogie, E., Mckenna, D., Cancelas-Peres, J., Szczepiorkowski, Z., Sacher, R., McMannis, J., Eichler, H., Garritsen, H., Takanashi, M., van de Watering, Stroncek, D. and Reems, J. 2013. Current practices and prospects for standardization of the hematopoietic colony-forming unit assay: a report by the cellular therapy team of the Biomedical excellence for safer transfusion (BEST) collaborative. Cytotherapy **15:** 255–62.

Pan, J., Chang, Q., Wang, X., Son, Y., Zhang, Z., Chen, G., Luo, J., Bi, Y., Chen, F. and Shi, X. 2011. Reactive oxygen species-activated Akt/ASK1/p38 signaling pathway in nickel compound-induced apoptosis in BEAS 2B cells. *Chemical research in toxicology **23*:** 568-577.

Pandey, R. and Srivastava, S., 2000. Spermatotoxic Effects of Nickel in Mice. *Bulletin of Environmental Contamination and Toxicology* **64:** 161-167.

Pareek, A., Godavarthi, A., Issarani, R. and Nagori, B. 2013. Antioxidant and Hepatoprotective Activity of Fagonia Schweinfurthii (Hadidi) Hadidi Extract in Carbon Tetrachloride Induced Hepatotoxicity in HepG2 Cell Line and Rats. *J. Ethnopharmacol.* **150**: 973–981.

Patrizi, B. and Siciliani de Cumis, M. 2018. TCDD toxicity mediated by epigenetic mechanisms *International Journal of Molecular Sciences* **19:** 4101.

Pérez, L., González-José, R. and García, P. 2016. Prediction of non-genotoxic carcinogenicity based on genetic profiles of short term exposure assays. *Toxicological Research* **32:** 289–300.

Peters, K., Unger, R.E., Barth, S., Gerdes, T. and Kirkpatrick, C. 2001. Induction of apoptosis in human microvascular endothelial cells by divalent cobalt ions. Evidence for integrin-mediated signaling via the cytoskeleton. *Journal of Materials Science: Materials in Medicine **12*****:*** 955-958.

Pirkle, J., Wolfe, W., Patterson, D., Needham, L., Michalek, J., Miner, J., Peterson, M. and Phillips, D. 1989. Estimates of the half-life of 2,3,7,8-tetrachlorodibenzo-p-dioxin in Vietnam veterans of operation ranch hand. *J. Toxicol. Environ. Health **27*****:*** 165–171.

Plitzko, B. and Loesgen, S. 2018. Measurement of Oxygen Consumption Rate (OCR) and Extracellular Acidification Rate (ECAR) in Culture Cells for Assessment of the Energy Metabolism. Bio Protoc. 8: e2850.

Polychloroprene: 9010-98-4. 2023. *ChemicalBook*. Available at: https://www.chemicalbook.com/ChemicalProductProperty_EN_CB0414643.htm

Poonkothai, M., Vijayavathi, B. 2012. Nickel as an essential element and a toxicant. Inernational Journal of Environmental Science **1:** 285-288.

Pozarowski, P. and Darzynkiewicz, Z. 2004. Analysis of Cell Cycle by Flow Cytometry. In: Schönthal, A.H. (eds) Checkpoint Controls and Cancer. Methods in Molecular Biology, vol 281. Humana Press.

Pratt, I. and Barron, T. 2003. Regulatory recognition of indirect genotoxicity mechanisms in the European Union. *Toxicology Letters* **140-141**:53–62.

PubChem. 2023. Sodium arsenite- *National Center for Biotechnology Information. PubChem Compound Database*. U.S. National Library of Medicine. Available at: https://pubchem.ncbi.nlm.nih.gov/compound/Sodium-arsenite.

Pubchem.ncbi.nlm.nih.gov. 2022. *Nickel chloride*. [online] Available at: <https://pubchem.ncbi.nlm.nih.gov/compound/24385>

Pubchem.ncbi.nlm.nih.gov. 2022. *Sodium arsenite.* [online] Available at: <https://pubchem.ncbi.nlm.nih.gov/compound/Sodium-arsenite#section=2D-Structure> [Accessed 28 March 2022].

Public Citizen. 2022. Petition to Ban Cholesterol-Lowering Drug Rosuvastatin (Crestor) - Public Citizen. [online] Available at: https://www.citizen.org/article/petition-to-ban-cholesterol-lowering-drug-rosuvastatin-crestor/.

Rabbani, G., Saha, S., Akhtar, M., Marni, F., Mitra, A., Ahmed, S., Alauddin, M., Bhattacharjee, M., Sultana, S., Chowdhury, A. 2003. Antioxidants in detoxification of arsenic-induced oxidative injury in rabbits: preliminary results. *J. Environ. Sci. Health Part A: Tox. Hazard Subst. Environ. Eng.* **38:** 273-287.

Raisuddin, S. and Jha, A. 2004. Relative sensitivity of fish and mammalian cells to sodium arsenate and arsenite as determined by alkaline single cell gel electrophoresis and cytokinesis-block micronucleus assay. *Environmental and Molecular Mutagenesis* **44:** 83-89.

Ramaiahgari, S., den Braver, M., Herpers, B., Terpstra, V., Commandeur, J., van de Water, B., Price, L. 2014. A 3D *in vitro* model of differentiated HepG2 cell spheroids with improved liver-like properties for repeated dose high-throughput toxicity studies. *Arch Toxicol.* **88:** 1083-95.

Randolph, N. 2021. Pipeline Logic and Culpability: Establishing a Continuum of Harm for Sacrifice Zones. *Frontiers in Environmental Science* **9**.

RCN. 2023. *Prevention is better than cure: Campaigns: Royal College of Nursing, The Royal College of Nursing*. Available at: https://www.rcn.org.uk/Get-Involved/Campaign-with-us/Prevention-is-better-than-cure#:~:text=The%20phrase%20%27prevention%20is%20better,Ireland%2C%20Scotland%2C%20Wales).

Refsvik, T., and Andreassen, T. 1995. Surface binding and uptake of nickel(II) in human epithelial kidney cells: modulation by ionomycin, nicardipine and metals. *Carcinogenesis* **16**:1107–1112.

Ren, N., Atyah, M., Chen, W. and Zhou, C-H. 2017. The various aspects of genetic and epigenetic toxicology: testing methods and clinical applications. *J Transl Med* **15**: 110.

Rhiouani, H., El-Hilaly, J., Israili, Z. and Lyoussi, B. 2008. Acute and sub-chronic toxicity of an aqueous extract of the leaves of Herniaria glabra in rodents. *Journal of Ethnopharmacology* **118:** 378-386.

Rimon, G., Bazenet, C., Philpott, K. and Rubin, L. 1997. Increased surface phosphatidylserine is an early marker of neuronal apoptosis. *J Neurosci Res.* **48:** 563–570.

Robertson Lab. 2023. *The chemistry behind the assay, The Robertson Lab | Robertson Lab | Perelman School of Medicine at the University of Pennsylvania*. Available at: https://www.med.upenn.edu/robertsonlab/

Robles, A., Bemmels, N., Foraker, A. and Harris, C. 2001. *APAF-1* Is a Transcriptional Target of p53 in DNA Damage-induced Apoptosis. *Cancer Res* **61**: 6660–6664.

Roederer, M. 2001. Spectral compensation for flow cytometry: visualization artifacts, limitations, and caveats. Cytometry **45:** 194-205.

Roesslein, M., Hirsch, C., Kaiser, J., Krug, H. and Wick, P. 2013. Comparability of *in vitro* tests for bioactive nanoparticles: A common assay to detect reactive oxygen species as an example. *International Journal of Molecular Sciences* **14:** 24320–24337.

Rong, Y., Durden, D., Van Meir, E. and Brat, D. 2006. 'Pseudopalisading' Necrosis in Glioblastoma: A Familiar Morphologic Feature That Links Vascular Pathology, Hypoxia, and Angiogenesis. *Journal of Neuropathology & Experimental Neurology* **65:** 529-539.

Rose, S., Frye, R., Slattery, J., Wynne, R., Tippett, M., Melnyk, S. and James, S. 2014. Oxidative stress induces mitochondrial dysfunction in a subset of autistic lymphoblastoid cell lines. *Transl Psychiatry* **4:** e377.

Rosefort, C., Fauth, E. and Zankl, H. 2004. Micronuclei induced by aneugens and clastogens in mononucleate and binucleate cells using the cytokinesis block assay. *Mutagenesis* **19:** 277–284.

Rossman, T. 2003. Mechanism of arsenic carcinogenesis: an integrated approach. *Mutation Research/Fundamental and Molecular Mechanisms of Mutagenesis* **533:** 37-65.

Rossman, T., Goncharova, E., Rajah, T. and Wang, Z. 1997. Human cells lack the inducible tolerance to arsenite seen in hamster cells. Mutat Res **386**: 307–314.

Rothe, G. and Valet, G. 1990. Flow Cytometric Analysis of Respiratory Burst Activity in Phagocytes With Hydroethidine and 2′,7′-Dichlorofluorescin. *Journal of Leukocyte Biology* **47:** 440-448.

Roy, J., Chatterjee, D., Das, N. and Giri, A. 2018. Substantial Evidences Indicate That Inorganic Arsenic Is a Genotoxic Carcinogen: a Review. *Toxicological Research* **34:** 311-324.

Royall, J. and Ischiropoulos, H. 1993. Evaluation of 2′,7′-Dichlorofluorescin and Dihydrorhodamine 123 as Fluorescent Probes for Intracellular H2O2 in Cultured Endothelial Cells. *Archives of Biochemistry and Biophysics* **302**: 348-355.

Ruch, W., Cooper, P. and Baggiolini, M. 1983. Assay of H2O2 production by macrophages and neutrophils with homovanillic acid and horse-radish peroxidase. *J. Immunol. Methods* **63:** 347–357.

Rudel, D., Douglas, C., Huffnagle, I., Besser, J. and Ingersoll, C. 2013. Assaying Environmental Nickel Toxicity Using Model Nematodes. *PLoS ONE* **8:** e77079.

Russell, W. and Burch, R. 1959. The Principles of Humane Experimental Technique. London, UK: Methuen.

Saha, K. 2003. Diagnosis of Arsenicosis. *Journal of Environmental Science and Health, Part A* **38:** 255-272.

Salami, J., Warraich, H., Valero-Elizondo, J., Spatz, E., Desai, N., Rana, J., Virani, S., Blankstein, R., Khera, A., Blaha, M., Blumenthal, R., Lloyd-Jones, D. and Nasir, K. 2017. National Trends in Statin Use and Expenditures in the US Adult Population From 2002 to 2013. *JAMA Cardiology* **2:** 56-65.

Salnikow, K. and Zhitkovich, A. 2008. Genetic and epigenetic mechanisms in metal carcinogenesis and cocarcinogenesis: nickel, arsenic, and chromium. *Chem. Res. Toxicol*. **21:** 28-44.

Salnikow, K., Davidson, T., Zhang, Q., Chen, L., Su, W. and Costa, M. 2003. The involvement of hypoxia-inducible transcription factor-1-dependent pathway in nickel carcinogenesis. *Cancer Res.* **63**: 3524–30.

Samizo, S and Kaneko, H. 2023 Predictive Modeling of HMG-CoA Reductase Inhibitory Activity and Design of New HMG-CoA Reductase Inhibitors. ACS Omega. **8**: 27247-27255.

Sangweni, N., Dludla, P., Chellan, N., Mabasa, L., Sharma, J. and Johnson, R. 2021. The Implication of Low Dose Dimethyl Sulfoxide on Mitochondrial Function and Oxidative Damage in Cultured Cardiac and Cancer Cells. *Molecules* **26**: 7305.

Santibáñez-Andrade, M., Quezada-Maldonado, E., Rivera-Pineda, A., Chirino, Y., García-Cuellar, C., Sánchez-Pérez, Y. 2023. The road to malignant cell transformation after particulate matter exposure: From oxidative stress to genotoxicity. *International Journal of Molecular Sciences* **24:** 1782.

Sarkar, S., Horn, G., Moulton, K., Oza, A., Byler, S., Koklus, S. and Longacre, M. 2013. Cancer development, progression, and therapy: An epigenetic overview. *International Journal of Molecular Sciences* **14**: 21087–21113.

Sax, S., Gentry, P., Van Landingham, C., Clewell, H. and Mundt, K. 2020. Extended Analysis and Evidence Integration of Chloroprene as a Human Carcinogen. *Risk Analysis* **40:** 294-318.

Schaap, M., Wackers, P., Zwart, E., Huijskens, I., Jonker, M., Hendriks, G., Breit, T., van Steeg, H., van der Water, B. and Luijten, M. 2015. A novel toxicogenomics-based approach to categorize (non-) genotoxic carcinogens. *Arch Toxicol* **89**, 2413–2427.

Schecter, A., Birnbaum, L., Ryan, J. and Constable, J. 2006. Dioxins: An overview. *Environmental Research* **101:** 419-428.

Scherer, W., Syverton, J. and Gey, G. 1953. Studies on the propagation *in vitro* of poliomyelitis viruses. IV. Viral multiplication in a stable strain of human malignant epithelial cells (strain HeLa) derived from an epidermoid carcinoma of the cervix. *J Exp Med* **97:** 695–710.

Schmid, W. 1976. The Micronucleus Test for Cytogenetic Analysis. In: Hollaender, A. (eds) Chemical Mutagens. Chemical Mutagens. Springer, Boston, MA. https://doi.org/10.1007/978-1-4684-0892-8_2

Schrenk, D. 2018. What is the meaning of 'a compound is carcinogenic'? *Toxicology Reports* **5:** 504–511.

Sen, P., and Costa, M. 1986. Pathway of nickel uptake influences its interaction with heterochromatic DNA. *Toxicol. Appl. Pharmacol*. **84:** 278–285.

Shah, U., de Oliveira Mallia, J., Singh, N., Doak, S. and Jenkins, G. 2018. A three-dimensional *in vitro* HEPG2 cells liver spheroid model for genotoxicity studies. *Mutation Research/Genetic Toxicology and Environmental Mutagenesis* **825**: 51–58.

Shelby, M. 1990. Results of NTP-sponsored mouse cytogenetic studies on 1,3-butadiene, isoprene, and chloroprene. *Environmental Health Perspectives* **86:** 71–73.

Shen, H. and Zhang, Q. 1994. Risk assessment of nickel carcinogenicity and occupational lung cancer. *Environ Health Perspect.* **102:** 275–82.

Shi, H., Shi, X. and Liu, K. 2004. Oxidative mechanism of arsenic toxicity and carcinogenesis. *Mol. Cell. Biochem.* **255:** 67–78.

Siegel, R., Miller, K. and Jemal, A. 2018. Cancer statistics, 2018. *CA Cancer J. Clin*. **68**: 7–30.

Sigma aldrich (2023) *RPMI vs. DMEM. RPMI 1640 media*. Available at: https://www.sigmaaldrich.com/GB/en/products/cell-culture-and-analysis/cell-culture-media-and-buffers/classical-media-and-buffers/rpmi-1640-media#rpmi-vs-dmem

Sills, R., Hong, H., Melnick, R., Boorman, G., Devereux, T. 1999. High frequency of codon 61 KRAS A→T transversions in lung and Harderian gland neoplasms of B6c3f1 mice exposed to chloroprene (2-chloro-1,3-butadiene) for 2 years, and comparisons with the structurally related chemicals isoprene and 1,3-butadiene. *Carcinogenesis* **20:** 657–662.

Silva Lima, B. and Van der Laan, J. 2000. Mechanisms of Nongenotoxic Carcinogenesis and Assessment of the Human Hazard. *Regulatory Toxicology and Pharmacology* **32:** 135-143.

Silva, R. and Tamburic, S. 2022. A State-of-the-Art Review on the Alternatives to Animal Testing for the Safety Assessment of Cosmetics. *Cosmetics* **9:** 90.

Smirnova, L., Harris, G., Leist, M. and Hartung, T. 2015. Cellular resilience. ALTEX **32:** 247–260.

Smith, A., Lingas, E. and Rahman, M. 2000. Contamination of drinking-water by arsenic in Bangladesh: a public health emergency. *Bulletin of the World Health Organization* **78:** 1093–1103.

Smith, M., Guyton, K., Gibbons, C., Fritz, J., Portier, C., Rusyn, I., DeMarini, D., Caldwell, J., Kavlock, R., Lambert, P., Hecht, S., Bucher, J., Stewart, B., Baan, R., Cogliano, V. and Straif, K. 2016. Key Characteristics of Carcinogens as a Basis for Organizing Data on Mechanisms of Carcinogenesis. *Environmental Health Perspectives* **124:** 713-721.

Sommer, S., Buraczewska, I. and Kruszewski, M. 2020. Micronucleus Assay: The State of Art, and Future Directions. *Int J Mol Sci.* **21:** 1534.

Song, X., Fiati Kenston, S., Kong, L. and Zhao, J., 2017. Molecular mechanisms of nickel induced neurotoxicity and chemoprevention. *Toxicology* **392:** 47-54.

Stambolic, V., Suzuki, A., de la Pompa, J., Brothers, G., Mirtsos, C., Sasaki, T., Ruland, J., Penninger, J., Siderovski, D. and Mak, T. 1998. Negative Regulation of PKB/Akt-Dependent Cell Survival by the Tumour Suppressor PTEN. *Cell* **95:** 29-39.

Stannard, L., Doak, S., Doherty, A. and Jenkins, G., 2016. Is Nickel Chloride really a Non-Genotoxic Carcinogen?. *Basic & Clinical Pharmacology & Toxicology* **121:** 10-15.

Stellman, J. and Stellman, S. 2018. Agent orange during the Vietnam War: The lingering issue of its civilian and military health impact. *American Journal of Public Health* **108:** 726–728.

Stellman, J., Stellman, S., Christian, R, Weber T, Tomasallo C. 2003. The extent and patterns of usage of Agent Orange and other herbicides in Vietnam. Nature. **422**: 681–687.

Stewart, Z., Westfall, M. and Pietenpol, J. 2003. Cell-cycle dysregulation and anticancer therapy. *Trends Pharmacol Sci.* **24:** 139–145.

Suarez-Torres, J., Alzate, J. and Orjuela-Ramirez, M. 2019. The NTP Report on carcinogens: A valuable resource for public health, a challenge for regulatory science. *Journal of Applied Toxicology* **40:** 169–175.

Sugiura, A. and Rathmell, J. 2018. Metabolic Barriers to T Cell Function in Tumours. *The Journal of Immunology* **200:** 400-407.

Sun, W., Zhou, Y., Zhang, Z., Cao, L. and Chen, W. 2017. The Trends in Cardiovascular Diseases and Respiratory Diseases Mortality in Urban and Rural China, 1990–2015. *International Journal of Environmental Research and Public Health* **14:** 1391.

Swenberg, J., Richardson, F., Boucheron, J., Deal, F., Belinsky, S., Charbonneau, M. and Short, B. 1987. High-to low-dose extrapolation: critical determinants involved in the dose response of carcinogenic substances. *Environ. Health Perspect*. **76:** 57.

Szmant, H. 1975. Physical properties of dimethyl sulfoxide and its function in biological systems. Ann. N. Y. Acad. Sci. **243:** 20-30.

Szybowska, P., Kostas, M., Wesche, J., Wiedlocha, A., Haugsten, E. 2019. Cancer Mutations in FGFR2 Prevent a Negative Feedback Loop Mediated by the ERK1/2 Pathway. Cells. **8:** 518.

Szychowski, K., Rybczyńska-Tkaczyk, K., Leja, M., Wójtowicz, A. and Gmiński, J. *2016.* Tetrabromobisphenol A (TBBPA)-stimulated reactive oxygen species (ROS) production in cell-free model using the H_2DCFDA assay—limitations of method. *Environ Sci Pollut Res* **23**: 12246–12252.

Tait, J., Gibson, D. and Fujikawa, K. 1989. Phospholipid binding properties of human placental anticoagulant protein-I, a member of the lipocortin family. *J Biol Chem*. **264:** 7944–7949.

Tanida, T., Warita, K., Ishihara, K., Fukui, S., Mitsuhashi, T., Sugawara, T., Tabuchi, Y., Nanmori, T., Qi, W.-M, Inamoto, T., Yokoyama, T., Kitagawa, H. and Hoshi, N. 2009. Fetal and neonatal exposure to three typical environmental chemicals with different mechanisms of action: Mixed exposure to phenol, phthalate, and dioxin cancels the effects of sole exposure on mouse midbrain dopaminergic nuclei. *Toxicology Letters* **189**: 40–47.

Tapio, S. and Grosche, B. 2006. Arsenic in the aetiology of cancer. *Mutation Research/Reviews in Mutation Research* **612:** 215-246.

Tarpey, M., Wink, D. and Grisham, M. 2004. Methods for detection of reactive metabolites of oxygen and nitrogen: *in vitro* and *in vivo* considerations. *Am. J. Physiol. Regul. Integr. Comp. Physiol.* **286:** 431–444.

Terpilowska, S. and Siwicki, A. 2018. Interactions between chromium(III) and iron(III), molybdenum(III) or nickel(II): Cytotoxicity, genotoxicity and mutagenicity studies. *Chemosphere*, **201:** 780-789.

Tezuka, M., Hanioka, K., Yamanaka, K. and Okada, S. 1993. Gene Damage Induced in Human Alveolar Type II (L-132) Cells by Exposure to Dimethylarsinic Acid. *Biochemical and Biophysical Research Communications* **191:** 1178-1183.

Thermofisher. 2023. DAPI (4',6-diamidino-2-phenylindole): Thermo Fisher Scientific - US, DAPI (4',6-diamidino-2-phenylindole) | Thermo Fisher Scientific - US. Available at: https://www.thermofisher.com/uk/en/home/life-science/cell-analysis/fluorophores/dapi-stain.html.

Thompson, D., 1993. A chemical hypothesis for arsenic methylation in mammals. *Chemico-Biological Interactions* **88:** 89-114.

Thornton, I. and Farago, M. 1997. The geochemistry of arsenic, in: C. O. Abernathy, R. L. Calderon, W. R.Chappell (Eds.), Arsenic: Exposure and Health Effects, Chapman and Hall, Kluwer Academic Publishers, London 1-16.

Tice, R., Boucher, R., Luke, C., Paquette, D., Melnick, R. and Shelby, M., 1988. Chloroprene and isoprene: cytogenetic studies in mice. *Mutagenesis* **3:** 141-146.

Tomásek, L. and Darby, S. 1995. Recent results from the study of West Bohemian uranium miners exposed to radon and its progeny. *Environmental Health Perspectives* **103:** 55-57.

Ton, T., Hong, H., Devereux, T., Melnick, R., Sills, C. and Kim, Y. 2007. Evaluation of genetic alterations in cancer-related genes in lung and brain tumours from B6C3F1 mice exposed to 1,3-butadiene or chloroprene. *Chemico-Biological Interactions* **166:** 112–120.

Torreilles, J. and Guérin, M., 1990. Nickel (II) as a temporary catalyst for hydroxyl radical generation. *FEBS Letters* **272**: 58-60.

Tung, C. and Jheng, J. 2014. Interpretable prediction of non-genotoxic hepatocarcinogenic chemicals. *Neurocomputing* **145**: 68-74.

Uddin, A., Burns, F., Rossman, T., Chen, H., Kluz, T. and Costa, M. 2007. Dietary chromium and nickel enhance UV-carcinogenesis in skin of hairless mice. *Toxicological Applied Pharmacology* **221:** 329-38.

Uneyama, C., Toda, M., Yamamoto, M. and Morikawa, K. 2007. Arsenic in various foods: Cumulative data. *Food Additives & Contaminants* **24:** 447-534.

Valentine, R. and Himmelstein, M., 2001. Overview of the acute, subchronic, reproductive, developmental and genetic toxicology of β-chloroprene. *Chemico-Biological Interactions* **135-136:** 81-100.

van Acker, S., van den Berg, D., Tromp, M., Griffioen, D., van Bennekom, W., van der Vijgh, W. and Bast, A. 1996. Structural aspects of antioxidant activity of flavonoids. *Free Radic. Biol. Med.* **20:** 331–342.

van Delft, J., van Agen, E., van Breda, S., Herwijnen, M., Staal, Y. and Kleinjans, J. 2004. Discrimination of genotoxic from non-genotoxic carcinogens by gene expression profiling. *Carcinogenesis* **25:** 1265–1276.

Van den Berg, M., Birnbaum, L., Denison, M., De Vito, M., Farland, W., Feeley, M., Fiedler, H., Hakansson, H., Hanberg, A., Haws, L., Rose, M., Safe, S., Schrenk, D., Tohyama, C., Tritscher, A., Tuomisto, J., Tysklind, M., Walker, N. and Peterson, R. 2006. The 2005 World Health Organization Reevaluation of Human and Mammalian Toxic Equivalency Factors for Dioxins and Dioxin-Like Compounds. *Toxicological Sciences* **93:** 223–241.

Vega, L., Styblo, M., Patterson, R., Cullen, W., Wang, C. and Germolec, D. 2001. Differential Effects of Trivalent and Pentavalent Arsenicals on Cell Proliferation and Cytokine Secretion in Normal Human Epidermal Keratinocytes. *Toxicology and Applied Pharmacology* **172:** 225-232.

Vermeulen, K., Van Bockstaele, D. and Berneman, Z. 2003. The cell cycle: a review of regulation, deregulation and therapeutic targets in cancer. *Cell Proliferation* **36:** 131-149.

Veselenak, R., Miller, A., Milligan, G., Bourne, N. and Pyles, R. 2015. Development and utilization of a custom PCR array workflow: analysis of gene expression in mycoplasma genitalium and guinea pig (Cavia porcellus). *Mol Biotechnol.* **57:** 172-83.

Vinken, M., Doktorova, T., Ellinger-Ziegelbauer, H., Ahr, H., Lock, E., Carmichael, P., Roggen, E., van Delft, J., Kleinjans, J., Castell, J., Bort, R., Donato, T., Ryan, M., Corvi, R., Keun, H., Ebbels, T., Athersuch, T., Sansone, S., Rocca-Serra, P., Stierum, R., Jennings, P., Pfaller, W., Gmuender, H., Vanhaecke, T., Rogiers, V. 2008. The carcinoGENOMICS project: Critical selection of model compounds for the development of omics-based *in vitro* carcinogenicity screening assays, Mutation Research/Reviews in Mutation Research **659**: 202-210.

Vogt, B. and Rossman, T. 2001. Effects of arsenite on p53, p21 and cyclin D expression in normal human fibroblasts-a possible mechanism for arsenite's comutagenicity. *Mutation Research* **478**:159–168.

Wagner, S. and Weswig, P. 1974. Arsenic in Blood and Urine of Forest Workers. *Archives of Environmental Health: An International Journal* **28:** 77-79.

Walmsley, R. and Billinton, N. 2011. How accurate is *in vitro* prediction of carcinogenicity? *British Journal of Pharmacology* **162:** 1250–1258.

Wang, C., Tao, W., Wang, Y., Bikow, J., Lu, B., Keating, A., Verma, S., Parker, T., Han, R. and Wen, X., 2010. Rosuvastatin, Identified From a Zebrafish Chemical Genetic Screen for Antiangiogenic Compounds, Suppresses the Growth of Prostate Cancer. *European Urology* **58:** 418-426.

Ward, E., Schulte, P., Bayard, S., Blair, A., Brandt-Rauf, P., Butler, M., Dankovic, D., Hubbs, A., Jones, C., Karstadt, M., Kedderis, G., Melnick, R., Redlich, C., Rothman, N., Savage, R., Sprinker, M., Toraason, M., Weston, A., Olshan, A., Stewart, P., Zahm, S. 2003. National Occupational Research Agenda Team. Priorities for development of research methods in occupational cancer. *Environ Health Perspect*. **111:** 1-12.

Ward, N., Watts, G. and Eckel, R. 2019. Statin toxicity. *Circulation Research* **124:** 328–350.

Wareham, M. and Rosney, D. 2020 Living in America's cancer alley is like Death row. *BBC News*. BBC. Available at: https://www.bbc.co.uk/news/av/newsbeat-54773957.

Webmd.com. 2022. *Rosuvastatin Oral: Uses, Side Effects, Interactions, Pictures, Warnings & Dosing - WebMD*. [online] Available at: <https://www.webmd.com/drugs/2/drug-76701/rosuvastatin-oral/details> [Accessed 23 September 2022].

Weinberg, R. 1996. How Cancer Arises. Scientific American **275**: 62–70. JSTOR, http://www.jstor.org/stable/24993349.

White, C., 2002. A Review of the Pharmacologic and Pharmacokinetic Aspects of Rosuvastatin. *The Journal of Clinical Pharmacology* **42:** 963-970.

WHO. 2023. Cancer, World Health Organization. World Health Organization. Available at: https://www.who.int/news-room/fact-sheets/detail/cancer.

WHO. 2001. Arsenic Compounds, Environmental Health Criteria 224, 2nd ed., World Health Organisation, Geneva.

Wilde, E., Chapman, K., Stannard, L., Seager, A., Brüsehafer, K., Shah, U., Tonkin, J., Brown, M., Verma, J., Doherty, A., Johnson, G., Doak, S. and Jenkins, G. 2017. A novel, integrated *in*

vitro carcinogenicity test to identify genotoxic and non-genotoxic carcinogens using human lymphoblastoid cells. *Archives of Toxicology* **92:** 935-951.

Williams, P., Villada, A., Deacon, C., Raab, A., Figuerola, J., Green, A., Feldmann, J. and Meharg, A. 2007. Greatly Enhanced Arsenic Shoot Assimilation in Rice Leads to Elevated Grain Levels Compared to Wheat and Barley. *Environmental Science & Technology* **41:** 6854-6859.

Wills, J., Summers, H., Hondow, N., Sooresh, A., Meissner, K., White, P., Rees, P., Brown, A. and Doak, S. 2017. Characterizing Nanoparticles in Biological Matrices: Tipping Points in Agglomeration State and Cellular Delivery *In Vitro*. *ACS Nano* **11**: 11986–12000.

Wolfe, W., Michalek, J., Miner, J., Pirkle, J., Caudill, S., Patterson, D. and Needham, L. 1994. Determinants of TCDD half-life in veterans of operation ranch hand. *J. Toxicol. Environ. Health **41*:** 481–488

Woo, S., Park, I., Park, M., Lee, H., Lee, S., Chun, Y., Lee, S., Hong, S. and Rhee, C. 2002. Arsenic trioxide induces apoptosis through a reactive oxygen species-dependent pathway and loss of mitochondrial membrane potential in HeLa cells. *International Journal of Oncology* **21**: 57-63.

Wu, C., Ko, J., Pan, H., Chiu, L., Kang, Y. and Hsiao, Y. 2019. Ni-induced TGF-β signaling promotes VEGF-a secretion via integrin β3 upregulation. *Journal of Cellular Physiology* **234:** 22093-22102.

Wu, S., Powers, S., Zhu, W. and Hannun, Y. 2016. Substantial contribution of extrinsic risk factors to cancer development. *Nature* **529**: 43–47.

Xi, H., Frenkel, K., Klein, C. and Costa, M., 1993. Nickel Induces Increased Oxidants in Intact Cultured Mammalian Cells as Detected by Dichlorofluorescein Fluorescence. *Toxicology and Applied Pharmacology* **120:** 29-36.

Xu, G., Liu, J., Yoshimoto, K., Chen, G., Iwata, T., Mizusawa, N., Duan, Z., Wan, C. and Jiang, J., 2014. 2,3,7,8-Tetrachlorodibenzo-p-dioxin (TCDD) induces expression of p27kip1 and FoxO3a in female rat cerebral cortex and PC12 cells. *Toxicology Letters* **226:** 294-302.

Xu, J., Ye, Y., Huang, F., Chen, H., Wu, H., Huang, J., Hu, J., Via, D., Wu, Y. 2016. Association between dioxin and cancer incidence and mortality: A meta-analysis. *Scientific Reports* **6**.

Yamakage, K., Kusakabe, H. and Tanaka, N. 1998. Comparative studies of MCL-5 cells and human lymphocytes for detecting indirect-acting clastogens. *Mutation Research/Genetic Toxicology and Environmental Mutagenesis* **412**: 55-61.

Yamamoto, S., Konishi, Y., Matsuda, T., Murai, T., Shibata, M., Matsui-Yuasa, I., Otani, S., Kuroda, K., Endo, G., Fukushima, S. 1995. Cancer Induction by an Organic Arsenic Compound, Dimethylarsinic Acid (Cacodylic Acid), in F344/DuCrj Rats after Pretreatment with Five Carcinogens. *Cancer Research **55:** 1271-1276.*

Yamanaka, K., Hayshi, H., Kato, K., Hasegawa, A., Oku, N. and Okada, S. 1997. DNA Single-Strand Breaks in L-132 Cells Resulting from Inhibition of Repair Polymerization Shortly after Exposure to Dimethylarsinic Acid. *Biological and Pharmaceutical Bulletin* **20:** 163-167.

Yang, M. 2011. A current global view of environmental and occupational cancers. *Journal of Environmental Science and Health, Part C* **29**: 223-249.

Yao, Y., Lu, Y., Chen, W., Jiang, Y., Cheng, T., Ma, Y., Lu, L. and Dai, W. 2014. Cobalt and Nickel Stabilize Stem Cell Transcription Factor OCT4 through Modulating Its Sumoylation and Ubiquitination. *PLoS ONE* 9: p.e86620.

Yen, Y., Tsai, K., Chen, Y., Huang, C., Yang, R. and Liu, S. 2012. Arsenic induces apoptosis in myoblasts through a reactive oxygen species-induced endoplasmic reticulum stress and mitochondrial dysfunction pathway. *Archives of Toxicology* **86:** 923-933.

Yin, S., Cui, H., Peng, X., Fang, J., Zuo, Z., Deng, J., Wang, X., Wu, B. and Guo, H. 2015. Toxic effect of $NiCl_2$ on development of the bursa of Fabricius in broiler chickens. *Oncotarget* **7:** 125-139.

Zeisel, S. 1996. Choline. A nutrient that is involved in the regulation of cell proliferation, cell death, and cell transformation. Adv. Exp. Med. Biol. **399:** 131–141.

Zhao, S. 2016. Amendment of the low-density lipoprotein cholesterol target in the 'Chinese Guidelines for the Prevention and Treatment of Adult Dyslipidemia': Opinion. *Chronic Diseases and Translational Medicine* **2:** 7–9.

Zhao, S., Tsuchida, T., Kawakami, K., Shi, C. and Kawamoto, K., 2002. Effect of As2O3 on cell cycle progression and cyclins D1 and B1 expression in two glioblastoma cell lines differing in p53 status. *International Journal of Oncology* **21:** 49-55.

Zhao, Y., Xie, P. and Fan, H. 2012. Genomic profiling of microRNAs and proteomics reveals an early molecular alteration associated with tumourigenesis induced by MC-LR in mice. *Environ Sci Technol* **46:** 34–41.

Zong, W., Rabinowitz, J. and White, E. 2016. Mitochondria and Cancer. *Mol Cell*. **61:** 667-676.

Zoumpourlis, V., Solakidi, S., Papathoma, A. and Papaevangeliou, D. 2003. Alterations in signal transduction pathways implicated in tumour progression during multistage mouse skin carcinogenesis. *Carcinogenesis* **24**: 1159-1165.

2,3,7,8-tetrachlorodibenzo-p-dioxin. 2023. *National Center for Biotechnology Information. PubChem Compound Database*. Available at: https://pubchem.ncbi.nlm.nih.gov/compound/2_3_7_8-Tetrachlorodibenzo-P-dioxin